OTS: 60-41,412

JPRS: 5610
20 October 1960

NEWS OF HIGHER EDUCATIONAL INSTITUTIONS,

MINISTRY OF HIGHER EDUCATION USSR

RADIOPHYSICS SERIES

VOL. II, No 4, MOSCOW, 1959

Distributed by:

OFFICE OF TECHNICAL SERVICES
U. S. DEPARTMENT OF COMMERCE
WASHINGTON 25, D. C.

U. S. JOINT PUBLICATIONS RESEARCH SERVICE
205 EAST 42nd STREET, SUITE 300
NEW YORK 17, N. Y.

F O R E W O R D

This publication was prepared under contract by the UNITED STATES JOINT PUBLICATIONS RESEARCH SERVICE, a federal government organization established to service the translation and research needs of the various government departments.

JPRS: 5610

CSO: 4341-N/RF4

NEWS OF HIGHER EDUCATIONAL INSTITUTIONS,

MINISTRY OF HIGHER EDUCATION USSR

RADIOPHYSICS SERIES

Izv Vysshikh Ucheb Zaved Radiofiz

[Following is the complete translation of Seriya Radiofizika (Radiophysics Series) Vol. II, No 4, Moscow, 1959, pages 521-673.]

ERRATA

ЗАМЕЧЕННЫЕ ОПЕЧАТКИ

Page / Стр. *	Page / Стр. **	Line / Строка	Designated / Напечатано	Correction / Должно быть
		from top		
46	547	14 сверху	$\ldots - 2M\gamma_2 \cos\varphi_2$	$\ldots - M\gamma_2 \cos\varphi_2$
50	549	21 снизу	$\left[1-\exp\left(-\frac{2\omega}{c}\,xy\right)\right]$	$\left[1-\exp\left(-\frac{2\omega}{c}\,xz\right)\right]$
62	556	7 сверху	$\overline{(\ln\lvert E\rvert - \ln\lvert E\rvert)^2}\ldots$	$\overline{(\ln\lvert E\rvert - \ln\lvert E\rvert)^2}\ldots$
67	558	6 снизу	$\ldots = -p^3(r \quad z_0)$	$\ldots = -p^3(r - r_0)$
71		15 сверху	$\overline{\xi_r^2} = \overline{\xi_l^2}$	$\overline{\xi_r^2} = \overline{\xi_l^2}$
71	561	17 сверху	$\ldots = \frac{\lvert\overline{E^2}\rvert}{2\lvert\overline{E}\rvert^2}\ldots$	$\ldots = \frac{\lvert\overline{E^2}\rvert}{2\lvert\overline{E}\rvert^2}\ldots$
73	562	8 снизу	$\ldots(L/z/\ z_{\text{макс}})^2$	$\ldots(L\,k\,l_\perp z_{\text{макс}})^2$
87	571	27 снизу	$\ldots\frac{\overline{l}L^3}{L_0^4}\ldots$	$\ldots\frac{\overline{l}L^3}{z_0^4}\ldots$
92		2 сверху	$\ldots\frac{(\omega_2-\Omega)^2}{4a_0^2\omega_0^2}\ldots$	$\ldots\frac{(\omega_2-\Omega)^2}{4a_0^2\omega_0^2L^2}\ldots$
97	578	6 сверху	$\ldots\frac{(\omega_2-\Omega)^2}{4a_0^2\omega_0^2L}\ldots$	$\ldots\frac{(\omega_2-\Omega)^2}{4a_0^2\omega_0^2L^2}\ldots$
100	579	13 снизу	$\ldots+\frac{p_1\Delta_1\sin 2\beta_1}{p_1^2+\Omega^2}\ldots$	$\ldots+\frac{p_1\Delta_2\sin 2\beta_1}{p_1^2+\Omega^2}\ldots$
229	654	19 сверху	$\sim e^{ikr}$	$\sim e^{ikz}$
246	661	12 снизу	γ_{13} и γ_{12}	γ_{13} и γ_{12}

*[translation page]
**[Russian book page]

CONTENTS

SOME ASPECTS OF THE THEORY OF WAVE PROPAGATION IN MEDIA WITH RANDOM INHOMOGENEITIES - REVIEW .

Pages 521-542

by N.G. Denisov & V.A. Zverev.

Introduction

The study of the effect of random variations in the properties of a medium on a wave propagated in it is of considerable interest to many branches of applied physics, solar physics, the physics of the earth's atmosphere and ionosphere and acoustics, for example. There is a very extensive literature related to the propagation of waves in media with random inhomogeneities.

Recently reviews and monographs, devoted to this theme, have been published. Thus, for example, references [1,2] offer a systematic exposition of the problems of the scattering of waves by turbulent atmospheric inhomogeneities. There is also a review of research devoted to the diffraction of radiowaves by chaotic inhomogeneities in the solar corona and the ionosphere [3].

In recent years a lot of work has been done on the scattering of radiowaves in the troposphere. The book [4] describes this work fairly thoroughly. The basic data relating to ionospheric scattering can be found in article [5].

In this article we shall consider methods of solving phenomenological problems of the theory of wave propagation in media with

random inhomogeneities. This implies, above all, methods of calculating the statistical properties of the field of a wave, passing through a non-homogeneous layer, i.e. methods of calculating fluctuations in amplitude, phase and the corresponding correlation functions. This, of course, abuts on methods of solving problems of diffraction at irregular screens and certain matters in the theory of scattering.

This review is primarily focused on work which has not been covered in existing reviews and monographs. Moreover, as distinct from the procedure in previous reviews and monographs, the above problems are solved while taking into account regular wave refraction in a non-homogeneous layer.

1. The approximation of geometrical optics

Finding the statistical properties of the field of a wave passing through a layer, containing large-scale inhomogeneities, is a comparatively simple problem. A detailed exposition of the results of investigating these problems by a method, based on the solution of the equations of the ray theory, is given in article [1]. In this connection we shall simply dwell very briefly on certain results of the geometrical theory.

If the dimensions of the inhomogeneities l are large compared with the wavelength, then at a small distance from the non-homogeneous layer the character of the field is determined by the lens action of the inhomogeneities. At distances considerably exceeding the radius of correlation of fluctuations in the refractive index the process of ray propagation may be considered to be a random process without consequence and multiple scattering (i.e. scattering by a large mass of the medium) can be described with the aid of the Einstein-Fokker equation [1,6] *.

* This question has recently been dealt with in reference [7].

Under these conditions it is possible to introduce the probability $W(z, \vartheta, \varphi) \sin \vartheta$, defining the orientation of a ray along a path z (ϑ and φ are polar and azimuthal angles in the spherical system of coordinates). The statistical scheme of this random process coincides with that describing the rotational Brownian motion of molecules. In this case the function $W(z, \vartheta, \varphi)$ obeys a known equation of the parabolic type. The solution of this equation can be written in closed form for any angle of scatter. Below, however, we shall consider only the case of small angles.

If a plane wave falls on an inhomogeneous layer (at the beginning of the layer the function $W(0, \vartheta) = \delta(\vartheta)/2\pi\vartheta$ is given), then at the end of the path z the angular spectrum $W(z, \vartheta)$ will have the form [1]:

$$W(z, \vartheta) = \frac{1}{4\pi D z} e^{-\vartheta^2/4Dz}, \qquad (1.1)$$

where D is the so-called diffusion coefficient of the rays. The mean square of fluctuations in the angle of arrival will be equal to

$$\overline{\vartheta^2} = 4 D z. \qquad (1.2)$$

Basing ourselves on the equations of the ray theory, we can get the following expression for the coefficient D [6]:

$$D = \frac{1}{4} \frac{\overline{\vartheta^2}}{\Delta z} = -\frac{1}{2n^2} \int_0^\infty \nabla^2 R(r)\, dr, \qquad (1.3)$$

where $\overline{\vartheta^2}$ is the mean square of the fluctuational deviation of the angle of arrival of the ray for the path Δz and $R(r) = \overline{\Delta n_1 \Delta n_2}$ is the correlation function of fluctuations in the refractive index n.

In this solution it is assumed that the mean value of the refractive index does not depend on the coordinates (homogeneous medium). Frequently, however, we encounter the case in which the mean parameters of the medium also vary. In the general case the problem

is a very complex one. Much more simple is the case of a plane-stratified medium, when the mean value of the refractive index $n(z)$ depends only on the one coordinate z.

When random inhomogeneities are present in layer, the dimensions of which are large compared with the wavelength and at the same time small compared with the scale of regular variation in $n(z)$, this problem can be solved (just as in the case of a homogeneous medium) with the aid of the statistical model known from the theory of the rotational Brownian motion of molecules. The regular deviation of the ray on account of refraction in the layer is analogous to the regular deviation of the dipole moment of a molecule under the action of an external field.

The function $W(\vartheta, z)$, defining the probability that a ray at the level z will have a direction ϑ (normalized angular energy spectrum), now satisfies, for small angles ϑ, the expression [8]:

$$\vartheta \frac{\partial W}{\partial z} = \frac{\partial}{\partial \vartheta}\left\{ D\,\vartheta \frac{\partial W}{\partial \vartheta} + \frac{1}{n}\frac{dn}{dz}\vartheta^2 W \right\}. \qquad (1.4)$$

The solution of this equation, similar to that of (1.1), has the form:

$$W(z,\vartheta) = \frac{1}{4\pi f(z)}\, e^{-\vartheta^2/4f(z)}; \qquad f(z) = \frac{1}{n^2(z)}\int_0^z D(\zeta)\, n^2(\zeta)\, d\zeta. \qquad (1.5)$$

For the mean square of fluctuations in the angle of arrival we get the formula

$$\overline{\vartheta^2} = 4f(z) = \frac{4}{n^2(z)}\int_0^z D(\zeta)\, n^2(\zeta)\, d\zeta. \qquad (1.6)$$

According to (1.6), on leaving a non-homogeneous layer of thickness z_0 $[n(z_0) = 1]$

$$\overline{\vartheta^2} = 4\int_0^{z_0} D(\zeta)\, n^2(\zeta)\, d\zeta. \qquad (1.7)$$

Note that the diffusion coefficient D is inversely proportional to to $n^2(\zeta)$ (see (1.3)). Formula (1.7) shows that the multiplier

$B^{-2}(\varsigma)$ is eliminated on account of refraction of the rays.

Equally simple is the treatment of other statistical characteristics of a wave, passing through a layer, containing large-scale inhomogeneities. First we shall find the correlation function of phase fluctuations [9]. In the ray approximation the fluctuational variation in phase for a path L_0 is equal to $S = k_0 \int_0^{L_0} \Delta n \, dz$ ($k_0 = \omega/c$) and the correlation function is written thus :

$$\overline{S(r_1)\, S(r_2)} = k_0^2 \int_0^{L_0}\int_0^{L_0} \overline{\Delta n_1 \Delta n_2}\, dz_1\, dz_2 . \qquad (1.8)$$

Assuming that the correlation function $\overline{\Delta n_1 \Delta n_2}$ depends only on the distance between the points r_1 and r_2 ($\overline{\Delta n_1 \Delta n_2} = (\overline{\Delta n})^2 \rho(r)$) and proceeding in (1.8) to integration with respect to $\zeta = z_1 - z_2$ and $z = (z_1 + z_2)/2$, we find :

$$R_S \equiv \overline{S(x, y)\, S(x+\xi, y+\eta)} = 2k_0^2 \int_0^{L_0} \rho(\xi, \eta, \varsigma)\, d\varsigma \int_{\varsigma/2}^{L_0 - \varsigma/2} \overline{(\Delta n)^2}\, dz . \qquad (1.9)$$

Here it is considered that for distances of the order of the scale of the random inhomogeneities l the function $(\overline{\Delta n})^2$ varies insignificantly. Taking into account, furthermore, that $L_0 \gg l$, we shall write (1.9) approximately in the form :

$$R_S(\xi, \eta) = 2k_0^2 \int_0^{L_0} \overline{(\Delta n)^2}\, dz \int_0^{\infty} \rho(\xi, \eta, \varsigma)\, d\varsigma . \qquad (1.10)$$

Hence we find the mean square phase fluctuation

$$S^2 = R_S(0, 0) = 2k_0^2 \int_0^{L_0} \overline{(\Delta n)^2}\, dz \int_0^{\infty} \rho(0, 0, \varsigma)\, d\varsigma . \qquad (1.11)$$

Note that in a medium without absorption the phase correlation function (1.10) coincides with the complex phase correlation function. The latter is closely linked with the correlation function of a complex field and, accordingly, with the angular energy spectrum (see section 3).

Fluctuations in the amplitude or intensity of a ray, passing

through a layer, containing large-scale inhomogeneities, are determined by the lens action of these inhomogeneities. Of course, these quantities can be found by calculating the variation in the cross section of a beam tube. In this case we get the following formula for the mean square of intensity fluctuations [8]:

$$\overline{(\Delta J/J)^2} = \int_0^{L_0} |v(L_0) - v(z)|^2 \overline{(\Delta n)^2}\, dz \int_{-\infty}^{+\infty} \nabla^4 \rho(\xi, \eta, \varsigma)\, d\varsigma. \quad (1.12)$$

Here $\nabla^4 = \left(\frac{\partial^2}{\partial \xi^2} + \frac{\partial^2}{\partial \eta^2}\right)^2$, $\rho(\xi, \eta, \varsigma)$ is the correlation coefficient of fluctuations in the refractive index. The function $v(z) = \int_0^z dz/n(z)$ is the group path of the ray for the plasma. For a layer with constant mean parameters $n(z) = \text{const} = 1$ we get [1]:

$$\overline{(\Delta J/J)^2} = \frac{2}{3} \overline{(\Delta n)^2} L_0^3 \int_0^{\infty} \nabla^4 \rho(\xi, \eta, \varsigma)\, d\varsigma. \quad (1.13)$$

We shall not deal with the solution of other problems by the method of the ray theory, since, in the first place, they have been treated thoroughly in the book reference [1] and, in the second, the same solutions can be obtained by starting from the more rigorous solutions, considered in the following sections.

On setting out more rigorous solutions, it is possible to establish the limits of applicablity of the approximation of geometrical optics. These conditions are [10]:

$$\lambda \ll l; \qquad \lambda L_1 \ll l^2, \quad (1.14)$$

where l is the scale of the inhomogeneities, L_1 is the distance from the beginning of the scattering layer to the point of observation (for a refinement of this condition taking into account refraction in the layer see section 2).

In the problem of the propagation of light through a turbulent atmosphere $\lambda \sim 10^{-5}$ cm, $l \sim 1$ cm and, consequently, the second condition (1.14) is fulfilled when $L_1 \ll 10^5$ cm. Thus, geometrical

optics is practically inapplicable to this problem.

In the propagation of radiowaves through the upper ionosphere ($l \sim 10^3$ m) the second condition (1.14) is fulfilled when $L \ll 10^6$ m ($\lambda = 1$ m) and $L_1 \ll 10^5$ m ($\lambda = 10$ m). Consequently in the range $\lambda \sim 10$ m the approximation of geometrical optics becomes incorrect. In describing the scattering of radiowaves in the lower ionosphere the ray theory is practically never applicable ($l \sim 200$ m, $\lambda \sim 20$ m and $l^2/\lambda \sim 10^3$ m).

In the instance of the propagation of sound in the sea ($l \sim 10^2$ cm) geometrical optics can be employed only up to distances $L_1 \ll 10^4$ cm ($\lambda \sim 1$ cm).

Note, finally, that the solution of the problem of the propagation of waves in a layer, containing random inhomogeneities, by the method of geometrical optics is comparatively simple. However, this simplification is obtained only in the case of weak, regular gradients and small scattering angles. Considerable mathematical difficulties arise, when it is necessary to consider large deviations of the rays and also when there are sharp, regular gradients of the refractive index in the layer. However, we shall not touch on these subjects, since they have not yet been discussed in the literature.

2. The method of smooth perturbations

The conditions of applicability of geometrical optics $l \gg \lambda$ and $\sqrt{\lambda L_1} \ll l^2$ impose limitations not only on the dimensions of the inhomogeneities but also on the distance L_1, which the scattered wave traverses to the point of observation. The latter limitation requires that the dimension of the Fresnel zone be much smaller than the scale of the inhomogeneities. Under these conditions their influence is reduced merely to a ray-focusing effect. A more rigorous approach, based on a solution of the wave equation, ought also to

take into account diffraction effects.

A widespread method of solving the wave equation, when weak inhomogeneities are present in the medium, is the method of perturbations. However, the solution employed in connection with another problem by Rytov [11] (the method of smooth perturbations) is most effective for calculating amplitude and phase fluctuations in a wave passing through a non-homogeneous layer. This method has been used by Obukhov [12] in connection with the problem of fluctuations in amplitude and phase. Below the method of smooth perturbations is used to solve the same problem for a layer, in which the mean value of the dielectric constant depends on the level z .

If we consider that the scale of the random inhomogeneities is sufficiently large ($l \gg \lambda$), then it is possible to neglect polarization effects and describe the field by means of the scalar equation

$$\Delta E + k_0^2 [\varepsilon(z) + \Delta\varepsilon(x, y, z)] E = 0. \qquad (2.1)$$

Here $k_0 = \omega/c$ is the wave number in a vacuum. We shall consider that the fluctuational deviation of the dielectric constant $\Delta\varepsilon(x,y,z)$ at any point is much less than the mean value of $\varepsilon(z)$.

We shall write the solution of eq. (2.1) in the form

$$E = e^{\Phi(x, y, z)}.$$

Then the function $\Phi(x,y,z)$ will satisfy the equation

$$\Delta\Phi + (\nabla\Phi)^2 + k_0^2 [\varepsilon(z) + \Delta\varepsilon(x, y, z)] = 0. \qquad (2.2)$$

If we now put the function Φ in the form $\Phi = \Phi_0 + \Phi_1$ and require the function Φ_0 to satisfy the equation

$$\Delta\Phi_0 + (\nabla\Phi_0)^2 + k_0^2 \varepsilon(z) = 0, \qquad (2.3)$$

then we get the following equation for the function Φ_1 :

$$\Delta\Phi_1 + \nabla\Phi_1 (2\nabla\Phi_0 + \nabla\Phi_1) + k_0^2 \Delta\varepsilon(x, y, z) = 0. \qquad (2.4)$$

Here we shall restrict ourselves to a consideration of a layer with smoothly varying average properties ($\lambda d\varepsilon(z)/dz \ll \varepsilon(z)$). For such a layer the solution of equation (2.3) can be written in the approximation of geometrical optics. We shall select the solution describing a wave traveling along z (normal incidence on the layer):

$$\Phi_0 = ik_0 \int_0^z \sqrt{\varepsilon}\, dz - \frac{1}{4}\int_0^z d\varepsilon/\varepsilon + \ln A_0, \qquad (2.5)$$

where A_0 is the amplitude of the unperturbed wave at the beginning of the non-homogeneous layer (when $z = 0$, $\varepsilon(0) = 1$).

Eq. (2.4) can be linearized, if it is admitted that $|\nabla\Phi_1| \ll |\nabla\Phi_0|$. Since for a smoothly varying layer $|\Delta\Phi_0| \approx k_0\sqrt{\varepsilon} = 2\pi/\lambda$, this condition means that with respect to the wavelength in the medium the variation in the function Φ_1 must be small.

Below we shall consider the case in which the dimension of the random homogeneities is much greater than the wavelength in the medium. Then if $\varepsilon(z)$ is not small, just as in the case in which $\varepsilon(z)$ = const. [12], the overall Laplace operator in (2.4) can be replaced with the transverse $\Delta_1 = \frac{\partial^2}{\partial x^2} + \frac{\partial^2}{\partial y^2}$. When the above assumptions are made, the linearized version of (2.4) may be written in the following form :

$$\Delta_1\Phi_1 + 2ik_0\sqrt{\varepsilon(z)}\,\partial\Phi_1/\partial z + k_0^2\,\Delta\varepsilon(x, y, z) = 0. \qquad (2.6)$$

We shall seek a solution of this equation, as in the case of a homogeneous medium ($\varepsilon(z)$ = const) [13], in the form of a Fourier expansion with respect to the variables x and y. We shall introduce the following notation:

$$\varphi(\varkappa_1, \varkappa_2, z) = \frac{1}{(2\pi)^2}\int_{-\infty}^{+\infty}\int \Phi_1 e^{-i(\varkappa_1 x + \varkappa_2 y)}\, dx\, dy\,; \qquad (2.7)$$

$$f(x_1, x_2, z) = \frac{1}{(2\pi)^2} \int_{-\infty}^{+\infty}\int \Delta\varepsilon(x, y, z) e^{-i(x_1 x + x_2 y)}\, dx\, dy. \qquad (2.7)$$

Multiplying eq. (2.6) by $e^{-i(x_1 x + x_2 y)}$ and integrating with respect to x and y, we get the following expression for the function $\varphi(x_1, x_2, z)$:

$$2ik_0\sqrt{\varepsilon(z)}\,\partial\varphi/\partial z - x^2\varphi + k_0^2 f(x_1, x_2, z) = 0 \qquad (x^2 = x_1^2 + x_2^2). \quad (2.8)$$

For a non-homogeneous layer the coefficient attached to the derivative $\partial\varphi/\partial z$ depends on z . However, a simple substitution of the variable

$$v = \int_0^z dz/\sqrt{\varepsilon(z)}$$

reduces eq. (2.8) to the equation with constant coefficients, discussed by Tatarskiy [13]. If a non-homogeneous layer has a thickness $L(\varepsilon(0) = \varepsilon(L) = 1)$ and within it there is a layer of thickness L_0, containing random inhomogeneities, the solution of eq. (2.8) in the point $z = L_1$, satisfying the initial condition $\varphi(0) = 0$, is written in the form :

$$\varphi(x_1, x_2, L_1) = \frac{ik_0}{2} \int_0^{L_0} f(x_1, x_2, z)\, e^{-i(x^2/2k_0)|v(L_1) - v(z)|} \frac{dz}{\sqrt{\varepsilon(z)}}. \qquad (2.9)$$

Note that the point of observation $z = L_1$ may even be outside the layer ($L_1 > L$).

The real part of the solution (2.9) is the amplitude level spectrum $\ln A_1 = \ln(A/A_0)$ and the imaginary part is the phase spectrum S_1. From (2.9) we find that

$$\mathrm{Re}\,\varphi = \frac{k_0}{2} \int_0^{L_0} f(x_1, x_2, z) \sin\left\{\frac{x^2}{2k_0}\,|v(L_1) - v(z)|\right\} \frac{dz}{\sqrt{\varepsilon(z)}}; \qquad (2.10)$$

$$\operatorname{Im}\varphi = \frac{k_0}{2}\int_0^{L_0} f(x_1, x_2, z)\cos\left\{\frac{x^2}{2k_0}\left|v(L_1)-v(z)\right|\right\}\frac{dz}{\sqrt{\varepsilon(z)}}. \quad (2.11)$$

A further problem consists in seeking the statistical quantities, characterizing a random field. The statistical properties of fluctuations in the dielectric constant are usually taken as known. Let $\overline{\Delta\varepsilon} = 0$ and the correlation function $R(r_1-r_2) = \overline{\Delta\varepsilon(r_1)\Delta\varepsilon(r_2)} = \overline{(\Delta\varepsilon)^2}\,\rho(r_1-r_2)$ be known. We shall make a Fourier expansion of this function with respect to the variables x,y and introduce the spectral density of the correlation function

$$F(x_1, x_2, z_1-z_2) = \frac{1}{(2\pi)^2}\int_{-\infty}^{+\infty}\int R(r_1-r_2)\,e^{-i(\alpha_1 x+\alpha_2 y)}\,dx\,dy. \quad (2.12)$$

From (2.10) we find the spectrum of the correlation function for the level $R_A(r_1-r_2) = \overline{\ln\left[A(r_1)/A_0\right]\ln\left[A(r_2)/A_0\right]}$ in the plane $z = L_1$:

$$F_A(x_1, x_2) = \frac{k_0^2}{4}\int_0^{L_0}\int \sin\left\{\frac{x^2\left|v(L_1)-v(z_1)\right|}{2k_0}\right\}\sin\left\{\frac{x^2\left|v(L_1)-v(z_2)\right|}{2k_0}\right\}\times$$
$$\times\frac{F(x_1, x_2, z_1-z_2)}{\sqrt{\varepsilon(z_1)\,\varepsilon(z_2)}}\,dz_1\,dz_2. \quad (2.13)$$

Analogously, from (2.11) we get the spectrum of the phase correlation function for $R_S(r_1-r_2) = \overline{S_1(r_1)S_1(r_2)}$ $(S_1 = \operatorname{Im}\Phi_1)$:

$$F_S(x_1, x_2) = \frac{k_0^2}{4}\int_0^{L_0}\int \cos\left\{\frac{x^2\left|v(L_1)-v(z_1)\right|}{2k_0}\right\}\cos\left\{\frac{x^2\left|v(L_1)-v(z_2)\right|}{2k_0}\right\}\times$$
$$\times\frac{F(x_1, x_2, z_1-z_2)}{\sqrt{\varepsilon(z_1)\,\varepsilon(z_2)}}\,dz_1\,dz_2. \quad (2.14)$$

If, for distances of the order of the scale of the random inhomogeneities, the regular variations in the properties of the medium are small, then we can write the following equation :

$$\frac{F(x_1, x_2, z_1 - z_2)}{\sqrt{\varepsilon(z_1)\,\varepsilon(z_2)}} = C(z_1, z_2)\, F_0(x_1, x_2, z_1 - z_2), \qquad (2.15)$$

where the coefficient

$$C(z_1, z_2) = \frac{\overline{(\Delta\varepsilon)^2}}{\varepsilon} = 4\,\overline{(\Delta n)^2} \qquad (2.16)$$

can be reckoned a function of the coordinate $(z_1 + z_2)/2$.

In formulas (2.13) and (2.14) it is possible to proceed to integration with respect to the coordinates $\zeta = z_1 - z_2$; $z = (z_1 + z_2)/2$. Substituting the variables and taking into account that $F_0(x_1, x_2, \zeta) = F_0(x_1, x_2, -\zeta)$, we get:

$$F_{\substack{A\\S}}(x_1, x_2) = \frac{k_0^2}{2} \int_0^{L_0} F_0(x_1, x_2, \zeta)\, d\zeta \int_{\zeta/2}^{L_0 - \zeta/2} C(z) \begin{matrix}\sin\\ \cos\end{matrix}\left\{ \frac{\varkappa^2}{2k_0} [v(L_1) - v(z_1)] \right\} \times$$

$$\times \begin{matrix}\sin\\ \cos\end{matrix}\left\{ \frac{\varkappa^2}{2k_0} [v(L_1) - v(z_2)] \right\} dz. \qquad (2.17)$$

The function $F_0(x_1, x_2, \zeta)$, the spectrum of the correlation coefficient $\rho(r_1 - r_2) = \overline{\Delta\varepsilon(r_1)\,\Delta\varepsilon(r_2)}/\overline{(\Delta\varepsilon)^2}$, in practice differs from zero only in the interval from $\zeta = 0$ to $\zeta \sim l$. If, moreover, $\sqrt{\varepsilon}\, k_0 l \gg 1$, then, since $\varkappa \sim 1/l$, for the area of integration we get $\varkappa^2 \zeta/2k_0\sqrt{\varepsilon} \sim 1/\sqrt{\varepsilon}\, k_0 l \ll 1$.

Formula (2.17) includes the quantities $v(z_{1,2}) = v(2z \pm \zeta)/2$. The variation in the function $v(z_{1,2}) = \int_0^{z_{1,2}} dz/\sqrt{\varepsilon}$ in the area of integration is equal to $\Delta v = \zeta/\sqrt{\varepsilon} \sim l/\sqrt{\varepsilon}$, and, consequently, the arguments of the trigonometrical functions, entering into formula (2.17), very insignificantly. Since $C(z)$ is also a slowly varying function, the integral with respect to the variable z can be taken out from the integral with respect to ζ with the value for $\zeta = 0$. The final result is written in the form:

$$F_{\substack{A\\S}}(x_1, x_2) = \frac{k_0^2}{2}\int_0^{L_0} C(z)\begin{matrix}\sin^2\\ \cos^2\end{matrix}\left\{\frac{\varkappa^2}{2k_0}[v(L_1) \quad v(z)]\right\} dz \int_0^{\infty} F_0(x_1, x_2, \varsigma)\, d\varsigma \qquad (2.18)$$

In the integral with respect to ς the upper limit can be taken as infinity.

Formulas (2.18) differ from the formulas obtained by Tatarskiy for the case in which $\varepsilon \approx 1$ [14] in that they contain v(z) and $v(L_1)$ instead of the linear coordinates z and L_1. For a plasma this represents the group path of the ray; thus, taking refraction into account gives a noticeable effect even for a smoothly varying medium, when $\int_0^L dz/\sqrt{\varepsilon(z)}$ differs substantially from the geometrical path L.

It is interesting to note that on taking refraction into account there is some variation in the boundaries of applicability of the approximation of geometrical optics. This follows from (2.18) if the argument of the trigonometrical functions is small, i.e. if $(\varkappa^2/2k_0)v(L_1) \ll 1$ or $\lambda_0 v(L_1)/l^2 \ll 1$ (in the second inequality it is considered that $\varkappa \sim 1/l$). Then, for the spectra of the correlation functions F_A and F_S we get the formulas :

$$\left.\begin{aligned} F_A &= \frac{1}{8}\int_0^{L_0} C(z)\,|v(L_1) - v(z)|\, dz \int_0^{\infty} \varkappa^4 F_0(x_1, x_2, \varsigma)\, d\varsigma; \\ F_S &= \frac{k_0^2}{2}\int_0^{L_0} C(z)\, dz \int_0^{\infty} F_0(x_1, x_2, \varsigma)\, d\varsigma. \end{aligned}\right\} \qquad (2.19)$$

The correlation functions of level and phase in the plane $z = L_1 \geqslant L_0$ will be equal to :

$$R_A(\xi, \eta) = \int_{-\infty}^{+\infty}\int F_A(x_1, x_2)\, e^{i(x_1\xi + x_2\eta)}\, dx_1\, dx_2 = \qquad (2.20)$$

$$= \frac{1}{8}\int_0^{L_0} C(z)\,|v(L_1)-v(z)|^2\,dz \int_0^{\infty} \nabla^4 \rho(\xi, \eta, \zeta)\,d\zeta; \qquad (2.20)$$

$$R_S = \frac{k_0^2}{2}\int_0^{L_0} C(z)\,dz \int_0^{\infty} \rho(\xi, \eta, \zeta)\,d\zeta, \qquad (2.21)$$

where $C(z) = \overline{(\Delta\varepsilon)^2}/\varepsilon = 4\,\overline{(\Delta n)^2}$ and $\rho(\xi, \eta, \zeta)$ is the correlation coefficient of fluctuations in the dielectric constant. From formulas (2.20) and (2.21) we get the mean squares of the fluctuations in level and phase :

$$\overline{\left(\ln\frac{A}{A_0}\right)^2} = R_A(0,0) = \frac{1}{8}\int_0^{L_0} C(z)\,|v(L_1)-v(z)|^2\,dz \int_0^{\infty} \nabla^4 \rho(0, 0, \zeta)\,d\zeta; \qquad (2.22)$$

$$\overline{S^2} = R_S(0, 0) = \frac{k_0^2}{2}\int_0^{L_0} C(z)\,dz \int_0^{\infty} \rho(0, 0, \zeta)\,d\zeta. \qquad (2.23)$$

It should be noted that these formulas can be obtained directly from the ray theory equations (see section 1, formulas (1.11) and (1.12)).

The correlation functions of level (2.20) and phase (2.21) show that, when geometrical optics is applicable, the transverse scale of inhomogeneities in level and phase, just as when ε = const, coincides with the transverse scale of the inhomogeneities. The effect of refraction is felt only in fluctuations in intensity. In this connection it should be noted that the refraction of scattered waves may be important both in the propagation of radiowaves in the ionosphere and the solar corona and in the propagation of sound waves in the sea. As far as the propagation of light and radiowaves in the atmosphere is concerned, where the refractive index is close to unity and $v(z) \approx z$, taking refraction into account does not introduce

significant changes.

Whereas the intensity of atmospheric turbulence depends on height, the function $C(z)$ increases with increase in z (diminishes with height). Accordingly, the main contribution to the integral (2.23) is made by the lower layers of the atmosphere, which are generally also responsible for phase fluctuations (vibration of images of stars). From formula (2.22) it follows that the scintillation of stars is determined by the higher layers of the atmosphere [14].

A solution in the approximation of geometrical optics is limited by the inequality $\lambda_0 v(L_1)/l^2 \ll 1$. More general solutions, taking into account diffraction effects, are expressed in formulas (2.18). Using these formulas, we find the correlation functions of phase and level :

$$R_{S}^{A}(\xi, \eta_1) = \int_{-\infty}^{+\infty}\int F_{S}^{A}(x_1, x_2) e^{i(x_1\xi + x_2\eta)}\, dx_1\, dx_2 .$$

We shall introduce the notation

$$\int_0^{\infty} F_0(x_1, x_2, \zeta)\, d\zeta = a(x_1, x_2); \qquad (2.24)$$

then the Fourier conjugate of the function $a(x_1, x_2)$ will be equal to : $(\xi, \eta) = \int_0^{\infty} \rho(\xi, \eta, \zeta)\, d\zeta$.

From (2.18) we find :

$$R_{S}^{A}(\xi, \eta) = \frac{k_0^2}{2}\int_0^{L_1} C(z)\, dz \int_{-\infty}^{+\infty}\int \sin^2\cos^2\left\{\frac{\varkappa^2}{2k_0}\left|v(L_1) - v(z)\right|\right\} \times$$

$$\times\, a(x_1, x_2)\, e^{i(x_1\xi + x_2\eta)}\, dx_1\, dx_2. \qquad (2.25)$$

Substituting (2.24) and integrating with respect to x_1 and x_2,

we get :

$$R_{A,S}(\xi,\eta) = \frac{k_0^2}{4}\int_0^{L_0} C(z)\left|M(\xi,\eta) \mp \int_{-\infty}^{+\infty}\int M(x+\xi,y+\eta)\frac{1}{\pi P}\sin\frac{r^2}{P}\,dx\,dy\right|dz, \tag{2.26}$$

where

$$P(z) = 4\,|v(L_1) - v(z)|/k_0\,,\quad r^2 = x^2 + y^2.$$

For a homogeneous layer $C(z) = 4(\overline{\Delta n})^2 = \text{const.}$, $v(L_1) - v(z) = L_1 - z$ and in formula (2.26) it is possible to integrate with respect to z :

$$R_{A,S}(\xi,\eta) = k_0^2(\overline{\Delta n})^2\left\{M(\xi,\eta)\,L_0 \pm \frac{k_0}{4\pi}\int_{-\infty}^{+\infty}\int M(x+\xi,y+\eta)\times\right.$$
$$\left.\times\left[\mathrm{si}\,\frac{k_0 r^2}{4L_1} - \mathrm{si}\,\frac{k_0 r^2}{4(L_1-L_0)}\right]dx\,dy\right\}, \tag{2.27}$$

where

$$\mathrm{si}\,u = -\int_u^{\infty}(\sin u/u)\,du.$$

Chernov [1] has investigated formula (2.27) in detail for $L_1 = L_0$ and for a Gaussian correlation function. Tatarskiy [2,13,14] has made calculations with the function $M(\xi,\eta)$ defined by the "two-thirds" law. We shall not dwell on formulas (2.27), since this question has been satisfactorily dealt with in references [1,2]. We shall merely note that for large values of the parameter $k_0 l^2/L_0$ we obtain from (2.27) the simple ray theory formulas (2.20), (2.21) and in this region the scale of the correlation functions R_A and R_S coincides with the scale of correlation of fluctuations in the refractive index. As calculations show [1], the same may occur even for small values of the parameter $k_0 l^2/L_0$. In this case, as can easily be shown, the second addend in formulas (2.27) is small compared with the first and

$$R_{A,S} \simeq k_0^2\,\overline{(\Delta n)^2}\,L_0\,M(\xi,\eta);\qquad M(\xi,\eta) = \int_0^{\infty}\rho(\xi,\eta,\zeta)\,d\zeta\,.$$

Thus, the correlation functions R_A and R_S are identical and differ by the factor 2 from the phase correlation function, obtained for the region $k_0 l^2/L_0 \gg 1$ (see (2.21)). Analogous results are also obtained for $L_1 > L_0$ [15]. It must be noted that these results are obtained only when the correlation function $M(\xi, \eta)$ is a Gaussian function (the inhomogeneities are characterized by a single scale l). Calculations based on the theory of local-isotropic turbulence show the following [2,13]. The correlation of the log of amplitude extends to distances of the order of the scale of the inhomogeneities only on the condition that $\sqrt{\lambda L_1} \ll l_0$ (l_0 is the internal scale of the turbulence), i.e. in the zone of geometrical optics. If $l_0 \ll \sqrt{\lambda L_1} \ll l_m$ (l_m is the external scale of turbulence), the scale of correlation of fluctuations in level is determined by the radius of the first Fresnel zone $\sqrt{\lambda L_1}$.

We shall now find the complex phase correlation function. This function is closely linked with the angular energy spectrum of the scattered field (see section 3). It is easy to show that the complex phase correlation function R_Φ is expressed by R_A and R_S:

$$R_\Phi(\xi, \eta) = \overline{\Phi_1(x, y, L_1)\, \Phi_1(x+\xi, y+\eta, L_1)} = R_A + R_S. \quad (2.28)$$

Using formula (2.18), for the spectrum of the function $R_\Phi(\xi, \eta)$ we get the simple formula:

$$F_A + F_S = \frac{k_0^2}{2} \int_0^\infty F_0(x_1, x_2, \varsigma)\, d\varsigma \int_0^{L_0} C(z)\, dz. \quad (2.29)$$

Hence (or from (2.25)) we find:

$$R_\Phi(\xi, \eta) = R_A + R_S = \frac{k_0^2}{2} \int_0^{L_0} C(z)\, dz \int_0^\infty \rho(\xi, \eta, \varsigma)\, d\varsigma. \quad (2.30)$$

From formula (2.30) it is evident that the scale of the complex phase correlation function $R_\Phi(\xi, \eta)$ is determined by the

transverse scale of the correlation function of the random inhomogeneities $M(\xi,\eta)=\int_0^\infty \rho(\xi,\eta,\zeta)d\zeta$. Moreover, the function $R_\varphi(\xi,\eta)$ does not depend on the distance between the point of observation $z = L_1$ and the edge of the dispersive layer $z = L_0$ [16-18]. Thus, in any plane, parallel to the dispersive layer (screen), the function $R_\varphi(\xi,\eta)$ is the same, in spite of the refraction of scattered waves in the remaining part of the layer with regular variation in the refractive index. Note, finally, that formula (2.29) does not contain the factor $(\varkappa^2/k_0)v(L_1)$, since on adding F_A and F_S (see (2.18)) it is eliminated. Thus, we arrive at an expression for the complex phase correlation function in the form (2.30), which practically coincides (when $l \gg \lambda$) with the value, obtained on the basis of simple calculations within the framework of the ray theory [19] (see 1.10). Formula (2.30), although it does have the character of an approximation of geometrical optics, is applicable when the method of smooth perturbations holds true. Actually this means that when $l \gg \lambda$ a whole series of formulas, obtained by methods of the ray theory, have a wider area of applicability. This relates, for example, to the angular energy spectrum and, consequently, to fluctuations of the angle of arrival of the ray (see section 3).

3. Diffraction of waves at an irregular screen.

The passage of a wave through a layer with random inhomogeneities can be considered as diffraction at an irregular screen. The action of such a screen consists in a plane wave passing through it being modulated with respect to amplitude and phase. The distribution of the field of the wave on leaving the screen depends on the properties of the non-homogeneous layer; the statistical characteristics of this field may be computed, for example, by the methods of the preceding section. A further theoretical problem consists in demonstrat-

ing means of computing the statistical characteristics of the field in the region beyond the screen. The latter are completely determined by the distribution of the field in the plane forming the boundary of the non-homogeneous layer. In this connection we shall sometimes refer below to the non-homogeneous layer as a plane infinitely thin screen.

Suppose that a plane wave of unit amplitude falls on a plane screen, disposed at the level z = 0. Since, generally speaking, the screen changes the amplitude and phase of the incident wave, beyond the screen there is established a certain field distribution f(x,y,0). Below we shall consider the scalar problem; in the case of the diffraction of an electromagnetic field at a one-dimensional screen the component of electric field intensity, parallel to the screen, may serve as the function f(x,y,0).

We shall expand the function f(x,y,0) in the Fourier range :

$$f(x, y, 0) = \int_{-\infty}^{+\infty}\int F(\varkappa_1, \varkappa_2)\, e^{i(\varkappa_1 x + \varkappa_2 y)}\, d\varkappa_1\, d\varkappa_2. \qquad (3.1)$$

Using the formula for manipulating a double Fourier integral, we get :

$$F(\varkappa_1, \varkappa_2) = \frac{1}{(2\pi)^2} \int_{-\infty}^{+\infty}\int f(x, y, 0)\, e^{-i(\varkappa_1 x + \varkappa_2 y)}\, dx\, dy. \qquad (3.2)$$

The field below the screen may be represented in the form of a superposition of plane waves :

$$f(x, y, z) = \int_{-\infty}^{+\infty}\int F(\varkappa_1, \varkappa_2)\, e^{i(\varkappa_1 x + \varkappa_2 y + \varkappa_3 z)}\, d\varkappa_1\, d\varkappa_2, \qquad (3.3)$$

where $\varkappa_3 = \sqrt{k_0^2 - \varkappa_1^2 - \varkappa_2^2}$ $(k_0 = \omega/c)$.

The function $F(\varkappa_1, \varkappa_2)$ is the angular spectrum of the diffracted field.

Thus, knowing the angular spectrum and the phases of the waves of its components, it is possible to find the distribution of

the field in any plane, parallel to the screen.

In the case of a chaotic screen f(x,y,0) is a random function of the variables x,y . Let us determine the correlation function of the complex field

$$\rho_f(\xi,\eta) = \int_{-\infty}^{+\infty} f(x,y) f^*(x+\xi, y+\eta)\, dx\, dy \Big/ \int_{-\infty}^{+\infty} f(x,y) f^*(x,y)\, dx\, dy \quad (3.4)$$

or

$$\rho_f(\xi,\eta) = \overline{f(x,y) f^*(x+\xi, y+\eta)} \Big/ \overline{f(x,y) f^*(x,y)} \quad (3.5)$$

(the line denotes the average with respect to the whole screen). This function describes the statistical properties of a random field in the plane z = 0. It is easy to show that the function $\rho(\xi,\eta)$ is closely connected with the angular energy spectrum [3]. For this purpose, using formula (3.2), we determine the correlation function [20] :

$$\overline{F(\varkappa') F^*(\varkappa'')} = \frac{1}{(2\pi)^4} \int\int\int\int \overline{f(r') f^*(r'')}\, e^{-i(\varkappa' r' - \varkappa'' r'')}\, dr'\, dr''. \quad (3.6)$$

Here $\varkappa$ is a vector with the components $\varkappa_1$ and $\varkappa_2$ and r' is a vector with the components x,y. In formula (3.6) we shall integrate with respect to the variables r = r' - r'' and r'' :

$$\overline{F(\varkappa') F^*(\varkappa'')} = \frac{1}{(2\pi)^4} \int\int\int R(r)\, e^{-i\varkappa' r}\, dr \int\int\int e^{-i r''(\varkappa' - \varkappa'')}\, dr'', \quad (3.7)$$

where it is assumed that the function $R(r) = \overline{f(r')f^*(r'')}$ depends only on the distance between the points r' and r'' : $r = |r' - r''|$. Using the definition of a δ -function, we shall write (3.7) in the form :

$$\overline{F(\varkappa') F^*(\varkappa'')} = \frac{1}{(2\pi)^2} \int\int R(r)\, e^{-i\varkappa' r}\, dr\, \delta(\varkappa_1' - \varkappa_1'')\, \delta(\varkappa_2' - \varkappa_2''). \quad (3.8)$$

Denoting the Fourier-conjugate correlation function of R(r) by $F_0^2(\varkappa_1, \varkappa_2)$, we have :

$$F_0^2(x_1, x_2) = \frac{1}{(2\pi)^2} \int_{-\infty}^{+\infty}\int R(\xi, \eta)\, e^{-i(x_1\xi + x_2\eta)}\, d\xi\, d\eta. \qquad (3.9)$$

Inverting this integral gives :

$$R(\xi, \eta) = \overline{f(x, y) f^*(x+\xi, y+\eta)} = \int_{-\infty}^{+\infty}\int F_0^2(x_1, x_2)\, e^{i(x_1\xi + x_2\eta)}\, dx_1\, dx_2. \qquad (3.10)$$

whence follows, in particular, the relationship :

$$R(0,0) = \overline{|f(x, y)|^2} = \int_{-\infty}^{+\infty}\int \overline{|f(x, y)|^2}\, dx\, dy = \int_{-\infty}^{+\infty}\int F_0^2(x_1, x_2)\, dx_1\, dx_2.$$

Thus, the function $F_0^2(x_1, x_2)$ is the angular energy spectrum of a wave passing through the screen.

Using (3.10) we can also write :

$$\rho_f(\xi, \eta) = R(\xi, \eta)/R(0,0) =$$

$$= \int_{-\infty}^{+\infty}\int F_0^2(x_1, x_2)\, e^{i(x_1\xi + x_2\eta)}\, dx_1\, dx_2 \Big/ \int_{-\infty}^{+\infty}\int F_0^2(x_1, x_2)\, dx_1\, dx_2. \qquad (3.11)$$

Expression (3.9) shows that the correlation function of the complex field and the energy spectrum are Fourier conjugates (Wiener-Hinchin theorem). Note that this relationship holds true only for a screen and a diffraction pattern, the structure of which does not vary with time. For a non-stationary screen the same relationships between the mean correlation function and the mean angular energy spectrum will occur when quasi-static conditions prevail.

For the sake of simplicity we shall also consider that

$$\int_{-\infty}^{+\infty}\int |f(x, y)|^2\, dx\, dy = \int_{-\infty}^{+\infty}\int F_0^2(x_1, x_2)\, dx_1\, dx_2 = 1.$$

Then the functions $\rho_f(\xi, \eta)$ and $F_0^2(x_1, x_2)$ will be Fourier conjugates :

$$\rho_f(\xi, \eta) \longleftrightarrow F_0^2(x_1, x_2). \qquad (3.12)$$

We shall note two evident properties of the correlation function and the angular spectrum. If the grating moves parallel to itself, then $\rho_f(\xi, \eta)$ and, consequently, the angular spectrum do not change. In any plane parallel to the screen and lying far from the screen, the complex amplitude correlation functions are the same and coincide with the correlation function of the complex field at the screen itself. This is evident from the fact that the amplitudes of plane waves in different planes $z = \text{const}$, disposed sufficiently far from the screen, will differ from each other only by a multiplier the modulus of which is equal to unity.

Thus, the angular spectrum is determined by the correlation function of the complex field. We shall write the field as it leaves the screen in the form :

$$f(x, y, 0) = e^{i\Phi(x, y)}, \tag{3.13}$$

where $\Phi(x,y)$ is the variation in complex phase introduced by the non-homogeneous layer (the screen). In the case of diffraction in a non-homogeneous layer of thickness L_0 this function and its statistical characteristics can be found, for example, as they were in section 2 . It is known that if the fluctuations in the dielectric constant are distributed in accordance with a normal law, then the correlation function of the complex field can be written in the form [21] (see also [3]) :

$$\rho_f(\xi, \eta) = e^{R_\Phi(\xi, \eta) - R_\Phi(0,0)}, \tag{3.14}$$

where $R_\Phi(\xi, \eta)$ is the complex phase correlation function. The latter can be determined by the usual method (see formula (2.30)). Thus, knowing the complex phase correlation function, we can easily compute the angular spectrum also.

As an example, we shall consider the concrete case, in which the correlation coefficient of fluctuations $\Delta\varepsilon$ is defined by the

Gaussian function

$$\rho(\xi, \eta, \zeta) = e^{-(\xi^2+\eta^2+\zeta^2)/l^2}. \qquad (3.15)$$

Then, on the basis of (2.30) we can write :

$$R_\Phi(\xi, \eta) - R_\Phi(0,0) = \Phi_m^2 \left[e^{-(\xi^2+\eta^2)/l^2} - 1 \right], \qquad (3.16)$$

where $\Phi_m^2 = R_\Phi(0,0)$ is the mean square fluctuation in the modulus of the complex phase. Now it is also easy to calculate the angular spectrum of a scattered field. For simplicity we shall consider the case of a one-dimensional screen, the properties of which depend only on the coordinate x . In this case the normalized correlation function of the complex field will be equal to

$$\rho_f(\xi, \eta) = e^{\Phi_m^2 (e^{-\xi^2/l^2} - 1)}. \qquad (3.17)$$

If we now take the Fourier conjugate of the function $\rho_f(\xi, \eta)$ then for the angular spectrum we get the expression [3] :

$$F_0^2(x) = \exp\left(-\Phi_m^2\right) \left[\delta(x) + \frac{l}{2\sqrt{\pi}} \sum_{n=1}^{\infty} \frac{\Phi_m^{2n}}{\sqrt{n\,n!}} \exp\left(-\frac{x^2 l^2}{4n}\right) \right], \qquad (3.18)$$

from which it follows that the angular spectrum is composed of an unperturbed wave with the amplitude $\exp(-\Phi_m^2/2)$ and of a large number of side waves. The energy going into the side waves is equal to $1 - \exp(-\Phi_m^2)$. On comparing the energy of the scattered waves with the energy of the unperturbed wave, it is possible to determine the "signal to noise ratio"

$$b = \exp\left[-\Phi_m^2\right] / \left[1 - \exp\left(-\Phi_m^2\right)\right] = \left(e^{\Phi_m^2} - 1\right)^{-1}.$$

For small Φ_m^2 $b \approx \Phi_m^{-2} \gg 1$ and the angular spectrum is composed, basically, of the unperturbed component (mirror-reflected

wave in the case of reflection from an ionospheric screen) and weak side waves. The correlation function of the complex field is then equal to :

$$\rho_f(\xi, \eta) \simeq 1 - \Phi_m^2 [1 - \rho(\xi, \eta)], \qquad (3.19)$$

and, consequently, the scale of the field inhomogenaities coincides with the scale of the non-homogeneous screen structure.

If $\Phi_m^2 \gg 1$, then the "mirror" component is small and the angular spectrum is composed, basically, of side waves. The complex field correlation function (3.16) can now be written approximately in the form (for the region $\xi \gg l$) :

$$\rho_f(\xi, \eta) \simeq \exp\left(-\Phi_m^2 \xi^2/l^2\right). \qquad (3.20)$$

In this case the diffraction pattern becomes finer; its inhomogeneities are Φ_m times less than the scale of the random inhomogeneities of the layer (screen).

In certain cases knowing the correlation function of the complex field enables one to evaluate the correlation function of amplitude $\rho_A(\xi)$. However, for this it is necessary to know the law of amplitude distribution. For example, for a Rayleigh distribution of amplitudes we have the relationship [3] :

$$\rho_{A^2}(\xi) = |\rho_f(\xi)|^2 \simeq \rho_A(\xi).$$

A detailed calculation of the function $\rho_{A^2}(\xi)$ can be found in [22].

Let us consider in greater detail the case $\Phi_m^2 \gg 1$. Since the correlation of the complex field then extends to small distances, the exponent in (3.14) can be expanded in a series. For an isotropic screen we get :

$$\rho_f(r) = \exp\left[\frac{1}{2}\left(\frac{d^2 R_\Phi}{dr^2}\right)_{r=0} r^2\right]. \qquad (3.21)$$

The angular spectrum is found from the formula

$$F_0^2(x_1, x_2) = \frac{1}{(2\pi)^2} \int_{+\infty}^{-\infty} \int \rho_f(\xi, \eta)\, e^{-i(x_1\xi + x_2\eta)}\, d\xi\, d\eta,$$

which, for an isotropic screen, can be written in the form :

$$F_0^2(x) = \frac{1}{2\pi} \int_0^\infty \rho_f(r)\, J_0(xr)\, r\, dr, \qquad (3.22)$$

where J_0 is a Bessel function.

In this case, when $\rho_f(r)$ is described by a Gaussian function, (3.20), the angular spectrum

$$F_0^2(x) = \frac{1}{4\pi a^2} \exp\left(-\frac{x^2}{4a^2}\right), \qquad a^2 = -\frac{1}{2}\left(\frac{d^2 R_\Phi}{dr^2}\right)_{r=0} \qquad (3.23)$$

is Gaussian; the breadth of the spectrum can be determined in the following way:

$$\overline{x^2} = 2\pi \int_0^\infty F_0^2(x)\, x^3\, dx = \frac{1}{2a^2} \int_0^\infty \exp\left(-\frac{x^2}{4a^2}\right) x^3 dx = 4a^2 = -2\left(\frac{d^2 R_\Phi}{dr^2}\right)_{r=0}. \qquad (3.24)$$

This quantity characterizes fluctuations in the angle of arrival of a ray.

In conclusion it is interesting to note the following: Feijer [23] solved the problem of the diffraction of waves in an extended layer by another method. It is possible to divide the medium into a number of layers and consider the effect of each one in succession. Of course, in this problem the effect of multiple wave-scattering is taken into account. However, it appears that the solution obtained by Feijer coincides with the solution obtained by Fourier transformation of formula (3.14), where the correlation function of the complex phase $R_\Phi(\xi, \eta)$ is found from the simple formulas of geometrical optics [24]. The fact that calculations based on the approximation

of geometrical optics give a good result is understandable, if one takes into account that, although it also has the character of an approximation of geometrical optics, formula (2.30) for the function $R_\varphi(\xi, \eta)$ (and the angular spectrum) has a wider area of applicability, not limited by the condition $\lambda L \ll$ [illegible] ^{2} (see end of section 2).

4. Scattering of waves at weak inhomogeneities

In many problems of wave propagation in media with fluctuating parameters it is required to find the intensity of the scattered radiation or the effective diameter of scatter. Ordinarily this problem is solved by the method of perturbations. If the scattered field is small and it is possible to neglect secondary scattering, then the total field at a sufficiently great distance R from the scatter region can be represented as the sum of the scattered waves:

$$E = \frac{E_0 k_0^2 \sin \chi}{4\pi R} \int_V \Delta\varepsilon \, e^{i\psi} \, dV . \qquad (4.1)$$

Here E_0 is the amplitude of the primary field, $\Delta\varepsilon$ is the fluctuational deviation of the dielectric constant from the mean, χ is the angle between the vector E_0 and the direction of propagation of the scattered wave.

Now let a plane wave fall on the scattering volume V . If it is not plane, it is possible to resolve it into a sum of plane waves and take one component. At a great distance from the scattering volume the front of the scattered spherical waves can be considered plane. Scattered waves with different directions of the wavefront arrive at the point where the receiver is located. These waves are summed at the output of the receiving device within the limits of its directional diagram. To find the total effect we shall first compute the energy of the scattered wave with a definite direction of wavefront; then we shall find the total effect. In this case we

I shall consider the wave vector of the scattered wave k to be fixed and the quantity Ψ in formula (4.1) will represent the phase difference between two plane waves with wave vectors k_0 (wave E_0) and k (wave E) :

$$\Psi = (k_0 - k)\, r = K r.$$

Here r is the radius vector, $K = k_0 - k$, $|k| = |k_0| = \omega/c$ and, consequently,

$$|K| = 2 k_0 \sin(\vartheta/2), \tag{4.2}$$

where ϑ is the angle between the vectors k_0 and k, i.e. the angle of scatter.

Now we can write the field of the scattered wave in the form

$$E = \frac{E_0 k_0^2 \sin\chi}{4\pi R} \varepsilon_k. \tag{4.3}$$

Here ε_k is the expansion as a triple Fourier integral of the function $\Delta\varepsilon(x,y,z)$:

$$\varepsilon_k = \int_V \Delta\varepsilon(x, y, z)\, e^{iKr}\, dV. \tag{4.4}$$

The quantity ε_k is a function of K_x, K_y, K_z, i.e. depends on the angle of scatter.

We turn now to a solution of the statistical problem. In this case the function ε_k is not known. Ordinarily the correlation function of $\Delta\varepsilon$ is considered known :

$$\overline{\Delta\varepsilon(r_1)\,\Delta\varepsilon(r_2)} = \overline{(\Delta\varepsilon)^2}\, \rho(|r_1 - r_2|). \tag{4.5}$$

Since, moreover, we shall assume the isotropism of the statistical properties of the medium, the function $\rho(r)$ is taken in spherically symmetrical form. Ordinarily the solution of the statistical problem comprises finding the mean squares of the field. From (4.3) we get

$$\overline{E^2} = \frac{E_0^2 k_0^4 \sin^2\chi}{(4\pi)^2 R^2}\, \overline{\varepsilon_k^2}. \tag{4.6}$$

On the basis of (4.4) we then have :

$$\overline{\varepsilon_k^2} = \int_{V_1}\int_{V_1} \overline{\Delta\varepsilon(r_1)\,\Delta\varepsilon(r_2)}\, e^{iK(r_1 - r_2)}\, dV_1\, dV_2 . \qquad (4.7)$$

If in (4.7) we change to the variables x_1, y_1, z_1 and if $\xi = x_1 - x_2$; $\eta = y_1 - y_2$; $\zeta = z_1 - z_2$, then, integrating with respect to x_1, y_1, z_1, we get:

$$\overline{\varepsilon_k^2} = \overline{(\Delta\varepsilon)^2}\, V \int_{-\infty}^{+\infty}\int\int \rho(r)\, e^{iKr}\, d\xi\, d\eta\, d\zeta . \qquad (4.8)$$

In (4.8) the limits of integration are extended to infinity, since $\rho(r)$ decreases in a smaller radius than $V^{1/3}$.

Formula (4.8) is a solution of the problem posed. It is possible to give it a somewhat different form on the basis of the spherical symmetry of $\rho(r)$. We shall take a spherical system of coordinates with the axis directed along K . Then

$$\overline{\varepsilon_k^2} = \overline{(\Delta\varepsilon)^2}\, V \int_0^{\infty}\int_0^{\pi}\int_0^{2\pi} \rho(r)\, e^{iKr\cos\vartheta}\, r^2 \sin\vartheta\, dr\, d\vartheta\, d\varphi . \qquad (4.9)$$

Integrating with respect to ϑ and φ, we get :

$$\overline{\varepsilon_k^2} = 4\pi V \overline{(\Delta\varepsilon)^2} \int_0^{\infty} \rho(r)\, r^2\, \frac{\sin(Kr)}{Kr}\, dr . \qquad (4.10)$$

Finally, the intensity of the scattered field will be equal [25-27] to

$$\overline{E^2} = \frac{E_0^2 k_0^4 V\, \overline{(\Delta\varepsilon)^2} \sin^2 Z}{4\pi R^2} \int_0^{\infty} \rho(r)\, r\, \frac{\sin(Kr)}{K}\, dr . \qquad (4.11)$$

It is usual to introduce into the theory of scattering the effective diameter of scatter σ , which is equal to the energy flux, scattered by a unit volume within a unit solid angle, related to the energy flux in the primary wave. According to (4.11),

$$\sigma = \frac{\overline{E^2}}{E_0^2}\frac{R^2}{V} = \frac{k_0^4\,\overline{(\Delta\varepsilon)^2}\sin^2\chi}{4\pi}\int_0^\infty \rho(r)\,r^2\,\frac{\sin(Kr)}{Kr}\,dr. \qquad (4.12)$$

Formulas (4.11) and (4.12) solve the problem posed, reducing it to a quadrature. Calculations with concrete $\rho(r)$ functions are well known (see for example [4]) and we shall not dwell on this point here.

Of course, the solution thus obtained holds true when the mean value of the refractive index is close to unity. Meanwhile, we frequently encounter the problem of the scattering of waves in a medium, the average parameters of which vary. In these circumstances it is necessary to take into account refraction of the scattered waves. It appears that the exposition given above can easily be generalized to include the case of a medium with smoothly varying average properties [28]. If the properties of the medium vary with respect to the height z, then the mean square of the scattered field will be defined by the following formula, analogous to (4.11):

$$\overline{E^2} = \frac{E_0^2 k_0^4 V\,\overline{(\Delta\varepsilon)^2}\sin^2\chi(z)}{4\pi}\,\frac{d\Omega(z)}{ds_0}\int_0^\infty \frac{\sin[K(z)r]}{K(z)}\,\rho(r)\,r\,dr. \qquad (4.13)$$

Here it is assumed that the scattering volume is at level z and that the primary wave is plane ($d\Omega(z)$ is the solid angle of the beam at the point of scattering, ds_0 is the area, normal to the ray, on which the beam bears on leaving the non-homogeneous layer). Note moreover, that in formula (4.13) the quantities χ, the angle between the vector E_0 for the unperturbed wave and the scattered wave (k') at the level z and $K = |(k - k')| = 2k\sin(\vartheta/2)$ (ϑ is the angle between the vectors k and k' at the level z) depend on z. In calculating the scattering of a spherical wave it is necessary to take into account the spread in the beam of the fundamental wave [28,29].

The solutions obtained are still insufficient to determine the

mean intensity of a signal received by some antenna device. Generally speaking, in calculating the average characteristics of a signal it is necessary to take into account the effect of the antenna directional diagram [30,31]. Here we have a complete analogy with the phenomenon of the passage of noise through a filter. In the case of scattering the role of the resonance characteristic is played by the antenna directional diagram.

Formula (4.11) gives the mean square of the amplitude of a wave, scattered in a given direction. In the case of a high-directional antenna this solution is sufficient. In fact, let the receiving device have a directional diagram $g(\Omega)$, where Ω is a solid angle. Waves, scattered in different directions, are not correlated and, consequently, the total energy received by the antenna, taking into account its directional diagram, will be equal to

$$\overline{E_n^2} = \int \overline{E_\vartheta^2}\, g(\Omega)\, d\Omega. \qquad (4.14)$$

Further, by assuming the function $g(\Omega)$ considerably narrower than the scattering diagram (antenna with a large gain), it is possible to take $\overline{E_\vartheta^2}$ out from under the integral sign:

$$\overline{E_n^2} = \overline{E_{\vartheta^*}^2} \int g(\Omega)\, d\Omega = \overline{E_{\vartheta^*}^2}\, g(\Omega^*)\, \Delta\Omega. \qquad (4.15)$$

Here ϑ^* is the direction of maximum radiation of the antenna and $\Delta\Omega$ is the effective width of its directional diagram. Then $\overline{E_\vartheta^2}$ is given by formula (4.11), where the value of ϑ is so chosen that the direction of scatter coincides with the axis of the directional diagram.

If it is not assumed in advance that the function $g(\Omega)$ is sharper than $\overline{E_\vartheta^2}$, then on the basis of (4.6), (4.7) and (4.14) we get for $\overline{E_n^2}$:

$$\overline{E_n^2} = \frac{E_0^2 k_0^4 V}{(4\pi)^2 R^2} \overline{(\Delta\varepsilon)^2} \sin^2\chi \int_\Omega \int_V \varphi(r)\, g(\Omega)\, e^{iKr}\, dV d\Omega; \qquad (4.16)$$

When the function $g(\Omega)$ displays axial symmetry it is possible to perform one integration in (4.16).

Let us compute the integral

$$I = \int_{\Omega} e^{iKr} g(\Omega)\, d\Omega .$$

For this purpose we shall put the vector K in the form

$$K = K_0 + K_1 ,$$

where K_c is the difference between the wave vector of an unperturbed wave and the wave vector of a wave scattered along the axis of symmetry of the antenna directional diagram. Thus, the end of the vector K_o lies on the axis of symmetry of the antenna.

For an antenna with a narrow directional diagram ($a \gg \lambda$) it is possible to take the vector K_1 perpendicular to the antenna axis. Introducing the angles ϑ and φ of a spherical system of coordinates with the axis directed along the axis of symmetry of the antenna and the center at its point of location, we find :

$$I = e^{iK_0 r} \int e^{iK_1 r} g(\Omega)\, d\Omega = e^{iK_0 r} \int_0^{2\pi}\int_0^{\pi} g(\vartheta)\, e^{iK_1 r_\perp \cos\varphi} \sin\vartheta\, d\vartheta\, d\varphi .$$

Here $r_\perp$ is the projection of r on a plane normal to the axis of the antenna. After integration with respect to φ we have :

$$I = e^{iK_0 r} 2\pi \int_0^{\pi} g(\vartheta) \sin\vartheta\, J_0(K_1 r_\perp)\, d\vartheta .$$

The vector K_1 represents the difference between the wave vectors of the scattered waves along the antenna axis and with respect to an arbitrary direction (within the limits of the directional diagram). In virtue of this

$$|K_1| = 2K_0 \sin(\vartheta/2),$$

where ϑ is the angle read from the antenna axis. Putting $\sin\vartheta \approx \vartheta$ for a high-directional antenna, we finally have :

$$I = e^{i\kappa_0 r} 2\pi \int_0^{\infty} g(\vartheta)\,\vartheta J_0(k_0\,\vartheta\, r_\perp)\,d\vartheta = e^{i\kappa_0 r}\,\Phi(r_\perp).$$

In the last integral the upper limit may be put equal to infinity. Thus, the function $\Phi(r_\perp)$ is equal to:

$$\Phi(r_\perp) = 2\pi \int_0^{\infty} g(\vartheta)\,\vartheta\, J_0(k_0\,\vartheta\, r_\perp)\,d\vartheta\,. \qquad (4.17)$$

Subsituting the result of the computations in (4.16), we find that

$$\overline{P_n^2} = \frac{E_0^2 k_0^4 V}{(4\pi)^2 R^2}\,\overline{(\Delta\varepsilon)^2}\sin^2\chi \int_V p(r)\,\Phi(r_\perp)\,e^{i\kappa_0 r}\,dV\,. \qquad (4.18)$$

It follows from expression (4.17) that the function $\Phi(r_\perp)$ is a Fourier-Bessel conjugate of the function $g(\vartheta)$, the square of the modulus of the antenna directional diagram. In its turn the antenna directional diagram is a Fourier-Bessel conjugate of the function f(r), which represents the amplitude distribution of the oscillations along the antenna radius. On the basis of the properties of a Fourier-Bessel transformation it is possible to express a function, which is the Fourier-Bessel conjugate of the square of the modulus of a function, as a conjugate of the same function, allying the function $\Phi(r_\perp)$ itself and f(r). Such a link between functions conjugate in the Fourier sense is a contraction, i.e. the integral of the product of these functions, considered as the displacement function of one of them. For functions, conjugate in the Fourier-Bessel sense, there is an analogous relationship, employing which gives us:

$$\Phi(k_0 r_\perp) = \frac{k_0^2}{2\pi}\int_0^{\infty}\int_0^{2\pi} f(k_0 r) f\left(\sqrt{k_0^2 r_\perp^2 + k_0^2 r^2 + 2k_0^2 r_\perp r\cos\vartheta}\right) r\,dr\,d\vartheta, \qquad (4.19)$$

Like an ordinary contraction, expression (4.19) is an integral of the product of two functions, one of which is displaced with

respect to the other by the distance $r_\perp$. If the size of the antenna is limited by a maximum radius a , then, when $r_\perp$ is greater than a , neither of the functions has a common point, in virtue of which $\Phi(k_0 r_\perp) = 0$ when $r_\perp$ is greater than a . In this case we shall get the field described by (4.14), only when $\rho(r)$ decreases considerably in the distance a . Otherwise we get a field described by a function without spherical symmetry and in this case it is impossible to carry out the transformation leading to the quadrature of (4.17).

Together with (4.19) formula (4.18) is a general expression for the intensity of fluctuations, applicable for any shape of antenna directional diagram with axial symmetry.

The case of a high-directional antenna system, which we discussed above, can be obtained as a consequence of (4.18) on condition that the function $\rho(r)$ varies rapidly compared with $\Phi(r_\perp)$. For this it is necessary that the transverse dimensions of the antenna system considerably exceed the magnitude of the correlation radius of the random inhomogeneities l . Thus, the condition $a \gg \lambda$ still does not give us the right to consider the antenna high-directional and use formula (4.15) for calculating the intensity of the fluctuations. It is necessary that the directionality of the antenna be considerably sharper than the angular spectrum of scattering, which boils down to the condition $a \gg l$.

Expression (4.18) also yields a formula for the other extreme case, namely, for the case of a point, nondirectional receiver. Generally speaking, this approximation is useful when the function $\Phi(r_\perp)$ decreases considerably more rapidly than the function $\rho(r)$. This occurs when the size of the inhomogeneities (correlation radius l) is much greater than the dimensions of the antenna. In this case in (4.18) we can carry out the integration with respect to $r_\perp$, assuming that only Φ is dependent on this coordinate, while $\rho(r)$

can be considered constant over the whole interval of integration with respect to $r_\perp$. In this case the integration of (4.18) can be carried out using (4.17) and the inversion formula for a Fourier-Bessel transformation. Then:

$$\overline{E_n^2} = \frac{\overline{E_0^2}\, k_0^4\, V\, g(\vartheta_0)}{(4\pi)^2 R^2 \quad k_0^2} \int_0^\infty \rho(z, 0)\, dz. \qquad (4.20)$$

Here ϑ_0 is the angle between the direction of the unperturbed wave and the antenna axis. The coordinate z is taken along the antenna axis.

Expression (4.20) can be put in a form corresponding to the formulas obtained by Obukhov [12]. For this it is sufficient to put $\vartheta_0 = 0$ (scattering at an angle coinciding with the direction of propagation of the wave) and the scattering volume V into the form:

$$V = z\pi (R\vartheta)^2, \qquad (4.21)$$

where ϑ is the span of the antenna directional diagram and z is the linear dimension of the scattering volume along the direction of propagation. We then get the following expression:

$$\overline{E_n^2} = \frac{\overline{E_0^2}\, k_0^2\, z\vartheta}{16\pi} \int_0^\infty \rho(z, 0)\, dz. \qquad (4.22)$$

Thus, the reasoning leading to formula (4.18) enables us to look at the two approaches to scattering phenomena from a single point of view; one of these approaches, discussed in the work of Obukhov [12], Chernov [1] and certain other authors, considers fluctuations at a certain point in the wavefront and the second, discussed in works on the scattering of radio waves [23], aims at a solution of the problem of the intensity of scattering in a given direction. It appears that the applicability of one or the other of these approaches to the solution of a concrete problem of the

fluctuations picked up by a receiver depends on the relationship between the directional diagram of the receiving device and the spatial spectrum of scattering at inhomogeneities.

Bibliography

1. Chernov, L.A.: Rasprostraneniye voln v srede so sluchaynymi neodnorodnostyami (Propagation of waves in a medium with random inhomogeneities), Publ. AS USSR, M., 1958.
2. Tatarskiy, V.I.: Flyuktuatsionnye yavleniya pri rasprostraneniyi voln v turbulentnoy atmsofere (Fluctuation phenomena in the propagation of waves in a turbulent atmosphere), Publ. AS USSR, M., 1959.
3. Ratcliff, D.Zh.: Nekotorye voprosy teorii diffraktsii i ikh primeneniye k ionosfere (Some questions in the theory of diffraction and their application to the ionosphere), Problems of modern physics, 10 (1957) 5.
4. Vysokovskiy, D.M.: Nekotorye voprosy dal'nevo troposfernovo rasprostraneniya ul'trakorotkikh radiovoln (Some questions relating to the long-range tropospheric propagation of ultra-short radiowaves), Publ. AS USSR, M., 1958.
5. Al'pert, Ya.L.: Nekotorye voprosy fiziki ionosfery. Flyuktuatsii elektronnoy plotnosti i rasseyaniye radiovoln (Some questions of ionospheric physics. Fluctuations in electron density and the scattering of radiowaves), UFN, 61 (1957) 423.
6. Chernov, L.A.: Rasprostraneniye zvuka v statisticheski neodnorodnoi srede (Propagation of sound in a statistically inhomogeneous medium), ZhETF, 24 (1953) 210.
7. Scheffler, H: Strahlenoptische Ausbreitung in Medien mit statistisch verteilten Inhomogenitaten (I. Unregelmassige Refraktion als Markoff-Prozess), Astr. Nachr. 284 (1958) 227; II. Streuung in kleine Winkelbereiche, Astr. Nachr. 284 (1959) 269. (Ray propagation in media with statistically distributed inhomogeneities. (I. Irregular refraction as the Markoff process). II. Small-angle scattering.
8. Denisov, N.G.: O rasprostraneniyi voln v ploskosloistoy srede, soderzhashchey statisticheskiye neodnorodnosti (On the propagation of waves in a plane-stratified medium containing statistical inhomogeneities), Radiofizika, 1 (1958) 5-6, 34.
9. Chandrasekhar, S.: A statistical basis for the theory of stellar scintillation, Monthly not. Roy. Astr. Soc., 112 (1952) 475.
10. Tatarskiy, V.I.: O kriterii primenimosti geometricheskoi optiki v zadachakh o rasseyaniyi voln v srede so statisticheskimi neodnorodnostyami pokazatelya prelomleniya (On the criterion for the

applicability of geometric optics to problems on the scattering of radiowaves in a medium with statistical inhomogeneities of the refractive index), ZhETF 25 (1953) 84.
11. Rytov, S.M.: Diffraktiya sveta na ul'trazvukovykh volnakh (Diffraction of light in ultrasonic waves), Trans. AS USSR, Phys. Ser. 2 (1937) 223.
12. Obukhov, A.M.: Vliyaniye neodnorodnostey atmosfery na rasprostraneniye zvuka i sveta (Effect of atmospheric inhomogeneities on the propagation of sound and light), Trans. AS USSR, Geograph. and Geophys. Ser. 2 (1953) 155.
13. Tatarskiy, V.I.: O pulsatsiyakh amplitudy i fazy volny, rasprostranyayushcheysya v slabo neodnorodnoy atmosfere (On pulsations of phase and amplitude in a wave propagated in a slightly inhomogeneous atmosphere), Rep. AS USSR, 107 (1956) 245.
14. Tatarskiy, V.I.: O rasprostraneniyi voln v lokal'no izotropnoy turbulentnoy srede s plavno menyayushchimisya kharakteristikami (Propagation of waves in a locally isotropic turbulent medium with smoothly varying characteristics), Rep. AS USSR 120 (1958) 289.
15. Krotova, A.A.: Diffraktsiya v sloye so sluchaynymi neodnorodnostyami (Diffraction in a layer with random inhomogeneities), Sci. Notes of the Chitinskiy Ped. Institute, 2 (1958) 39.
16. Scheffler, H.: Astronomische Szintillation und atmospharische Turbulenz (Astronomical scintillation and atmospheric turbulence), Astr. Nachr. 282 (1956) 193.
17. Scheffler, H: Bemerkung zur Theorie der astron. Sicht (Note on the theory of astron. visibility), Astr. Nachr. 283 (1956) 87.
18. Denisov, N.G.: O flyuktuatsiyakh amplitudy i fazy volny, proshedshey cherez sloy so sluchaynymi neodnorodnostyami (On fluctuations in amplitude and phase in a wave passing through a layer with random inhomogeneities), Radiofizika, 2 (1959) 316.
19. Scheffler, H.: Streuung von Radiowellen in der Sonnenkorona und die Mitte-Rand-Variation der ruhigen solaren Meterwellenstrahlung (Scattering of radiowaves in the solar corona and the center-edge variation in stationary solar meter wave radiation), Zeit. f. Astrophys. 45 (1958) 113.
20. Rytov, S.M.: Teoriya elektricheskikh flyuktuatsiy i teplovovo izlucheniya (Theory of electric fluctuations and thermal radiation), Publ. AS USSR, M., 1953, 25.
21. Keller, G.: Astronomical "seeing" and its relation to atmospheric turbulence, Astr. J. 58 (1953) 113.
22. Pisareva, V.V.: O diffraktsii radiovoln na khaoticheskikh neodnorodnostyakh i kolebaniya intensivnosti solnechnovo i kosmicheskovo radioizlucheniya (Diffraction of radiowaves at chaotic inhomogeneities and fluctuation in the intensity of solar and cosmic radiation), Astron. Zh. 35 (1958) 112.

23. Feijer, J.A.: The diffraction of waves in passing through an irregular refracting medium, Proc. Roy. Soc., A220 (1953) 459.
24. Bremley, E.N.: The diffraction of waves by an irregular refracting medium, Proc. Roy. Soc., A225 (1954) 515.
25. Pekeris, C.L.: Note on the scattering of radiation in an inhomogeneous medium, Phys. Rev. 71 (1947) 268.
26. Booker, H.G.; Gordon, E.: A theory of radio scattering in the troposphere, Proc. IRE 38 (1950) 401.
27. Villars, F.; Weisskopf, V.F.: The scattering of electromagnetic waves by turbulent atmospheric fluctuations, Phys. Rev. 94 (1954) 232.
28. Denisov, N.G.: Rasseyaniye voln v ploskoslоistoy srede (Scattering of waves in a plane-stratified medium), Radiofiz. 1, 5-6, (1958) 41.
29. Benediktov, E.A.; Mityakov, N.A.: O rasseyaniyi radiovoln v ionosfere (Scattering of radiowaves in the ionosphere), Radiofiz. 2 (1959) 3.
30. Zverev, V.A.: Vliyaniye napravlennosti priemnovo ustroistva na srednyuyu intensivnost' signala, prinimayemovo za schet rasseyaniya (Effect of the directionality of the receiving device on the mean intensity of a signal, received on account of scattering), Akustich. Zh. 3 (1957) 329.
31. Wheelon, A.D.: Relation of radiomeasurements to the spectrum of tropospheric dielectric fluctuations, J. Appl. Phys. 28 (1957) 684.

Radiophysics Research Institute
Gor'kiy University

Submitted 15 June 1959.

DISTORTION OF RADIOWAVES PROPAGATED IN THE IONOSPHERE

Pages 543-552

by I.M. Vilenskiy & N.A. Zykova.

A discussion is offered on nonlinear distortions of the modulation of a wave propagated in the ionosphere. The calculating technique employed makes it possible to consider such distortions for arbitrary modulation frequencies. Numerical values for the nonlinear distortions are derived.

1. The question of the distortion of a powerful radiowave propagated in the ionosphere has been discussed in [1]. It was shown that if a radiowave, modulated with respect to amplitude with a frequency Ω, is propagated in the ionosphere, then the non-linearity of the ionosphere leads to an increase (compared with the linear case) in the coefficient of absorption of the wave, to a variation in the depth of the fundamental tone of amplitude modulation, to the appearance of overtones (2Ω, 3Ω) of amplitude modulation, to a change in the phase of the wave, the phenomenon of phase modulation (the periodic frequency terms Ω, 2Ω come into the expression for phase) and to the appearance of overtones of the carrier frequency. The following technique was used in making the calculations: the kinetic equations were used to compute the current produced in the ionosphere by the radiowave and the expression obtained was substituted in the wave equation. Both the kinetic equations and the wave equation were solved by the method of successive approximations. The non-linearity was taken into account in the first

approximation. Only collisions between electrons and neutral molecules were taken into account, as it had previously been shown (see, for example, [2,3]) that collisions between electrons and ions and electrons and electrons play an inconsiderable part in nonlinear effects.

[1] gives expressions for nonlinear distortions only for the case of high and low modulation frequencies, as the kinetic equations are easily solved only in these extreme instances.

On the other hand, we know (see [2], for example) that, while taking into account only collisions between electrons and neutral molecules, we can achieve sufficient accuracy by using merely the so-called elementary theory, in which it is assumed that all the electrons move with a certain common velocity (distribution of electrons with respect to velocity is disregarded). The advantage of the elementary theory is that with its help it is easily possible to get expressions for nonlinear distortions for any modulation frequency.

2. In this article we shall proceed in the following manner: with the help of the elementary theory we shall compute the current produced in the ionosphere by the action of a powerful radiowave and then, just as in [1], and with the same approximation, we shall solve the wave equation. For the sake of simplicity we shall consider the case of the vertical incidence of a wave on a homogeneous layer and we shall restrict ourselves to calculating the nonlinearity merely as a first approximation*. We shall neglect the Earth's magnetic field.

---

* This leads to a result which does not hold for very large values of the field intensity in the ionosphere. Gurevich [4] has dealt with nonlinear distortions for arbitrary values of the field intensity. He also showed that for broadcast stations of a power of 200 kilowatts or less taking the non-linearity as a first approximation gives sufficiently accurate results.

Here we shall only consider changes due to the fundamental carrier and we shall not touch on the question of the overtone 3ω due to the non-linearity of the medium, since this question has been discussed in [1] using the kinetic theory and the elementary theory does not add anything on this point.

Let there fall on the ionosphere an amplitude-modulated radiowave with a field, which, at the lower boundary of the ionosphere, may be written in the form:

$$E = E_0 (1 + M \cos \Omega t) \cos (\omega t - \varphi) = E_{10} \cos (\omega t - \varphi), \qquad (1)$$

where ω is the circular carrier frequency, Ω is the modulation frequency ($\Omega \ll \omega$) and M is the modulation depth.

This wave causes changes in the velocities of the electrons and, accordingly, in the number of collisions between electrons and molecules. The magnitude of these changes is easily obtained from a consideration of the energy balance of an electron, acquiring energy from the wave and losing it in collisions [2]:

$$\frac{d}{dt}\left(\frac{mv^2}{2}\right) + \delta \frac{mv^2}{2} \nu_{eff} = e (\dot{r}E), \qquad (2)$$

where δ is the mean relative fraction of the kinetic energy of the electron lost in collision with a molecule. In elastic impact $\delta = \delta_{el} \cong 2m/\mu$, but ordinarily, as experiments have shown, $\delta \gg \delta_{el}$; $\nu_{eff} = v/l$ is the effective number of collisions, l is the length of the free run, which we consider as not depending on the velocity, $\dot{r}$ is the ordered electron velocity. The latter is easily found from the equation of motion (disregarding the Earth's magnetic field):

$$m\ddot{r} + m\nu_{eff}\dot{r} = eE. \qquad (3)$$

Assuming that δ is independent of ν_{eff} (or considering $\delta = \delta_0(1 - \nu_{eff}^2/\nu_1^2)$, where ν_1 is the value of ν_{eff} corresponding to thermal equilibrium) and bearing in mind that the change in the

effective number of collisions under the influence of an external field is small ($\Delta \nu_{eff} \ll \nu_{eff}$), taking into account (1) and making use of the known solution of equation (3), we get from (2) :

$$\nu_{э\phi\phi} = \nu_0 + \Delta \nu_{э\phi\phi}; \quad \Delta \nu_{э\phi\phi} = \Delta \nu_0 + \Delta \nu^{(\Omega)} + \Delta \nu^{(\omega)}; \tag{4}$$

$$\Delta \nu_0 = \frac{e^2 E_0^2 (1 + M^2/2) \nu_0}{2\delta v^2 m^2 (\omega^2 + \nu_0^2)}; \tag{5}$$

$$\Delta \nu^{(\Omega)} = \nu_0 \left[M_1 \cos (\Omega t - \varphi_1) + M_2 \cos (2\Omega t - \varphi_2) \right] E_0^2;$$

$$M_1 = \frac{e^2 \nu_0 M}{m^2 v^2 (\omega^2 + \nu_0^2) \sqrt{\Omega^2 + (\delta \nu_0)^2}};$$

$$M_2 = \frac{e^2 \nu_0 M^2}{4 m^2 v^2 (\omega^2 + \nu_0^2) \sqrt{4\Omega^2 + (\delta \nu_0)^2}}; \tag{6}$$

$$\operatorname{tg} \varphi_1 = \Omega / \delta \nu_0; \qquad \operatorname{tg} \varphi_2 = 2\Omega / \delta \nu_0;$$

$$\Delta \nu^{(\omega)} = - A \cos (2\omega t + \varphi); \qquad \operatorname{tg} \varphi = \nu_0 / \omega;$$

$$A = \frac{e^2 E_0^2 (1 + M \cos \Omega t)^2 \nu_0}{4 m^2 v^2 \omega (\omega^2 + \nu_0^2)^{1/2}}, \tag{7}$$

where $\nu_0 = \pi a^2 N_m \overline{v}$ is the value of ν_{eff} when E = 0. In writing equations (4) - (7) we reckoned that $\Omega \ll \omega$.

If we consider that $|\Delta \nu^{(\Omega)}| \ll \nu_0$ и $|\Delta \nu^{(\omega)}| \ll |\Delta \nu^{(\Omega)}|$*, and if we are not interested in the amplitude of the carrier overtone 3ω due to the non-linearity of the medium, then it is possible to neglect the term $\Delta \nu^{(\omega)}$, as we shall do below.

Making use of known formulas for the conductance and the specific inductive capacitance:

$$\sigma = \frac{e^2 N \nu_{э\phi\phi}}{m (\omega^2 + \nu^2_{э\phi\phi})_{eff}}; \quad \varepsilon = 1 - \frac{4\pi e^2 N}{m (\omega^2 + \nu^2_{э\phi\phi})_{eff}} = 1 - \frac{\omega_0^2}{\omega^2 + \nu^2_{э\phi\phi}}, \tag{8}$$

* Actually, is of the same order when $\varphi \to 0$ and of the order of $\Omega / \nu_0 \ll 1$ for high Ω, when $\Omega \gg \delta \nu_0$.

where N is the number of electrons in 1 cm^3. ν_{eff} in (8) should be understood as the value of this quantity, determined from formulas (4) - (6). Then clearly, we can write:

$$\sigma \simeq \frac{e^2 N (\nu_0 + \Delta \nu_{eff})}{m (\omega^2 + \nu_0^2 + 2\nu_0 \Delta \nu_{eff})} \simeq \sigma_0 + \sigma_0 \frac{\Delta \nu_{eff}}{\nu_0} \frac{\omega^2 - \nu_0^2}{\omega^2 + \nu_0^2},$$

$$\varepsilon \simeq 1 - \frac{\omega_0^2}{\omega^2 + \nu_0^2 + 2\nu_0 \Delta \nu_{eff}} \simeq \varepsilon_0 + \frac{2\omega_0^2 \nu_0 \Delta \nu_{eff}}{(\omega^2 + \nu_0^2)^2}; \quad (9)$$

$$\sigma_0 = \frac{e^2 N \nu_0}{m (\omega^2 + \nu_0^2)}; \quad \varepsilon_0 = 1 - \frac{\omega_0^2}{\omega^2 + \nu_0^2}.$$

We shall now consider the expression for the density of the total ionospheric current (see [2], for example):

$$j = E_{10} \left[\sigma \cos(\omega t - \xi) - \frac{\omega}{4\pi} (\varepsilon - 1) \sin(\omega t - \xi)\right] =$$

$$= E_{10} \left[\sigma_0 \cos(\omega t - \xi) - \frac{\omega}{4\pi} (\varepsilon_0 - 1) \sin(\omega t - \xi)\right] + \quad (10)$$

$$+ E_{10}^2 \sigma_1 [\cos(\omega t - \xi) - a \sin(\omega t - \xi)],$$

where

$$\sigma_1 = \sigma_0 \frac{\omega^2 - \nu_0^2}{(\omega^2 + \nu_0^2)(1 + M \cos \Omega t)^2} \left[\frac{e^2 (1 + M^2/2)}{2\delta m^2 v^2 (\omega^2 + \nu_0^2)} + \right.$$

$$\left. + M_1 \cos(\Omega t - \varphi_1) + M_2 \cos(2\Omega t - \varphi_2)\right]; \quad (11)$$

$$a = \frac{\omega}{4\pi} \frac{2\omega_0^2 \nu_0^2}{(\omega^2 + \nu_0^2)(\omega^2 - \nu_0^2)\sigma_0} = \frac{2\omega\nu_0}{\omega^2 - \nu_0^2}.$$

The quantities E_{10} and ξ in formula (10) must be considered as still unknown functions of the coordinates. If we take the case of vertical incidence of the wave on the layer, then denoting the

corresponding coordinate by z and counting it upwards from the beginning of the layer, at the boundary of which z = 0, we may write:

$$E_{10} = E_0(z)\,[1 + M\cos(\Omega t)]; \qquad \xi = \xi(z).$$

As we know [2], for the case of normal incidence of the wave on the layer, in the absence of the Earth's magnetic field, the wave equation has the form:

$$\frac{\partial^2 E_{10}}{\partial z^2} - \frac{1}{c^2}\frac{\partial^2 E_{10}}{\partial t^2} - \frac{4\pi}{c^2}\frac{\partial j}{\partial t} = 0, \tag{12}$$

where E_{10} and j are to be understood as projections of the vectors E_{10} and j either on the x-axis or on the y-axis. Using formula (10) for j and collecting terms with $\sin(\omega t - \xi)$ and $\cos(\omega t - \xi)$, we get:

$$\begin{aligned} &\frac{d^2E_{10}}{dz^2} - E_{10}\left[\left(\frac{d\xi}{dz}\right)^2 - \frac{\omega^2}{c^2}\varepsilon_0\right] + \frac{4\pi\omega}{c^2}\,a\,\sigma_1 E_{10}^3 = 0; \\ &2\frac{dE_{10}}{dz}\frac{d\xi}{dz} + E_{10}\frac{d^2\xi}{dz^2} + \frac{4\pi\omega}{c^2}\sigma_0 E_{10} + \frac{4\pi\omega}{c^2}\sigma_1 E_{10}^3 = 0. \end{aligned} \tag{13}$$

As in [1], we shall solve system (13) by the method of successive approximations, assuming that

$$\begin{aligned} &E_{10} = E_{10}^{(0)} + E_{10}^{(1)}, \qquad (|E_{10}^{(1)}| \ll |E_{10}^{(0)}|); \\ &\xi = \xi^{(0)} + \xi^{(1)}, \quad (|\xi^{(1)}| \ll |\xi^{(0)}|) \end{aligned} \tag{14}$$

and neglecting powers of $E_{10}^{(1)}$ and $\xi^{(1)}$ higher than the first and their products. The solution sought, satisfying the boundary conditions

$$\begin{aligned} &(E_{10}^{(0)})_{z=0} = E_0(1 + M\cos\Omega t); \quad (E_{10}^{(1)})_{z=0} = 0; \\ &(\xi^{(0)})_{z=0} = (\xi^{(1)})_{z=0} = 0, \end{aligned} \tag{15}$$

has the form :

$$E_{10}^{(0)} = E_0 (1 + M \cos \Omega t) \exp\left(-\frac{\omega}{c} \varkappa z\right); \quad \xi^{(0)} = \frac{\omega}{c} n z;$$

$$E_{10}^{(1)} = -\frac{1}{2} \frac{\varepsilon_1}{\varepsilon_0} E_{10}^{(0)} \exp\left(-\frac{\omega}{c} \varkappa z\right) \left[1 - \exp\left(-\frac{2\omega}{c} \varkappa z\right)\right]; \quad (16)$$

$$\xi^{(1)} = \left(\frac{\varkappa}{n} + \frac{a}{2}\right) \frac{\varepsilon_1}{\varepsilon_0} E_{10}^{(0)} \left[1 - \exp\left(-\frac{2\omega}{c} \varkappa z\right)\right].$$

In the computations it was reckoned that, provided $\varepsilon_0 \gg \frac{4\pi\sigma_0}{\omega}$, a condition which, for the sake of simplicity, was assumed fulfilled, (except for the vicinity of the reflection point, where $\varepsilon_0 \to 0$, this inequality is ordinarily fulfilled closely enough), the indices of absorption and refraction $\varkappa$ and n were linked with ε_0 and σ_0 by the relationships (see [2], for example):

$$n \simeq \sqrt{\varepsilon_0}; \quad \varkappa \simeq 2\pi\sigma_0/\omega \sqrt{\varepsilon_0}. \quad (17)$$

Using formulas (4), (5), (6), (11), (16) and assuming that $\overline{v^2} = \overline{v^2} = \delta kT/m$ (k is Boltzmann's constant, T is the kinetic temperature of the electrons), we get for the field at the receiving point:

$$E = E_0 \exp\left(-\frac{\omega}{c} \varkappa z\right) \left\{1 - \gamma \left[1 + M^2 \left(\frac{1}{2} + \frac{(\delta\nu_0)^2}{\Omega^2 + (\delta\nu_0)^2}\right)\right]\right\} \times$$

$$\times \left[1 + M_\Omega \cos(\Omega t - \zeta_1) + M_{2\Omega} \cos(2\Omega t - \zeta_2) + M_{3\Omega} \cos(3\Omega t - \zeta_3)\right] \times$$

$$\times \cos\left[\omega t - \frac{\omega}{c} n z + a + \beta_\Omega \cos(\Omega t - \chi_1) + \beta_{2\Omega} \cos(2\Omega t - \chi_2)\right], \quad (18)$$

where

$$\gamma = \frac{\pi e^2 E_0^2 (\omega^2 - \nu_0^2)}{32 \delta mkT (\omega^2 + \nu_0^2)^2} \left[1 - \exp\left(-\frac{2\omega}{c} \varkappa z\right)\right]. \quad (18a)$$

Then we have the following relationships for the quantities characterizing the distortions of amplitude modulation:

$$M_2 = M - \Delta M_2; \quad \Delta M_2 = 2\gamma M (\delta\nu_0)^2 \left\{ \frac{1 - M^2/2}{\Omega^2 + (\delta\nu_0)^2} + \frac{M^2}{8\left[4\Omega^2 + (\delta\nu_0)^2\right]} \right\};$$

$$M_{2\Omega} = \frac{1}{2} \gamma M^2 (\delta\nu_0) \sqrt{\frac{25\,\Omega^2 + 9\,(\delta\nu_0)^2}{\left[\Omega^2 + (\delta\nu_0)^2\right]\left[4\Omega^2 + (\delta\nu_0)^2\right]}};$$

$$\operatorname{tg}\zeta_1 = \frac{2\gamma_1 \sin\varphi_1 + M\gamma_2 \sin\varphi_2}{2(1-\gamma)M - 2\gamma_1 \cos\varphi_1 - 2M\gamma_2 \cos\varphi_2}; \qquad (19)$$

$$\operatorname{tg}\zeta_2 = \frac{M\gamma_1 \sin\varphi_1 + 2\gamma_2 \sin\varphi_2}{M\gamma_1 \cos\varphi_1 + 2\gamma_2 \cos\varphi_2};$$

$$\varphi_1 = \operatorname{arc\,tg}\,(\Omega/\delta\nu_0); \quad \varphi_2 = \operatorname{arc\,tg}\,(2\Omega/\delta\nu_0);$$

$$\gamma_1 = 2\gamma M (\delta\nu_0) \Big/ \sqrt{\Omega^2 + (\delta\nu_0)^2}; \quad \gamma_2 = \gamma M^2 (\delta\nu_0)/2 \sqrt{4\Omega^2 + (\delta\nu_0)^2}$$

For the sake of simplicity we omit formulas for the overtone M_3.

It is interesting to note that, according to formulas (18a) and (19), the quantity ΔM_Ω can be not only positive but negative. The latter case will occur when $\omega < \nu_0$, where ν_0 is the value of the effective number of collisions in the region of interaction.

In the case under consideration the changes in phase are characterized by the quantities:

$$\alpha = 2\gamma \left(1 + \frac{M^2}{2}\right)\left(\frac{\chi}{n} + \frac{\omega\nu_0}{\omega^2 - \nu_0^2}\right);$$

$$\beta_\Omega = \frac{4\gamma M (\delta\nu_0)}{\sqrt{\Omega^2 + (\delta\nu_0)^2}}\left(\frac{\chi}{n} + \frac{\omega\nu_0}{\omega^2 - \nu_0^2}\right); \qquad (20)$$

$$\beta_{2\Omega} = \frac{\gamma M^2 (\delta\nu_0)}{\sqrt{4\omega^2 + (\delta\nu_0)^2}}\left(\frac{\chi}{n} + \frac{\omega\nu_0}{\omega^2 - \nu_0^2}\right).$$

It is interesting to compare our results with results obtained in [1] with the aid of the kinetic theory. For low modulation frequencies the author of [1] got the following value for a quantity characterizing the increase in the absorption of a radio-wave (compared with the linear case) :

$$\frac{\Delta E}{E} = \frac{e^2 E_0^2 \left(1 + \frac{3}{2} M^2\right)}{12\, mkT\, \omega^2\, \delta_{\text{эл}}} \left[1 - \exp\left(-\frac{2\omega}{c} \varkappa z\right)\right]. \qquad (21)$$

Here ΔE is the variation in the amplitude of the wave due to the non-linearity of the medium, E is the value of the amplitude in a linear approximation.

For the same case ($\Omega \ll \delta\nu_0$) it follows from formula (18) that:

$$\frac{\Delta E}{E} = \gamma \left(1 + \frac{3}{2} M^2\right) = \qquad (18b)$$

$$= \frac{\pi e^2 E_0^2 \left(1 + \frac{3}{2} M^2\right) (\omega^2 - \nu_0^2)}{32\, mkT\, (\omega^2 + \nu_0^2)^2\, \delta} \left[1 - \exp\left(-\frac{2\omega}{c} \varkappa z\right)\right].$$

Neglecting in (18b) the quantity ν_0^2 as compared with ω^2 and assuming in (21) $\delta_{el} \cong 2m/\mu = \delta$, we can see that in this case the quantities compared differ only by the factor $8/3\pi \cong 0.85$.

In the case of low modulation frequencies ($\Omega \ll \delta\nu_0$), for the other quantities characterizing the non-linearity formulas (19) and (20) give:

$$\Delta M_2 = 2\gamma M \left(1 - \frac{3}{8} M^2\right); \quad M_{2e} = \frac{3}{2} \gamma M^2; \qquad (19a)$$

$$\alpha = 2\gamma \left(1 + \frac{M^2}{2}\right) \left(\frac{\varkappa}{n} + \frac{\omega\nu_0}{\omega^2 - \nu_0^2}\right); \qquad (20a)$$

$$\beta_2 = 4\gamma M \left(\frac{\varkappa}{n} + \frac{\omega\nu_0}{\omega^2 - \nu_0^2}\right); \quad \beta_{2e} = \beta_2 \frac{M}{4},$$

where γ is determined from formula (18a).

A comparison between (19a) and (20a) and formulas obtained for corresponding quantities by means of the kinetic theory [1]

also shows that the quantities compared differ by a factor of about 0.85. This inaccuracy is clearly not significant, as a number of quantities occurring in the final formulas (E_o, T, δ and so on) can be determined only approximately. Moreover, the results obtained above must be considered no less accurate than results of the kinetic theory. In fact, when kinetic formulas are applied to concrete calculations, it is necessary to make a series of allowances which sharply reduce their accuracy; for example, replace $\delta_{el} = 2m/\mu$ with the experimental value of δ, take for granted the condition $\omega^2 \gg \nu_o^2$, which we know is not fulfilled for long waves, propagated, mainly, in the lower part of the E-layer (thinking in terms of night-time), etc.

For high modulation frequencies ($\Omega \gg \delta\nu_o$), according to (18) - (20),

$$\frac{\Delta E}{E} \cong \gamma \left(1 + \frac{M^2}{2}\right);$$

$$\Delta M_2 \cong 2\gamma M (\delta\nu_0/\Omega)^2 \left(1 - \frac{15}{32} M^2\right); \quad M_{2\Omega} \cong \frac{5}{4} \gamma M^2 \frac{\delta\nu_0}{\Omega}; \quad (22)$$

$$\beta_2 \cong 4\gamma M \frac{\delta\nu_0}{\Omega} \left(\frac{\varkappa}{n} + \frac{\omega\nu_0}{\omega^2 - \nu_0^2}\right); \quad \beta_{2\Omega} = \beta_2 \frac{M}{8}.$$

The results obtained for the given case in [1] are erroneous. As the expression for $\Delta\nu^{(\Omega)}$, obtained in the case of high Ω with the aid of the kinetic theory, contains terms orthogonal to terms contained in the initial expression for E_{10} (if, for example, cos (Ωt) enters into E_{10}, then sin (Ωt) [2] will enter into $\Delta\nu^{(\Omega)}$), then clearly the distortions of modulation will be quadratic with respect to the absolute magnitude of $\Delta\nu^{(\Omega)}$, i.e. of the order of E_o^4. We have not taken such variations into account. Therefore it is possible to state that in the kinetic theory, for high Ω and in the approximation concerned, we must have $\Delta M_\Omega \simeq M_{2\Omega} \simeq \beta_\Omega \simeq \beta_{2\Omega} \simeq 0$. This circumstance, that in

the elementary theory it proved possible to take into account terms proportional to $\delta \nu_0 / \Omega$ and $(\delta \nu_0 / \Omega)^2$ while in the kinetic theory these corrections are not taken into account, is linked with the fact that in solving the kinetic equation terms of the order of $\delta \nu_0 / \Omega$ are discarded.

Formulas for intermediate modulation frequencies are not obtained in the kinetic theory; thus, it was not possible to check the above dependence of nonlinear distortions on the modulation frequency (see formulas (18) - (20)) by comparing it with the kinetic theory. However, the fact that the dependence of cross-modulation on the modulation frequency, found by the elementary theory, is well confirmed by experiment, permits us to hope that the above results will be sufficiently accurate for any Ω.

According to formula (19), when $\omega^2 \gg \nu_0^2$, on account of the non-linearity of the ionosphere the depth of modulation M ought to diminish both for low and for high modulation frequencies. The deduction in [1] about the increase in the fundamental tone of modulation is based on the error pointed out above.

We shall now compare our results with the results of the authors of [5,6,7].

Tselishchev's article [5] was the first to be devoted to the question of the dependence of the absorption of a radiowave on the magnitude of the intensity of the field. As already mentioned in [1], besides using a successive solution for equation (12) the author employs the so-called "quasi-stationary" method of reasoning. This method consists in making use of the solution of the wave equation obtained for a linear medium, i.e. for a medium, in which the current depends linearly on the intensity of the field E, while the value of the index of absorption $\varkappa$, as affected by the field of a powerful station, is substituted only in the final formulas.

The result obtained in [5] differs from formula (18)

[(/5/ deals with the case where M = 0) in that instead of the quantity $\left[1 - \exp\left(-\frac{2\omega}{c} \varkappa \Omega\right)\right]$, which figures in formula (18), the formulas obtained in /5/ contain the quantity $\frac{2\omega}{c} \varkappa z$. If $\frac{2\omega}{c} \varkappa z \ll 1$, then, clearly, the two formulas coincide.

However, ordinarily in the ionosphere $(\omega/c) \varkappa z \gg 1$ (for not too short waves); then the results of /5/ and our results are quite different: whereas according to /5/ the quantities characterizing the non-linearity grow without limit with increase in the path of the wave z, according to formula (18) they tend as it were to a point of saturation, occurring at $(\omega/c) \varkappa z \gg 1$ (see Fig. 1).

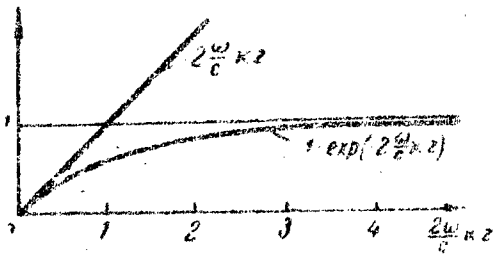

Fig. 1

Nerovnya /6/ uses the same methods as in /5/ to deal with distortions of amplitude-modulation. Accordingly, everything stated above in connection with /5/ applies equally to /6/*.

A more consistent calculation of the variation in the depth of modulation has been made by Hibberd /7/. Using the elementary theory and an integral approach (suggested by Shaw /8/ in connection with cross-modulation), he obtained the following result for ΔM_{Ω}:

$$\Delta M_{\Omega} = \frac{M}{1 - M^2/2\ \Omega^2 + (\delta\nu_0)^2} \int_0^S \frac{w_0}{\overline{Q}} \frac{\partial \eta}{\partial \nu} \nu_0\, dS, \qquad (23)$$

---

* There have been numerous references in the literature to the inadequacy of the method used in /5/ for dealing with nonlinear effects (see, for example, /1,2,3/).

where $\bar{Q}$ is the mean oscillatory energy of an electron under the action of an external field, w_o is the power communicated to the electron by the field, S is the path of the wave in the ionosphere and $\eta = (\omega/c)\varkappa$.

Since for a homogeneous layer $w_0 \sim E^2 \sim E_0^2 \exp(-2\eta S)$, then (23), after integration, gives us :

$$\Delta M_\Omega \sim \left[1 - \exp\left(-\frac{2\omega}{c} \varkappa S\right)\right],$$

which agrees with our results. The fact that the dependence of ΔM_Ω on the modulation frequency in formula (23) differs somewhat from that in (19) is a result of certain terms, governed by the presence of the overtone 2Ω, being disregarded in (23).

Formula (23) has the shortcoming that it does not reveal the character of the dependence of ΔM_Ω on the carrier frequency of the radiowave; as indicated above, this has great significance. The method used by Hibberd does not permit a correct investigation of nonlinear distortions of the phase of the wave or of the formation of overtones of the carrier frequency.

Thus, we see that by using the "elementary" theory to calculate the current density and then solving the wave equation, it is possible to obtain a sufficiently accurate picture of the nonlinear distortions which occur in the ionosphere, when not very powerful radiowaves are propagated in it. A certain lack of rigor in the argument (compared with the kinetic theory) is compensated for by the possibility of investigating the phenomena for arbitrary values of the modulation frequency.

Finally, everything we have stated here holds true only insofar as we are justified in assuming that the ionosphere does not contain very high concentrations of negative ions, considerably exceeding the electron densities (on this point see [2,3].)

2. Using the formulas obtained above, we shall evaluate the magnitude of the nonlinear distortions, which it is possible to expect in concrete cases. The computations will be made on the basis of the following simplifying assumptions:

a) oblique incidence of the wave on the layer will be taken into account only in determining the point of reflection; the trajectory of the ray is considered rectilinear;

b) the Earth's magnetic field is taken into account only in computing the coefficients of absorption and refraction, while considering the case of quasi-longitudinal propagation / 2 /;

c) the following simplified model of the lower part of the nocturnal E-layer of the ionosphere: the layer begins at an altitude of 80 km; the electron density varies with altitude in accordance with the law $N = N_0 + cz_1$, where $N_0 = 50$ el.cm^{-3} is the electron density at an altitude of from 80 to 90 km, c is a proportionality factor equal to $9 \cdot 2.10^{-4}$ el.cm^{-4}, and z_1 is the altitude read from the 90 km level; the number of collisions varies with altitude in accordance with an exponential law: $\nu_0 = \nu_0' \exp(-z/h)$, $\nu_0' = 5 \cdot 4.10^6$ is the number of collisions at an altitude of 80 km;

d) the power of the transmitter is equal to 100 kilowatts; the depth of modulation $M = 0.8$.

Figs. 2-4 give the results of a calculation of the variation in amplitude modulation in dependence on the distance between the receiver and the transmitter $\Delta M_1 = f_1(L)$, on the modulating frequency $\Delta M_2 = f_2(F)$ and on the carrier frequency $\Delta M_3 = f_3(\lambda)$.

As is evident from Fig. 2, the amount of demodulation falls sharply with increase in the distance between the receiver and the transmitter. This is due to the fact that as the distance between receiver and transmitter increases, the depth to which the ray penetrates into the ionosphere decreases.

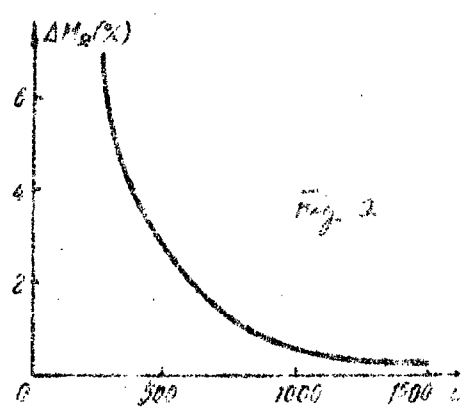

Fig. 2

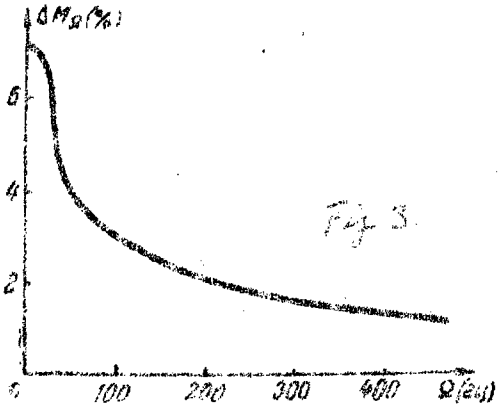

Fig. 3

Fig. 2: Dependence of ΔM_Ω on the distance L between receiver and transmitter.

Fig. 3: Dependence of ΔM_Ω on the modulation frequency.

According to Fig. 3, the change in the depth of modulation becomes less with increase in the modulation frequency.

The dependence of the variation in the depth of amplitude modulation on the carrier frequency (Fig. 4) is also of interest. As is evident from the graph, for low carrier frequencies ($\omega < \nu_c$) the quantity ΔM_Ω is negative and, consequently, the modulation due to the non-linearity must then increase. Increase in the carrier frequency will bring an increase in modulation in the lower part of the E-layer, i.e. at the very beginning of the wave path, and a decrease in it on further penetration into the layer. The resulting value of ΔM_Ω may become positive. For a certain value of ω ($\omega \approx \nu_{eff}$) ΔM_Ω may clearly become equal to zero. Moreover, this value of ω will evidently be different for different distances L between receiver and transmitter.

In character the dependences obtained by calculation coincide with certain others obtained experimentally. Thus, for example, a series of experiments was carried out in Cambridge [9] in 1955 under conditions very close to the theoretical ones. The dependence

of demodulation on the modulating frequency, obtained as a result of these experiments, coincides qualitatively with the graph in Fig. 3.

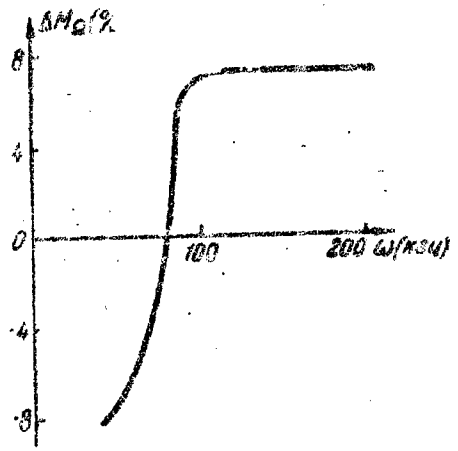

Fig. 4: Dependence of ΔM_Ω on the carrier frequency ω. (ω in kcs)

Note, however, that the experiments of Cutolo et al (see, for example, [10]) with respect to demodulation at gyromagnetic frequency gave results substantially different from those obtained above. For example, in Cutolo's experiments the depth of modulation decreased from 60% to 35-40% for a comparatively small transmitter power, while at high modulation frequencies this decrease was more substantial.

We shall make no attempt to explain these results here. We shall note only that Bayley's assumption [11], which reduces to the decrease in the depth of modulation being governed by a different absorption of the fundamental carrier and side frequencies of a wave, the carrier frequency of which is close to the local gyro frequency, is not confirmed by concrete calculations. Moreover, it is not possible to explain in this way the experimentally observed dependence of demodulation on the modulation frequency.

In conclusion we shall note that further experimental and theoretical study of the nonlinear distortion of powerful radio-waves may, as remarked in [1], give information valuable in plotting

the lower part of the ionosphere. For example, an experimental study of the dependence of demodulation on the distance between transmitter and receiver may throw light on the question of the distribution of electron density in the lower part of the ionosphere, since, as calculations have shown, this dependence is different for different electron distributions. A study of the dependence of demodulation on the carrier frequency might prove very useful in determining the effective number of collisions in the region of interaction. In fact, an experimental determination of the value of ω, at which the quantity ΔM_{Ω} vanishes, would at the same time permit a conclusion about the mean value of ν_{eff} in the region of interaction. By varying the distance between receiver and transmitter it is possible to trace the dependence of ν_{eff} on altitude in the lower part of the ionosphere.

Finally, a further experimental investigation of nonlinear distortions close to the gyro frequency would also be of great interest. The foremost question requiring clarification here would be the character of the polarization picked up by the receiver of the gyromagnetic wave, as this might be found useful for explaining the causes of modulation distortion at the gyro frequency.

The authors wish to thank A.V. Gurevich for his valuable comments on reading the article in manuscript.

Bibliography

1. Vilenskiy, I.M.: Symp. in mem. A.A. Andronov, Publ. AS USSR, M., 1955, 582.
2. Al'pert, Ya.L.; Ginzburg, V.L.; Feinberg, E.L.: Rasprostraneniye radiovoln (Propagation of radiowaves), Gostekhizdat, M., 1953.
3. Vilenskiy, I.M.: ZhETF, 22 (1952) 514.
4. Gurevich, A.V.: Radiotekhnika i Elektronika, 1 (1956) 704; Radiofizika, 1 (1958) 4, 21.
5. Tselishchev, V.P.: ZhTF, 10 (1940) 1630.
6. Nerovnya, L.K.: Vestnik MGU, math.-phys. ser., 2 (1956) 99.
7. Hibberd, F.H.: J.Atm.Terr.Phys. 6 (1955) 268.
8. Shaw, J.: Proc.Phys.Soc. 64 (1951) 1.

9. Cutolo, M.: Nature, 167 (1951) 314; Ann. telecommuns. 12 (1957) 150.
10. Bayley, V.A.: Nuovo Cimento Suppl., 4 (1956) 1430.

Novosibirsk Electrotechnical Institute
of Communications

Submitted 29 Nov. 58
after correction
27 Apr. 1959.

THE PROPAGATION OF ELECTROMAGNETIC WAVES IN A MEDIUM WITH RANDOM INHOMOGENEITIES ABOVE AN IDEALLY CONDUCTING PLANE

Pages 553-564

by E.A. Kaner & F.G. Bass.

This article develops a theory of the propagation of electromagnetic waves in a statistically homogeneous medium above an ideally conducting plane. Computations are made for the basic statistical characteristics (mean field, mean square of fluctuations in phase and amplitude) and their dependence on the frequency and polarization of the radiowaves, the distances and heights of the receiving and transmitting antennas. An investigation is made of the observed sharp increase in fluctuations close to the interference minima of the mean field and at the edge of the first lobe.

A considerable amount of theoretical [1] and experimental [2] work has been devoted to studies of the effect of fluctuations on the propagation of waves in a statistically homogeneous and unbounded medium. These studies have made it possible to explain such phenomena as stellar scintillation, fading, etc., to determine the mean dimensions of inhomogeneities and certain other characteristics of media. However, in many cases, especially in connection with the propagation of electromagnetic waves in the troposphere*, the effect of the boundary surface (the surface of the earth) is sub-

* For the sake of definiteness we shall discuss only the propagation of radiowaves in the atmosphere, although the final results are also applicable to the propagation of waves in other media.

stantial. The presence of a boundary surface leads to an interference structure of the radiation field and, therefore, experimental data may differ considerably from the results of a calculation of fluctuation effects in an unbounded medium. Taking into account the boundary surface leads to qualitatively new phenomena. We shall draw attention to two of these in particular.

If the boundary surface is an ideally conducting plane, then, firstly, the mean field may vanish at certain points in space as a result of interference of the direct and surface-reflected waves. Close to these points there is a sharp increase in the relative fluctuations in the amplitude and phase of the field. Secondly, at the edge of the first lobe, where the tangential components of the mean field decrease in inverse proportion to the square and not to the first power of the distance from the source (region of applicability of the so-called "square-law" formula of Vvedenskiy [3]), a considerable increase in the intensity of the fluctuations also ought to be observed.

As proved by Men', Gorbacn and Fraude [4] with the aid of simple and graphic arguments, in this region the mean squares of the relative fluctuations in amplitude and phase are proportional to the cube of the distance from the source and do not depend on the wavelength, whereas in an unbounded medium these quantities are proportional to the first power of the distance and the square of the frequency. The comparison with experimental data made in [4] confirms the results of calculations.

The present article is devoted to a theoretical consideration of the statistical characteristics of a radiation field in a medium with random fluctuations in the dielectric constant in the presence of a plane, ideally conducting boundary surface*.

*Some results given in the present article were published in abbreviated form in article [7].

1. Statistical characteristics of the electromagnetic field

For a complete statistical description of a radiation field it is, generally speaking, necessary to know the distribution function $f(\delta\varepsilon)$ of the random deviations of the dielectric constant $\delta\varepsilon$ from the mean value $\overline{\varepsilon}$, which for simplicity we shall take as unity. However, in its present state the theory does not give an unambiguous answer to the question of the distribution of $\delta\varepsilon$. If we consider the law of distribution of $\delta\varepsilon$ to be normal or limit ourselves to a consideration of small fluctuations, then for a complete statistical description it is sufficient to know merely the second moment of $f(\delta\varepsilon)$ or the correlation function $\overline{\delta\varepsilon(r_1)\,\delta\varepsilon(r_2)}$. Leaving aside the question of determining this function, in investigating the characteristics we shall consider that the correlation function has the form:

$$\overline{\delta\varepsilon(r_1)\,\delta\varepsilon(r_2)} = \overline{\delta\varepsilon^2}\,W(|x_1 - x_2|, |y_1 - y_2|, |z_1 - z_2|), \qquad (1.1)$$

where $\overline{\delta\varepsilon^2}$ does not depend on the coordinates (statistically homogeneous medium), while the correlation factor W depends only on the modulus of the difference in the components of the vectors r_1 and r_2. Ordinarily in an unbounded medium we assume that W depends on $|r_1 - r_2|$ (model of isotropic and homogeneous turbulence). The presence of a boundary surface may lead to anisotropy of the correlation radii: the correlation of fluctuations in $\delta\varepsilon$ with respect to the normal to the boundary surface z = 0 may be other than in the plane xy. Below we shall not detail the form of the correlation function, as in the limiting cases it is possible to get results for an arbitrary form of W.

An important point is to find the distribution function for random fluctuations in the electromagnetic field. In the case in which the point, at which the field is computed, is at such a great distance R away from the emitter that $R \gg l$ (l is the char-

acteristic correlation radius) and it is possible to restrict oneself to the calculation of a single scattering, clearly the distribution of the electromagnetic field will be normal for any law of distribution of $\delta\varepsilon$*. Actually, by dividing the whole distance, along which the electromagnetic wave is propagated, into sections with dimensions of the order of $l \ll R$, it is easy to see that the fluctuations in the field at a distance R from the source are defined by the sum of fluctuations in the field in each of these sections. As the number of sections is large and the fluctuations of the field in each of them are practically independent, the field in question is defined by the sum of a large number ($\sim R/l$) of independent random components, which in accordance with the central limit theorem of the theory of probability is normally distributed.

Thus, the distribution function of each of the components of the field $E = E_r + iE_i$ (E_r and E_i are the real and imaginary parts of E) has the form:

$$f(E_r, E_i) = A_0 \exp\left[-\frac{\xi_r^2}{a^2} - \frac{\xi_i^2}{b^2} + 2q\frac{\xi_r \xi_i}{ab}\right], \qquad (1.2)$$

where

$$\begin{aligned} \xi_r &= E_r - \overline{E_r}; & \xi_i &= E_i - \overline{E_i}; \\ a^2 &= 2(1-q^2)\overline{\xi_r^2}; & b^2 &= 2(1-q^2)\overline{\xi_i^2}; \\ q &= \overline{\xi_r \xi_i}/(\overline{\xi_r^2}\,\overline{\xi_i^2})^{1/2}; & A_0 &= \sqrt{1-q^2}/\pi ab. \end{aligned} \qquad (1.3)$$

---

* If $\delta\varepsilon$ is distributed in accordance with a normal law, then the field will also be distributed normally at any distance from the source, since, in the approximation mentioned, the random fluctuations of the field are a linear functional of $\delta\varepsilon$ (see below).

Accordingly, it is necessary to determine mean values of the real and imaginary parts of each of the components of the field, their m-s values and the autocorrelation factors of the real and imaginary parts of the field. The remaining sections of this article are devoted to the computation of these quantities.

We shall show the connection between these quantities and the other important statistical characteristics of the radiation field - fluctuations in amplitude $|E|$, phase φ and their autocorrelations.

From formula (1.2) it is easy to find the distribution function for amplitude and phase of each of the random components of the field:

$$f(\varphi) = \frac{1}{2} A_0 \left| \cos^2\varphi/a^2 + \sin^2\varphi/b^2 - (2q/ab)\sin\varphi\cos\varphi \right|^{-1};$$

$$f(\xi) = 2\pi A_0 \xi \exp\left[-\xi^2 2^{-1} (a^{-2} + b^{-2}) \right] I_0 \left(\xi^2 2^{-1} a^{-2} b^{-2} \times \right.$$

$$\left. \times \sqrt{(a^2 - b^2)^2 + 4q^2 a^2 b^2} \right),$$

where $\xi = \sqrt{\xi_r^2 + \xi_i^2}$, I_0 and I_o is a Bessel function of the imaginary argument.

Remote from the minima of the mean field, where the mean phase is equal to

$$\bar{\varphi} \equiv \overline{\operatorname{arctg}(E_i/E_r) + \pi s(E_r)} = \varphi_0 + \frac{\overline{\xi_r^2} - \overline{\xi_i^2}}{|E|^2} (\sin\varphi_0 \cos\varphi_0 + \cos 2\varphi_0), \tag{1.4}$$

where φ_0 is the phase of the mean field

$(\bar{E} = |\bar{E}| \exp i\varphi_0)$; $s(x) = 1$ $(x < 0)$; $s(x) = 0$ $(x > 0)$.

The mean-square fluctuation in phase is

$$\overline{\delta\varphi^2} \equiv \overline{(\varphi - \bar{\varphi})^2} = |E|^2 (\overline{\xi_r^2} \sin^2\varphi_0 + \overline{\xi_i^2} \cos^2\varphi_0 - \overline{\xi_r \xi_i} \sin 2\varphi_0). \tag{1.5}$$

The mean amplitude is :

$$|\bar{E}| \equiv \overline{(E_r^2 + E_i^2)^{1/2}} \simeq |\bar{E}| + \frac{1}{2|\bar{E}|} \left(\overline{\xi_r^2} \sin^2\varphi_0 + \overline{\xi_i^2} \cos^2\varphi_0 - \overline{\xi_r \xi_i} \sin 2\varphi_0 \right). \tag{1.6}$$

The mean square of the fluctuation in amplitude is:

$$\overline{\delta A^2} = \overline{(|E| - |\bar{E}|)^2} = \overline{\xi_r^2}\cos^2\varphi_0 + \overline{\xi_i^2}\sin^2\varphi_0 - \overline{\xi_r \xi_i}\sin 2\varphi_0 . \quad (1.7)$$

The cross-correlation of amplitude and phase is:

$$-\overline{\delta\varphi \frac{\delta A}{|\bar{E}|}} = \frac{(|E| - |\bar{E}|)}{|\bar{E}|}(\varphi - \bar{\varphi}) = \frac{1}{2|E|^2}(\overline{\xi_i^2} - \overline{\xi_r^2})\sin 2\varphi_0 + \frac{\overline{\xi_r \xi_i}}{|\bar{E}|^2}\cos 2\varphi_0 . \quad (1.8)$$

In the important special case in which $\overline{\xi_r^2} = \overline{\xi_i^2} = |\xi|^2/2$, $q \ll 1$, the fluctuations in phase and the relative fluctuations in amplitude are distributed in accordance with a normal law with uniform dispersion:

$$\sigma = \overline{\delta\varphi^2} = \overline{\delta A^2}/|\bar{E}|^2 = |\xi|^2/2|\bar{E}|^2. \quad (1.9)$$

The cross-correlation of amplitude and phase $\sigma_{A\varphi}$ is then small compared with unity:

$$\sigma_{A\varphi} \equiv \frac{\overline{\delta A\, \delta\varphi}}{(\overline{\delta A^2}\,\overline{\delta\varphi^2})^{1/2}} \sim q \ll 1. \quad (1.10)$$

In the same case close to the minima of the mean field ($|\bar{E}|^2 \ll |\xi^2|$) the distribution of phase is equiprobable, the amplitude is distributed in accordance with Rayleigh's law, the mean phase is equal to $\pi/2$ and the mean square of the fluctuation in phase is $\pi^2/3$. For the fluctuation in amplitude it is convenient to introduce the following characteristic (analogous to the square of the fluctuations in amplitude level usually introduced):

$$\overline{(\ln|E| - \ln|\bar{E}|)^2} = \pi^2/24, \quad (1.11)$$

which, like the phase characteristics, is in this case independent of the concrete properties of the fluctuating medium.

Although absolute fluctuations in a random component of the field are close to zeroes of the mean field, these fluctuations, like relative fluctuations remote from these points, in particular

fluctuations in phase and "level", increase sharply.

2. Fundamental equations and boundary conditions

It follows from the results of the preceding section that a complete statistical description of the radiation field is given by a knowledge of the mean values of the field and the corresponding mean-square quantities. The starting equations for computing the latter are those of Maxwell, which, after the magnetic field has been excluded, reduce to the form:

$$\text{rot rot } \boldsymbol{E} = k^2 \boldsymbol{D}; \qquad k = \frac{\omega}{c}. \tag{2.1}$$

The time-dependence is given by the factor $\exp(-i\omega t)$. The intensity of the electric field E and the induction vector D are connected by the relationship $D = \varepsilon E$. Assuming that $\varepsilon = 1 + \delta\varepsilon$, $E = \bar{E} + \xi$, we find:

$$\text{rot rot } (\bar{E} + \xi) = k^2 (1 + \delta\varepsilon)(\bar{E} + \xi). \tag{2.2}$$

We obtain equations for the regular and random components of the field separately. With this object we shall average equation (2.2) and then compute an averaged equation from (2.2). As a result

$$\text{rot rot } \bar{E} = k^2 (\bar{E} + \overline{\xi \delta\varepsilon}); \tag{2.3}$$

$$\text{rot rot } \xi = k^2 (\xi + \bar{E}\delta\varepsilon). \tag{2.4}$$

In equation (2.3) we have retained the small component $\overline{\xi \delta\varepsilon}$ as this term insures the effect of the attenuation of the mean field at infinity (see [5]). Analogous small terms in (2.4) can be neglected.

The latter equations are necessary to complete the boundary conditions at the boundary surface. We shall assume that the boundary

is an ideally conducting plane*. Accordingly, the tangential components of the field are equal to zero :

$$\overline{E}_{z0} = \xi_{z0} = 0. \qquad (2.5)$$

The subscript zero denotes that the corresponding quantities are taken for z = 0 . The z-axis is directed along the outward normal to the boundary surface z = 0 and passes through the point z_o, in which the emitter is located. The x-axis is directed along the projection of the line joining the observation point r(L,0,z) with the emitter $r_o(0,0,z)$.

The boundary condition for the vertical component of the field E_z can be obtained in the ordinary way [6] by taking the divergence from equations (2.3) and (2.4) and reducing z to zero. After a few simple calculations we get:

$$(\partial \overline{E}_z / \partial z)_0 = -(\overline{\xi_z \partial \delta\varepsilon / \partial z})_0 ; \quad (\partial \xi_z / \partial z)_0 = -\overline{E}_{z0} (\partial \delta\varepsilon / \partial z)_0. \qquad (2.6)$$

In the following we shall restrict ourselves merely to an investigation of large-scale fluctuations, scattering at which is a matter of special interest. In other words we shall consider that $|\nabla \delta\varepsilon| \ll k |\delta\varepsilon|$ or $k\ell \gg 1$, i.e. assume a small variation in the properties of random inhomogeneities at the wavelength. In this case it is clearly possible to turn away from polarization corrections with a relative order not less than $1/k\ell \ll 1$. With the same degree of accuracy it is possible to neglect terms in the right-hand member of the boundary conditions (2.6) due to polarization corrections.

Accordingly, the vector equations (2.3) and (2.4) break down into scalar wave equations for the individual components:

---

* The assumption of finite conductivity is linked only with somewhat more clumsy computations and, in principle, can be introduced by employing an analogous method. This question is discussed qualitatively below.

$$(\Delta + k^2)\overline{E} + k^2\overline{\xi\delta\varepsilon} = -p\delta(r - r_0); \qquad (2.7)$$

$$(\Delta + k^2)\xi + k^2\bar{E}\delta\varepsilon = 0 \qquad (2.8)$$

with the boundary conditions

$$\bar{E}_{/0} = \xi_{/0} = (\partial\bar{E}_z/\partial z)_0 = (\partial\xi_z/\partial z)_0 = 0. \qquad (2.9)$$

The term with the δ-function in the right-hand member of (2.7) is connected with the presence of the source in the point r_0.

3. Solution of the equations. Mean field.

The solution of equation (2.8) for a random component of the field ξ is easy to write in explicit form, if we make use of the known Green functions for the operator $\Delta + k^2$. For tangential components this solution has the form:

$$\xi_-(r) = k^2 \int_{z' \geqslant 0} dr'\, \varphi_-(r, r')\, \bar{E}_t(r')\, \delta\varepsilon(r'), \qquad (3.1)$$

and for the z component:

$$\xi_+(r) = k^2 \int_{z' \geqslant 0} dr'\, \varphi_+(r, r')\, \bar{E}_z(r')\, \delta\varepsilon(r'), \qquad (3.2)$$

where

$$\varphi_+(r, r') = \varphi(|r - r'|) \pm \varphi(|r_1 - r'|);$$

$$\varphi(\rho) = \exp(ik\rho)/4\pi\rho.$$

The point r_1 is a mirror reflection of the point r in the plane z=0 .

Substituting (3.1) and (3.2) in (2.7), we arrive at the following integral-differential equation, defining the mean field*:

$$(\Delta + k^2)\,\bar{E}(r) + k^4\overline{\delta\varepsilon^2}\int_{z' \geqslant 0} dr'\, \varphi_\mp(r, r')\,\bar{E}(r')\, W(|r - r'|) = -p\delta(r - r_0). \qquad (3.3)$$

* In finding the mean field we shall assume for the sake of simplicity that $W(\rho) = W(|\rho|)$.

(For tangential components it is necessary to take φ_- in the integral and for the z-component φ_+.)

The integral term in equation (3.3) contains a small parameter $\overline{\delta\varepsilon^2}$ which is ordinarily neglected. However, as shown in [5], neglecting this component leads to a contradiction of the law of conservation of energy. Since the integral component plays a part only at large distances from the source, we shall replace it with an asymptotic expression for large r*. It is possible to show that for a sufficiently large L, when the quantity $D = 2L/kl^2 \gg 1$ (remote zone),

$$\int\limits_{z'\geqslant 0} dr'\, \varphi_{\mp}(r, r')\, W(|r-r'|)\, \bar{E}(r') = \int\limits_{-\infty}^{+\infty} dr'\, \varphi_{\mp}(|r-r'|)\, W(|r-r'|)\, \bar{E}(r')\,|1+O(1/D)|. \tag{3.4}$$

With this object we shall turn from the integral-differential equation (3.3) to the integral equation:

$$\bar{E}(r) = p\varphi_{\mp}(r, r_0) + k^4\overline{\delta\varepsilon^2}\int\limits_{z'\geqslant 0} dr'\, \varphi_{\mp}(r, r')\int\limits_{z''\geqslant 0} dr''\, \varphi_{\mp}(r', r'') \times W(|r'-r''|)\, E(r''). \tag{3.5}$$

The solution of this equation by the usual iteration method is appropriate only when $\delta\varepsilon^{-2}\, k^2 l L \ll 1$, i.e. where the effect of the fluctuations on the mean field is negligibly small. We shall therefore find a solution without this limitation.

Let us make the substitution $r'' = r' + \rho$ in the integral :

---

* At small distances the form of this term is not material, as it is generally possible to neglect it.

$$\int_{z''\geq 0} dr''\, \psi_{\mp}(r', r'')\, W(|r' - r''|)\, \bar{E}(r'') =$$

$$= \int_{z\geq -z'} d\rho\, W(\rho)\, |\varphi(\rho) \mp \varphi(|2z'\mathbf{e} + \rho|)|\, \bar{E}(r' + \rho) \qquad (3.6)$$

(choice of **e** parallel to the z-axis).

Standard evaluations using the stationary phase method [6] show that for sufficiently large L the basic contribution to the integral with respect to **r'** is made by values of $z' \lesssim z + \sqrt{L/k}$. Therefore, with an accuracy of the order of $W(\sqrt{L/k}) \ll 1$ when $D \gg 1$ it is possible to replace the lower limit in (3.6) with $-\infty$ and neglect the second term in the square brackets (with an accuracy which in any event is not worse than $O(1/\sqrt{D})$*. Thus, at large distances equation (3.3) takes on the form:

$$(\Delta + k^2)\bar{E}(r) + k^4 \overline{\delta\varepsilon^2} \int_{-\infty}^{\infty} d\rho\, W(\rho)\varphi(\rho)\, \bar{E}(r + \rho) = -p^2 (r - z_0). \qquad (3.7)$$

At these distances, with a relative accuracy of O(1/D), the solution of this equation has the form:

$$\bar{E}(r) = p_+ \varphi_+^{\varkappa}(r, r_0), \qquad (3.8)$$

where $\varphi^{\varkappa}(\rho)$ differs from $\varphi(\rho)$ in that instead of κ in $\exp(ik\rho)$ it is necessary to substitute the value of $\varkappa$ from the equation

$$\varkappa^2 = k^2 + \overline{\delta\varepsilon^2} k^4 \int_{-\infty}^{\infty} d\rho\, W(\rho)\varphi(\rho)\cos \varkappa\rho. \qquad (3.9)$$

In fact, substituting (3.8) in (3.7), we find:

---

* As more accurate evaluations show, the relative correction due to this component is much less, namely of the order of $D^{-1/2} \exp(-k^2 l^2/2)$ when $W(\rho) = \exp(-\rho^2/l^2)$.

$$\left(-\varkappa^2+k^2\right)\varphi_{\mp}^{\varkappa}(r, r_0)+\overline{\delta\varepsilon^2}\,k^4\int_{-\infty}^{\infty}d\rho\, W(\rho)\,\varphi(\rho)\,\varphi_{\mp}^{\varkappa}(r+\rho; r_0)=0. \quad (3.10)$$

At large distances $\varphi^{\varkappa}(r+\rho; r_0)=\varphi^{\varkappa}(|r-r_0|)\exp(i\varkappa_2\rho)\mp\varphi^{\varkappa}(|r_1-r_0|)\exp(i\varkappa_2\rho)$ correct to terms of the order of $k\rho^2/L\sim 1/D\ll 1$ ($\varkappa_1=\varkappa(r-r_0)/|r-r_0|$, $\varkappa_2=\varkappa(r_1-r_0)/|r_1-r_0|$). Since the integral in (3.10) does not depend on the direction of the vector $\varkappa$, equation (3.10) reduces to (3.9).

Thus, to find the mean field above an ideally conducting plane, it is sufficient to replace the propagation constant k with the quantity $\varkappa = k\sqrt{\varepsilon_{eff}}$ with the effective dielectric constant

$$\varepsilon_{эфф}=1+4\pi\,\overline{\delta\varepsilon^2}\,k^2\int_0^{\infty}d\rho\,\rho^2\,W(\rho)\,\varphi(\rho)\,\frac{\sin k\rho}{k\rho}\approx 1+\frac{1}{2}\,i\overline{\delta\varepsilon^2}\,k\int_0^{\infty}W(\rho)\,d\rho, \quad (3.11)$$

coinciding with the value of ε_{eff} in an unbounded medium (see [5]).

4. Statistical characteristics of the radiation field in the remote zone.

In calculating the intensity of absolute fluctuations in the field $|\xi^2|$ the attenuation of the mean field, connected with the deviation of ε_{eff} from unity, can be taken into account by multiplying $|\xi^2|$ in the final formulas by $\exp(-2kL\,\mathrm{Im}\sqrt{\varepsilon_{eff}})$, as the intensity of the fluctuating and regular components becomes attenuated with distance in accordance with one and the same law.

The formulas for fluctuations in phase and relative amplitude fluctuation, presented below, relate to the case in which these fluctuations are small and the attenuation of the mean field can be neglected.

Bearing this in mind, we shall compute:

$$\overline{|\xi^2(r)|}=\overline{\delta\varepsilon^2}\,k^4|p^2|\iint_{z',z''\geq 0}dr'\,dr''\,\varphi_{\mp}(r, r')\,\varphi_{\mp}(r', r_0)\times \quad (4.1)$$

$$\varphi^*_{\pm}(r, r'')\,\varphi^*(r'', r_0)\,W(|x'-x''|;|y'-y''|;|z'-z''|) \quad (4.1)\ \text{cont.}$$

(the minus sign relates to the horizontal, the plus sign to the vertical component of the field).

We shall assume that the following inequalities are fulfilled:

$$\lambda \ll l \ll \sqrt{\lambda L}, \quad z, z_0 \ll L \qquad (\lambda = 1/k = c/\omega). \tag{4.2}$$

In finding the asymptotic of (4.1) we make use of the known fact that the main contribution to the integral is made by a small region along the path of propagation of the waves, bounded by a strongly prolate ellipsoid, the transverse dimensions of which are of the order of $\sqrt{\lambda L}$. Therefore, the functions φ, entering into (4.1) can be expanded with respect to powers of the ratio of transverse to longitudinal components. The result of the expansion is thus:

$$\overline{|\mathcal{E}^2_{\mp}(r)|} = \overline{\delta\varepsilon^2}\,(k/4\pi)^4\,|p^2_{\mp}| \times$$

$$\times \int_{-\infty}^{\infty}\int \frac{dx'\,dx''\exp|ik(|x'|+|L-x'|-|x''|-|L-x''|)|}{|x'|\,|L-x'|\,|x''|\,|L-x''|} \times$$

$$\times \int_{-\infty}^{\infty}\int dy'\,dy''\exp\left[\frac{ik}{2}\left(\frac{y'^2}{|L-x'|}+\frac{y'^2}{|x'|}-\frac{y''^2}{|L-x''|}-\frac{y''^2}{|x''|}\right)\right]\times \tag{4.3}$$

$$\times \int_0^{\infty}\int_0^{\infty} dz'\,dz''\,W(|x'-x''|;|y'-y''|;|z'-z''|)\exp\left[\frac{ik}{2}\times\right.$$

$$\left.\times\left(\frac{z^2+z'^2}{|L-x'|}+\frac{z_0^2+z'^2}{|x'|}-\frac{z^2+z''^2}{|L-x''|}-\frac{z_0^2+z''^2}{|x''|}\right)\right]\times$$

$$\times 16\begin{matrix}\sin\\ \cos\end{matrix}\left(\frac{kzz'}{|L-x'|}\right)\begin{matrix}\sin\\ \cos\end{matrix}\left(\frac{kz_0z'}{|x'|}\right)\begin{matrix}\sin\\ \cos\end{matrix}\left(\frac{kzz''}{|L-x''|}\right)\begin{matrix}\sin\\ \cos\end{matrix}\left(\frac{kz_0z''}{|x''|}\right).$$

Calculations show that, when the inequalities (4.2) are fulfilled, it is sufficient to integrate over the interval from 0 to L in the integrals with respect to x' and x". In this connection it is possible to put x" equal to x' everywhere except in the function of W while integrating from $-\infty$ to $+\infty$ with respect to the difference $\xi = x'' - x'$. The double integral with respect to y' and y" is easily evaluated and as a result we get:

$$\overline{|\xi_{\mp}^2(r)|} = \delta\varepsilon^2 |p_{\mp}^2| \left(\frac{k}{4\pi}\right)^3 \frac{4}{L} \int_0^\infty d\xi \int_0^L \frac{dx'}{x'(L-x')} \times$$

$$\times \int_0^\infty \int_0^\infty dz'\, dz''\, W(\xi, 0, |z'-z''|) \cos\left(\frac{kL}{2} \frac{z'^2 - z''^2}{x'(L-x')}\right) \times \qquad (4.4)$$

$$\times \left[\cos\frac{kz(z'-z'')}{L-x'} \mp \cos\frac{kz(z'+z'')}{L-x'}\right] \left[\cos\frac{kz_0(z'-z'')}{x'} \mp \right.$$

$$\left. \mp \cos\frac{kz_0(z'+z'')}{x'}\right].$$

Further computations making use of the inequality $D \gg 1$ lead to the following expression:

$$\overline{|\xi_{\mp}^2(r)|} = \delta\varepsilon^2 |p_{\mp}^2| \left(\frac{k}{4\pi}\right)^2 \frac{1}{L} \times$$

$$\times \int_\delta^\infty d\xi \int_0^1 dt \left\{ W(\xi, 0, 0) + \frac{1}{2} W(\xi, 0, 2zt + 2z_0(1-t)) + \right. \qquad (4.5)$$

$$+ \frac{1}{2} W(\xi, 0, |2zt - 2z_0(1-t)|) \mp \cos\frac{2kzz_0}{L} \left| W(\xi, 0, 2zt) + \right.$$

$$\left. \left. + W(\xi, 0, 2z_0 t)\right|\right\} \left[1 + O\left(\frac{l}{L}, \frac{1}{kl}, \frac{\ln D}{D}\right)\right].$$

The formula obtained makes it possible to explain the dependence of all the fluctuation characteristics on the frequency and polarization of the radiowave and the distance and height of the receiving and transmitting antennas. It is possible to show that:

$$\frac{\overline{\xi^2(r)}}{|\xi^2|} = \frac{\overline{\xi_r^2} - \overline{\xi_i^2} + 2i\overline{\xi_r \xi_i}}{|\overline{\xi^2}|} \sim O\left(\frac{\ln D}{D}\right), \qquad (4.6)$$

i.e. with the accuracy mentioned $\overline{\xi_r^2} = \overline{\xi_i^2}$ and $q \equiv 2\overline{\xi_r \xi_i}/|\overline{\xi^2}| = 0$. Therefore in the remote zone far from the minima of the mean field

$$\varkappa = \sigma_\varphi^2 = \frac{\overline{\delta A^2}}{|\bar{E}|^2} = \frac{|\xi^2|}{2|\bar{E}|^2} = \frac{1}{4}\overline{\delta\varepsilon^2}\,\frac{k^2 L}{|1 \mp \cos(2kzz_0/L)|}\int_0^\infty d\xi \times$$

$$\times \int_0^1 dt \left\{ W(\xi, 0, 0) + \frac{1}{2} W(\xi, 0, 2zt + 2z_0(1-t)) + \right. \qquad (4.7)$$

$$+ \frac{1}{2} W(\xi, 0, |2zt - 2z_0(1-t)|) \mp \cos\frac{2kzz_0}{L} \left| W(\xi, 0, 2zt) + \right.$$

$$\left. \left. + W(\xi, 0, 2z_0 t) \right| \right\}.$$

Formula (4.7) shows that the principle of reciprocity is fulfilled for the fluctuations: they are symmetrical functions of z and z_0.

Let us consider various limiting cases.

If the altitudes z, z_0 are such that $(k z z_0 / L)^2 \ll 1$, then the dependence of fluctuations in phase and of relative amplitude fluctuations on distance and frequency is essentially different for the vertically and horizontally polarized components. For horizontal polarization :

$$\sigma_- = \frac{1}{8}\overline{\delta\varepsilon^2}\,\frac{L^3}{(z z_0)^2}\int_0^\infty d\xi \int_0^1 dt \left\{ W(\xi,0,0) + \frac{1}{2} W(\xi,0,2zt + 2z_0(1-t)) + \right.$$

$$\left. + \frac{1}{2} W(\xi,0,2zt - 2z_0(1-t)) \right| - \left(1 - 2\frac{k^2 z^2 z_0^2}{L^2}\right) \times \qquad (4.8)$$

$$\left. \times \left| W(\xi,0,2zt) + W(\xi,0,2z_0 t) \right| \right\}$$

The fluctuations are proportional to the cube of the distance and do not depend on the frequency. For vertical polarization:

$$\sigma_+ = \frac{1}{8}\overline{\delta\varepsilon^2}\,k^2 L \int_0^\infty d\xi \int_0^1 dt \left\{ W(\xi,0,0) + \frac{1}{2} W(\xi,0,2zt + 2z_0(1-t)) + \right.$$

$$\left. + \frac{1}{2} W(\xi,0,|2zt - 2z_0(1-t)|) + W(\xi,0,2zt) + W(\xi,0,2z_0 t) \right\} \qquad (4.9)$$

The fluctuations are proportional to the first power of the distance and the square of the frequency.

If the receiving and transmitting antennas are raised to relatively great heights, when $l_\perp \ll z, z_0 \ll \sqrt{L/k}$ ($l_\perp$ is the correlation radius with respect to the normal to the boundary surface),

$$\sigma_- / \sigma_+ \simeq (L/kzz_0)^2 \gg 1, \qquad (4.10)$$

where

$$\sigma_+ = \frac{1}{8}\overline{\delta\varepsilon^2}\,k^2 L \bar{l}_1; \qquad \bar{l}_1 = \int_0^\infty W(\xi,0,0)\,d\xi.$$

At small heights ($z, z_0 \ll l_\perp$)

$$\sigma_- = \frac{1}{60}\overline{\delta\varepsilon^2}\,\frac{L^3}{l_\perp^4}\int_0^\infty d\xi\, W_\zeta^{(IV)}(\xi,0,0); \qquad (4.11)$$

$$\sigma_+ = \frac{1}{2}\overline{\delta\varepsilon^2}\,k^2 L \bar{l}_\parallel. \qquad (4.12)$$

In expanding we assumed that $W(\xi,0,\zeta)$ was an even function of ζ of the form $W(\xi,0,\zeta/l_\perp)$. In this case too the ratio of the fluctuations is large:

$$\sigma_-/\sigma_+ \simeq (L/kl_\perp^2)^2 \gg 1. \qquad (4.13)$$

Finally, when one of the quantities z or z_0 is much greater than $l_\perp$ but the other is much less than $l_\perp$,

$$\sigma_- = \frac{1}{4}\overline{\delta\varepsilon^2}\,k^2 \int_0^\infty d\xi \Big| W(\xi,0,0) + \frac{1}{3}(L/k z_{\text{макс}} l_\perp)^2 \times$$

$$\times \Big| W_\zeta''(\xi,0,0)\Big|\Big|; \qquad (4.14)$$

$$\sigma_\mp = \frac{1}{4}\overline{\delta\varepsilon^2}\,k^2 L\,\overline{l_\parallel};$$

$$\sigma_\mp/\sigma_+ \simeq 1 + \frac{1}{3}(L/z l_\perp z_{\text{макс}})^2$$

($z_{\text{макс}}$ is equal to the greater of the quantities z, z_0). Analogous formulas may also be easily obtained in the case where $(k z z_0/L)^2$ is not small compared with unity.

For large values of $z/l_\perp$, $z_0/l_\perp \gg 1$

$$\sigma_\mp = \frac{1}{4}\,\frac{\overline{\delta\varepsilon^2}\,k^2 L\,\overline{l_\parallel}}{(1 \mp \cos 2kzz_0/L)}. \qquad (4.15)$$

When $z/l_\perp \gg 1$, $z_0/l_\perp \ll 1$,

$$\sigma_\mp = \sigma_+ = \frac{1}{4}\overline{\delta\varepsilon^2}\,k^2 L\,\overline{l_\parallel}. \qquad (4.16)$$

In conclusion we present a general formula for fluctuations in amplitude and phase in the case, in which it is possible to approximate the correlation function $\overline{\delta\varepsilon^2}\,W(x,y,z)$ with $\overline{\delta\varepsilon^2}\exp -(x^2+y^2)/l_\parallel^2 - z^2/l_\perp^2$:

$$\sigma_{\mp}^2 = \frac{\overline{\delta\varepsilon^2}\, k^2 L \bar{l}_{\parallel}}{4\,|1 \mp \cos(2kzz_0/L)|}\left\{1 + \frac{\bar{l}_{\perp}}{2(z^2 - z_0^2)}\left[z\,\mathrm{erf}(2z/l_{\perp}) - z_0\,\mathrm{erf}(2z_0/l_{\perp})\right] \mp \cos\frac{2kzz_0}{L}\left[\mathrm{erf}(2z/l_{\perp})/(2z/l_{\perp}) + \mathrm{erf}(2z_0/l_{\perp})/(2z_0/l_{\perp})\right]\right\}, \qquad (4.17)$$

where $$\mathrm{erf}(x) = \frac{2}{\sqrt{\pi}}\int_0^x \exp(-t^2)\,dt, \quad \bar{l} = l\frac{\sqrt{\pi}}{2}.$$

An analogous formula, obtained in [4] from qualitative reasoning, correctly describes the dependence of the fluctuations on the frequency ω and the distance L. However, the height dependences agree only for $z, z_0 \gg l_{\perp}$; for low heights the corresponding formula in [4] diverges substantially from the result obtained.

The increase in fluctuations close to the minima of the mean field is connected with the interference structure of the electromagnetic field in space. The interference effects are expressed most distinctly when the amplitudes of the direct and reflected waves are identical. If the modulus R of the amplitude coefficient of reflection $R\exp(i\psi)$ is different from unity, the interference phenomena do not lead to such a powerful increase in the fluctuations. In the limiting case of small coefficients of reflection it is possible to use formulas obtained for an unbounded medium.

In the case of finite but sufficiently large electric conductivity of the boundary surface the difference in the laws of growth of the relative fluctuations with distance for horizontal and vertical polarization at the edge of the first interference lobe decreases. This is connected with the fact that for relatively small heights the phase ψ of the reflection coefficient for a vertically polarized wave varies sharply from 0 to π while the amplitude R

remains close to unity. Accordingly, the vertical component of the regular field decreases proportionally to L^{-2} and not to L^{-1}, as in the case of ideal conductivity, and the fluctuations of the vertical component increase with distance in accordance with the same law as in horizontal polarization, i.e. $\sigma_+ \sim L^3$. Finally, if the modulus R of the reflection coefficient is not close to unity, the fluctuations in this region must increase with the distance L more rapidly than L but more slowly than L^3.

By comparing the results obtained with experimental data it is possible to determine such important statistical characteristics as the mean square of fluctuations in the dielectric constant, the correlation radii in different directions, and so on. Thus, there is no doubt about the importance of making similar experimental investigations. The first results have already been obtained: in [4] it was shown that in accordance with theory the fluctuations in amplitude and phase of a horizontally polarized radiowave do not depend on the frequency and increase proportionally to L^3. In our opinion these investigations need to be supplemented by a study of fluctuations close to the interference minima of the mean field, of the height and frequency dependence of the fluctuations, etc.

Note that the effect characterized by a sharp increase in the relative fluctuations close to the interference minima and in the remote zone is connected not with an increase in the absolute fluctuations but with a decrease in the regular component of the field. From this point of view it is natural to expect that on taking into account the curvature of the boundary surface (for example, the curvature of the earth) outside the zone of direct visibility, where the regular component of the radiation field decreases exponentially with distance, the relative fluctuations will increase in accordance with an exponential law. The theoretical investigation of this

question is the subject of a separate report.

In conclusion we shall take the opportunity to thank S.Ya. Braude and A.V. Men' for their useful discussions which brought our attention to the problems treated in the article.

Bibliography

1. Chernov, L.A.: Rasprostraneniye voln v srede so sluchaynymi neodnorodnostyami (Propagation of waves in a medium with random inhomogeneities), Publ. AS USSR, M., 1958; Reports of the AS USSR, 98 (1954) 953; Akust. Zh., 3 (1957) 192; Obukhov, A.M.: Trans. AS USSR, Geophys. Ser., 2 (1953) 155; Krasil'nikov, V.A.; Obukhov, A.M.: Akust. Zh., 2 (1956) 107; Muchmore, R.B.; Wheelon, A.D.: Proc. IRE, 43 (1955) 1437, 1450; Tatarskiy, V.I.: Rep. AS USSR, 120 (1958) 289; ZhETF, 25 (1953) 74; Karavaynikov, V.N.: Akust. Zh., 3 (1957) 165.
2. Herbstrait, J.W.; Thomson, M.C.: Proc. IRE, 43 (1955) 1391. Deam, A.P.; Tannin, B.M.: Proc. IRE, 43 (1955) 1402.
3. Vvedenskiy, B.A.; Arenberg, A.G.: Rasprostraneniye ul'trakorotkikh voln (Propagation of ultrashort waves), Svyaz'izdat, M., 1934.
4. Men', A.V.; Gorbach, V.I.; Braude, S.Ya.: Radiofizika, 2 (1959) 388.
5. Kaner, E.A.: Radiofizika, in print.
6. Al'pert, Ya.L.; Ginzburg, V.L.; Feinberg, E.L.: Rasprostraneniye radiovoln (Propagation of radiowaves), GITTL, M., 1953.
7. Kaner, E.A.; Bass, F.G.: Rep. AS USSR, 127 (1959) 792.

Institute of radiophysics and electronics AS USSR

Submitted 19 Mar. 1959

THE CORRELATION OF ELECTROMAGNETIC FIELD FLUCTUATIONS IN A MEDIUM WITH RANDOM INHOMOGENEITIES ABOVE AN IDEALLY CONDUCTING PLANE.

Pages 565-572

by F.G. Bass & E.A. Kaner.

The authors establish space correlation functions for fluctuations in amplitude and phase in an electromagnetic field, propagated in a medium with random inhomogeneities above an ideally conducting plane.

Article [1] gave mean squares for fluctuations in amplitude and phase in an electromagnetic field in a medium with random inhomogeneities above an ideally conducting plane. However, these quantities do not give a complete description of the statistical properties of the electromagnetic field. The correlation relationships among amplitudes and phases of fields at different points in space are also important statistical characteristics. The phase and amplitude correlations are of interest not only from the point of view of applications; they can also be used to determine the correlation function between fluctuations in the dielectric constant $\delta\varepsilon$.

The correlation of amplitudes and phases of an electromagnetic field in free space has been investigated by a number of authors (see, for example, [2]). As was shown in [1], the propagation of radiowaves in a medium with random inhomogeneities above an ideally conducting plane has a number of special features, connected with the

interference structure of the average field. In this connection it is of interest to investigate the phase and amplitude correlation dependences taking into account the boundary surface.

All the results in the present article are based on the assumption that $\lambda \ll l \ll \sqrt{\lambda L}$, z. $z_0 \ll L$. .

1. General formulas for the correlation functions

If the fluctuating part of the electromagnetic field is much less than the regular component (remote from zeroes of the latter), then the expressions for fluctuations in phase and amplitude have the form:

$$\delta\varphi = (\xi_i \bar{E}_r - \xi_r \bar{E}_i)/|\bar{E}^2|; \tag{1.1}$$

$$\delta A/|\bar{E}| = (\xi_r \bar{E}_r + \xi_i \bar{E}_i)/|\bar{E}^2|. \tag{1.2}$$

We shall compute the correlations between relative amplitude fluctuations and phase fluctuations at different points 1 and 2 :

$$K(\delta\varphi_1, \delta\varphi_2) = \overline{\frac{\xi_{i1}\bar{E}_{r1} - \xi_{r1}\bar{E}_{i1}}{|E_1^2|} \frac{\xi_{i2}\bar{E}_{r2} - \xi_{r2}\bar{E}_{i2}}{|E_2^2|}}; \tag{1.3}$$

$$K(\delta A_1, \delta A_2) = \overline{\frac{\xi_{r1}\bar{E}_{r1} + \xi_{i1}\bar{E}_{i1}}{|\bar{E}_1^2|} \frac{\xi_{r2}\bar{E}_{r2} + \xi_{i2}E_{i2}}{|\bar{E}_2^2|}}. \tag{1.4}$$

It is also easily possible to find the composite amplitude-phase correlation. However, in the majority of interesting limiting cases this correlation function is small compared with those mentioned above and, moreover, does not give essentially new data compared with the results of investigating the correlations of

---

* The notation of [1] is followed throughout.

amplitudes and phases. Therefore we shall not proceed to compute the composite correlation.

Formulas (1.3) and (1.4) may be considerably simplified, if we take into account that in the remote zone ($D = 2L/k^2 \gg 1$) the real and imaginary parts of the expression

$$\overline{\xi_1 \xi_2} = \overline{\xi_{r1}\,\xi_{r2}} - \overline{\xi_{i1}\,\xi_{i2}} + i\left(\overline{\xi_{i1}\,\xi_{r2}} + \overline{\xi_{r1}\,\xi_{i2}}\right)$$

are $D/\ln D \gg 1$ times less than $\overline{\xi_1 \xi_2^*}$, i.e. in the approximation in question are equal to zero. Taking these relationships into account the correlations of phases and amplitudes are equal to each other :

$$K(\delta\varphi_1, \delta\varphi_2) = K(\delta A_1, \delta A_2) = K = \frac{\mathrm{Re}}{2|\bar{E}_1\bar{E}_2|}\left\{\overline{\xi_1 \xi_2^*} \exp\left|i(\varphi_2 - \varphi_1)\right|\right\} \tag{1.5}$$

($\varphi_1 - \varphi_2$ is the difference in phase of the regular components of the field in the points r_1 and r_2).

Thus, the phase and amplitude correlation functions are completely defined by the quantity $\overline{\xi_1 \xi_2^*}$.

According to [1],

$$\xi_{1\pm} = \xi_{\pm}(r_1) = k^2 p_{\pm} \int_0^{z'} dr'\, \delta\varepsilon(r')\, \varphi_{\pm}(r_1, r')\, \varphi(r', r_0). \tag{1.6}$$

We shall not take into account the deviation of the effective dielectric constant from its mean value, since in what follows we only consider small fluctuations in the amplitude and phase of the electromagnetic field. From (1.6) we get:

$$\overline{(\xi_1 \xi_2^*)}_{\pm} = k^4 |p_{\pm}^2| \int_0^{z'}\int_0^{z''} dr'\, dr'' \varphi_{\pm}(r_1, r')\, \varphi_{\pm}(r_1, r_0) \times \\ \times \varphi_{\pm}^*(r_2, r'')\, \varphi_{\pm}^*(r'', r_0)\, \overline{\delta\varepsilon(r')\, \delta\varepsilon(r'')}. \tag{1.7}$$

2. Transverse correlation

Let us consider the case in which the points $r_1(L; -b/2; z - d/2)$ and $r_2(L; b/2; z + d/2)$ lie in the plane $x = L$. We shall describe as "transverse" the correlation of fluctuations for such an arrangement of the points 1 and 2. $\overline{\xi_1 \xi_2^*}$ may then be worked out in complete analogy with the computation of $\overline{|\xi^2|}$ in /1/ and gives the following result:

$$\overline{(\xi_1 \xi_2^*)}_{\pm} = |p_{\pm}|^2 (4\pi)^{-2} \overline{\delta\varepsilon^2} k^2 L^{-1} \exp(-ikzd/l) \int_0^{\infty} d\xi \int_0^1 dt \{ W(\xi/l_{\perp}; bt/l_{\parallel}; td/l_{\perp}) \times \cos(kz_0 d/L) + 1/2\, W(\xi/l_{\perp}; bt/l_{\parallel}; (2zt + 2z_0(1-t))/l_{\perp}) \exp(ikz_0 d/L) + 1/2\, W(\xi/l_{\parallel}; bt/l_{\parallel}; 2|zt - z_0(1-t)|/l_{\perp}) \exp(-ikz_0 d/L) \pm \{ W(\xi/l_{\parallel}; bt/l_{\perp}; 2zt/l_{\perp}) \cos(2kzz_0/L) + 1/2\, W(\xi/l_{\parallel}; bt/l_{\parallel}; (2z_0(1-t) + td)/l_{\perp}) \exp(2ikzz_0/L) + 1/2\, W(\xi/l_{\parallel}; bt/l_{\parallel}; |2z_0(1-t) - td|/l_{\perp}) \exp(-2ikzz_0/L) \} \quad (2.1)$$

We have the following expressions for the amplitudes of the mean fields:

$$|\bar{E}_{1\pm}| = (|p_{\pm}|/4\pi L)[2(1 \pm \cos(2kz_0(z - d/2)/L))]^{1/2}; \quad (2.2)$$
$$|\bar{E}_{2\pm}| = (|p_{\pm}|/4\pi L)[2(1 \pm \cos(2kz_0(z + d/2)/L))]^{1/2}.$$

Substituting (2.1) and (2.2) in formula (1.5), after a few simple transformations we get:

$$K_{\pm} = \frac{1}{4} \frac{\overline{\delta\varepsilon^2} k^2 L}{|\cos(kzd_0/L) \pm \cos(2kzz_0/L)|} \int_0^{\infty} d\xi \int_0^1 dt \{ \cos(kz_0 d/L) \times \{ W(\xi/l_{\parallel}; bt/l_{\perp}; td/l_{\perp}) + 1/2\, W(\xi/l_{\perp}; bt/l_{\parallel}; 2(zt + z_0(1-t))/l_{\perp}) + 1/2\, W(\xi/l_{\perp}; bt/l_{\parallel}; 2|zt - z_0(1-t)|/l_{\perp}) \} \pm \cos(2kzz_0/L) \{ W(\xi/l_{\parallel}; bt/l_{\perp}; 2zt/l_{\perp}) + 1/2\, W(\xi/l_{\parallel}; bt/l_{\perp}; (2z_0(1-t) + td)/l_{\perp}) + 1/2\, W(\xi/l_{\perp}; bt/l_{\perp}; |2z_0(1-t) - td|/l_{\perp}) \} \} \quad (2.3)$$

Formula (2.3) completely solves the problem posed and shows that in the plane parallel to z = 0, when d = 0, the transverse correlation of phases and amplitudes occurs at $b \sim l_{\parallel}$, while, when b = 0, it is effective up to distances of the order of $d \sim l_{\perp}$.

However, to get comprehensive results it is necessary to investigate various limiting cases. The most interesting limiting case is that of distances between receivers which are large compared with the correlation radius. For small distances we get inconsiderable corrections to the mean squares of phases and amplitudes.

First let us consider the case of large b. Let $b \gg z, z_0, l_{\parallel}$, d and let $(kzz_0/L)^2$ not be small. Then it follows from (2.3) that

$$K_{\pm} = \overline{\delta\varepsilon^2} \frac{k^2 l_{\parallel}^2 L}{4b} \int_0^{\infty} \int_0^{\infty} d\xi\, dt \left[W(\xi;\ t;\ 0) + W\left(\xi;\ t;\ 2z_0 / l_{\perp}\right) \right]. \quad (2.4)$$

At the edge of the first interference lobe, where $(kzz_0/L)^2 \ll 1$, it is possible to introduce into (2.3) an expansion in series with respect to powers of $(kzz_0/L)^2$ and $(kz_0 d/L)^2$. (Note that when $(kzz_0/L)^2 \ll 1$ $(kz_0 d/L)^2 \ll 1$, since by definition $d \leqslant 2z$.) As a result the expression for K_+ coincides with (2.4) and that for K_- has the form:

$$K_- = \frac{1}{4b} \overline{\delta\varepsilon^2} k^2 l_{\parallel}^2 L \int_0^{\infty} \int_0^{\infty} d\xi\, dt \left| W(\xi; t; 0) - \right.$$

$$\left. (l_{\parallel} L t / kz_0 l_{\perp})^2\ W^{(2)}\ (\xi;\ t;\ 0) \right| \text{ при } (2z_0 \gg l_{\perp}); \quad (2.4a)$$

$$K_- = \frac{1}{2b}\ \overline{\delta\varepsilon^2} k^2 l_{\parallel}^2 L \int_0^{\infty} \int_0^{\infty} d\xi\, dt \left| W(\xi;\ t;\ 0) + \right.$$

$$\left. + (l_{\parallel} L t / k l_{\perp}^2 b)^2\ W^{(4)}\ (\xi;\ t;\ 0) \right| \text{ при } (2z_0 \ll l_{\perp}).$$

Here and below :

$$W^{(n)} = \frac{\partial^n}{\partial \varsigma^n}\ W(\xi;\ \eta;\ \varsigma).$$

Below we shall denote formulas relating to the case $(2kzz_0/L)^2 \ll 1$ (region of applicability of the so-called "square-law" formula of Vvedenskiy's) by means of primed figures, without mentioning them specially.

Note that in formula (2.4a) we may have different particular cases, depending on whether the quantities $(l_\parallel L/kz_0 b l_\perp)^2$ and $(l_\parallel L/k l_\perp^2 b)^2$ are large or small; if $2z_0 \gg l_\perp$, then

$$K_- = \frac{1}{4b}\overline{\delta\varepsilon^2} l_\parallel^2 L k^2 \int_0^\infty \int_0^\infty d\xi\, dt\, W(\xi;\, t;\, 0) \quad \text{for} \quad (l_\parallel L/k_0 b l_\perp)^2 \ll 1; \tag{2.4b}$$

$$K_- = -\frac{\overline{\delta\varepsilon^2}\, l_\parallel^4 L^3}{4b^3 z_0^2 l_\perp^2} \int_0^\infty d\xi \int_0^\infty dt\, t^2 W^{(2)}(\xi;\, t;\, 0) \quad \text{for} \quad (l_\parallel L/kz_0 b l_\perp)^2 \gg 1;$$

if $2z_0 \ll l_\perp$, then

$$K_- = \frac{1}{2b}\overline{\delta\varepsilon^2} l_\parallel^2 L k^2 \int_0^\infty \int_0^\infty d\xi\, dt\, W(\xi;\, t;\, 0) \quad \text{for} \quad (l_\parallel L/k l_\perp^2 b)^2 \ll 1; \tag{2.4c}$$

$$K_- = \frac{\overline{\delta\varepsilon^2} l_\parallel^4 L^3}{2b^3 l_\perp^4} \int_0^\infty \int_0^\infty d\xi\, dt\, t^2 W^{(4)}(\xi;\, t;\, 0) \quad \text{for} \quad (l_\parallel L/k l_\perp^2 b)^2 \gg 1.$$

We shall pass to a consideration of the dependence of the correlation function on height. Here we shall examine four limiting cases.

a) $z, z_0 \gg l_\perp$, b. We shall also put $d \ll 2z$. Then the formulas for $K_\pm$ have the following form:

$$K_\pm = \frac{1}{4} \frac{\overline{\delta\varepsilon^2} k^2 l_\parallel L \cos(kz_0 d/L)}{\cos(kz_0 d/L) \pm \cos(2kzz_0/L)} \int_0^\infty d\xi \int_0^1 dt\, W(\xi;\, bt/l_\perp;\, td/l_\perp). \tag{2.5}$$

Note that $K_\pm$ vanishes if the condition $(kz_0 d/L) = (2n+1)\pi/2$

(where n is an integer) is fulfilled.

When $(2kzz_0/L)^2 \ll 1$

$$K_+ = \frac{1}{8}\overline{\delta\varepsilon^2}k^2 l_\parallel L\int_0^\infty d\xi\int_0^1 dt\ W(\xi;\ bt/l\ ;\ td/l\ )\ ; \qquad (2.5a)$$

$$K_- = \frac{1}{8}\overline{\delta\varepsilon^2}\, l_\parallel\ l^3\,(zz_0)^2\int_0^\infty d\xi\int_0^1 dt\ W(\xi;\ bt/l_\parallel;\ td/l_\parallel). \qquad (2.5b)$$

When $b \gg l_\parallel$, $d \gg l_\perp$, the asymptotic of the integral J, entering into formulas (2.5), has the form:

$$J \sim l_\parallel/b \quad (b \gg d); \quad J \sim l_\perp/d \quad (b \ll d). \qquad (2.6)$$

b) $z, z_0 \ll l_\perp$. In this case we have the inequality $(2kzz_0/L)^2 \ll 1$ and

$$K_+ = \frac{1}{2}\overline{\delta\varepsilon^2}k^2 l_\parallel L\int_0^\infty d\xi\int_0^1 dt\ W(\xi;\ bt/l_\parallel;0); \qquad (2.7)$$

$$K_- = \frac{1}{2}\,\delta\varepsilon^2\, l_\parallel\ l_\perp^{-4}L^3\int_0^\infty d\xi\int_0^1 dt\ W^{(4)}(\xi;\ bt/l_\parallel;\ 0)\ t^2(1-t)^2. \qquad (2.7a)$$

When $b \gg l_\perp$ (2.7a) goes over into the second of the formulas (2.4b).

c) $z_0 \gg l_\perp$; $z \ll l_\perp$. Then

$$K_+ = K_- = \frac{1}{4}\overline{\delta\varepsilon^2}k^2 l_\parallel L\int_0^\infty d\xi\int_0^1 dt\ W(\xi;\ bt/l_\parallel;\ 0). \qquad (2.8)$$

If $(2kzz_0/L)^2 \ll 1$, then the expression for K_+ coincides with (2.8) but the formula for K_- has the following form :

$$K_- = \frac{1}{4}\overline{\delta\varepsilon^2}k^2 l_\parallel L\int_0^\infty d\xi\int_0^1 dt\,\{W(\xi;\, bt/l_\parallel;\, 0) - (Lt/kl_\perp z_0)^2 \times \tag{2.8a}$$

$$\times\, W^{(2)}(\xi;\, bt/l_\parallel;\, 0)\}.$$

— r) $z_0 \ll l_\perp$; $z \gg l_\perp, b$; $d \gg l_\perp, b$. Then

$$K_\pm = \frac{1}{8zd}\overline{\delta\varepsilon^2} l_\parallel l_\perp k^2 L(d+2z)\int_0^\infty\int_0^\infty d\xi\, d\varsigma\, W(\xi;\, 0;\, \varsigma). \tag{2.9}$$

At the edge of the first lobe K_+ coincides with (2.9) and K_- is equal to :

$$K_- = \frac{\overline{\delta\varepsilon^2}k^2 l_\parallel\, l_\perp L(d+2z)}{8zd}\left[\int_0^\infty\int_0^\infty d\xi\, d\varsigma\, W(\xi;\, 0;\, \varsigma) + \right. \tag{2.9a}$$

$$\left. + 2\,\frac{L^2}{k^2 z d l_\perp (d+2z)}\int_0^\infty d\zeta\, W(\xi;\, 0;\, 0)\right].$$

It is possible to draw certain conclusions from a consideration of these limiting cases. For vertical polarization the correlation is always proportional to $L\omega^2$. For horizontal polarization the correlation function K_- may be proportional to $L\omega^2$ or to L^3, in the latter case K_- being independent of the frequency. These conclusions, like the fact that transverse correlation occurs at distances of the order of the corresponding correlation radii, do not depend on the concrete form of the function W.

To conclude this section we shall introduce an expression for the correlation functions $K_\pm$ in the case where $b = 0$. On substituting in (2.3) $W(\rho) = \exp\left[-(\xi^2 \pm \eta^2)l_\parallel^{-2} - \varsigma^2 l_\perp^{-2}\right]$ we get:

$$K_{\pm} = \frac{\overline{\delta\varepsilon^2}\, k^2 L\, \bar{l}_{\parallel}\, \bar{l}_{\perp}}{4\,|\cos(kz_0 d/L)\quad \cos(2kzz_0/L)|}\left\{\left[\frac{\operatorname{erf}(d/l_{\perp})}{d} + \right.\right.$$

$$+\left.\frac{z\operatorname{erf}(2z/l_{\perp}) - z_0\operatorname{erf}(2z_0/l_{\perp})}{2(z^2 - z_0^2)}\right]\cos\left(\frac{kz_0 d}{L}\right) + \left[\operatorname{erf}(2z/l \quad 2z\right. \tag{2.10}$$

$$\left.\left. + \frac{d\operatorname{erf}(d/l_{\perp}) - 2z_0\operatorname{erf}(2z_0/l_{\perp})}{d^2 - 4z_0^2}\right]\cos\frac{2kzz_0}{L}\right\},$$

where

$$\operatorname{erf}(x) = \frac{2}{\sqrt{\pi}}\int_0^x \exp(-t^2)dt, \quad \bar{l} = l\frac{\sqrt{\pi}}{2}.$$

3. Longitudinal correlation

By longitudinal correlation we understand the correlation of fluctuations in two points, disposed on a single straight line in a plane parallel to the boundary surface, i.e. we assume that $z = z_0$. Moreover, for the sake of simplicity we shall consider that $z = z_0 \gg l_{\perp}$ and we shall also assign an explicit form to the correlation function of fluctuations in the dielectric constant $\delta\varepsilon^2 W(\rho)$:

$$W(\rho) = \exp\left|-(\xi^2 + \eta^2)\, l_{\parallel}^{-2} - \zeta^2 l_{\perp}^{-2}\right|. \tag{3.1}$$

The coordinates of the points 1 and 2 are then $(L,0;\ z_0)$ and $(L + \Delta,\ 0;\ z_0)$, $\Delta \ll L$.
Then from (1.7) we get:

$$(\xi_1 \xi_2^*)_{\pm} = \delta\varepsilon^2\left(\frac{k}{4\pi}\right)^2 |P_{\pm}|^2 \frac{\bar{l}_{\parallel}}{L}\exp(-ik\Delta)\times$$

$$\times\int_0^1 \frac{dt}{|(1 + i2\Delta t^2/kl_{\parallel}^2)(1 + i2\Delta t^2\, kl_{\perp}^2)|^{1/2}}. \tag{3.2}$$

If the correlation radii are the same ($l_{\parallel} = l_{\perp} = l$), then:

$$\overline{(\xi_1 \xi_2^*)}_{\pm} = |p_{\pm}|^2 \overline{\delta\varepsilon^2} \left(\frac{k}{4\pi}\right)^2 \frac{\overline{I}}{l} \exp\left[i\left(\frac{\pi}{4} - k\Delta\right)\right] \left(\frac{kl^2}{8\Delta}\right)^{1/2} \times \left\{ \ln\left[\frac{(1 + 4\Delta^2/k^2l^4)^{1/2}}{1 + 2\Delta/kl^2 - (4\Delta/kl^2)^{1/2}} \right] - i\left[\pi s\left(\frac{2\Delta}{kl^2} - 1\right) \times \operatorname{arctg} \frac{(4\Delta/kl^2)^{1/2}}{1 - 2\Delta/kl^2} \right] \right\},$$

where $s(x) = 1$ $(x > 0)$, $s(x) = 0$ $(x < 0)$.

It is evident from formulas (3.2) and (3.3) that longitudinal decorrelation occurs at distances of the order of kl^2, i.e. roughly at the same length as in an unbounded medium. In other words, longitudinal correlation extends to distances considerably exceeding the length of transverse correlation. It is possible to show that this general conclusion does not depend on the relationship between z_0 and $l_\perp$.

In the case in which the distance Δ between receivers is large compared with kl^2,

$$\overline{\xi_1 \xi_2^*} \quad |p|^2 \, \pi \overline{\delta\varepsilon^2} \frac{\overline{I}}{l} \left(\frac{k}{4\pi}\right)^2 \left(\frac{kl^2}{8\Delta}\right)^{1/2} \exp\left(-\frac{\pi i}{4} - ik\Delta \right) \qquad (3.4)$$

and the correlation of fluctuations decreases in inverse proportion to $\sqrt{\Delta}$.

Substituting formula (3.4) and the expression for the average field in (1.5), we get:

$$K_\perp = \frac{\pi}{8} \frac{\overline{\delta\varepsilon^2} k^2 l L}{|\cos(kz_0^2\Delta/L^2) \pm \cos(2kz_0^2/L)|} \left(\frac{kl^2}{\Delta}\right)^{1/2} \times \cos\frac{2kz_0^2\Delta}{L^2}. \qquad (3.5)$$

At the edge of the first lobe the expression for $K_{\pm}$ has the form :

$$K_{\pm} = \frac{\pi}{16}\overline{\delta\varepsilon^2}k^2\overline{l}L\left(\frac{kl^2}{\Delta}\right)^{1/2};$$

$$K_{\pm} = \frac{\pi}{16}\overline{\delta\varepsilon^2}\,\frac{\overline{l}L^3}{L_0^4}\left(\frac{kl^2}{\Delta}\right)^{1/2}.$$

In the region of lobed structure of the average field it follows from (3.5) that $K_{\pm}$ is an oscillating function of Δ and vanishes when

$$\Delta = (L^2/kz_0^2)(2n + 1/2)\,\pi/2.$$

In the region of applicability of Vvedenskiy's "square-law" formula, the oscillations disappear and with increase in Δ $K_{\pm}$ decreases as $1/\sqrt{\Delta}$. Note that in [3], where the longitudinal correlation of the fluctuations was worked out for free space, an error has been admitted in the course of integrating: the function of s (see (3.3)) was not taken into account, as a result of which the asymptotic expression for the correlation function proves incorrect ($K \sim \Delta^{-1}$).

In this article we have investigated phase and amplitude correlation assuming that the relative fluctuations in the electromagnetic field were small, i.e. remote from the zeroes of the average field. Phase and amplitude correlation functions close to the interference minima of the latter can be worked out in the same way as in [1]. However, it is easy to see that decorrelation of phases and amplitudes close to the zeroes of the average field enters the picture at the same distances as in the case under consideration. Actually, by virtue of the central limit theorem ξ_1 and ξ_2 are normally distributed. At distances, at which the fluctuations in fields at different points in space are practically uncorrelated, the joint distribution

function for the quantities ξ_1 and ξ_2 breaks down into the product of the distribution functions of ξ_1 and ξ_2. Accordingly, the decorrelation of any quantities, depending on ξ_1 and ξ_2, occurs at the same distances as those at which the electromagnetic field is decorrelated.

Bibliography

1. Kaner, E.A.; Baos, F.G.: Radiofizika, 2 (1959) 553.
2. Chernov, L.A.: Rasprostraneniye voln v srede so sluchaynymi neodnorodnostyami (Propagation of waves in a medium with random inhomogeneities), Publ. AS USSR, M., 1958.
3. Karavaynikov, V.N.: Akust. Zh., 3 (1957) 165.

Institute of radiophysics and electronics AS USSR

Submitted 19 Mar. 1959.

ON THE INFLUENCE OF THE FLICKER EFFECT ON SELF-OSCILLATOR LINE-WIDTH

Pages 573-580

by V.S. Troitskiy.

It is shown that the effect of flicker noise is not directly connected with the non-isochronism of the oscillator and occurs only when there is a dependence of the frequency on the grid transconductance.

Article [1] gave a method of calculation, which made it possible to take into account the effect of periodic unsteadiness in tube noise on fluctuations in the amplitude and frequency of the oscillations of a self-escillator, using a first approximation in the solution of the nonlinear problem.

In this article the method referred to is used to analyze fluctuations in a concrete self-oscillator circuit, while taking into account a second approximation in the solution of the dynamic problem. This proves essential to an explanation of the influence of the flicker effect on the spectral line-width of a self-oscillator. An attempt is made to calculate the effect of flicker noise from fluctuations in the dynamic capacitance of the oscillator tube, which, as is known, depends on the transconductance and the operating regime [2]. Although some of the results of the effect of flicker noise obtained could be arrived at quasi-statically, nevertheless, the inclusion of slow fluctuations in the general scheme of calculation

appeared to us expedient, especially when it is necessary to take into account the correlation of factors acting in different ways.

1. The general relationships

We shall consider an oscillator arrangement with a plate circuit, the capacitance of which is equal to $C(t) = C_0 + \varkappa(t)$ (where $\varkappa(t)$ is the fluctuating part of the capacitance), while $\varkappa \ll C_0$ and $\overline{\varkappa} = 0$. The equation for the current x in the inductive branch of the circuit, taking into account its thermal e.m.f., $\xi_0(t)$, has the following form:

$$L\frac{d^2x}{dt^2} + r\frac{dx}{dt} + \frac{d}{dt}\left(\frac{q}{C}\right) = \frac{d\xi_0}{dt}.$$

Taking into account that

$$q = \int (x - J_a)\,dt;$$

$$\frac{d}{dt}\left(\frac{q}{C}\right) = \frac{x}{C} - \frac{1}{C}J_a - \frac{q}{C^2}\frac{dC}{dt} \simeq \frac{x}{C} - \frac{1}{C}J_a + \frac{L}{C}\frac{dx}{dt}\frac{dx}{dt},$$

we finally get:

$$\frac{d^2x}{dt^2} + \left(\frac{r}{L} + \frac{\varkappa}{C}\right)\frac{dx}{dt} + \omega^2 x = \frac{1}{L}\frac{d\xi_0}{dt} + \omega^2 J_a(t), \qquad (1)$$

where $\omega^2 = 1/L\,(C_0 + \varkappa)$ and $J_a(t)$ is the instantaneous value of the total plate current:

$$J_a(t) = J_a(t) + \xi_1(t)\sqrt{J_a\gamma_1} + \xi_2(t)\sqrt{J_a\gamma_2}. \qquad (2)$$

Here $\overline{J_a}$ is the dynamic value of the plate current, $\xi_1\sqrt{\overline{J_a}\gamma_1} = i_D(t)$ is the shot-noise current and $\xi_2 J_a\sqrt{\gamma_2} = i_\Phi(t)$ is the flicker-noise current of the tube, while γ_1 and γ_2 are depression factors, allowing for the reduction in noise in the presence of a space charge and $\xi_1(t)$ and $\xi_2(t)$ are random steady-state functions. It is easy to see that if the spectral densities of these

functions have the values

$$\overline{\xi_1^2}(\Omega) = 2e; \quad \overline{\xi_2^2}(\Omega) = \varsigma(\Omega), \tag{3}$$

where e is the charge of an electron, then, with the adopted notation $i_D(t)$ and $i_\phi(t)$, for a direct plate current $\overline{J_a}$ we get the familiar expressions for the spectral densities:

$$\overline{i_a^2}(\Omega) = \overline{i_a^2}(f)/\Delta f = \overline{\xi_1^2}(\Omega)\, J_a\, \gamma_1 = 2e\, \overline{J_a}\, \gamma_1;$$

$$\overline{i_\phi^2}(\Omega) = \overline{\xi_2^2}(\Omega)\, \overline{J_a^2}\, \gamma_2 = \overline{J_a^2}\, \gamma_2\, \varsigma(\Omega),$$

where $\varsigma(\Omega) = mF^{-\lambda}$ is a function of the form of the flicker-noise spectrum. The quantity m and the index λ depend on the individual properties of the tube; ordinarily $1 \leqslant \lambda \leqslant 2$ and m is such that $i_\phi^2(\Omega)$ becomes much less than the spectral density of the shot-noise even for frequencies $F = 10^3 - 10^4$ cps [7].

For an alternating $\overline{J_a}$ the expressions for $i_D(t)$ and $i_\phi(t)$ are, obviously, preserved but their spectra will present other relationships. Note that writing the flicker-noise current in the form $i_\phi(t) = \overline{J_a}\sqrt{\gamma_2}\ \xi_2(t)$ in the presence of self-oscillations is equivalent to assuming that the parameters of the tube grid characteristic undergo fluctuations. Actually, in a first approximation the plate current $\overline{J_a} = J_0 + J_1 \sin \omega t = J_0 + SV_D \sin \omega t$, where $J_1 = SV_D$ is the first harmonic of the plate current, V_D is the amplitude of voltage at the grid and S is the transconductance. Then

$$i_\phi(t) = \overline{J_a}\sqrt{\gamma_2}\,\xi_2(t) = J_0\sqrt{\gamma_2}\,\xi_2 + S\sqrt{\gamma_2}\,\xi_2\, V_a \sin \omega t =$$

$$= \Delta J_0(t) + \Delta S(t)\, V_a \sin \omega t,$$

where $\Delta J_0(t) = J_0\, \xi_2 \sqrt{\gamma_2}$ and $\Delta S(t) = S\, \xi_2 \sqrt{\gamma_2}$ are the fluctuations in the direct component and the transconductance. This means that the flicker-noise current is the result of random swinging of the whole tube characteristic about its point of intersection with

the abscissa. For a small linear element of the static tube characteristic about a given point the flicker effect reduces to the displacement of the element by $\Delta J_0 = J_0 \xi_2 \sqrt{\gamma_2}$ with respect to the current axis and its rotation by $S \xi_2 \sqrt{\gamma_2} = \Delta S$ in accordance with the same random law.

In the more general case it is possible not to assume complete correlation between $\Delta J_0(t)$ and $\Delta S(t)$, considering for example that there is a supplementary uncorrelated part of the displacement current, i.e. $\Delta J_0(t) = J_0 \xi_2 \sqrt{\gamma_2} + J_0 \xi_3$. However, as will appear below, noise, proportional to the direct component of the plate current, does not affect either amplitude or frequency fluctuations and, consequently, may in general be disregarded.

Since flicker-noise is connected with transconductance fluctuations, one of the possible ways in which it may affect frequency is through fluctuations in the dynamic capacitance of the tube. For the sake of generality we shall assume that fluctuations in dynamic capacitance are only partially correlated with the flicker-noise current, i.e. $\varkappa(t) = \Delta C \sqrt{\gamma_2} \xi_2 + \delta C \xi_3$, where ξ_3 is a certain random function, having a spectrum in the low-frequency range and taking in all other causes of fluctuations in the dynamic capacitance (due to power supply conditions, for example).

Substituting $\omega^2 \simeq \omega_0^2 \left(1 - \frac{\Delta C}{C_0} \sqrt{\gamma_2} \xi_2 - \frac{\delta C}{C_0} \xi_3\right)$

and expression (2) in (1), we get :

$$\frac{d^2x}{dt^2} + \omega_0^2 x = \mu f(x, \dot{x}) + \mu^2 \xi(t, x, \dot{x}),$$

$$\mu f(x, \dot{x}) = -(\omega_0/Q)\, \dot{x} + \omega_0^2 \overline{J}_a(t); \qquad (4)$$

where

$$\overline{J}_a(t) = F(x, \dot{x});$$

$$\mu^2 \xi(t, x, \dot{x}) = 1/l - d\xi_0/dt + \omega_0^2 (\Delta C/C_0) \sqrt{\gamma_2} \xi_2 + x \omega_0^2 (\delta C/C_0) \xi_3 +$$

$$+ \omega_0^2 \sqrt{\overline{J}_a \gamma_0} \xi_1 + \omega_0^2 \overline{J}_a \sqrt{\gamma_2} \xi_2$$

(the term $\dot{\varkappa}\dot{x}/C_0$ is very small compared with the others as a result of the slowness of the variation in $\varkappa(t)$ and has therefore been omitted).

An equation in the form of (4) describes fluctuations in a self-oscillator with one degree of freedom. It differs from equations previously investigated [3,4] in the dependence of the random force on the state of the system. The calculation of the resulting periodic unsteadiness of the noise leads to qualitatively new results in investigating the effect of tube noise on fluctuations in oscillation.

In article [1] (4) is solved with the aid of a first approximation of the solution of the dynamic problem. It is expedient to consider a more accurate solution, using a second approximation in the solution of the dynamic problem. This question has not been dealt with in the literature. (In Rytov's method [4] regular phase and amplitude corrections of the second order are obtained but for the noise discussed by the author, acting under steady-state conditions, their effect on the fluctuations is unimportant). Our solution of (4) will be based on the use of a method of solving nonlinear problems in the theory of oscillations, developed in [5] for an autonomous oscillatory system, showing, however, only the manner of solving the problem and quoting the final conclusions (without the laborious intermediate calculations).* The validity of applying the above method to the solution of the non-autonomous equation (4), when the effective force, moreover, is known to contain a Fourier component with a frequency, equal to the resonance frequency of the circuit (case of "resonance"), requires proof. However, it is clear that thanks to the statistical properties of

---

* The method, developed in [5], was also used in [6] for solving an oscillatory equation of the first order, containing a random quantity.

the force and its Fourier components it cannot lead to a systematic deviation of the amplitude of the system from its value in the absence of the force even in the "resonance" case. A rigorous treatment of the question* shows the correctness of the calculations, if the random force is at least of the order of μ.

In accordance with [5] we shall seek a solution of (4) in the form $x = a\cos\psi + u_1(a,\psi)$, where a is the amplitude, ψ the phase of the oscillation and $u_1(a,\psi)$ is a correction of the second order to the solution of first approximation, representing its nearest harmonic.

Making use of [5] it is possible to show that

$$\frac{da}{dt} = \mu A_1(a) + \mu^2 A_2(a) - \frac{\mu^2}{2\pi\omega_0}\int_0^{2\pi} \xi(t, a\cos\psi, \ldots)\sin\psi\, d\psi;$$

$$\frac{d\psi}{dt} = \omega_0 + \mu B_1(a) + \mu^2 B_2(a) - \frac{\mu^2}{2\pi a\omega_0}\int_0^{2\pi} \xi(t, a\cos\psi, \ldots)\cos\psi\, d\psi,$$

where μA_1, μB_1, $\mu^2 A_2$ and $\mu^2 B_2$ are known functions (see [5], p. 58). Substituting here $a = a_0(1 + \alpha)$ and $\psi = \omega_0 t + \vartheta_1 + \varphi(t)$, where $\alpha(t)$, $\varphi(t)$ are functions of the amplitude and phase fluctuations, and expanding A(a) and B(a) in series with respect to the small quantity $a_0\alpha$ [3], after certain simple transformations we get:

$$\frac{dx}{dt} = (p_1 + p_2)x - \frac{\mu^2}{2\pi\omega_0 a_0}\int_0^{2\pi} \xi(t, a_0\cos\psi, \ldots)\sin\psi\, d\psi;$$

$$\frac{d\vartheta}{dt} = \nu(t) = (\Delta_1 + \Delta_2)\alpha - \frac{\mu^2}{2\pi\omega_0 a_0}\int_0^{2\pi} \xi(t, a_0\cos\psi, \ldots)\cos\psi\, d\psi, \qquad (5)$$

where the functions $p_1 = \mu dA_1/da$; $p_2 = \mu^2 dA_2/da$; $\Delta_1 = a_0\mu dB_1/da$; $\Delta_2 = a_0\mu^2 dB_2/da$ are taken for the value $a = a_0$.

* Computed by V.N. Nikonov.

When $p_2 = 0$, $\Delta_2 = 0$ expression (5) coincides with the corresponding expression introduced in [1].

2. Calculation of fluctuations

Taking the cubic characteristic of the tube $J_a = SV_D - S_1 V_D^3$ we get, in accordance with (4):

$$\ddot{x} + \omega_0^2 x = \dot{x}h - (\dot{x})^3 b + \xi(t, x, \dot{x}),$$

where

$$h = -(\omega_0/Q) + \omega_0^2 SM; \quad b = \omega_0^2 S_1 M^3;$$

$$\xi(t, x, \dot{x}) = (1/L)\, d\, \xi_0/dt + x\, \xi_2\, \omega_0^2 (\Delta C/C_0) + x\, \xi_3\, \omega_0^2 (\delta C/C_0) +$$

$$+ \xi_1\, \omega_0^2 \sqrt{\overline{J_a}\, \gamma_1} + \xi_2\, \omega_0^2 \overline{J_a} \sqrt{\gamma_2},$$

while

$$\overline{J_a} = J_0 + SM\dot{x} - S_1 M^3 (\dot{x}^3). \tag{6}$$

To the first approximation $x = a \cos \omega_1 t$, $\omega_1 = \omega_0 + B_1(a)$ there correspond the values :

$$A_1(a) = \frac{a}{2}\left(h - \frac{3}{4}\omega_0^2 a^2 b\right); \quad B_1 \equiv 0 \quad (\Delta_1 \equiv 0); \quad p_1 \equiv -h.$$

For the second approximation $x = a \cos \omega_2 t + (\omega_0 a^3 b/32) \sin 3\omega_2 t$

$$B_2(a) = \frac{1}{8}\left[\frac{9}{32} b^2 a^4 \omega_0^3 - \frac{h^2}{\omega_0}\right]; \quad B_2(a_0) = -\frac{h^2}{16\omega_0}; \quad \Delta_2 = \frac{p_1^2}{4\omega_0} \tag{7}$$

$$\omega_2 = \omega_0 + B_2(a_0); \quad A_2 \equiv 0; \quad p_2 \equiv 0.$$

Note that the second-order frequency correction $B_2(a_0)$ depends on the transconductance S_1.

We shall put (6) into the expression for $\xi(t,x)$; then neglecting small nonlinear terms we shall have:

$$\xi(t, a_0 \cos\psi) = (1/l)\, d\xi_0/dt + a_0 \cos\psi \xi_2 \sqrt{\gamma_2}\, \omega_0^2 (\Delta C/C_0) +$$

$$+ a_0 \cos\psi \xi_3\, \omega_0^2 (\delta C/C_0) + \xi_1 \omega_0^2 \sqrt{(J_0 - SMa_0\, \omega_0 \sin\psi)\, \gamma_1} +$$

$$+ \xi_2\, \omega_0^2 \sqrt{\gamma_2}\, (J_0 - SMa_0\, \omega_0 \sin\psi).$$

Substituting this expression in (5), in the right-hand member we get integrals of products of random functions and periodic functions of the form $\xi \sin n\psi$, $\xi \cos n\psi$ $(n = 0,1,2,\ldots)$. Since the frequency of oscillations in radiofrequency oscillators lies outside the limits of the flicker-noise band,

$$\int_0^{2\pi} \xi_2 \begin{pmatrix} \cos n\psi \\ \sin n\psi \end{pmatrix} d\psi = 0$$

where $n = 1,2,\ldots$. The remaining products can be integrated, since the frequencies in their spectrum may be as low as desired [1].

As a result we get :

$$\frac{d\alpha}{dt} = p_1 \alpha - \frac{1}{a_0 \omega_0 L} \frac{d\xi_0}{dt} \sin\omega_2 t - \frac{\omega_0}{a_0} \sqrt{\gamma_1} \sqrt{J_0 - J_1 \sin\omega_2 t}\; \xi_1 \sin\omega_2 t +$$

$$+ \frac{\omega_0}{2a_0} J_1 \sqrt{\gamma_2}\, \xi_2;$$

(8

$$\nu(t) = \Delta_2 \alpha - \frac{1}{a_0 \omega_0 L} \frac{d\xi_0}{dt} \cos\omega_2 t -$$

$$- \frac{\omega_0}{a_0} \sqrt{\gamma_1} \sqrt{J_0 - J_1 \sin\omega_2 t}\; \xi_1 \cos\omega_2 t - \frac{\omega_0 \Delta C}{2C_0} \sqrt{\gamma_2}\, \xi_2 - \frac{\omega_0 \delta C}{2C_0} \xi_3.$$

It is clear from this expression that the flicker-noise does not act directly on the frequency of the oscillations. This effect, apart from the obvious capacitance effect, is due only to the non-isochronism of the oscillator. In fact, by virtue of the linearity of equations (8) the functions of frequency and amplitude fluctuations due to the flicker effect (capacitance fluctuations are not taken into account) will be defined by the equations:

$$\frac{d\alpha_\Phi}{dt} = p_1 \alpha_\Phi + \frac{\omega_0}{2a_0} J_1 \sqrt{\gamma_2}\,\xi_2; \quad \nu_\Phi(t) = \Delta_2 \alpha_\Phi .$$

Denoting the spectral density of the fluctuations in amplitude and frequency, produced by the flicker effect, by $w_{\alpha\Phi}$ and $w_{\nu\Phi}$ respectively and bearing in mind expressions (3), (7) and $a_0 = J_1 Q$, where Q is the Q-factor of the circuit, we get:

$$w'_{\nu\Phi} = \Delta_2^2\, w_{\alpha\Phi}(\Omega) - \Delta_2^2 \frac{\omega_0^2}{4Q^2} \frac{\gamma_2}{p_1^2 + \Omega^2} \simeq \frac{\gamma_2 \varsigma(\Omega)}{64} \frac{p_1^2}{Q^2}. \qquad (9)$$

In proceeding to this expression it was assumed that $a_0 = J_1 Q$, where Q is the Q-factor of the circuit.

In order to evaluate these quantities we shall introduce a complete solution of (8), which can be found by means of a Fourier expansion. In this connection we assume that γ_1 and γ_2 do not depend on the current (on time). Simple, but rather laborious calculations give (see [1]):

$$w'_\alpha(\Omega) = \frac{1}{p_1^2 + \Omega^2} \left\{ \frac{(\omega_2 - \Omega)^2}{4a_0^2 \omega_0^2} \bar{\xi}_0^2 (\omega_2 - \Omega) + \frac{(\omega_2 + \Omega)^2}{4a_0^2 \omega_0^2 L^2} \xi_0^2 (\omega_2 + \Omega) + \right.$$
$$\left. + \frac{\omega_0^2}{2a_0^2} J_0 \bar{\xi}_1^2 (\omega_2) + \frac{\omega_0^2}{4a_0^2} J_1^2 \bar{\xi}_2^2 (\Omega) \right\}; \qquad (10)$$

$$w_\nu(\Omega) = \frac{(\omega_2 - \Omega)^2}{4a_0^2 \omega_0^2 L} \left(1 + \frac{2\Omega\Delta_2}{p_1^2 + \Omega^2} + \frac{\Delta_2^2}{p_1^2 + \Omega^2} \right) \bar{\xi}_0^2 (\omega_2 - \Omega) +$$
$$+ \frac{(\omega_2 + \Omega)^2}{4a_0^2 \omega_0^2 L^2} \left(1 - \frac{2\Omega\Delta_2}{p_1^2 + \Omega^2} + \frac{\Delta_2^2}{p_1^2 + \Omega} \right) \bar{\xi}_0^2 (\omega_2 + \Omega) +$$
$$+ \frac{\omega_2^2}{2a_0^2} J_0 \gamma_1 \left(1 + \frac{\Delta_2^2}{p_1^2 + \Omega^2} \right) \bar{\xi}_1^2 (\omega_2) + \frac{\omega_0^2 \delta C^2}{4C_0} \xi_3^2 (\Omega) + \qquad (11)$$
$$+ \frac{\Delta_2^2}{p_1^2 + \Omega^2} \frac{J_1^2 \omega_0^2 \gamma_2}{4a_0^2} \bar{\xi}_2^2 (\Omega) + \frac{\omega_0^2 \Delta C^2}{4C_0^2} \gamma_2 \bar{\xi}_2^2 (\Omega) + \frac{2p_1 \Delta_2}{p_1^2 + \Omega^2} \frac{\omega_0^2 J_1 \Delta C}{4a_0 C_0} \gamma_2 \bar{\xi}_2^2 (\Omega).$$

In the last expression the terms in Δ_2 and Δ_2^2 reflect the effect of fluctuations in amplitude on fluctuations in frequency, which is observed during non-isochronism of the oscillator. The first, second and third terms determine the fluctuations in frequency due to thermal and shot-effect noise. The fifth, sixth and seventh terms are linked with the action of flicker noise; the fifth term is connected with the effect of amplitude fluctuations on the frequency, the sixth with the effect of fluctuations in capacitance and the seventh with the intercorrelation of these processes. Since $p_1 < 0$, this term is negative and may compensate to some degree the action of the fifth and sixth terms.

Expressions (10) - (11) can be substantially simplified, by taking into account the fact that the terms of the form $2\Omega\Delta_2/(p_1^2 + \Omega^2)$ and $\Delta_2^2/(p_1^2 + \Omega^2)$ are ordinarily small compared with unity and can be neglected; in view of the sharp limitation of the spectrum of $\xi_2^2(\Omega)$ to the low-frequency range it is possible to put $p_1^2 + \Omega^2 = p_1^2$ in the fifth and sixth terms. Also taking into account that at room temperature T $\xi_0^2(\omega_2 + \Omega) = \xi_0^2(\omega_2 - \Omega) = 4kTr$ for radiofrequencies and that $a_0 = J_1 Q$, $a_0^2 r = 2P$ (P is the power of the oscillations produced by the oscillator), we get the final expressions:

$$w_1(\Omega) = \frac{1}{p_1^2 + \Omega^2}\frac{\omega_0^2}{Q^2}\left|\frac{kT}{P} + \frac{J_0 e\,\gamma_1}{J_1^2} + \frac{\gamma_2\zeta(\Omega)}{4}\right|; \qquad (12)$$

$$w_1(\Omega) = \frac{\omega_0^2}{Q^2}\left|\frac{kT}{P} + \frac{J_0 e\,\gamma_1}{J_1^2}\right| + \left|\frac{p_1}{8Q} + \frac{\omega_0 \Delta C}{2C_0}\right|^2 \gamma_2\zeta(\Omega). \qquad (13)$$

We shall evaluate the effect of different kinds of noise on fluctuations in frequency in an amplifier tube oscillator with the following parameters: $f_0 = 10^6$ cps, $Q = 50$, $J_1 = 7$ ma, $J_0 = 10$ ma, $C_0 = 200$ mumufarads and, consequently, $r = 16$ ohms, $P = ra_0^2/2 \approx 1$ watt. Let $\gamma_1 = 0.7$ and $\gamma_2\zeta(\Omega) = \gamma_{2m}F^{-2}$, where $\gamma_{2m} = 10^{-13}$

cps, $p_1 \cong -\omega_0/Q$ and $\Delta C = 2.10^{-3}$ mumufarads. In accordance with (13),

$$\omega_1 = 6\cdot 10^{-11} + 4\cdot 10^{-7} + (-300 + 120)^2\, 10^{-13}\, f^{-2}.$$

Hence it is clear that in the case in question the two flicker fluctuation terms are of the same order of magnitude. Without taking into account capacitance fluctuations, the flicker-width of the spectrum for an observation time exceeding $2\pi/\delta = 100$ secs will be equal [1] to $\Delta F_{fl} = (p_1/8\pi Q)\sqrt{m/2\delta} = 10^{-4}$ cps, whereas the natural width $\Delta F_e \cong 3\cdot 3.10^{-8}$ cps.

In conclusion it should be noted that not every non-isochronism of the oscillator leads to the flicker effect influencing the frequency of the oscillations. In fact, we shall consider the same oscillator setup but with a quadripole included in the grid circuit to displace the phase of the voltage through a small angle ρ. Then, the oscillator is not isochronous, even to a first approximation, since the first-order correction to the frequency $B_1(a)$ depends on the amplitude of the oscillation. In this case:

$$B_1(a) = \frac{1}{2} S\omega_0^2 M \sin\rho - \frac{3}{8} M^3 S_1 \omega_0^4 \sin\rho\, a^2;$$

$$A_1(a) = \frac{a}{2}\left[-\frac{r}{L} + M\omega_0^2 S\cos\rho + \frac{3}{4} S_1 M^3 \omega_0^4 a^2 \cos\rho\right].$$

However, this does not lead to fluctuations in frequency due to the flicker effect, since, as is clear from the expression for $B_1(a)$, the latter acts on the frequency through fluctuations in the transconductance (direct action) and fluctuations in amplitude, governed, in their turn, by fluctuations in the transconductance. Assuming that $S = S_0 + \Delta S$ and making a quasi-static calculation, it is possible to show qualitatively that both effects are mutually compensating. If $A_1(a) = 0$, then

$$a^2 = \left(-\frac{r}{l} + MS_0\omega_0^2 \cos\rho + M\omega_0^2 \cos\rho\Delta S \right) \left(\frac{3}{4} S_1 M^3 \omega_0^4 \cos\rho \right)^{-1};$$

substituting this in $B_1(a)$ we get:

$$\Delta B_1 = B_1 - \frac{1-r}{2-l} \operatorname{tg}\rho \quad \frac{1}{2}\omega_0^2 M \sin\rho\Delta S - \frac{1}{2}\omega_0^2 M \sin\rho\Delta S = 0,$$

which it was required to prove.

More rigorously the absence in the first approximation of the effect of flicker-noise in an oscillator circuit with phase displacement in the grid can be demonstrated by using the general accurate solution for fluctuations of frequency in this circuit presented in [1] (formulas (25), (26)), which, somewhat transformed (taking into account (23)), for the part of the spectral density connected with flicker-noise, can be written in the form*:

$$w_{\nu\varphi} = \frac{\omega_0^2}{4Q^2} \left| \cos^2\beta_1 + \frac{p_1\Delta_1 \sin^2\beta_1}{p_1^2 + \Omega^2} + \frac{\Delta_1^2 \sin^2\beta_1}{p_1^2 + \Omega^2} \right| \gamma_2 \zeta(\Omega), \qquad (14)$$

where β_1 is the angle of phase displacement between the current in the inductive branch of the circuit and the first harmonic of the plate current. For the setup in question $\beta_1 = \rho + \pi/2$ and, moreover, $\Delta_1 = p_1 \tan\rho$; therefore,

$$w_{\nu\varphi} = \frac{\omega_0}{4Q^2} \left[\sin^2\rho - \frac{2p^2\sin^2\rho}{p^2 + \Omega^2} + \frac{p^2\sin^2\rho}{p^2 + \Omega^2} \right| \gamma\zeta(\Omega)$$

$$= \frac{\omega_0^2}{4Q^2} \frac{\Omega^2}{(p_1^2 + \Omega^2)} \gamma_2\zeta(\Omega).$$

Since $\zeta(\Omega) \sim \Omega^{\lambda}$, $\lambda \leqslant 2$, in this case the flicker-noise does not form a spectrum of frequency fluctuations increasing as $\Omega \to 0$ and,

---

* There was a printer's error in formula (26) [1]; as can be seen from (25) $p\Delta \sin 2\beta_1$ should have been given instead of $p\Delta\cos^2\beta_1$.

consequently, does not lead to a broadening of the line*. Thus, for the flicker effect to influence the frequency it is necessary that the latter depend on the transconductance. A solution of first approximation, evidently, does not give this dependence, i.e. does not reflect the features of the oscillator which are of interest in connection with this particular question.

The author wishes to thank A.N. Malakhov for his helpful criticism and S.M. Rytov for reviewing the manuscript as well as V.N. Nikonov for assistance with the calculations.

Bibliography

1. Troitskiy, V.S.: Radiofizika, 1, 1 (1958) 20.
2. Shitikov, G.T.: Radiotekhnika, 10, 12 (1955) 54.
3. Bershtein, I.L.: Trans. AS USSR, Phys. Ser., 14 (1950) 145.
4. Rytov, S.M.: ZhETF, 29, (1955) 301, 315.
5. Bogolyubov, N.N.; Mitropol'skiy, Yu.A.: Asimptoticheskiye metody v teorii nelineynykh kolebaniy (Asymptotic methods in the theory of nonlinear oscillations), GITTL, M., 1958.
6. Tikhonov, V.N.; Amiantov, I.N.: Radiotekhnika i Elektronika, 1, (1958) 428.
7. Malakhov, A.N.: Radiotekhnika i Elektronika, 4 (1959) 54.

Radiophysics Research Institute
Gor'kiy University

Submitted 10 Apr. 1959.

* In [1] the expression (14) for $\omega_{\nu\varphi}$ was incorrectly discussed, as p_1, Δ_1 and β_1 were considered independent to a known extent. My attention was brought to this and the singular compensation of the action of flicker-noise in the solution of first approximation by A.N. Malakhov.

ON THE SPECTRUM OF THE E.M.F. INDUCED BY PERIODIC REVERSAL OF FERROMAGNETIC POLARITY

Pages 581-587

by K.A. Goronina & A.A. Grachev.

A report is given on the results of experiments in connection with an investigation of the continuous spectrum of the induced e.m.f. A comparison is made between the spectrum of the induced e.m.f. and the shot-noise spectrum.

The spectrum of the e.m.f. induced by reversing the polarity of a ferromagnetic by means of a periodic field contains harmonics, multiples of the reversal frequency, and a continuous spectrum. We shall call the continuous component of the induced e.m.f. spectrum magnetic noise. The presence of magnetic noise shows that the process of polarity reversal is not strictly periodic.

It is necessary to study the continuous spectrum in order to get data for determining the threshold of sensitivity of magnetic amplifiers and probes; moreover, we may thus hope to get new information on the processes of reversal of polarity in ferromagnetics. There are numerous experimental and theoretical articles on this question [1-10]. Biorci and Pescetti note [9] that the value for the spectral density of magnetic noise, observed in their experiments, and its dependence on the frequency agree with magnetic noise calculations made by the same method as used to calculate the shot-noise in electron tubes. Similar calculations are made in

[7 1,6 7]. The spectral density thus obtained is constant, starting from zero frequency to frequencies comparable with $1/\tau_0$, where τ_0 is the duration of the e.m.f. pulses occurring in Barkhausen jumps. The magnetic noise spectrum, measured in [7 10 7], has another character: the spectral density increases with increase in frequency; the experimental curves, illustrating the dependence of the spectral power density G on the frequency f, at which the spectral density is measured, are extrapolated to the value G = 0 for f = 0. (We shall call f the spectrum observation frequency as distinct from the polarity reversal frequency F). A spectrum of this nature was also observed for materials investigated by Biorci and Pescetti. The ranges of observation frequencies in the two studies overlapped. In the range of frequencies, where, according to [7 9 7], the spectral density is constant, according to [7 10 7] it grows several times less when the observation frequency is reduced. One gets the impression that the experimental data are contradictory. It is not clear whether it is possible to treat magnetic noise like shot-noise. Bearing in mind this state of things we shall present the results of our latest experiments and compare them with the results of other authors.

If we denote the induced e.m.f. at the moment of time t by u(t), then it is possible to write an expression which constitutes a definition of the spectral power density :

$$G(f) = \lim_{\theta \to \infty} \frac{1}{2\theta} \left| \int_{-\theta}^{\theta} u(t)\, e^{i2\pi ft}\, dt \right|^2 ; \qquad (1)$$

here the horizontal line denotes averaging with respect to the ensemble of realizations of the random function u(t).

For the spectral density at zero frequency this expression takes the form:

$$G(0) = \lim_{\theta \to \infty} \frac{1}{2\theta} \overline{\left| \int_{-\theta}^{+\theta} u(t)\, dt \right|^2}.$$

If we reckon that $\int_{-\theta}^{+\theta} u(t)\, dt$ is equal to the change in flux over the interval of time from $-\theta$ to $+\theta$ and, accordingly, will be a finite quantity for any θ, we get $G(0) = 0$ independently of the specimen being investigated and the other experimental conditions. As already pointed out, this conclusion is in conformity with experiment [10]. In order to establish whether the results of Biorci and Pescetti contradict this conclusion, it is necessary to turn our attention to the dependence of magnetic noise on the polarity reversal frequency and take into account that in their experiments the spectrum was investigated for polarity reversal frequencies F very much lower than those in [10].

The dependence of the spectrum on the polarity reversal frequency is more straightforward in ferrites, where the phenomenon is not complicated by a skin-effect. Fig. 1 shows our data for the noise spectrum of a ferrite*. The frequency ratio f/F is plotted along the abscissa and $\sqrt{G/F}$ along the ordinate axis. (The amplitude of the polarity-reversing field is the same for all the frequencies F.) This figure shows that for a constant f/F the quantity $\sqrt{G/F}$ does not depend on f anf F. This law must hold in those cases in which the mean value of the magnetic flux for a given magnetic field and the statistical characteristics of the random deviations of the flux from the mean value do not depend on the rate at which the magnetic field changes. In order to convince oneself of this, it is enough to transform the expression for spectral density (1) taking into

---

* This figure does not show the spectral density close to harmonics of the frequency (in a band of the order of 10 cps). The spectrum close to the harmonics will be treated separately.

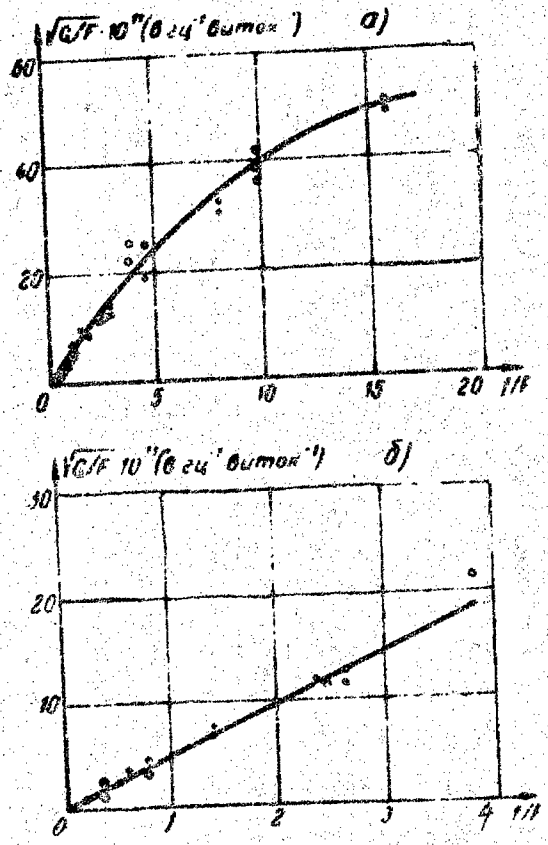

Fig. 1: Magnetic noise spectrum for a ferrite , NTs-1000 (amplitude of polarity-reversing field 0.18 oersteds, . . . f = 44 kc, + + + f = 21 kc, o o o f = 11 kc).

account the fact that in the case described the magnetic flux Φ, connected with the e.m.f. by the expression $u(t) = -d\Phi/dt$, may be considered a function of the relative time $\tau = t/T$ ($T = 1/F$ is the period of polarity reversal). Expression (1) then becomes:

$$G(f) = F \lim_{\theta F \to \infty} \frac{1}{2\theta F} \left| \int_{-\theta F}^{+\theta F} \left(\frac{d\Phi}{d\tau} e^{i2\pi(f/F)\tau} \right) d\tau \right|^2 .$$

From this expression it is clear that the ratio G/F depends only on the ratio of the frequencies f and F.

In conductors the quantity $\sqrt{G/F}$ depends not only on the ratio of the frequencies; for a given f/F it decreases for increase in F,

while in thin specimens the decrease is less than in thick ones (Fig. 2). The reason for this dependence on the polarity-reversal frequency may be a skin effect.

In Figs. 1 and 2 the spectral density decreases when f/F decreases only in the region of small values of f/F. For ferrites and iron this decrease occurs when f/F is less than 30. In the experiments of Biorci and Pescetti the least f/F was 30; therefore the fact that they did not observe a decrease in the spectral density when the observation frequency was reduced does not contradict our experiments. However, the dependence of the spectral density G on the polarity-reversal frequency F, observed in [9], does not agree with our findings (in [9] the spectrum was measured for only two polarity-reversal frequencies 1.5 and 3 cps).

We may therefore conclude that in the region of small f/F the magnetic noise spectrum differs from the shot-noise spectrum. Whereas the shot-noise spectrum does not depend on the frequency f, the spectral density of the magnetic noise is equal to zero for zero frequency f and increases with increase in f to a certain frequency f_1, which depends on the polarity-reversal frequency.

Let us consider what results from a comparison of the shot-noise spectrum with the magnetic noise spectrum for large frequency ratios f/F. Our experiments, like those of Biorci and Pescetti, show that for large ratios f/F the spectral density at first hardly changes with increase in f but then diminishes.

If we compute the spectral density of the magnetic noise, considering the e.m.f. pulses due to the reversal of magnetization in different domains to be independent, then we get a spectrum coinciding with the shot-noise spectrum (as the current pulses in the shot effect are independent). In this case the spectral density of the magnetic noise is written in the form

$$G(f) = \overline{|S(f)|^2}\, NF \qquad (2)$$

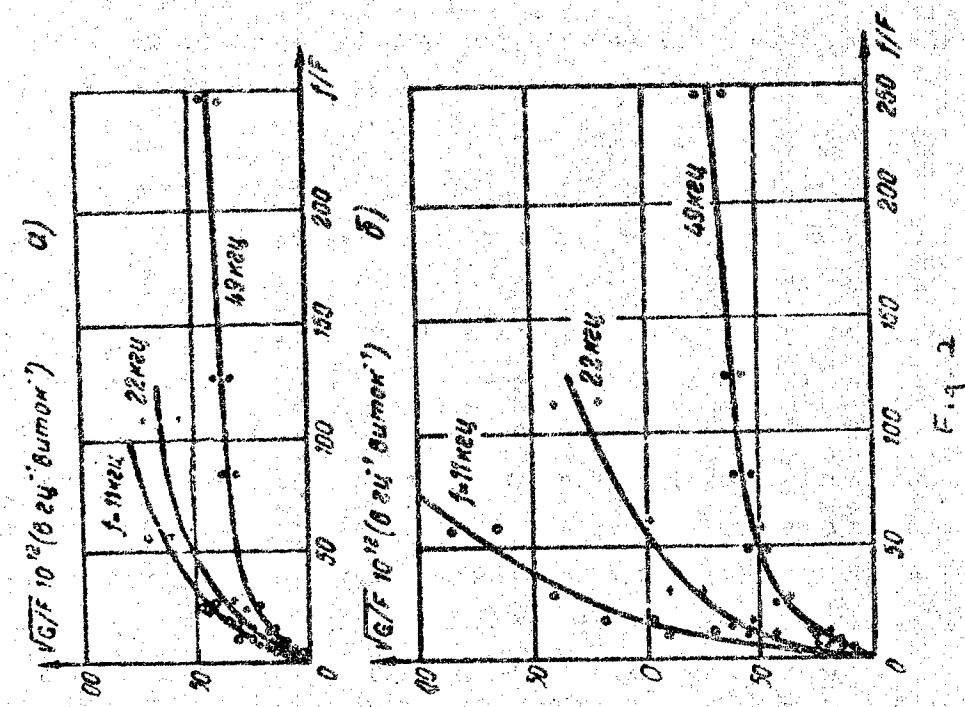

Fig. 2: Magnetic noise spectrum of "armco" iron (amplitude of polarity-reversing field 0.92 oersteds, . . . f = 49 kc, + + + f = 21 kc, o o o f = 11 kc):

a) strip 3 mu thick; b) strip 110 mu thick.

(here S(f) is the Fourier expansion of the e.m.f. pulse, generated in one Barkhausen jump, the horizontal line is the sign of averaging with respect to all the jumps, N is the number of jumps in a complete cycle of polarity reversal).

For the frequency range $f \ll 1/\tau_0$ S(f) = S(0) and is equal to the change in magnetic flux for a jump Φ. For these frequencies we get a constant spectral density

$$G(f) = \overline{\Phi^2} NF.$$

If we denote the average value of the modulus of the e.m.f. over the period by $|\bar{e}| = N\overline{\Phi}F/2$, then

$$G(f) = 2\frac{\overline{\Phi^2}}{\overline{\Phi}}|\tilde{e}|. \qquad (3)$$

To compare the calculations with experiment it is necessary to have data on the magnitude, duration and shape of the e.m.f. pulses, generated in the Barkhausen jumps. We do not have all these data. For unannealed permalloy and "armco" iron we know $\overline{\Phi^2}$, $\overline{\Phi}$ and the order of magnitude of the duration of the e.m.f. pulses, generated in polarity reversal with a slowly increasing field (10^{-4} oersteds per second)*. The duration of the pulses is from 10^{-3} to 10^{-5} sec. There are few long pulses but their contribution to the change in flux is substantial. In reversing the polarity with frequencies of hundreds of cps up to several kc, at which the noise was measured, the pulse lengths will clearly be less.

Unfortunately, the nature of the experimental spectrum cannot be compared with formula (2) in the region in which $|S(f)|$ and $G(f)$ diminish with increase in f, as we have not sufficient data on the shape and duration of the pulses. In the magnetic noise spectrum it is possible to single out the range of observation frequencies in which the spectral density has a maximum and depends only slightly on the observation frequency: this is the frequency range in which $1/\tau_0 < f < f_1$ (τ_0 is the duration of the e.m.f. pulses in Barkhausen jumps). It is proper to compare the magnitude of the spectral density in this section with the value computed from formula (3). The quantities required for the comparison are given in Table 1.

Table 1.

Specimen	$\overline{\Phi}$ v.sec.turns^{-1}	$\overline{\Phi^2}/\overline{\Phi}$ v.sec.turns^{-1}	$\tilde{e}$ v.turns^{-1}	$\sqrt{G_{cal}}$ v.cps$^{-\frac{1}{2}}$. turns^{-1}	$\sqrt{G_{max}}$ v.cps$^{-\frac{1}{2}}$. turns^{-1}
"armco" iron	4.10^{-13}	$5{\cdot}6.10^{-13}$	1.10^{-4}	1.10^{-8}	$0{\cdot}9.10^{-8}$
Permalloy	$2{\cdot}7.10^{-12}$	$1{\cdot}2.10^{-11}$	$1{\cdot}8.10^{-4}$	$6{\cdot}5.10^{-8}$	6.10^{-8}

The value of $\sqrt{G_{max}}$, where G_{max} is the experimentally obtained maximum value of the spectral density, is close to the value of $\sqrt{G_{cal}}$, found from formula (3). If we take into account measuring errors, then we may say that the experiments are in accord with formula (3).

For ferrites and annealed Permalloy the quantities $\overline{\dot{\Phi}}$ and $\overline{\dot{\Phi}^2}$ were not determined but the Barkhausen jumps were observed and it is possible to state that they are finer than for the materials considered above. In accordance with formula (3) the spectral density of magnetic noise in ferrites and annealed Permalloy is less than in unannealed Permalloy and "armco" iron.

With ferrites shorter e.m.f. pulses were observed in Barkhausen jumps than with conducting materials. Correspondingly, the spectral noise density in ferrites did not diminish with increase in f over the frequency range investigated by us (max. frequency 44 kc), whereas the noise spectrum for conducting materials fell off notably. Biorci and Pescetti observed the beginning of a fall in the spectral density of a ferrite and iron at the same frequencies. It is possible that this may be due to the effect of the self-capacitance of the coil (they used an indicator coil with 7,500 turns).

Thus, we come to the following conclusions. The magnetic noise spectrum has the form shown schematically in Fig. 3a. The spectral density increases with increase in the observation frequency up to a certain frequency f_1, which depends on the polarity-reversal frequency and is different for different materials. For frequencies $f > f_1$ the spectrum has the same form as the shot-noise spectrum. The frequency f_2, starting from which the spectral density decreases, is of the order of $1/\tau_0$, where τ_0 is the duration of the Barkhausen jumps. The maximum value of the spectral density is equal to $\overline{\dot{\Phi}^2}NF$, i.e. is determined by the number of Barkhausen jumps and the magnitude of the e.m.f. pulses, generated in the jumps.

Fig. 3b is a schematic illustration of the correlation function

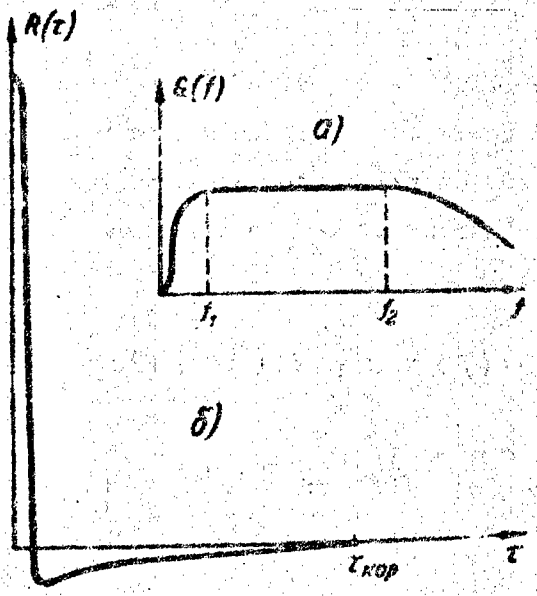

Fig. 3a: General form of the magnetic noise spectrum;
Fig. 3b: Magnetic noise correlation function.

$R(\tau)$, corresponding to the magnetic noise spectrum. Since $G(0)=0$ the integral $\int_0^\infty R(\tau)d\tau$ is also equal to 0 . The interval of time in which $R(\tau)^{\circ}>0$ is equal in order of magnitude to $\tau_0 = 1/f_2$. The whole interval, in which $R(\tau)$ differs markedly from zero, is determined by the frequency, starting from which the magnetic noise can be calculated like shot-noise . With respect to order of magnitude this interval τ_{kop} is equal to $1/f_1$.

If we take the values of f_1 from the experiments, then for Permalloy τ_{kop} is roughly equal to the time taken to run through the steep part of the hysteresis loop in one cycle of polarity reversal; for ferrites τ_{kop} is twenty times less than the time taken to run through the steep part of the loop.

The spectra of all the specimens reveal a linear increase in $\sqrt{G}$ with increase in f for small f/F. In order to emphasise this feature, in Fig. 1b the part of the spectrum corresponding to small f/F is shown to a larger scale.

We shall show that this property of the magnetic noise spectrum must always be present, if the correlation function is different from

zero only in a finite interval of time. Let $R(\tau) \equiv 0$ for $\tau > \tau_{kop}$. We shall consider small frequencies f, for which it is possible to limit ourselves to two terms in the expansion of $\cos(2\pi f \tau)$ with respect to its argument. For these frequencies we can write:

$$G(f) = 2\int_0^{\tau_{kop}} R(\tau)\cos(2\pi f \tau)\, d\tau =$$

$$= 2\int_0^{\tau_{kop}} R(\tau)\, d\tau - 4\pi^2 f^2 \int_0^{\tau_{kop}} R(\tau)\,\tau^2\, d\tau.$$

Since $G(0) = 0$, $\int_0^{\tau_{kop}} R(\tau)d\tau = 0$ and for the spectral density we get the expression: $G(f) = 4\pi^2 f^2 \left| \int_0^{\tau_{kop}} R(\tau)\,\tau^2\, d\tau \right|$,

according to which G(f) is proportional to f^2.

A simple model of the polarity reversal process, with a spectrum and correlation function of the form described, is considered in [3,7,8,10]. In these papers it is assumed that in polarity reversal that only the moments of remagnetization of the domains fluctuate, that all the domains are independent and that there is no correlation between the moments of remagnetization in different periods. We shall denote the moment of remagnetization of one of the domains in a certain cycle by t, its average value by $\bar{t}$ and the random magnitude of the deviation of t from the mean by $\varepsilon = t - \bar{t}$. If different domains give e.m.f. pulses of the same shape or magnitude, the spectral density, computed for such a model, may be written in the form:

$$G(f) = |\overline{S(f)}|^2 NF\,[1 - |\varphi(f)|^2]; \qquad (4)$$

here $\varphi(f) = \overline{\exp(i2\pi f\varepsilon)}$ is a characteristic function; the remaining quantities have the same significance as in the preceding formulas. For sufficiently large frequencies f the quantity $\varphi(f)$ is much less than unity and formula (4) coincides with formula (2), i.e. the magnetic noise in the model in question is analogous to the shot-noise. When f = 0, the characteristic function $\varphi(0) = 1$ and the spectral density is equal to zero. For small f, expanding $\varphi(f)$ in a series and limiting ourselves to terms of the order of f^2, we get :

$$G(f) = \overline{|S(0)|^2}\, NF\, 4\pi^2\overline{\varepsilon^2} f^2,$$

i.e. G(f) is proportional to f^2.

Thus, formula (4) agrees with experiment for sufficiently small and sufficiently large frequencies. It is possible to select a law of distribution of ε, in particular, the quantity $\overline{\varepsilon^2}$, such that (4) will correctly describe the spectrum, obtained experimentally, over the whole frequency range. Then, for Permalloy, for example, it is necessary to take $\sqrt{\overline{\varepsilon^2}}$ as being of the same order of magnitude as the time taken to run through the steep part of the hysteresis loop.

Although (4) gives a good description of the spectrum for a definite law of distribution of the random quantity ε, it is not possible to assume that the model of a ferromagnetic used in deriving this formula corresponds to reality. For example, from the coincidence of (4) with experiment in the case of Permalloy it is not possible to conclude that in the actual Permalloy specimen all the domains fluctuate independently, while each domain can be remagnetized at any section of the hysteresis loop (since $\sqrt{\overline{\varepsilon^2}}$ is of the order of the time taken to run through the steep part of the hysteresis loop). It is also possible to assume another model for a ferromagnetic. Let the reversal of the magnetization of the ferromagnetic start now from one nucleus now from another according

to a random law. The whole sequence of Barkhausen jumps occurring after the formation of the nucleus is unambiguously determined by what nucleus remagnetization starts from, but this sequence will be different for different nuclei. The parameters of the latter model (duration of the sequences of pulses, distribution of the pulses in them) may be chosen so that the noise spectrum, given by this model, will coincide with the spectrum obtained experimentally. Then $\tau_{кор}$ will be of the order of the average duration of the pulse sequence but the fluctuations in the moments of remagnetization of the individual domains will be much less than necessary for agreement with experiment in the first model.

Thus, as far as the magnetic noise spectrum is concerned, it is not possible to establish unambiguously the nature of the connection between fluctuations in the Barkhausen jumps in different zones of a ferromagnetic specimen.

Bibliography

1. Krumhansl, J.A.; Beyer, R.T.: J.Appl.Phys. 20 (1949) 582.
2. Grachev, A.A.: Reports AS USSR, 71 (1950) 269.
3. Gorelik, G.S.: Trans. AS USSR, Phys. Ser., 14 (1950) 174.
4. Williams, F.S.; Noble, S.W.: Proc. IEE, 97 II (1950) 445.
5. Grachev, A.A.: Rep. AS USSR, 85 (1952) 741.
6. Haneman, J.: J.Appl.Phys. 26 (1955) 355.
7. Bunkin, F.V.: ZhTF, 26 (1956) 1782.
8. Bunkin, F.V.: ZhTF, 26 (1956) 1790.
9. Biorci, G.; Pescetti, D.: J.Appl.Phys., 28 (1957) 777.
10. Grachev, A.A.: Radiofizika, 1, 2 (1958) 71.

Radiophysics Research Institute of
Gor'kiy University

Submitted 19 Mar. 1959.

EXCITATION OF A SMOOTH PERFECTLY CONDUCTING SOLID OF REVOLUTION - I.

Pages 588-595

by E.N. Vasil'ev

The author presents a numerical method of calculating the distribution of current in a solid of revolution excited by an electromagnetic wave. This method is based on the use of integral equations and is applicable to a solid of revolution of arbitrary shape.

Introduction

It is known that in the form, in which it is usually presented, the problem of the external excitation of an ideally conducting body by outside sources of electromagnetic waves can be reduced to the solution of integral equations [1-5]. In this article we make use of the equations for the electric current density [1] and the magnetic current density [2] at the surface of the body. These equations differ from each other only with respect to the sign in front of j(p) and can be written in the form :

$$\pm j(p) = -2j^{\text{перв}}(p) + \frac{1}{2\pi}\int_{(\Sigma)}\left[n_p\left[j(q)\,\text{grad}\,\frac{e^{-ip}}{\rho}\right]\right]d\sigma_q,$$

where p is the observation point, q is the integration point, j is the required density of the surface current, $j^{\text{перв}}$ is the density of the surface current corresponding to the primary field, ρ is the distance between the points p and q, Σ is the surface of the

body (it is assumed that it satisfies Lyapunov's conditions [6]), n_p is the unit vector of the normal to the surface Σ in the point p. The plus sign corresponds to the equation for magnetic current density (then $j^{nepB} = -|nE^{nepB}|$) and the minus sign corresponds to the equation for electric current density (then $j^{nepB} = |nH^{nepB}|$). In equation (1) all the space coordinates and distances are multiplied by the wave number α.

From the point of view of the existence and uniqueness of solutions the equation for magnetic current density is the one which has been most fully investigated. Muller [2] has shown that when the internal region, bounded by the surface Σ, is a resonance region, the integral equation for the magnetic current density does not have a solution; however, the electromagnetic field, generated by this current, always exists and is always unique.

As far as we know, the equation for the electric current density has not been investigated in detail, though the matter is of undoubted interest. As the two equations are almost completely identical, both the equation for the electric current density and that for the magnetic current density will have singular points.

The application of integral equations to the problem of external excitation is advantageous in that with their aid the three-dimensional problem in an infinite region is reduced to a two-dimensional problem on a bounded surface. If we assume that the surface Σ is a surface of revolution, then equation (1) reduces to a series of one-dimensional integral equations for azimuthal harmonics of the current density, which can be successfully solved by numerical methods.

1. Reduction of the integral equation

We shall employ an orthogonal rotating coordinate system u, v, φ, related to the Cartesian coordinates in the following way:

$$x = \eta(u, v)\cos\varphi; \quad y = \eta(u, v)\sin\varphi; \quad z = \xi(u, v). \tag{2}$$

Certain properties of orthogonal rotating coordinate systems are presented in article by Moon and Spencer [7]. It follows from this article, in particular, that the Lame coefficients h_1, h_2, h_3 of system (2) are independent of the azimuthal coordinate φ. Moreover, the orthogonality of the lines u and v leads to the two relationships :

$$\cos\Theta = \frac{\partial\xi(u, v)}{h_1\,\partial u} = \frac{\partial\eta(u, v)}{h_2\,\partial v}; \quad \sin\Theta = \frac{\partial\eta(u, v)}{h_1\,\partial u} = -\frac{\partial\xi(u, v)}{h_2\,\partial v}, \tag{3}$$

where Θ is the angle between the tangent to the line u in a certain point p with the coordinates (u,v) and the axis of rotation. Formulas (3) can easily be obtained by constructing differential triangles on the coordinate lines u and v .

We now require that one of the surfaces u = const of coordinate system (2) should coincide with the surface Σ and that the unit vector u^0, tangent to the coordinate line u, should coincide with respect to direction with the vector of the outside normal to the surface Σ .

We shall now formulate all the quantities, appearing in (1), as Fourier series with respect to the azimuthal coordinate φ :

$$j(v, \varphi) = \sum_{m=-\infty}^{\infty} j_m(v)\, e^{im\varphi}; \quad j^{\text{неорм}}(v, \varphi) = \sum_{m=-\infty}^{\infty} j_m^{\text{неорм}}(v)\, e^{im\varphi}; \tag{4}$$

$$\frac{e^{-ip}}{p} = \sum_{m=-\infty}^{\infty} S_m(u, u', v, v')\, e^{im(\varphi-\varphi')}. \tag{5}$$

Here and below the primes denote quantities, relating to the point q ; quantities, relating to the point p , are given without primes.

The validity of expansion (5) is not evident and will be proved below (see (16) and (17)).

In order to multiply the vectors in (1) and then integrate with respect to the coordinate φ, it is necessary to make a parallel transposition of the vector j(q) to the point p, stationary during integration. Parallel transposition formulas can be obtained by considering the vector j(q) as a first-order tensor and making use of the formulas for tensor transformation. As a result of this we get:

$$j_u = \left[\frac{\partial \eta}{h_1 \partial u}\frac{\partial \eta'}{h_1 \partial u'}\cos(\varphi-\varphi') + \frac{\partial \xi}{h_1 \partial u}\frac{\partial \xi'}{h_1 \partial u'}\right] j'_u +$$

$$+\left[\frac{\partial \eta}{h_1 \partial u}\frac{\partial \eta'}{h_2 \partial v'}\cos(\varphi-\varphi') + \frac{\partial \xi}{h_1 \partial u}\frac{\partial \xi'}{h_2 \partial v'}\right] j'_v + \frac{\partial \eta}{h_1 \partial u}\sin(\varphi-\varphi')\, j'_\varphi;$$

$$j_v = \left[\frac{\partial \eta}{h_2 \partial v}\frac{\partial \eta'}{h_1 \partial u'}\cos(\varphi-\varphi') + \frac{\partial \xi}{h_2 \partial v}\frac{\partial \xi'}{h_1 \partial u'}\right] j'_u + \qquad (6)$$

$$+\left[\frac{\partial \eta}{h_2 \partial v}\frac{\partial \eta'}{h_2 \partial v'}\cos(\varphi-\varphi') + \frac{\partial \xi}{h_2 \partial v}\frac{\partial \xi'}{h_2 \partial v'}\right] j'_v + \frac{\partial \eta}{h_2 \partial v}\sin(\varphi-\varphi')\, j'_\varphi;$$

$$j_\varphi = -\frac{\partial \eta'}{h_1 \partial u'}\sin(\varphi-\varphi')\, j'_u - \frac{\partial \eta'}{h_2 \partial v'}\sin(\varphi-\varphi')\, j'_v + \cos(\varphi-\varphi')\, j'_\varphi.$$

We shall substitute (4) and (5) in (1), effecting a parallel transposition of the vector j(q) to the point p with the aid of formulas (6).

We shall put the integral in (1) in coordinate form (with respect to the coordinates v' and φ'). In computing the integral with respect to φ', it is possible to make use of the orthogonality of the functions of $e^{im\varphi}$, putting the corresponding substitions for the exponents into Fourier series. As a result of integration with respect to φ' we get an expression in the form of an equation relating several Fourier series. Equating the coefficients of these series (the validity of the equating process is easy to prove), we find a system of integral equations for each azimuthal harmonic of the current density :

$$\pm j_{vm}(v) = -2j_{vm}^{\text{перв}}(v) + \int_{v'} \left| P_{m11}(v, v')\, j_{vm}(v') + P_{m12}(v, v')\, j_{\varphi m}(v') \right| h_2' h_3' dv'; \tag{7}$$

$$\pm j_{\varphi m}(v) = -2j_{\varphi m}^{\text{перв}}(v) + \int_{v'} \left| P_{m21}(v, v')\, j_{vm}(v') + P_{m22}(v, v')\, j_{\varphi m}(v') \right| h_2' h_3' dv'.$$

The kernels of this system of equations may be expressed by the formulas:

$$P_{m11} = \frac{\partial \eta'}{h_2' \partial v'} \frac{\partial \eta}{h_2 \partial v} \frac{\partial}{h_1 \partial u} \left(\frac{S_{m+1} + S_{m-1}}{2} \right) + \frac{\partial \xi'}{h_2' \partial v'} \frac{\partial \xi}{h_2 \partial v} \frac{\partial S_m}{h_1 \partial u} - \frac{\partial \eta'}{h_2' \partial v'} \frac{\partial \eta}{h_1 \partial u} \frac{\partial}{h_2 \partial v} \left(\frac{S_{m+1} + S_{m-1}}{2} \right) - \frac{\partial \xi'}{h_2' \partial v'} \frac{\partial \xi}{h_1 \partial u} \frac{\partial S_m}{h_2 \partial v}; \tag{8}$$

$$P_{m12} = \frac{\partial \eta}{h_2 \partial v} \frac{\partial}{h_1 \partial u} \left(\frac{S_{m-1} - S_{m+1}}{2i} \right) - \frac{\partial \eta}{h_1 \partial u} \frac{\partial}{h_2 \partial v} \left(\frac{S_{m-1} - S_{m+1}}{2i} \right); \tag{9}$$

$$P_{m12} = -\frac{\partial \eta'}{h_2' \partial v'} \frac{\partial \eta}{h_1 \partial u} i \frac{S_{m-1}(m-1) + S_{m+1}(m+1)}{2h_3} - \frac{\partial \xi'}{h_2' \partial v'} \frac{\partial}{h_1 \partial u} \left(\frac{S_{m-1} - S_{m+1}}{2i} \right) - \frac{\partial \xi'}{h_2' \partial v'} \frac{\partial \xi}{h_1 \partial u} \frac{imS_m}{h_3}; \tag{10}$$

$$P_{m22} = \frac{\partial}{h_1 \partial u} \left(\frac{S_{m+1} + S_{m-1}}{2} \right) \frac{S_{m-1}(m-1) - S_{m+1}(m+1)}{2h_3} \frac{\partial \eta}{h_1 \partial u}. \tag{11}$$

If the derivatives of the function S_m with respect to u and v in (8) and (9) are represented by derivatives with respect to the cylindrical coordinates R and z, then, bearing in mind (3) and the equations $\eta = R$, $\xi = z$, we get:

$$P_{m11} = \frac{\partial \eta'}{h_2' \partial v'} \frac{\partial}{\partial z} \left(\frac{S_{m+1} + S_{m-1}}{2} \right) \frac{\partial \xi' - \partial S_m}{h_2' \partial v' - \partial R}; \tag{12}$$

$$P_{m12} = \frac{\partial}{\partial z} \left(\frac{S_{m-1} - S_{m+1}}{2i} \right). \tag{13}$$

In the integral equation (1) the gradient from Green's function was taken with respect to the observation point p . It may be replaced with the gradient from the same function with respect to the point q , taken with sign reversed. Then making the analogous transformations, we get for P_{m12} and P_{m21} expressions easily reducible to the form of (9) and (10) and for P_{m11} and P_{m22} the expressions:

$$P_{m11} = -\frac{\partial}{h_1' \partial u'}\left(\frac{S_{m+1}+S_{m-1}}{2}\right)+ \\ + \frac{S_{m-1}(m-1)-S_{m-1}(m+1)}{2h_3}\frac{\partial \eta'}{h_1' \partial u'}; \qquad (14)$$

$$P_{m22} = -\frac{\partial \eta}{h_2 \partial v}\frac{\partial}{\partial z'}\left(\frac{S_{m+1}+S_{m-1}}{2}\right)+\frac{\partial \xi}{h_2 \partial v}\frac{\partial S_m}{\partial R'}, \qquad (15)$$

which differ from (8) and (11).

Thus as a result of integrating with respect to φ' instead of a single, two-dimensional, vector integral equation we get a number of scalar systems of unidimensional integral equations, which, as already mentioned above, can be successfully solved by numerical methods. Examples of solutions of the integral equations are given in the second section of this article.

2. Investigation of the kernel of the integral equation

As follows from the preceding section, the kernel of the integral equation is expressed by the function S_m and its derivatives. The function S_m was defined as the m-th coefficient of the Fourier expansion of the Green's function $e^{-i\varphi}/\rho$. Like the Green's function, the function S_m is a function of two points in space, the positions of which we shall characterize with cylindrical coordinates. The distance ρ between the two points with coordinates R, φ, z and R', φ', z' is expressed by the formula:

$$\rho = \sqrt{(z - z')^2 + R^2 + (R')^2 - 2RR' \cos(\varphi - \varphi')}, \quad (16)$$

in which all the distances are assumed normalized (multiplied by the wave number).

It is evident from (16) that the angles φ and φ' enter into the expression for ρ, and, accordingly, into $e^{-i\rho}/\rho$ also, only in the form of a difference. If we expand $e^{-i\rho}/\rho$ in a Fourier series with respect to the variable $\Psi = \varphi - \varphi'$, then we get the expansion (5) employed above. Correspondingly, the function S_m can be written in the form:

$$S_m = \frac{1}{2\pi} \int_0^{2\pi} \frac{e^{-i\sqrt{(z-z')^2 + R^2 + (R')^2 - 2RR'\cos\Psi}}}{\sqrt{(z-z')^2 + R^2 + (R')^2 - 2RR'\cos\Psi}} e^{-im\Psi} d\Psi. \quad (17)$$

From this expression it follows that the function S_m is, essentially, a function of two variables, since ρ can be written in the following form:

$$\rho = \sqrt{\rho_0^2 + 2\nu^2(1 - \cos\Psi)}, \quad (18)$$

where $\rho_0^2 = (z - z')^2 + (R - R')^2$; $\nu^2 = RR'$.

It also follows from (16) that ρ and $e^{-i\rho}/\rho$ are even functions of the angle Ψ: therefore we get the relationship $S_m = S_{-m}$. Using this equation it is easy to show that when $m = 0$ (this corresponds to the case of axial symmetry of the fields) the terms P_{012} and P_{021} are equal to zero and the system of integral equations (7) breaks down into two independent integral equations for TE and TM waves.

Values of the function S_m were computed by the methods of

practical harmonic analysis. Graphs of the functions S_0 and S_1 are shown in Fig. 1. It is evident from these graphs that for small ρ_0 the real part of the function S_m tends to infinity. In order to clarify the character of this phenomenon it is necessary to isolate the singular term in the function S_m, which is a Fourier expansion of the function $1/\rho$ and is expressed by the formula:

$$S_m^e = \frac{1}{2\pi} \int_0^{2\pi} \frac{e^{-im\psi}\, d\psi}{\sqrt{(z-z')^2 + R^2 + (R')^2 - 2RR' \cos\psi}}. \qquad (19)$$

After a simple substitution of the variables this integral reduces to complete elliptic integrals. For the first three values of the index m integral (19) has the form:

$$S_0^e = \frac{2}{\pi\rho_\pi} K(k);$$

$$S_1^e = \frac{2}{\pi\rho_\pi} |K(k) - 2B(k)|; \qquad (20)$$

$$S_2^e = \frac{2}{\pi\rho_\pi} \left[K(k) + \right.$$

$$\left. + \frac{8}{3} \frac{E(k) - 2B(k)}{k^2} \right],$$

where

$$\rho_\pi = \sqrt{(z-z')^2 + (R+R')^2},$$

$$k = 2\nu/\rho_\pi.$$

In formulas (20) we use the notation for complete elliptic integrals adopted in [8].

When ρ_0 tends to zero, i.e. when the points p and q approach, k (modulus of the elliptic integral) tends to unity. The functions E(k) and B(k) then remain bounded but K(k) has a logarithmic singularity of the form

$$\ln(1/k'), \qquad (21)$$

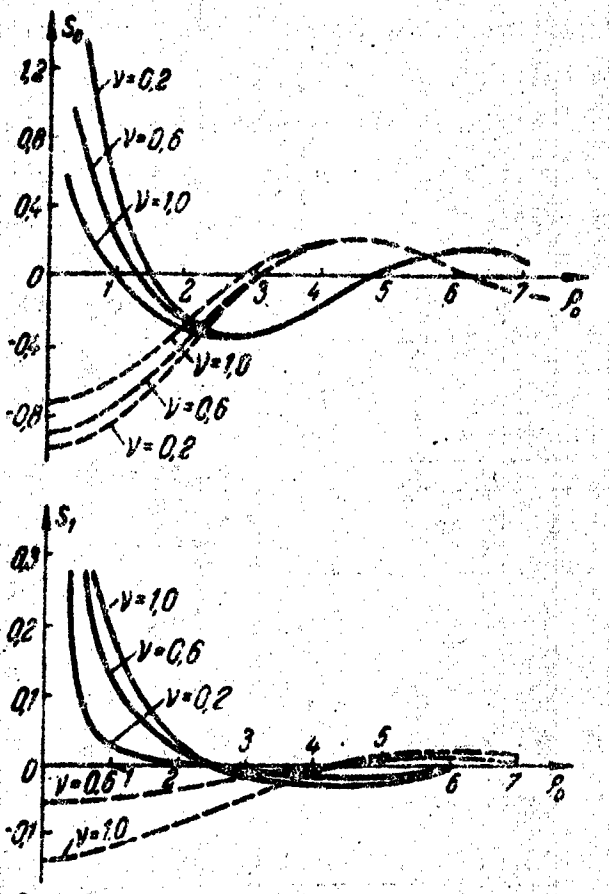

Fig. 1: Graphs of the functions S_0 and S_1 :
(——— real part; ----- imaginary part)

where $k' = \sqrt{1 - k^2} = \rho_0/\rho_\pi$ and the lengths ρ_0 and ρ_π are shown in Fig. 2. Thus, as follows from (20) and (21), when ρ_0 tends to zero, the functions S_0, S_1 and S_2 have the following singular term:

$$(1/\rho_\pi)\ln(\rho_\pi/\rho_0). \qquad (22)$$

It is possible to show that all the remaining functions S_m have the same singularity.

Apart from the function S_m itself, we find in the expression for the kernel derivatives of this function, which can be expressed

by means of derivatives with respect to cylindrical coordinates.

Among the derivatives of the function S_m with respect to R and z there is a simple relationship, which it is easy to find, by differentiating (17) with respect to R and with respect to z and equating the expressions obtained. As a result we get:

$$\frac{\partial S_m}{\partial R} = \frac{R}{z - z'} \frac{\partial S_m}{\partial z} - \frac{R'}{z - z'} \frac{\partial}{\partial z} \left(\frac{S_{m+1} + S_{m-1}}{2} \right). \tag{23}$$

Fig. 2: Determination of the lengths ρ_0 and ρ_π

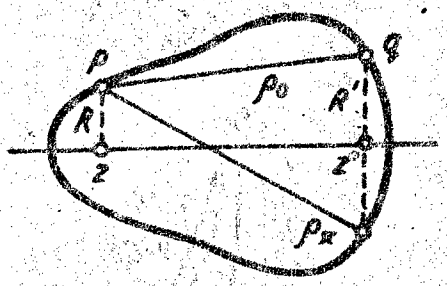

Moreover, by equating (12) and (14) while taking into account (3), it is possible to find the relationships between the function S_m itself and its derivatives:

$$\frac{\partial}{\partial R'} \left(\frac{S_{m+1} - S_{m-1}}{2} \right) - \frac{(m-1) S_{m-1} - (m+1) S_{m+1}}{2R'} + \frac{\partial S_m}{\partial R} = 0. \tag{24}$$

If in (24) the derivatives with respect to R and R' are replaced with derivatives with respect to z , using (23), then we get the more convenient formula:

$$S_m = \frac{RR'}{m(z - z')} \frac{\partial}{\partial z} \left(\frac{S_{m+1} - S_{m-1}}{2} \right). \tag{25}$$

It is evident from (23) and (25) that the function S_m and its derivatives are simply expressed by the function

$$Q_m = \frac{1}{z - z'} \frac{\partial S_m}{\partial z}. \tag{26}$$

We have partially tabulated the function Q_m; however, these tables are not reproduced here because of their bulkiness.

Derivatives of the functions $\eta(u,v)$ and $\xi(u,v)$ also enter into the expression for the kernel as well as the function S_m and its derivatives. The computation of these derivatives is not difficult, as they are expressed by means of sines and cosines of the angle between the outward normal to the body and the axis of rotation - (formulas (3)).

If we try to characterize the kernels of system of equations (7) in general, we may state the following. The graphs of all the kernels of the system have the form of damped oscillations. When the points p and q coincide, the real parts of the kernels P_{m11} and P_{m22} have a logarithmic singularity. The kernels P_{m12} and P_{m21} do not have singularities, which it is easy to confirm by transforming (10) and (13) with the aid of formulas (3), (23) and (25):

$$P_{m12} = \frac{z - z'}{RR'} \, imS_m; \tag{27}$$

$$P_{m21} = \left[\frac{\cos\Theta \sin\Theta'}{R} - \frac{\cos\Theta' \sin\Theta}{R'} \frac{z - z'}{RR'} \cos\Theta \cos\Theta'\right] imS_m. \tag{28}$$

When the points v and v' coincide, the function S_m has a logarithmic singularity but the multiplier in front of it reverts to zero like a linear function. As a result P_{m12} and P_{m21} also vanish when $v = v'$.

3. Computation of the azimuthal harmonics of fields from given sources

It is above all in computing the right-hand member of the system of integral equations (7) that we meet with the necessity of computing the azimuthal harmonics of fields from given sources. As is evident from (1), (4) and (7), in the case of a system of equations

for electric current density the right-hand member of this system (i.e. the functions $j_{m\nu}^{\text{перв}}(v)$ and $j_{m\varphi}^{\text{перв}}(v)$) represents azimuthal harmonics of the vector $[nH^{\text{перв}}]$, where $H^{\text{перв}}$ is the magnetic field of the primary sources in free space. The magnetic field of electric and magnetic side currents is expressed by means of the known formula, which, after multiplication by the vector of the outward normal to the solid of revolution and normalization, has the form:

$$|n_p H(p)| = -\frac{1}{4\pi a}\left[n_p \int\limits_{(W)} \left\{\left[j^{э\,ст}(q)\,\text{grad}\,\frac{e^{-ip}}{p}\right] + \right.\right.$$
$$\left.\left. + i\sqrt{\frac{\varepsilon}{\mu}}\,\text{grad}\,\text{div}\left[j^{м\,ст}(q)\frac{e^{-ip}}{p}\right] + i\sqrt{\frac{\varepsilon}{\mu}}\,j^{м\,ст}(q)\frac{e^{-ip}}{p}\right\} dw_q\right], \quad (29)$$

where $j^{э\,ст}$ and $j^{м\,ст}$ are respectively the densities of the electric and magnetic side currents, n_p is the vector of the outward normal to the surface of the solid of revolution, W is the volume occupied by the side sources and alpha is the wave number.

It should be noted that the first term in formula (29) has the same accuracy as the integral term in equation (1).

In order to get the azimuthal harmonics of the primary field, it is necessary to perform the same operations on (29) as were performed above on (1). We then get the following expressions:

$$j_{m\nu}^{\text{перв}}(v) = -\frac{1}{2a}\int\limits_{(F)} \left\{P_{m11}\,j_{m\tau}^{э\,ст} + \Pi_{m11}\,j_{m\tau}^{м\,ст} + P_{m12}\,j_{m\varphi}^{э\,ст} + \Pi_{m12}\,j_{m\varphi}^{м\,ст}\right\} h_3' df,$$

$$j_{m\varphi}^{\text{перв}}(v) = -\frac{1}{2a}\int\limits_{(F)} \left\{P_{m21}\,j_{m\tau}^{э\,ст} + \Pi_{m21}\,j_{m\tau}^{м\,ст} + P_{m22}\,j_{m\varphi}^{э\,ст} + \Pi_{m22}\,j_{m\varphi}^{м\,ст}\right\} h_3' df, \quad (30)$$

where $j_{m\tau}^{э\,ст}$ and $j_{m\tau}^{м\,ст}$ are azimuthal harmonics of of the components of the electric and magnetic side currents, lying in the meridional plane, $j_{m\varphi}^{э\,ст}$ and $j_{m\varphi}^{м\,ст}$ are azimuthal harmonics of the φ-th components of the electric and magnetic side currents and F is the

region in the meridional plane occupied by the side currents.

The functions P_{msl} are defined by formulas (8) - (15) but Π_{msl} is given by the following relationships:

$$\Pi_{m11} = \sqrt{\frac{\varepsilon}{\mu}}\left(-\frac{m}{h_3}\frac{\partial S_m}{h_2\partial v'} + \frac{\partial \eta'}{h_2'\partial v'}\frac{S_{m+1}+S_{m-1}}{2}\right); \quad (31)$$

$$\Pi_{m12} = \sqrt{\frac{\varepsilon}{\mu}}\left(+i\frac{m^2}{h_3h_3'}S_m - i\frac{S_{m-1}+S_{m+1}}{2}\right); \quad (32)$$

$$\Pi_{m21} = \sqrt{\frac{\varepsilon}{\mu}}\left(-i\frac{\partial^2 S_m}{h_2\partial v h_2'\partial v'} + i\frac{\partial \eta}{h_2\partial v}\frac{\partial \eta'}{h_2'\partial v'}\frac{S_{m-1}+S_{m+1}}{2} + \right. \quad (33)$$

$$\left. + i\frac{\partial \xi}{h_2\partial v}\frac{\partial \xi'}{h_2'\partial v'}S_m\right); \quad (34)$$

$$\Pi_{m22} = \sqrt{\frac{\varepsilon}{\mu}}\left(-\frac{m}{h_3'}\frac{\partial S_m}{h_2\partial v} + \frac{\partial \eta}{h_2\partial v}\frac{S_{m-1}-S_{m+1}}{2}\right).$$

In formulas (8) - (15) and (31) - (34) the direction v should be understood as the direction of the generator of the solid of revolution and the direction v' as the direction of the component of the current $j_{m\tau}$.

After the integral equation has been solved, there remains the problem of computing the electric and magnetic fields of the currents, induced in the solid of revolution. As all the calculations are carried out separately for each azimuthal harmonic of current density, it is rational to compute the fields in the form of azimuthal harmonics also.

Without going into details we note that the harmonics of the near fields can be found from formulas scarcely different from (30). To determine the azimuthal harmonics of a field in the far zone it is easy to get the simpler formulas:

$$E_{\vartheta m} = \sqrt{\frac{\mu}{\varepsilon}}\frac{e^{-ir}}{2r}\int_{v'}\left\{\left[-i^m\cos\Theta'\cos\vartheta\,\frac{d}{dR'\sin\vartheta}J_m(R'\sin\vartheta) - \right.\right.$$

$$\left.\left. - i^{m+1}\sin\Theta'\sin\vartheta\,J_m(R'\sin\vartheta)\right] j'_{vm} + \right. \tag{35}$$

$$\left. + \cos\vartheta\,\frac{mi^{m+1}}{R'\sin\vartheta}J_m(R'\sin\vartheta)\,j'_{\varphi m}\right\} e^{iz'\cos\vartheta}\,h'_2h'_3dv';$$

$$E_{\cdot m} = \sqrt{\frac{\mu}{\varepsilon}}\frac{e^{-ir}}{2r}\int_{v'}\left\{-\frac{mi^{m+1}\cos\Theta'}{R'\sin\vartheta}J_m(R'\sin\vartheta)\,j'_{vm} - \right. \tag{36}$$

$$\left. - i^m\frac{d}{dR'\sin\vartheta}J_m(R'\sin\vartheta)\,j'_{\varphi m}\right\} e^{iz'\cos\vartheta}\,h'_2h'_3dv'.$$

In these formulas r and ϑ are the spherical coordinates of the observation point, $J_m(R'\sin\vartheta)$ is a Bessel function, z', R' are the cylindrical coordinates of the point v' and Θ' is the angle between the vector of the outward normal and the axis of rotation in the point v'.

Bibliography

1. Fok, V.A.: ZhETF, 15, (1945), 693.
2. Muller, C.: Math. Ann. 123 (1951) 345.
3. Mane, A.W.: Zeits.f.Physik, 126 (1949) 606.
4. Kupradze, V.D.: Granichnye zadachi teorii kolebaniy i integral'nye uravneniya (Boundary problems in the theory of oscillations and some integral equations), Gostekhizdat, M., 1950.
5. Avazashvili, D.Z.: Soobshcheniya AN Gruz. SSR (Reports of AS of Georgian SSR), 14 (1953) 6.
6. Tikhonov, A.N.; Samarskiy, A.A.: Uravneniya matematicheskoy fiziki (Equations of mathematical physics), Gostekhizdat, M., 1953.
7. Moon, P.; Spencer, D.: J. Franklin Inst., 252 (1951) 327.
8. Yanke, E.; Emde, F.: Tablitsy funkstiy (Tables of functions) Gostekhizdat, M., 1949.

Moscow Institute of Energetics

Submitted 8 January 1958, after revision - 6 May 1959.

EXCITATION OF A SMOOTH PERFECTLY CONDUCTING SOLID OF REVOLUTION - II.

Pages 596-601

by E.N. Vasil'ev.

1. Axially symmetric excitation of a solid of revolution with a TM wave.

In the first part of this article [1] we discussed some general questions connected with the integral equations of the electrodynamic boundary problem for a perfectly conducting solid of revolution. Here we shall give some examples of solutions of the integral equations. In this connection we shall employ equations for the density of the electric current, the solution of which gives a picture physically more graphic than the solution of the equations for the magnetic current.

As the first example we shall discuss the problem of the axially symmetric excitation of a thick cylinder of finite length with a transverse slot. Because of the axial symmetry it is sufficient to consider the system of equations (7) [1] from the first part of this article for a single value, zero, of the index m . In this case system (7) [1] breaks down into two independent equations, of which we shall use only the one corresponding to the TM wave:

$$j_{0v}(v) = 2j_{0v}^{\text{перв}}(v) - \int_{v'} P_{011}(v, v')\, j_{0v}(v')\, h_2' h_3' dv'. \qquad (1)$$

Using expressions (3), (12), (23) and (26) from [1], we write:

$$P_{011}(v, v') = |(z - z')^2 \cos\Theta - R' \sin\Theta| Q_1 + R \sin\Theta' Q_2. \quad (2)$$

Here z,R are the cylindrical coordinates of the point v ; z', R' are the cylindrical coordinates of the point v' ; Θ' is the angle between the vector of the outward normal and the axis of revolution in the point v'.

As the coordinate of v in (1) we shall take the length of the arc of the generatrix of the solid of revolution. The Lamé coefficient h_2' will then be equal to unity. The Lamé coefficient h_3' is equal to R' in any rotating coordinate system.

The method of Krylov and Bogolyubov [2] proved suitable enough for solving equation (1) numerically. This method consists in equation (1) being replaced with the equation

$$j_{0v}(v) = 2j_{0v}^{\text{перв}}(v) - \sum_{l=1}^{n} j_{0v}(v_l') \int_{v_l' - \Delta v_l'/2}^{v_l' + \Delta v_l'/2} P_{011}(v, v') h_3' \, dv' + a, \quad (3)$$

where a is the error due to replacing the integral with a sum. Essentially the change from (1) to (3) means replacing the current density sought with a piecewise constant function.

In the transformed equation (3) the coordinate v is successively given the values $v_1', v_2', \ldots, v_n'$ and the small quantity a is assumed equal to zero, as a result of which we get a system of linear algebraic equations for determining the current density in the points v_l' :

$$j_{0v}(v_s') + \sum_{l=1}^{n} j_{0v}(v_l') C_{sl} = 2j_{0v}^{\text{перв}}(v_s') \quad (s = 1,2, \ldots, n), \quad (4)$$

where

$$C_{sl} = \int_{v_l' - \Delta v_l'/2}^{v_l' + \Delta v_l'/2} P_{011}(v, v') \, h_3' \, dv'. \quad (5)$$

The advantages of the method described are simplicity and the fact that it can be applied to equations with kernels having a singularity. The last point is especially important for equation (1), as the kernel $P_{011}(v,v')$ reverts to infinity when $v = v'$. The accuracy of the solution obtained in this way is not great, because the function sought is too roughly approximated. However, in the calculations connected with practical problems very high accuracy is not required.

Thus, from the computational point of view the solution of the integral equation reduces to the determination of the elements of a matrix and the right-hand members of the system of equations (4) and then the solution of this system.

Where the points v and v' do not coincide within the small intervals $\Delta v'$, the kernel $P_{011}(v,v')$ varies in accordance with a law which is nearly linear; therefore all the elements C_{sl}, apart from the diagonals, are computed from formula (5) as the product of the length of the interval and the value of the integrand in the center of this interval. The singular and regular parts of the diagonal elements are calculated separately. In evaluating integral (5) for the singular part of the kernel expression (2) was not found very convenient; better results are obtained with the kernel expression (14) in [1], which when $m = 0$ takes on the form :

$$P_{011} = -\frac{\partial S_1}{h_1' \partial u'} - \frac{S_1}{R'} \sin\vartheta . \qquad (6)$$

Substituting in (6) the expression for the singular part of the function S_1 (20) [1], we get the singular part of the kernel of the integral equation. In computing the integral from expression (6) it is convenient to use expansions of the complete elliptic integrals given in [3].

The evaluation of the regular part of the diagonal elements is made in the same way as that of the non-diagonal elements, i.e.

by multiplying the value of the integrand in the center of the interval by the magnitude of the interval Δv.

The right-hand member of system (4) represents the primary field of the side magnetic current, characterizing the slot. We are concerned with the excitation of a solid with a transverse slot with axially symmetric distribution of the field; this corresponds to a magnetic current with a unique azimuthal component and one which is independent of φ. To work out the right-hand member we use formula (30) [1], which in this concrete case has the simple form:

$$J_{0v}^{\text{перв}}(v) = \frac{i}{2}\sqrt{\frac{\varepsilon}{\mu}}\int J_{0\varphi}^{\text{маг}}(v')\,S_1 R'\,dv'. \qquad (7)$$

The integral in (7) is taken with respect to the slot.

The calculations described have been made for cylinders of finite length with the diameters 0.287λ, 0.192λ and 0.096λ, the end faces being bounded with hemispheres. In all the cylinders the length of the generatrix was 0.95λ. The magnitude of the interval Δv was taken as equal to about 0.1λ. Thus, the solution of the integral equation for each of the three cylinders was reduced to the solution of a system of ten linear algebraic equations with ten unknowns. The systems of equations were solved with the aid of a computer; the resulting current distributions are shown in Figs. 1-3. These figures also contain directional diagrams for the first and third cylinders. The directional diagrams were worked out by numerical integration from formula (35) in [1].

It is clear from the figures that the current distribution has the character of incident and reflected waves with marked attenuation and recalls the current distribution in a long line with losses. With increase in the diameter of the cylinder the attenuation of the wave propagated along it increases; this is clear from the fact that, for example, the ratio of the magnitude of the current at the

node to that of the current at the antinode is about 0.8 for a cylinder of 0.287 λ diameter and about 0.5 for a cylinder of 0.096 λ diameter.

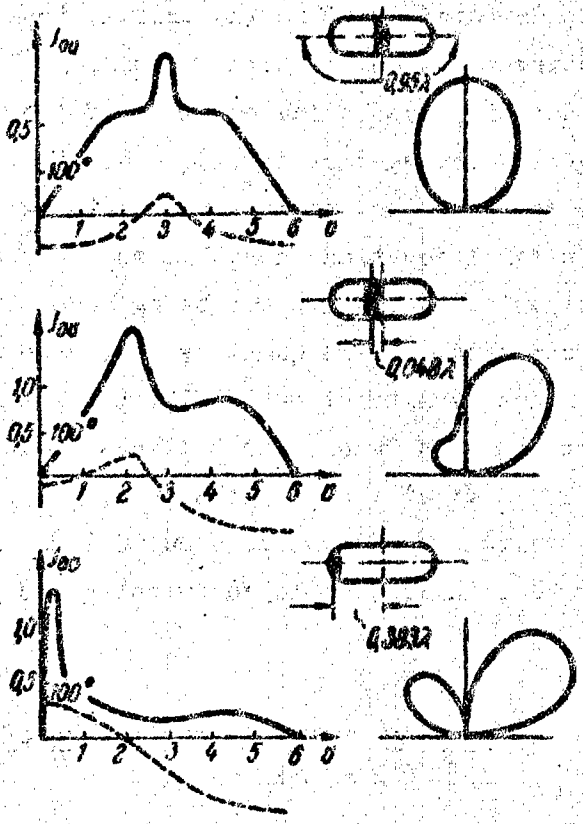

Fig. 1: Distribution of current density j_{cv} for a cylinder of 0.287 λ diameter and directional diagrams for the radiation:

——— modulus of current density; --- phase of current density.

At the slot there is a current maximum, which corresponds to the quasi-static field of the slot. The value of this maximum increases with increase in the diameter of the cylinder.

The directional diagrams, which are symmetrical if the slot is symmetrically disposed, are pulled in a direction opposite to that in which the slot moves, when the latter is displaced. If the slot

is displaced through a considerable distance, the directional diagrams take on a double-lobed appearance.

We shall briefly consider the accuracy of the results obtained. The fundamental error in the calculations will be the error due to replacing equation (1) with expression (3) (i.e. the quantity a). This quantity was evaluated by the following simple method. The integral, forming part of (1), was first evaluated from the rectangle formula (i.e. precisely as this was done in the solution of the integral equation) and then more accurately from Simpson's formula, the interval Δv being made twice as small. The results were compared. As the quantity $j_{0v}(v)$ we used one of the distributions of current density given in Fig. 1. The result was that at all points, except the point where the slot was located, the error did not exceed 2 - 3 %; at the slot the error was 7 %. Thus, for a length of the interval Δv equal to about 0.1 λ the method of solving the integral equation, employed by us, gives perfectly satisfactory accuracy.

2. Axially symmetric excitation of a solid of revolution with a TE wave

In this case as in the preceding one the system of equations (7) [1] is considered for a value of the index m equal to zero but the equation for $j_{0\varphi}(v)$ now corresponds to the TE wave :

$$j_{0\varphi}(v) = 2j_{0\varphi}^{\text{пер}}(v) - \int_{v'} P_{022}(v, v')\, j_{0\varphi}(v')\, h_2' h_3' dv'. \qquad (8)$$

When the points v and v' do not coincide, the kernel is computed from the formula:

$$P_{022} = |R \sin\Theta + (z - z')\cos\Theta|\, Q_1 - R' \sin\Theta\, Q_0 \qquad (9)$$

(the notation is perfectly analogous to the notation in (2)).

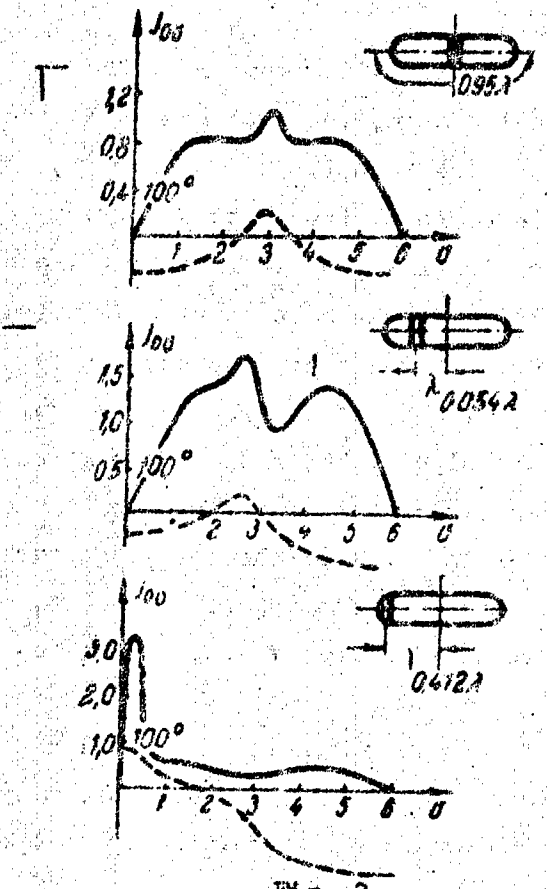

Fig. 2.

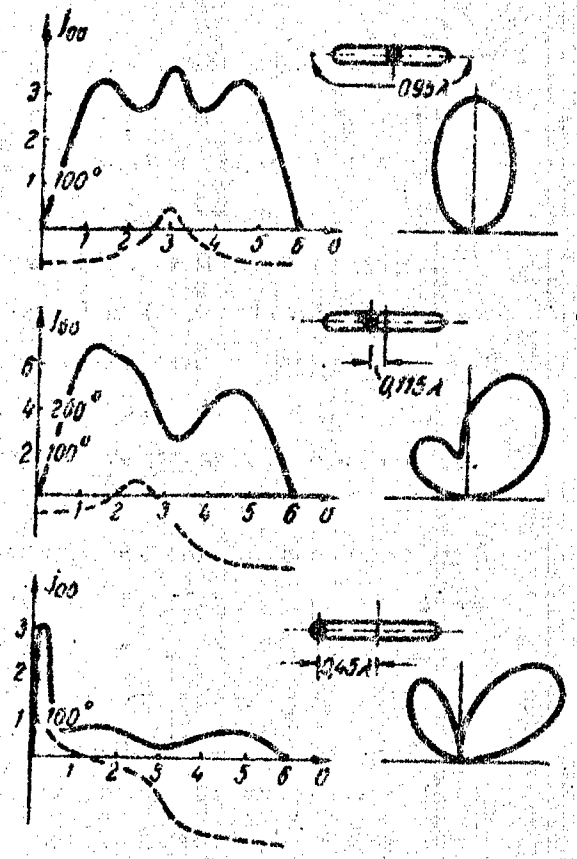

Fig. 3.

Fig. 2: Distribution of current density j_{ov} for a cylinder of diameter 0.192 λ and directional diagrams for the radiation : —— modulus of current density; ----- phase of current density.

Fig. 3: Distribution of current density j_{ov} for a cylinder of diameter 0.096 λ and directional diagrams for the radiation : —— modulus of current density; ----- phase of current density.

When the points coincide, it is more convenient to use the formula

$$P_{012} = \frac{\partial S_1}{h_1 \partial u} + \frac{S_1}{h_3} \sin \theta, \qquad (10)$$

analogous to (6).

The whole process of computation is the same as in the previous

case; the only difference is that the right-hand member of the system of algebraic equations is calculated, in correspondence with (30) [17], from the same formula as the kernel.

In the excitation of a solid of revolution with a TE wave the currents in the solid do not ordinarily play as important a part as in excitation with a TM wave. Therefore we have omitted detailed computations in this case. We worked out the current distribution for a cylinder of 0.287 λ diameter with end faces bounded by hemispheres, exciting it with a magnetic dipole. The results are given in Fig. 4. As can be seen from this figure, close to the dipole there is a sharp increase in current; over the rest of the solid the currents are very small. The field of currents, flowing in the solid, proves to be not large, so that the directional diagram is determined by the dipole radiation.

From this it follows that in our case, in which the solid does not have sharp angles at its surface, taking into account currents in the solid of revolution excited with a TE wave is relatively unimportant.

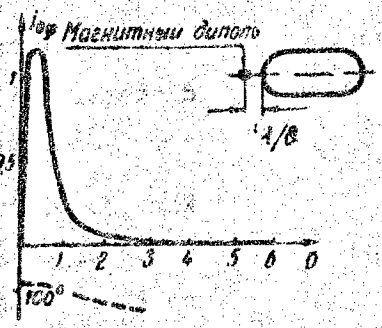

Fig. 4: Distribution of current density $j_{0\varphi}$ for a cylinder of 0.287 λ diameter and directional diagram for radiation:
—— modulus of current density;
---- phase of current density.
(Wording in figure: magnetic dipole).

The method proposed makes it possible to solve problems of excitation and diffraction for perfectly conducting solids of revolution. The examples in the second part of the article deal with axially symmetric problems. However, the method may equally well be applied to non-symmetrical problems also. The only difference will be that in the unsymmetrical case it will be a question of solving

not one integral equation but a whole system of equations (7) [1]. This leads to a doubling of the order of the corresponding system of linear algebraic equations for the same number of intervals Δv.

The method of numerically solving the integral equation, used here, and the limitations of computational techniques impose definite restrictions on the dimensions of the solid. We can solve without great difficulty excitation problems for solids with a generatrix length of the order of several wavelengths. It is natural to compare the method proposed here with the eigenfunction method, ordinarily used to solve such problems. In working out the directional diagrams of simple antennas, set up close to a cylinder of infinite length or a sphere, the eigenfunction method has definite advantages from the point of view of the simplicity of the calculations. However, even in the case of the symmetrical excitation of a spheroid the computational difficulties become comparable. In more complex cases the eigenfunction method is either generally inapplicable on account of difficulties connected with setting up a complete system of solutions of the vector wave equation or else with its aid the problem is reduced to a system of linear algebraic equations (as, for example, in the case of the unsymmetrical excitation of a spheroid [4]).

The method of integral equations has one other important advantage in that the solution provides a clear physical description of the distribution of currents over the body, making it possible to work out the close fields and judge the effect of different factors on the radiation characteristics.

In conclusion the author finds it his pleasant duty to thank G.T. Markov for valuable advice and comments.

Bibliography

1. Vasil'ev, E.N.: Radiofizika, 2 (1959) 588.
2. Kantorovich, L.V.; Krylov, V.I.: Priblizhennye metody vysshevo analiza (Approximate methods of higher analysis), Gostekhizdat,

Bibliography (cont.)

M.-L., 1952.
3. Yanke, E.; Emde, F.: Tablitsy funktsiy (Tables of functions), Gostekhizdat, M., 1949.
4. Markov, G.T.: Radiotekhnika i Elektronika, 2 (1957) 433.

Moscow Institute of Energetics

Submitted 8 Jan. 1958,
rev. 6 May 1959.

SIMULATING ELECTRICAL FIELD BY MEANS OF INDUCED CURRENT MEASUREMENTS

Pages 602-606

by G.M. Gershteyn

A previously proposed, new method of simulating stationary fields, based on the Shockley-Ramo theorem, is further developed. A means of broadening the boundary conditions is established; it is proposed that the method in question be modified by measuring the charge induced in the electrodes, when a charged probe is introduced at a certain point in the field. A technique of experimentally determining potential using an integrating capacitance is worked out.

In [1,2] the authors proposed a new method of simulating electric field using the Shockley-Ramo theorem on induced currents. It was shown that when a small charged body (the probe) is moved relative to a system of electrodes, if the charge on the probe and its rate of movement are constant, the current, induced in the external electrode circuit, is a function of time, proportional to the distribution function of the component of the stationary field along the corresponding space coordinate. Thus, there is a transition from the spatial distribution of the gradient of the field to the time-dependent function of the induced current. By writing out the latter, it is possible to get a direct picture of the distribution of the field component along the line of movement of the charged probe, i.e. a picture of the field which satisfies the Laplace equation for the boundary conditions, corresponding to the Shockley-

Ramo theorem.

In [2] attention was primarily paid to determining by this method the stationary electric field in models of the simplest systems reduced to two-electrode systems, in which the boundary conditions of the Shockley-Ramo theorem are easily satisfied. However, the significance of the method is broader than this. In fact, this is a method of simulating any physical field, satisfying the Laplace equation, taking into account limitations imposed on the boundary conditions by the way in which the Shockley-Ramo theorem is formulated. It can also be treated as an experimental method of solving problems of mathematical physics, reducible to a Laplace equation.

In this article we shall briefly state certain new results obtained from further development of the above method in connection with an exploration of the possibility of directly determining potential, broadening the boundary conditions and reducing the rate of movement of the charged probe.

1. Determination of probe potential

As already noted [2], during the movement of the charged probe q (Fig. 1) we get on the oscillograph screen a curve representing the dependence of the induced current on time $i_H(t)$, which reflects to a definite scale the distribution of the corresponding component of the intensity of the field E_s along the line of movement of the probe s. However, in many cases the information obtained is insufficient; it is often necessary to determine the potential of the field being studied and establish the equipotential pattern.

It is possible to show that the induced current method also makes it easy to determine the potential of the field. Thus, if we have a family of equipotentials of the section of the field in question through which the probe moves in an arbitrary direction, then to find

the potential we can make use of the known relationship between the potential φ and the intensity E_s:

$$\psi_2 - \psi_1 = \int_{s_1}^{s_2} E_s(s)\, ds, \qquad (1)$$

i.e. integrate the function $E_s(s)$. Taking into account the fact that $E_s(s)$ is proportional (correct to a constant scale factor α) to the time function of the induced current $i_H(t)$, we find that to determine φ it is sufficient to integrate the function $i_H(t)$:

$$\psi_2 - \psi_1 = \alpha \int_{t_1}^{t_2} i_H(t)\, dt \qquad (2)$$

(here t_1 and t_2 are moments of time at which the charged probe passes through the points s_1 and s_2 respectively).

The current induced in the external circuit can be fairly easily integrated by using the capacitance C (Fig. 2) as the integrating element. In this case the voltage $u_H(t)$, passed from the capacitance C to the input of the oscillograph, is determined from the expression :

$$u_H(t) = \frac{1}{C} \int_{t_1}^{t_2} i_H(t)\, dt. \qquad (3)$$

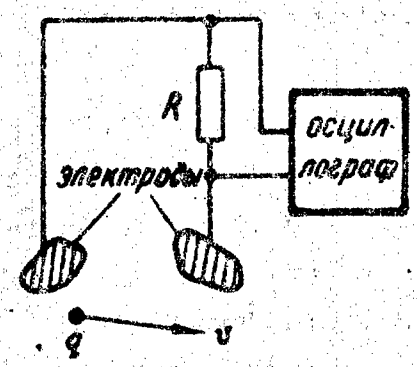

Fig. 1

(Left - electrodes; right - oscillograph)

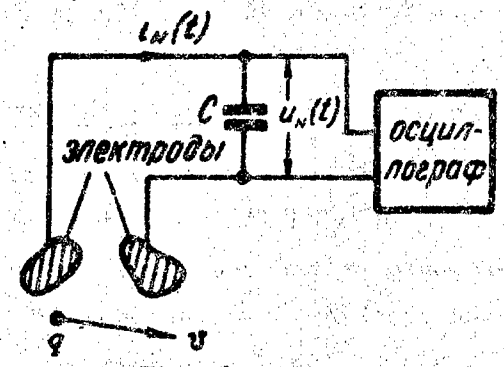

Fig. 2

(Left - electrodes; right - oscillograph)

Accordingly, on the oscillograph screen we shall get an integral curve, representing to a definite scale the distribution of potential along the line of movement of the probe $\varphi(s)$. By displacing, with the aid of some coordinator, the line of movement of the probe in a direction perpendicular to s, we shall get a family of these integral curves $\varphi(s)$. From these curves we can easily plot a family of equipotentials, by assigning definite values of the potential and finding the corresponding coordinates of points on the integral curves, at which the potential has the assigned values.

A positive feature of the above method of determining the potential is the fact that, obtaining a family of integral curves $\varphi(s)$ in the course of a brief experiment, it is then possible to assign any values of the potential, while finding the points of corresponding equipotentials, and thus plotting as dense a network of equipotentials as desired.

A family of integral curves $\psi(\varphi)$ was obtained for the segmental model and the setup with an integrating capacitance described in [2]. The equipotentials plotted from this family of curves satisfactorily coincided with the equipotential lines, obtained for a model of the same structure with the aid of an electrolytic bath.

It is necessary to stress that the proposed simulation method also makes it possible to investigate three-dimensional fields.

2. Broadening the boundary conditions

From the point of view of assigning boundary conditions for the potential of simulated fields certain serious difficulties in applying the proposed method are connected with limitations in the formulation of the Shockley-Ramo theorem [3,4], which allows for only definite values of the dimensionless potentials at the electrodes (+1 and 0). Accordingly, the method in its original form is easy to apply only when simulating fields produced by a small number of system

(for example, two-electrode systems of arbitrary form, pi-mode periodic structures and some others).

In order to broaden the class of systems which can be investigated, it is necessary to be able to simulate the boundary conditions corresponding to any values of the potentials at the electrodes, i.e. to any values of the dimensionless potentials from 0 to 1. To this end we represent the field at any point in the space being studied as a result of superimposing partial fields, obtained by alternately assigning the potential $\varphi = 1$ to one of the electrodes and the potential $\varphi = 0$ to the others. Then, when the charged, punctiform probe, moving at a constant speed v and bearing a charge q, passes through the given point, the component of field intensity, taken in the direction of movement of the probe, will be equal to

$$E_v = E_{v_1} + E_{v_2} + \ldots + E_{v_N}, \qquad (4)$$

and the current induced in the circuit of the n-th electrode (Fig. 3a) will be equal to

$$i_{H_k} = qv E_{v_k}. \qquad (5)$$

Then, clearly,

$$E_v = \frac{1}{qv}\left(i_{H_1} + i_{H_2} + \ldots + i_{H_N}\right), \qquad (6)$$

where N is the total number of electrodes. Connecting up all these electrodes and measuring the sum of the currents, as shown in Fig. 3b, we get the sum :

$$\sum_{k=1}^{N} i_{H_k} = i_{H_1} + i_{H_2} + \ldots + i_{H_N}.$$

Substituting in (6) gives the value of E_v corresponding to a dimensionless potential of + 1 at all these electrodes. We now assume that in adding the currents i_{H_1}, i_{H_2}, ..., i_{H_N} we somehow or other vary the magnitude of each of the currents and the ratio between them. This

is equivalent to varying the corresponding partial fields and (as a result of the linear relationship between the partial field E_{v_k} and the potential φ_k) to a variation of the dimensionless electrode potentials φ'_k satisfying the Shockley-Ramo theorem.

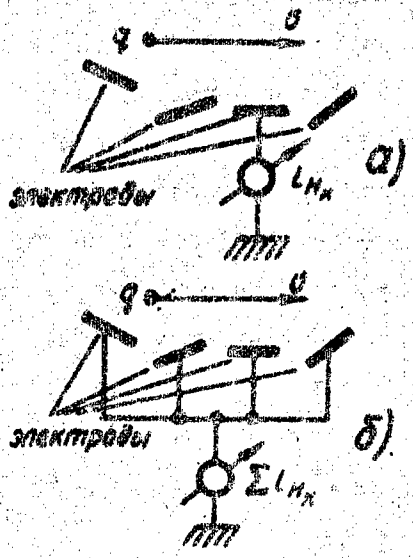

Fig. 3

(Heavy black lines = electrodes)

Since changing the magnitude of the induced current is not practically convenient, it is better to vary not the induced currents themselves but the voltages produced by these induced currents at specially connected resistances. Then , by varying the type of connection and the magnitudes of these resistances, it is easily possible to vary the ratio between the output voltages measured, this also being equivalent to definite variations in the currents of formula (6).

Fig. 4 shows one of the possible variants of the proposed method of assigning arbitrary boundary conditions for the potential with reference to a concrete electrode system (segmental structure). In this case, as the charged probe moves with respect to the segmental structure, the currents, induced as the probe passes the various slots

flow through the various resistances and create various induced voltages at the oscillograph input. By selecting different relationships among R_1 - R_4, it is possible to simulate boundary conditions corresponding to different values of the potentials at the electrodes 1,3,5,7. Preliminary experiments with this simulator confirm the argument outlined above.

The development of the proposed method of assigning boundary conditions makes it possible to simulate fields with arbitrary values of the potentials at the electrodes and, thus, to solve problems with boundary conditions of the first class (the Dirichlet problem). It is important to note that this simulation method makes it possible to solve both the inner and the outer boundary problems, as in this case there are no boundary walls.

3. Reducing the rate of movement of the probe

A fundamental shortcoming of the proposed field simulation method is the presence of the rapidly moving probe. The probe has to move relatively quickly in order to get an induced current big enough for indication purposes. However, this shortcoming is not one of principle; at the same time it is possible to reduce the speed of the probe at the expense of increasing the charge on the probe and varying the dimensions of the model electrodes. Thus, in the first experiments to investigate the field of segmental structures (number of segments - 4 - 8) with a very elementary method of charging the probe by friction, induced voltages sufficient to be recorded on an EO-7 oscillograph were obtained for a rotation of the structure of the order of 1,000-2,000 revs/min [1]. Increasing the number of segments to 24 makes it possible to reduce the rate of rotation to 3,000 revs/min (sic). It is perfectly possible that the use of electrets with a large charge will make it possible to employ comparatively small speeds (of the order of 50 - 100 revs/min).

In a number of cases, when it is required to find the potential at definite points in the field, another possibility, also derived from the Shockley-Ramo theorem, may prove useful. According to the latter it is possible to determine the charge q_{II} induced in a given electrode from the formula

$$q_{II} = q\psi(x_1, y_1, z_1), \qquad (7)$$

where q is the charge on a punctiform particle introduced at a definite point in the field with the coordinates x_1, y_1, z_1; (x_1, y_1, z_1) is the potential which would exist in the point x_1, y_1, z_1 on assigning to one electrode a dimensionless potential equal to + 1, the other electrodes being grounded. By bringing the charged probe to various points in the interelectrode space and measuring the charge thus induced at the electrodes with the aid of a sufficiently sensitive electrometer, it is possible directly to determine the potential at different points in the field. Preliminary experiments have confirmed the possibility of making such a modification in the field simulation method using the Shockley-Ramo theorem. In this case it is not generally necessary for the probe to move rapidly and complicated indicator instruments are not required; however, it is necessary to employ effective methods of screening against external electrostatic fields.

The method of simulating electrical field by measuring induced currents has the following positive features: a) ease with which it is possible to determine the potential distribution and the potential gradient along the line of movement of the charged probe; b) absence of the necessity of creating the field to be simulated, as a result of which power sources are not required; c) the possibility of simulating three-dimensional fields and of solving both inner and outer boundary problems.

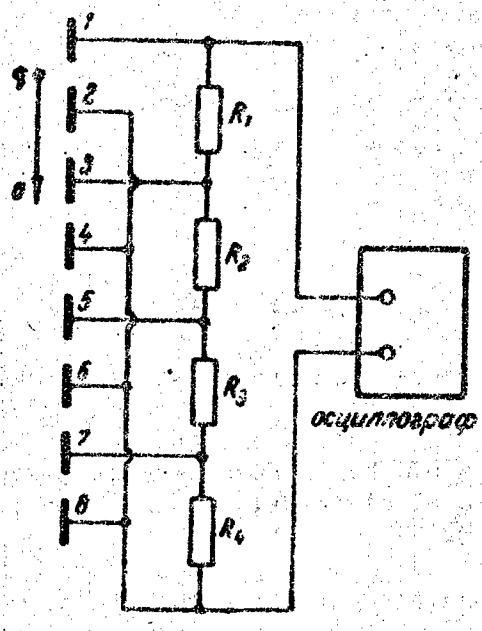

Fig. 4

The fundamental shortcomings of the method are connected with the necessity of making the probe move rapidly and of having a sufficiently sensitive induced current meter. However, these shortcomings are not matters of principle and can be eradicated.

It therefore would appear expedient to develop the proposed method further, since, together with the widely employed conducting layer methods, it can be useful for solving a series of problems in field simulation.

The author wishes to express his gratitude to the participants in the Saratov State University seminar and in particular to V.I. Kalinin, A.I. Shtyrov and V.M. Dashenkov for reviewing the contents of this article.

Bibliography

1. Gershteyn, G.M.: Preobrazovaniye prostranstvennykh harmonik kvasistatsionarnovo plya vo vremennye harmoniki navedennovo toka (Transformation of the spatial harmonics of a quasi-stationary field into time harmonics of the induced current), Report to the MVO conference on radio electronics, Saratov, 1957; see also Radiofizika, 1, 2 (1958) 13.

2. Gershteyn, G.M.: Radiotekhnika i elektronika, 4 (1959) 137.

3. Ramo, S.: Proc. IRE, 27 (1939) 584.

4. Lopukhin, V.M.: Vozbuzhdeniye elektromagnitnykh kolebaniy i voln elektronnymi potokami (Excitation of electromagnetic vibrations and waves by means of electron fluxes), Gostekhizdat, M., 1953.

Saratov State University

Submitted 8 Apr. 1959

CONTRIBUTION TO THE THEORY OF NONLINEAR DAMPERS

Pages 607-625

by M.I. Feygin

The author investigates the dynamics of impact dampers and dry-friction dampers by the point reflection method, while introducing the theory of bifurcations. The zones of existence and stability of the simplest periodic regimes with slipping motion and without slipping are established in the space of the parameters. Recommendations are given for the optimum adjustment of dampers. It is shown that the impact damper can completely extinguish the first harmonic. An explanation is offered of the erroneousness of the criterion of the energy capacity of a damper, used in selecting its optimum parameters.

The present article is devoted to an investigation of the dynamics of impact and dry-friction dampers, which are widely used in modern technology [1-5,12-15]. This question has often been treated theoretically, though not often enough by correct methods*. Accordingly even the simplest damper operating regimes have been inadequately studied**; for example, no investigations of stability have been made.

---

* A more simple problem with one degree of freedom was investigated sufficiently well in [10,19].

** By the simplest regimes we understand symmetrical motion with the period of the external force, with either one impact (impact damper) or one relative stop (dry-friction damper) per half period.

In this article we investigate the simplest periodic movements of a damper, considered as a nonlinear, nonautonomous system with two degrees of freedom, by the method of point reflections [17-19,22,23], introducing the theory of bifurcations [23]. The case of the dry-friction damper is first reduced to the equivalent relay system, thus making it possible to use the methods of studying periodic regimes and the slipping motion of relay systems, worked out in [20,21]. This investigation makes it possible to give practical recommendations for the optimum adjustment of dampers within the limits of the regimes considered and also to define in the space of the parameters the zones of existence and stability of the simplest forms of periodic motion both with and without slipping.

It has proved that part of the regions previously established for the simplest regimes without slipping [3,4,9,13] drops out on account of loss of stability and that part relates to regions with slipping motion.

Formulas are obtained for finding the parameters of dampers at which the amplitude of the fundamental harmonic close to the resonance frequency will be a minimum. We shall note that the impact damper can completely dissipate the first harmonic but that in this connection it is necessary to adjust to the frequency and magnitude of the external force.

A formula for the displaced resonance frequency is obtained for the dry-friction damper.

The erroneousness of the criterion of the energy capacity of a damper, widely used in selecting optimum parameters, is explained. Then, if an optimally tuned dry-friction damper has an energy capacity close to the maximum, the impact damper, on the other hand, can effectively extinguish vibrations, practically without dissipating energy.

1. The equations of motion

The model in question consists of an elastically supported (with a coefficient of elasticity k) mass M, on which there acts an external sinusoidal force (Fig. 1). The movement of the mass m is restricted by two stops, contact with which is accompanied by an instantaneous, inelastic impact with a coefficient of recovery R. Between the masses M and m there acts a dry-friction force F_1. Since basically energy is dissipated on impact and as the result of dry friction, we shall neglect viscous friction. Then in the intervals between impacts we shall have the following equations of motion:

$$M\ddot{x} + kx = F\sin\Omega t + F_1(\dot{x} - \dot{y}); \quad m\ddot{y} = -F_1(\dot{x} - \dot{y}) \qquad (|y - x| - D). \tag{1.1}$$

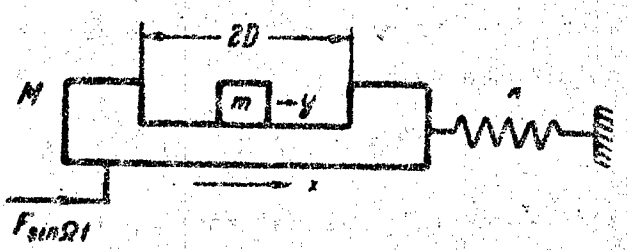

Fig. 1

For purposes of calculation the origin has been chosen as the position of the mass M, when the spring is in the undeformed state and the mass m is in the middle between the two stops. If in (1.1) we employ the dimensionless variables $\xi = F^{-1}M\Omega^2 x$, $\eta = F^{-1}M\Omega^2 y$, $\tau = \Omega t$, we get:

$$\ddot{\xi} + \omega^2\xi = \sin\tau + f(\dot{\xi} - \dot{\eta}); \quad \mu\ddot{\eta} = -f(\dot{\xi} - \dot{\eta}) \qquad (|\eta - \xi| < d). \tag{1.2}$$

The nonlinear function $f = F_1F^{-1}$ is determined in the following way:

$$f(\dot{\xi} - \dot{\eta}) = -h\,\mathrm{sgn}(\dot{\xi} - \dot{\eta}) \qquad (\dot{\xi} - \dot{\eta} \neq 0);$$
$$-h \leqslant f(\dot{\xi} - \dot{\eta}) \leqslant h \quad (\dot{\xi} - \dot{\eta} = 0); \tag{1.3}$$

the parameters μ, d and ω^2 are respectively equal to mM^{-1}, $F^{-1}M\Omega^2D$ and $kM^{-1}\Omega^{-2}$.

When $\eta - \xi = \pm d$ impact occurs. The velocities $\dot{\xi}_0$ and $\dot{\eta}_0$ immediately before impact are connected with the velocities $\dot{\xi}_0'$ and $\dot{\eta}_0'$ immediately after impact by the expression

$$(1+\mu)\dot{\xi}_0' = (1-\mu R)\dot{\xi}_0 + \mu(1+R)\dot{\eta}_0; \quad (1+\mu)\dot{\eta}_0' = (1+R)\dot{\xi}_0 + (\mu - R)\dot{\eta}_0. \tag{1.4}$$

In this article we shall not consider the general case of impact and dry friction but restrict ourselves to a study of two particular cases.

2. The case where h = 0 (impact damper)

Reduction to a point transformation.

In order to study the dynamics of an impact damper we put h = 0 in (1.2). We obtain the system

$$\ddot{\xi} + \omega^2\xi = \sin\tau; \quad \ddot{\eta} = 0 \quad (|\eta - \xi| < d), \tag{2.1}$$

which is characterized by the four parameters ω, d, μ, R, varying within the limits $0 \leqslant \omega, d, \mu < \infty$, $0 \leqslant R \leqslant 1$.

The phase-space of the system will be five-dimensional in the coordinates ξ, $\dot{\xi}$, η, $\dot{\eta}$, τ. It is divided into three regions by the surfaces $\eta - \xi = \pm d$ (we shall denote the latter by Π_+ and Π_-). We are interested only in motion in region G lying between Π_+ and Π_-. Let the initial moment correspond to the passing of the representative point M_0, with the coordinates ξ_0, $\dot{\xi}_0$, η_0, $\dot{\eta}_0$, τ_0, from G to Π_+. Then, if $R > 0$, it moves instantaneously along Π_+ to the point M_0' with the coordinates ξ_0, $\dot{\xi}_0'$, η_0, $\dot{\eta}_0'$, τ_0 and, leaving Π_+, moves again into G, until it once more falls on Π_+ or Π_- at a certain point M_1 (Fig. 2a). The equations for the transition from M_0 to M_1 are obtainable from (1.4) and (2.1):

$$\xi_1 = \omega^{-1}(\beta\dot{\xi}_0 - \alpha\cos\tau_0)\sin\omega(\tau_1-\tau_0) + (\xi_0 - \alpha\sin\tau_0)\cos\omega(\tau_1-\tau_0) + \alpha\sin\tau_1;$$

$$\dot{\xi}_1 = (\beta\dot{\xi}_0 - \alpha\cos\tau_0)\cos\omega(\tau_1-\tau_0) - \omega(\xi_0 - \alpha\sin\tau_0)\sin\omega(\tau_1-\tau_0) + \alpha\cos\tau_1; \qquad (2.2)$$

$$\eta_1 = \eta_0 + \gamma\dot{\xi}_0(\tau_1-\tau_0);\ (1+\mu)\dot{\eta}_1 = (\mu - R)\dot{\eta}_0 + (1+R)\dot{\xi}_0;\ \eta_1 - \xi_1 = \pm d,$$

where

$\alpha = (\omega^2-1)^{-1}$; $\beta = (1-R-2\mu R)(1-R+2\mu)^{-1}$; $\gamma = (1+R)(1-R+2\mu)^{-1}$

and τ_1 is the smaller root ($\tau_1 > \tau_0$).

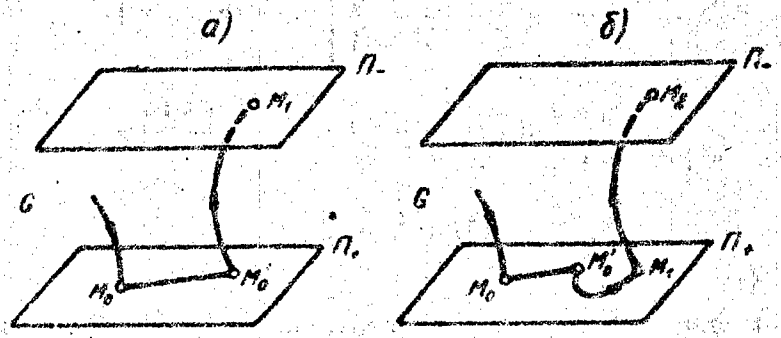

Fig. 2

Thus, the investigation of the motion of a representative point reduces, when $R > 0$, to the study of the point reflection of the surface Π_+ in itself or in Π_- (we shall call the latter a T_- - transformation), defined by (2.2).

If $R = 0$, then (2.2) will hold true when immediately after impact $\ddot{\xi}_0' > 0$. When $\ddot{\xi}_0' < 0$, the representative point moves from M_0' to M_1, without leaving Π_+. This corresponds to the common motion of the masses M and m. At the moment τ_1, definable as the least root of the equation $\ddot{\xi}(\tau) = 0$, the representative point leaves Π_+ and moves in G, until it again arrives at Π_+ or Π_- in the

point M_2 (Fig. 2b). The equations for the transformation, corresponding to the transition from M_0 to M_1, for $R = 0$ and $\dot{\xi}_0' < 0$ (we shall call it the S-transformation) are obtained from (1.4) and the solution of the equation

$$(1+\mu)\ddot{\xi} + \omega^2 \xi = \sin\tau \quad (\eta - \xi = d). \tag{2.3}$$

They have the form:

$$\begin{aligned}
\xi_1 = \eta_1 - d &= \frac{\nu}{\omega^2}\left[\dot{\xi}_0 + \frac{\omega^2-\nu^2}{\nu^2}\eta_0 - \frac{\cos\tau_0}{\nu^2-1}\right]\sin\nu(\tau_1-\tau_0) + \\
&+ \left[\xi_0 - \frac{\nu^2\sin\tau_0}{\omega^2(\nu^2-1)}\right]\cos\nu(\tau_1-\tau_0) + \frac{\nu^2\sin\tau_1}{\omega^2(\nu^2-1)}; \\
\dot{\xi}_1 = \eta_1 &= \frac{\nu^2}{\omega^2}\left[\dot{\xi}_0 + \frac{\omega^2-\nu^2}{\nu^2}\eta_0 - \frac{\cos\tau_0}{\nu^2-1}\right]\cos\nu(\tau_1-\tau_0) - \\
&- \nu\left[\xi_0 - \frac{\nu^2\sin\tau_0}{\omega^2(\nu^2-1)}\right]\sin\nu(\tau_1-\tau_0) + \frac{\nu^2\cos\tau_1}{\omega^2(\nu^2-1)}; \\
&\omega^2\xi_1 - \sin\tau_1 = 0,
\end{aligned} \tag{2.4}$$

where $\nu^2 = \omega^2(1+\mu)^{-1}$.

The equations of the T-transformation, corresponding to the transition from M_1 to M_2, are obtained from (2.1):

$$\begin{aligned}
\xi_2 &= \omega^{-1}\left|\dot{\xi}_1 - \alpha\cos\tau_1\right|\sin\omega(\tau_2-\tau_1) + \\
&+ \left[\xi_1 - \alpha\sin\tau_1\right]\cos\omega(\tau_2-\tau_1) + \alpha\sin\tau_2; \\
\dot{\xi}_2 &= \left|\dot{\xi}_1 - \alpha\cos\tau_1\right|\cos\omega(\tau_2-\tau_1) - \\
&- \omega\left[\xi_1 - \alpha\sin\tau_1\right]\sin\omega(\tau_2-\tau_1) + \alpha\cos\tau_2;
\end{aligned} \tag{2.5}$$

$$\eta_2 = \eta_1 + \dot{\eta}_1(\tau_2-\tau_1); \quad \dot{\eta}_2 = \dot{\eta}_1; \quad \eta_2 - \xi_2 = +d.$$

Here τ_1 and τ_2 must be the least roots of the equations, satisfying the conditions $\tau_1 > \tau_0$, $\tau_2 > \tau_1$.

Establishing regions in the space of the parameters corresponding to periodic movements.

Finding forms of periodic motion reduces to establishing closed trajectories in the phase space. By D we shall denote the region in the space of the parameters corresponding to the simplest regime. Then to each point in D there will correspond a stationary point of the transformation T_-T_+, if $R > 0$ or $R = 0$ and $\ddot{\xi}'_0 > 0$, and of the transformation ST_-ST_+, if $R = 0$ and $\ddot{\xi}'_0 < 0$. The stationary point is found from the condition $\tau_2 = \tau_0 + 2\pi$ and from the condition of coincidence of the phase coordinates of the final and initial points of the transformation.

To investigate the stability we form a characteristic equation $\chi(z) = 0$, for which we vary all the variables in the equations for the corresponding point transformation in the neighborhood of the stationary point and assume that $\delta\{M_2\} = z\,\delta\{M_0\}$.

Suppose that it is known that a certain point in the space of the parameters belongs to D. In varying the parameters sooner or later we shall hit on the boundary of D. The surfaces, bounding D, correspond to bifurcation values of the parameters, every logically possible bifurcation having a corresponding surface in the space of the parameters. Thus, to a breach of the conditions for the existance and stability of a stationary point of the transformation there correspond [23] boundary surfaces N_{+1}, N_{-1}, N_φ, the equations for which are obtained from $\chi(z) = 0$ by substituting $z = +1, -1, e^{i\varphi}$.

Another type of boundary surface is obtained from the condition that the period of movement of the representative point in the region G or on the surfaces Π_+ and Π_- be the least root of the equation $\Phi_1(\tau) = \eta(\tau) - \xi(\tau) \pm d = 0$ (or $\Phi_2(\tau) = \omega^2\xi(\tau) - \sin\tau = 0$). Let the function $\Phi(\tau)$ vanish when $\tau = \tau''$ and not have a zero when $\tau' < \tau < \tau''$. If, when the parameters are varied, at a certain value there appears a new root τ^* in the interval

mentioned, then $\Phi(\tau^*) = 0$ and $\Phi'(\tau^*) = 0$ must be fulfilled. On eliminating the parameter τ^* from the two equations, we shall get a certain surface in the space of the parameters, corresponding to the limit of the occurrence of extraneous roots. We shall denote the latter by C_τ. Then the equations of C_τ, corresponding to the $T_\pm$-transformation, have the form:

$$\eta(\tau^*) \quad \xi(\tau^*) \quad d = 0; \quad \eta(\tau^*) \quad \xi(\tau^*) = 0, \tag{2.6}$$

and those corresponding to the S-transformation the form:

$$\omega^2 \xi(\tau^*) - \sin\tau^* = 0; \quad \omega^2 \xi(\tau^*) - \cos\tau^* = 0. \tag{2.7}$$

For the simplest regime with slipping there is one more bifurcation surface, corresponding to the value of the parameters, at which the slipping movement disappears. We shall denote the latter by C_s. We get the equation of C_s from the condition that the acceleration of the system immediately after impact is equal to zero: $\ddot{\xi}_0' = 0$.

Since in the case of the impact damper there are no other logically possible bifurcations, to define D it is necessary and sufficient to construct in the space of the parameters the boundary surfaces N_{+1}, N_{-1}, N_φ, C_τ and C_s, mentioned above.

The simplest regime without slipping.

To the regime studied below there corresponds a stationary point of the transformation $T_- T_+$. However, in investigating a symmetrical regime it is sufficient to consider the T_--transformation of (2.2), putting

$$\xi_1 = -\xi_0; \quad \eta_1 = -\eta_0; \quad \dot{\xi}_1 = -\dot{\xi}_0; \quad \eta_1 = -\eta_0; \quad \tau_1 = \tau_0 + \pi. \tag{2.8}$$

After varying (2.2) with respect to all the variables close to the stationary point of the transformation and substituting $\delta\xi_1 = -z\,\delta\xi_0$ $\delta\eta_1 = -z\,\delta\eta_0$, $\delta\dot{\xi}_1 = -z\,\delta\dot{\xi}_0$, $\delta\dot{\eta}_1 = -z\,\delta\dot{\eta}_0$ and $\delta\tau_1 = z\,\delta\tau_0$, we get the characteristic equation

$$\begin{vmatrix} 0; & 1+z; & z\pi(-1+\mu R); & 2\gamma(z-1); \\ 1+R; & 0; & z(1-\mu R)- & 0; \\ & & -R(1+\mu); & \\ (1-\mu R)\omega^{-1}\sin\omega\pi; & z+\cos\omega\pi; & 0; & 2(1-z)- \\ & & & -(1+\beta)(1+\cos\omega\pi)- \\ & & & -A\omega^{-1}\sin\omega\pi; \\ z(1+\mu)+1-\mu R; & -\omega\sin\omega\pi; & -z\mu(1+R); & (z-1)\omega(1-\beta)\operatorname{tg}\omega\pi\,2+ \\ & & & +\omega(1+\beta)\sin\omega\pi- \\ & & & -A(z+\cos\omega\pi) \end{vmatrix} = 0, \quad (2.9)$$

where A is found from the expression

$$d^2\left|A^2+(1+\beta)^2\right| = \alpha^2\left|A-\pi\gamma-(1-\beta)\operatorname{tg}(\omega\pi/2)\right|^2. \quad (2.10)$$

Substituting $z = 1$, -1 and $e^{i\varphi}$ in (2.9) and eliminating A from (2.9) and (2.10), we get the equations of the surfaces N_{+1}, N_{-1} and $N\varphi$.

In Fig. 3 these boundaries are shown in the plane of the parameters d, ω, computed for R = 0.5, μ = 0.05 (Fig. 3a) and R = 0.5, μ = 0.5 (Fig. 3b). In both cases the region of stability is hatched.

It is characteristic that the simplest regime can be realized in a very small region of variation of the parameters and disappears at a frequency close to resonance*.

The more interesting case of resonance ($\omega = 1$) will be considered further. When $\omega = 1$, the characteristic equation (2.9) takes on the simpler form:

$$z^4+(k+2g)z^3+(2R-2k+g^2)z^2+(k+2Rg)z+R^2=0, \quad (2.11)$$

where

$$k=2(1+R)^2(1+\mu)^{-2}(\mu-\mu d+\pi^2/8);$$

$$g=(1+\mu)^{-1}(1+R)(\mu-1).$$

---

* The author of [8] notes the necessity of investigating the behavior of a damper close to resonance, since for certain values of the parameters it is very sensitive even to a small variation in frequency.

In this case the boundary N_{+1} will be $\mu = 0$; the boundary N_{-1} is described in the form: $8\mu(d-1) - \pi^2 + 4 = 0$ and the boundary N_0 breaks down into $R = 1$, $\mu = \infty$ and $8\mu(d-1) - \pi^2 - 8(1+\mu)(R-1)^2(R+1)^{-2} = 0$.

Fig. 4 shows the boundaries mentioned in various planes of the space of the parameters; the regions of existence and stability are hatched.

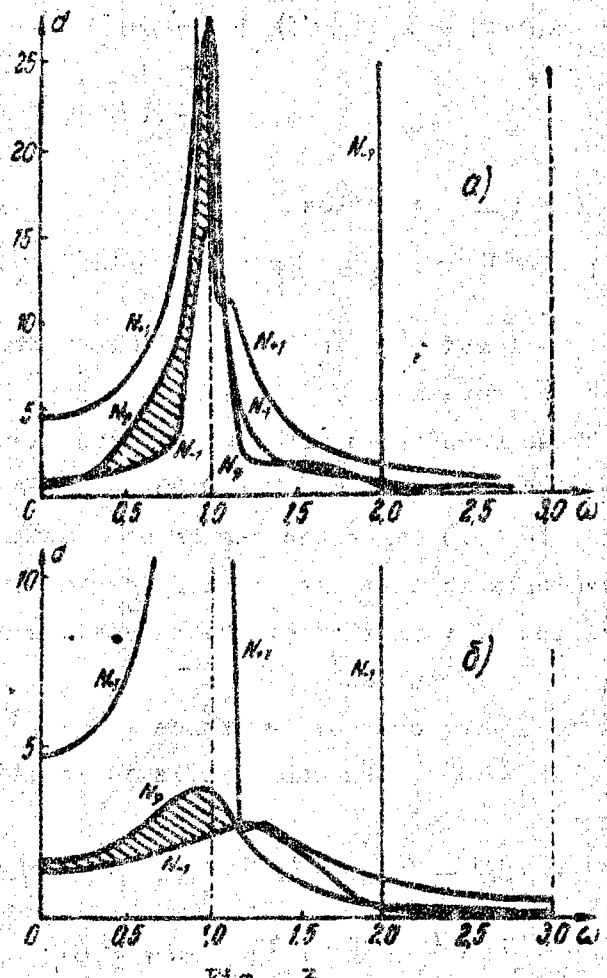

Fig. 3

The boundary surfaces C_τ (2.6) for $\omega = 1$ are written in the form:

$$(\pi^2 - 8\mu d)\cos\tau^* - 2|\pi(1-R-2\mu R)(1+R)^{-1} + 2\mu\tau^*|\sin\tau^* + 2\pi\tau^* - \pi^2 + 8\mu d = 0; \quad (2.12)$$

$$(\pi^2 - 8\mu d - 4\mu)\sin\tau^* - 2|\pi(1-R) - 2\mu R)(1-R)^{-1} \cdot \cdot \cdot - 2\mu\tau^*|\cos\tau^* - 2\pi = 0, \tag{2.12}$$

where the parameter τ^* varies within the limits $0 \leqslant \tau^* \leqslant \pi$. The $\pm$ sign in the first equation of (2.12) relates to the arrival of the representative point at Π_- or Π_+ respectively. In the first case the boundary C_τ does not intersect D* but in the second case it cuts out of D a small zone, corresponding to an additional impact against the stop, with which the last collision took place. In Fig. 4a this zone is indicated by double hatching.

We have not plotted C_τ in the general case in which $\omega \neq 1$. However, from a consideration of the case $\omega = 1$ it follows that C_τ can only reduce the regions of the existence and stability of the simplest regime established previously.

The greatest practical interest is offered by the value of the amplitude of the vibrations of the system close to the resonance frequency. We get the dependence $\xi(\tau)$ from (2.2) taking into account (2.8) and considering τ_1 a simply flowing coordinate.

Then putting $\omega = 1 - \Delta\omega$ and expanding $\xi(\tau)$ in series with respect to $\Delta\omega$, we shall confine ourselves to terms of the first order of smallness. Finally, on expanding the result as a Fourier series, we get the amplitude of the fundamental and higher harmonics:

$$\psi_1^2 = \left(d - \frac{1}{4} - \frac{\pi^2}{8\mu}\right)^2 + \frac{\pi^2(1+\mu)^2(1-R)^2}{16\mu^2(1+R)^2} + \Delta\psi_1^2; \tag{2.13}$$

$$\psi_n = (n^2-1)^{-1}|1 + \Delta\psi_n| \qquad (n = 3, 5, 7, \ldots),$$

where $\Delta\psi_1^2$ and $\Delta\psi_n$ are small quantities of the order of $\Delta\omega$. Fig. 4a shows curves of different amplitudes of the first harmonic. It is

---

* Since when $\tau^* = 0$ R = 0 and d = 0, the proof of this assertion reduces to the easily obtained proof of the absence of points of intersection of C_τ and N_{-1}. The corresponding boundary of C_τ is shown in Fig. 4a.

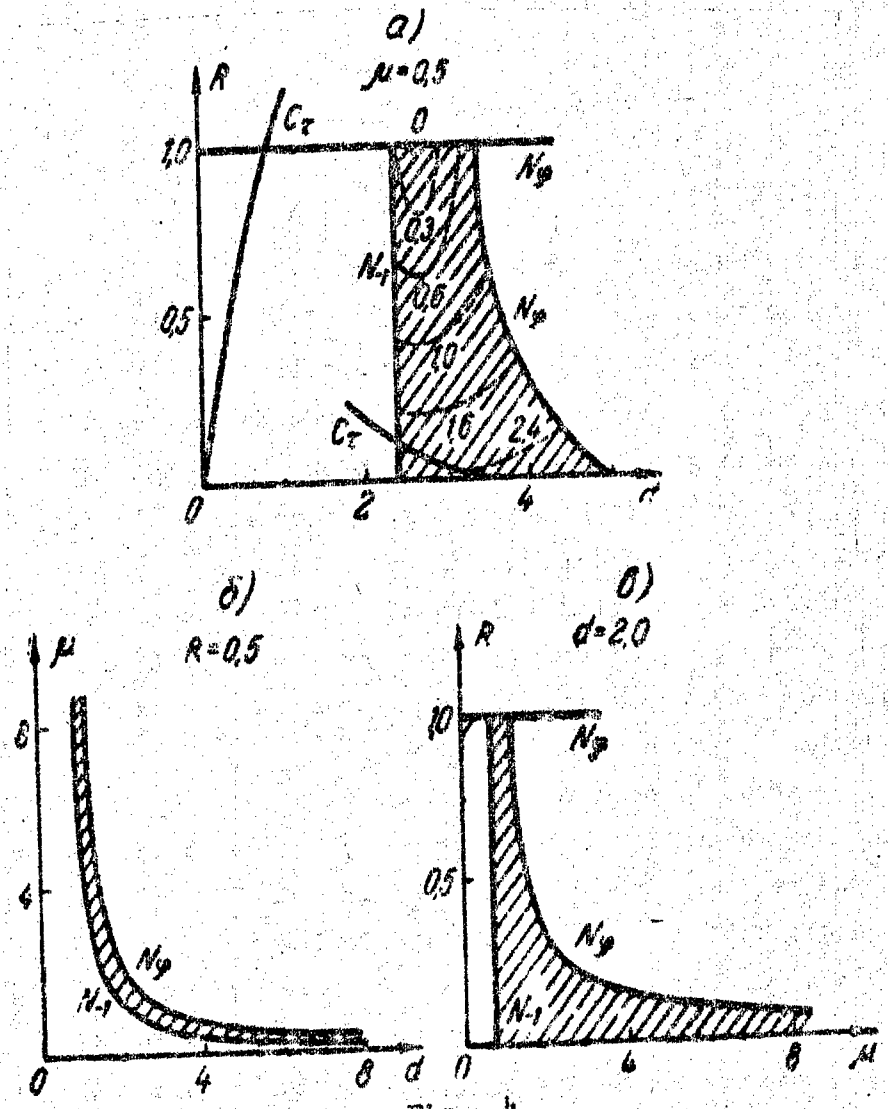

Fig. 4

clear from the figure and from (2.3) that for a value of the parameters corresponding to D there is no sharp increase in the amplitudes of the first harmonic on approaching the resonance frequency*.

It follows from (2.13) that when $\omega = 1$ the optimum distance between the stops $d^* = \pi^2/8\mu + 1/4$ or in dimensional parameters $D^* = (F/M\Omega^2)(1/4 + \pi^2 M/8m)$. The coefficient of recovery of speed R ought to be close to unity, in spite of the fact that the energy absorbed by the damper is then small. This confirms that selecting

* This corresponds with the results of the experiments described in [9].

optimum parameters for a damper on the basis of maximum energy capacity is not justified.

It is interesting to note that if, at the resonance frequency, $d = d^*$ and $R \to 1$, then the amplitude of the fundamental harmonic vanishes. Accordingly, the action of an impact damper is analogous to the action of a resonance dynamic damper in a system without viscous friction [15].

The simplest regime with slipping ($R = 0$).

The simplest periodic motion with slipping, considered in this section, corresponds to a symmetrical point in the transformation $ST_- ST_+$. Its coordinates satisfy expressions (2.4)-(2.5) and the condition:

$$\xi_2 = -\xi_0;\ \dot{\xi}_2 = -\dot{\xi}_0;\ \eta_2 = -\eta_0;\ \dot{\eta}_2 = -\dot{\eta}_0;\ \tau_2 = \tau_0 + \pi. \quad (2.14)$$

After varying (2.4) and (2.5) with respect to all the variables close to the stationary point of the transformation and substituting $\delta\xi_2 = -z\delta\xi_0;\ \delta\eta_2 = -z\delta\eta_0;\ \delta\dot{\xi}_2 = -z\delta\dot{\xi}_0;\ \delta\dot{\eta}_2 = -z\delta\dot{\eta}_0;\ \delta\tau_2 - z\delta\tau_0$ we get the following characteristic equation:

$$\begin{vmatrix} (1+z\cos\nu\tau)\,\omega^2 & \nu^2\,|1-\cos\omega(\pi-\tau)|; & z\omega\sin\nu\tau-\nu\sin\omega(\pi-\tau); \\ -z\omega^3\sin\nu\tau+\nu^3\sin\omega(\pi-\tau)+ & & \omega^2(z\cos\nu\tau+1)- \\ +\nu\omega(\omega^2-\nu^2)(\pi-\tau); & & -\nu^2\,|1-\cos\omega(\pi-\tau)| \end{vmatrix} = 0. \quad (2.15)$$

Here τ denotes the duration of the slip ($0 \leqslant \tau \leqslant \pi$). Substituting $z = +1, -1, e^{i\varphi}$ in (2.15), we get the equations of the boundary surfaces N_{+1}, N_{-1}, N_φ in the space of the parameters ω, ν, τ or (since $\nu = \omega(1+\mu)^{-1/2}$) in the space ω, μ, τ.

After simplifying the equation of N_φ reduces to the form:

$$\mu(1+\mu)^{-2}\,|\omega(\pi-\tau)\sin\omega(\pi-\tau) - 2 + 2\cos\omega(\pi-\tau)| = 0. \quad (2.16)$$

It follows from (2.16) that N_φ coincides with the surfaces corresponding to the limiting values of the parameter μ ($\mu = 0$ and $\mu = \infty$)

and also represents a family of cylindrical surfaces, parallel to the μ-axis. Each surface in the family corresponds to a root of the equation $x \sin x - 2(1 - \cos x) = 0$, the two surfaces $\omega = 0$ and $\tau = \pi$ corresponding to the zero root. A family of N_φ, shown as solid lines, is illustrated in Fig. 5 for $\mu = 0.05$.

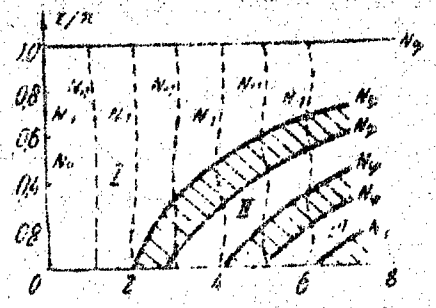

Fig. 5

Even after transformation the equations for N_{+1} and N_{-1} are too clumsy and we shall not present them. In Fig. 5 the boundaries N_{+1} and N_{-1} are shown by dotted lines. The extreme N_{-1} boundary coincides with $\omega = 0$; the succeeding ones are disposed close to integer values of the frequency ω, alternating with each other. However, as can be seen in the figure, in which the region of existence and stability is shown hatched, N_{+1} and N_{-1} define only an infinitely narrow strip of instability. "Large" regions of instability are defined by the boundaries N_φ.

As far as the regions of existence and stability thus defined are concerned, it is necessary to check that the period of movement of the representative point in the region G or on the surfaces Π_+, Π_- is the least root of the equations (2.4) and (2.5), for which it is necessary to plot the boundaries C_π. From (2.6) and (2.7), bearing in mind (2.4), (2.5) and (2.14), we get the equations of C_π for the S-transformation:

$$\frac{\nu}{\omega^2}\left[\dot{\xi}_0 + \frac{\omega^2 - \nu^2}{\nu^2}\,\eta_0 - \frac{\cos\tau_0}{\nu^2 - 1}\right]\sin\nu(\tau^* - \tau_0) +$$

$$+\left[\xi_0-\frac{\nu^2\sin\tau_0}{\omega^2(\nu^2-1)}\right]\cos\nu(\tau^*-\tau_0)+\frac{\sin\tau^*}{\omega^2(\nu^2-1)}=0;$$

$$\frac{\nu^2}{\omega^2}\left|\xi_0+\frac{\omega^2-\nu^2}{\nu^2}\cdot\eta_0-\frac{\cos\tau_0}{\nu^2-1}\right|\cos\nu(\tau^*-\tau_0)- \tag{2.17}$$

$$-\nu\left[\xi_0-\frac{\nu^2\sin\tau_0}{\omega^2(\nu^2-1)}\right]\sin\nu(\tau^*-\tau_0)+\frac{\cos\tau^*}{\omega^2(\nu^2-1)}=0,$$

where the parameter τ^* varies within the limits $\tau_0\leqslant\tau^*\leqslant\tau_0+\tau$, and the equation C for the T-transportation:

$$\eta_0(\pi+\tau_0-\tau^*)-\eta_0-\alpha\sin\tau^*+\omega^{-1}(\alpha\cos\tau_0-\dot\xi_0)\sin\omega(\pi-\tau_0-\tau^*)+$$
$$+(\xi_0-\alpha\sin\tau_0)\cos\omega(\pi+\tau_0-\tau^*)\mp d=0;$$

$$\eta_0+\alpha\cos\tau^*+(\alpha\cos\tau_0-\dot\xi_0)\cos\omega(\pi+\tau_0-\tau^*)- \tag{2.18}$$
$$-\omega(\xi_0-\alpha\sin\tau_0)\sin\omega(\pi+\tau_0-\tau^*)=0,$$

where the parameter τ^* varies within the limits $\tau_0+\tau\leqslant\tau^*\leqslant\tau_0+\pi$. Constants (2.17) and (2.18) have not been plotted. However, for concrete values of the parameters of region I a check showed that τ_1 and τ_2 actually are the least roots of (2.4) and (2.5). Accordingly, C_τ can only reduce the region I. No check of this kind was made for the other regions of stability in Fig. 5.

Finally, it is necessary to make sure that after the arrival of the representative point on Γ_+ $\ddot\xi_0'<0$, i.e. slipping occurs. Since the equation of the surface C_s, bounding the corresponding region in the space of the parameters, coincides with $\tau=0$, it is sufficient to check the condition $\ddot\xi_0'<0$ for any point in the plane ω,τ (Fig. 5). A check confirms that the regions defined correspond to a regime with slipping. Note that when ω and μ are fixed to each value of the parameter τ there corresponds a value of the parameter d. They are connected by the equations of the stationary point of the transformation. For example, when $\omega=1$, the simplest regime exists and is stable when $0<\nu<1$ and $0<\tau<\pi$. Expressing τ by means

of d, we find that $\tau = \pi$ corresponds to d = 0 and that $\tau = 0$ corresponds to the boundary $d = 1 + \nu^2\pi^2/8(1-\nu^2)$, which, by the way, will be the boundary C_s in the plane of the parameters d, μ.

Since for values of the parameters corresponding to N_{+1} or N_{-1} the dynamics of the system require special study, we shall consider the case $\omega = 0$ separately. In this case the equations of motion are : $\ddot{\xi} = \sin\tau$, $\ddot{\eta} = 0$ when $|\eta - \xi| < d$ and $(1+\mu)\ddot{\xi} = \sin\tau$ if $|\eta - \xi| = d$. Disregarding the uniform motion of the whole system, permitted by the equations written, we shall introduce a new variable $y = \eta - \xi$. Then at any moment of time the state of the system will be completely defined by the three quantities $y, \dot{y}$ and τ , the phase-space of which we shall also discuss.

The equation of independent motion of the masses in the variable y is:

$$\ddot{y} = -\sin\tau \quad (|y| < d). \tag{2.19}$$

At the moment when $|y| = d$ the impact occurs. Since R = 0, immediately after the impact $\dot{y} = 0$ but for slipping the condition $\ddot{\xi} < 0$ (or $\sin\tau < 0$) must also be fulfilled, if the representative point passed to Π_+, or $\ddot{\xi} > 0$ ($\sin\tau > 0$), if it passed to Π_-. The slipping $y = \pm d$ when $\sin\tau \lessgtr 0$ ceases when $\sin\tau = 0$.

Let the initial point of the transformation M_0 correspond to the moment τ_0 of breaking away of the masses after slipping at Π_+ (according to (2.20) we can take $\tau_0 = 0$). Then three constraints are imposed on the coordinates for M_0: $y_0 = d$, $\dot{y}_0 = 0$ and $\sin\tau_0 = 0$. Hence it follows that: if there is any periodic motion, it is stable, because it corresponds to a zero-dimensional point transformation.

It remains to settle the question of the presence of stationary points in the transformation.

After break-away the motion continues in accordance with (2.19) until there is a new impact in the point M_1. From the equations of transition from $M_0(d,0,0)$ to $M_1(y_1, \dot{y}_1, \tau_1)$

$$y_1 = d + \sin\tau_1 - \tau_1; \quad \dot{y}_1 = \cos\tau_1 - 1; \quad y_1 = -d$$

it is evident that the coordinate $y(\tau)$ is monotone decreasing. Accordingly, the representative point, leaving Π_+, certainly arrives at Π_-. Then, the equation $y_1 = -d$ or $\tau_1 - \sin\tau_1 = 2d$ has a unique root.

If d is such that $\sin \tau_1 > 0$ (i.e. $2\pi n < \tau_1 < (2n+1)\pi$ or $2\pi n < 2d < \pi(2n+1)$), after impact there is slipping with respect to the point M_2 ($y_2 = -d$; $\dot{y}_2 = 0$; $\tau_2 = (2n+1)\pi$). Comparing the coordinates M_2 and M_0 we see that there is a symmetrical stationary point of the transformation, and thus symmetrical motion with the period $2\pi(2n+1)$.

This proves, then, that at one of the boundaries N_{-1} there are simplest regimes with slipping which are stable; the intervals of d corresponding to them are also established.

3. The special case $d = \infty$ (dry-friction damper)

Reduction to a relay system. Phase-space. Classification of possible periodic motions.

In order to study the dynamics of the dry-friction damper, we shall make the distance between stops in eq. (1.2) $d = \infty$ and reduce the problem in question to a study of some relay system, thus making it possible to apply the methods worked out in [20,21].

By $x(\tau)$ we shall denote the output of the relay and the input of the linear link, by $y(\tau)$ the input of the relay, equal to the sum of the output of the linear link and the function $(\omega^2 - 1)^{-1} \cos\tau = \varkappa \cos\tau$, the derivative of the solution of the inhomogeneous equation $\ddot{\xi} + \omega^2 \xi = \sin\tau$.

The transmission factor of the linear link $K(p)$ is equal to the sum of the transmission factors of links corresponding to the equations $\ddot{\xi} + \omega^2 \xi = f(\dot{\xi} - \dot{\eta})$ and $\mu\ddot{\eta} = -f(\dot{\xi} - \dot{\eta})$:

$$K(p) = \frac{p}{p^2 + \omega^2} + \frac{1}{\mu p} = \sum_{i=1}^{3} \frac{c_i}{p - \lambda_i}, \tag{3.1}$$

where

$$\lambda_{1,2} = \pm j\omega; \quad \lambda_3 = 0; \quad c_{1,2} = 0{,}5; \quad c_3 = \mu^{-1}. \tag{3.2}$$

We shall assume the following relay characteristic:

$$x(\tau) = -h \operatorname{sgn} y(\tau) \quad (y(\tau) \neq 0); \qquad -h \leqslant x(\tau) \leqslant h \quad (y(\tau) = 0). \tag{3.3}$$

Furthermore, we shall introduce new variables y_i :

$$y_i = \frac{c_i}{p - \lambda_i} x; \qquad \dot{y}_i - \lambda_i y_i = c_i x. \tag{3.4}$$

Then the output of the linear link is in the form of a sum of the new variables:

$$\sum \frac{c_i}{p - \lambda_i} x = K(p)\, x.$$

Since the input of the relay is fed by an external force, the phase-space of the system will be four-dimensional in the coordinates y_1, y_2, y_3, τ , where τ is the phase. It follows from the form of the relay characteristic (3.3) that in the phase-space two regions of motion can be defined.

a) A region G_{+h}, where the relay input $y = \sum y_i + \alpha \cos \tau < 0$. Here the relay output $x(\tau) = +h$ and the equation of motion is:

$$\dot{y}_i - \lambda_i y_i = c_i h. \tag{3.5}$$

b) A region G_{-h}, where the relay input $y > 0$. Here the relay output $x(\tau) = -h$ and the equation of motion is:

$$\dot{y}_i - \lambda_i y_i = -c_i h. \tag{3.6}$$

The boundary of these regions is the relay switching surface, defined by the condition that the relay input is equal to zero:

$$y(\tau) = \sum y_i(\tau) + \alpha \cos \tau = 0. \tag{3.7}$$

The structure of the phase-space close to this surface is defined by the sign of $\dot{y}(\tau)$. If $\dot{y} < 0$, then the phase trajectories are directed towards the surface (3.7) in G_{-h} and away from it in G_{+h}; if $\dot{y} > 0$, then the pattern is reversed. Consequently, the inter-

Section of the surface $\dot{y} = \sum \dot{y}_i - \alpha \sin\tau = 0$ with (3.7) divides the latter into regions with different structures of the phase trajectories close to it. In accordance with (3.2), (3.5) and (3.6) the equation $\dot{y} = 0$ can be rewritten in the form:

$$\begin{aligned} &\sum \lambda_i y_i - \alpha \sin\tau + h\mu^{-1}(1+\mu) = 0 \quad (\text{region } G_{+h}) \\ &\sum \lambda_i y_i - \alpha \sin\tau - h\mu^{-1}(1+\mu) = 0 \quad (\text{region } G_{-h}) \end{aligned} \tag{3.8}$$

The surfaces (3.8), on intersecting (3.7), define a so-called slip plate (Fig. 6). If it is known that the phase point lies at (3.7), then, as follows from (3.8), it will be found outside the slip plate on condition that

$$\left| \sum \lambda_i y_i - \alpha \sin\tau \right| > h\mu^{-1}(1+\mu). \tag{3.9}$$

The part of surface (3.7) belonging to the plate will be denoted by A_s and the parts of (3.7) bordering it by A_+ and A_- (Fig. 6).

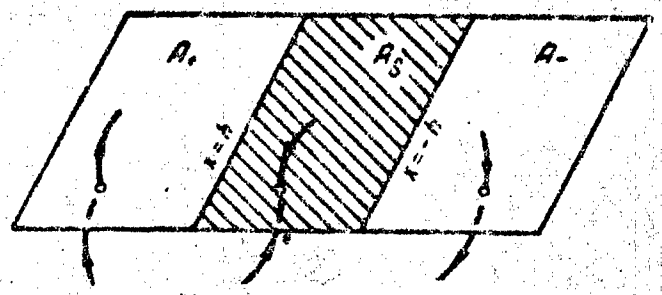

fig. 6

The arrival of the representative point at A_s is accompanied by slipping motion, which ceases when the point reaches the edges of the plate $x = h$ or $x = -h$, after which it leaves (3.7) and moves into G_{+h} or G_{-h} as the case may be.

The equations of the slipping motion are:

$$\dot{y}_i - \lambda_i y_i = c_i x; \quad \sum y_i + \alpha \cos\tau = 0; \quad |x| < h. \tag{3.10}$$

Let the point y_i^0, τ^0 lie on the surface (3.7). It further motion is determined by the part of the surface to which it belongs. In this connection it is possible to consider three types of point transformation of the surface (3.7) onto itself: a T_+-transformation of the region A_+ into the region A_- or A_s; a T_--transformation of A_- into A_+ or A_s and an S-transformation of A_s to the edge of the region A_+ or A_-.

It is clear from Fig. 6 that each of these transformations may be preceded by any other. In the general case it is possible to consider a point transformation composed of those mentioned above, which may be as complex as desired.

Finding and investigating the stability of the periodic motion reduces to finding the stationary points of the corresponding point transformation and the investigation of their stability. Thus, the simplest periodic motion, represented in Fig. 7a, corresponds to a stationary point of the transformation T_+T_-; the periodic motion with slipping, shown in Fig. 7b, corresponds to a stationary point of the transformation T_+ST_-S.

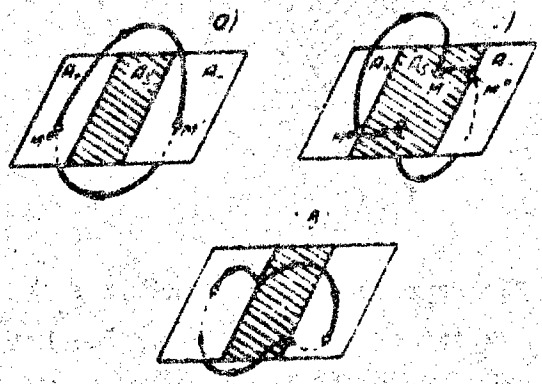

Fig. 7

The simplest regime without slipping.

We shall take a starting point y_i^0, τ^0 in the region A_+. We get

the equations of the transformation T_+T_- by integrating (3.5) and (3.6):

$$y_i' = -h\frac{c_i}{\lambda_i} + \left(y_i + h\frac{c_i}{\lambda_i}\right)e^{\lambda_i(\tau'-\tau)}; \qquad (3.11)$$

$$y_i'' = h\frac{c_i}{\lambda_i} + \left(y_i' - h\frac{c_i}{\lambda_i}\right)e^{\lambda_i(\tau''-\tau')} \qquad (3.12)$$

The moments τ' and τ'' are found as the least roots $\tau' > \tau^0$, $\tau'' > \tau'$ of the equations

$$\sum y_i' + a\cos\tau' = 0; \quad \sum y_i'' + a\cos\tau'' = 0. \qquad (3.13)$$

It is easy to show* that the simplest regime exists, if the stationary point of the transformation is symmetrical. It is found from the condition:

$$y_i' = -y_i^0; \quad \tau' = \tau^0 + \pi \qquad (3.14)$$

with the aid of eqs. (3.11) and (3.13):

$$y_i = -h\frac{c_i}{\lambda_i}\,\mathrm{th}\,\frac{\pi\lambda_i}{2}; \quad h\sum\frac{c_i}{\lambda_i}\,\mathrm{th}\,\frac{\pi\lambda_i}{2} - a\cos\tau = 0. \qquad (3.15)$$

In addition to the surfaces N_{+1}, N_{-1}, $N\varphi$ and $C\tau$, the region of existence and stability of the simplest regime in the space of the parameters is bounded by another surface C_h, corresponding to the bifurcation of the simplest regime due to the stationary point of

---

* Eliminating y_i' from (3.11) and (3.12), we get the dependence between the coordinates of the points M^0 and M''. To find the coordinates of the stationary point we put $y_i'' = y_i^0$ and $\tau'' = \tau^0 + 2\pi$. Then

$$y_i = h\frac{c_i}{\lambda_i}\left[1 - 2e^{\lambda_i(2\pi-\tau'-\tau)} + e^{2\pi\lambda_i}\right]\left[1 - e^{2\pi\lambda_i}\right]^{-1}.$$

Since $\lambda_3 = 0$, to find y_3^0 we consider the limit of this expression when $\lambda_3 \to 0$. After evaluating the indeterminate form we find at once that the limit is finite, if $\tau' - \tau^0 = \pi$.

the transformation falling on the slip plate. We get the equation of C_h from condition (3.9), if instead of y_i and τ we put the coordinates of the stationary point from (3.15) and take into account (3.2)

$$\left(\frac{1+\mu}{\mu}\right)^2+\left(\frac{1}{\omega}\operatorname{tg}\frac{\pi\omega}{2}+\frac{\pi}{2\mu}\right)^2=h^{-2}\pi^2. \qquad (3.16)$$

To formulate the equations of N_{+1}, N_{-1} and N_φ we make use of the characteristic equations for the simplest periodic motion of a relay system, obtained in [20]:

$$\frac{\alpha}{2}\sin\tau^0+h\sum\frac{c_i e^{\lambda_i\pi}}{1+e^{\lambda_i\pi}}-h\sum\frac{c_i e^{\lambda_i\pi}}{z+e^{\lambda_i\pi}}=0. \qquad (3.17)$$

Of the three boundary surfaces for the regime in question there is only one N_{+1}, the equation for which we get from (3.17) by substituting $z = +1$ and from (3.15):

$$\frac{\alpha^2}{h^2}=\left(\frac{1}{\omega}\operatorname{tg}\frac{\pi\omega}{2}+\frac{\pi}{2\mu}\right)^2. \qquad (3.18)$$

On comparing (3.16) and (3.18) it is clear that with increase in the friction h the simplest regime disappears due to the stationary point falling on the slip plate and not due to loss of stability. Consequently, it is enough to consider C_h. It also follows from (3.16) that when $\omega = 3,5,7,\ldots$ there is no simplest regime even when $h \to 0$.

We get the equation of the surface C_τ from the condition of contact with the phase trajectory of the slip plate at a point on its edge at a certain moment $\tau^0 + \tau^*$ (Fig. 7c)

$$\sum y_i(\tau+\tau^*)+\alpha\cos(\tau+\tau^*)=0;\quad \sum y_i(\tau+\tau^*)-\alpha\sin(\tau+\tau^*)=0. \qquad (3.19)$$

Eliminating τ^0 with the aid of (3.15), we arrive at an equation for C_τ in the parameter form:

$$\mu = \omega\,|\sin\tau^* - (\tau^* - \pi/2)\cos\tau^* - \pi/2|\,\{|\sin(\omega\tau^*) - \operatorname{tg}(\omega\pi/2)\cos(\omega\tau^*)|\cos\tau^* -$$
$$\omega\sin\tau^*\cos(\omega\tau^*) + \operatorname{tg}(\pi\omega/2)\,|\,|-\omega\sin\tau^*\sin(\omega\tau^*)|\}^{-1}; \qquad (3.20)$$
$$|\mu^{-1}\cos(\omega\tau^*) + \sin(\omega\tau^*)\operatorname{tg}(\pi\omega/2) - \delta\sin\tau^*|^2 + |\delta^2 - \alpha^2 h^{-2}|\cos^2\tau^* = 0$$

where $$\delta = \omega^{-1}\operatorname{tg}(\pi\omega/2) + \pi/2\mu,$$

and the parameter varies within the limits $0 \leqslant \tau^* \leqslant \pi$. Fig. 8 shows boundaries C_h and C_τ, plotted for $\omega = 2.8$. The boundary C_τ corresponds to the phase trajectory touching the edge of the slip plate (fig. 7c) and the region between C_h and C_τ obviously corresponds to periodic motion with slipping. In the case of resonance $\omega = 1$, the region which interests us is bounded only by C_h and is not intersected by the boundary C_τ. In fact, for $\omega = 1$ we get from (3.20):

$$\mu = |2\pi\sin\tau^* + \pi(\pi - 2\tau^*)\cos\tau^* - \pi^2|\,|2\sin\pi^*|^{-2} < 0$$

over the whole interval of variation of the parameter τ^*.

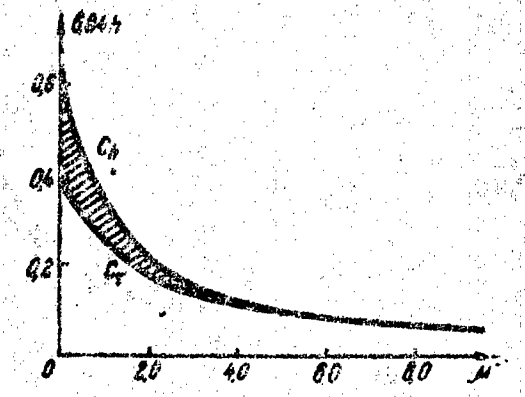

Fig. 8

In practice the most interesting region is that close to the resonance frequency $\omega = 1$. We shall introduce a new parameter $\Delta\omega = \omega - 1$ and expand with respect to $\Delta\omega$ all the equations in which we are interested. Thus, eq. (3.16) for C_h takes on the form:

$$h = \frac{\pi\mu}{4} \frac{1 - 1{,}5\ \Delta\omega}{\mu - \Delta\omega\,(0{,}25\,\pi^2 + 2\mu)} \qquad (3.21)$$

The boundary (3.21) is shown in Fig. 9a, from which it is clear that on reducing the relative mass μ or increasing the friction h the simplest regime without slipping (region I) goes over into a regime with slipping (region II).

The amplitude of vibrations in the damping system.

Since the relay input $y(\tau)$ represents the difference in the velocities of the system and the damper, we shall get the change in velocity of a single damping system by extending the summation merely to the system without the damper:

$$\dot{\xi}(\tau) = y_1(\tau) + y_2(\tau) + a\cos\tau .$$

We get the expression $y_i(\tau)$ from 3.11 by substituting τ' for τ and inserting the values of y_i^0 from (3.15):

$$\dot{\xi}(\tau) = h\omega^{-1}\left[\sin\omega(\tau - \tau^0) - \operatorname{tg}\left(\pi\omega/2\right)\cos\omega(\tau - \tau^0)\right] + a\cos\tau . \qquad (3.22)$$

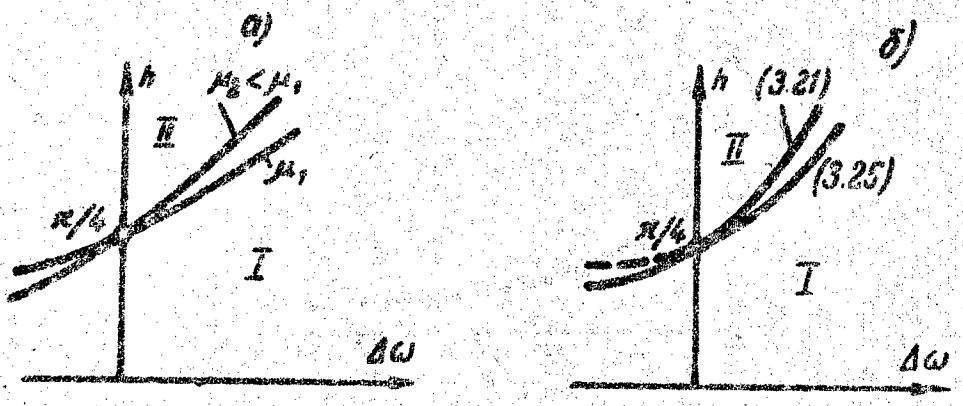

Fig. 9

Integrating (3.22) and expanding $\xi(\tau)$ in a Fourier series, after the corresponding transformations and after substituting τ^0 from (3.15) we get the amplitudes of the fundamental and higher harmonics:

$$\psi_1^2 = a^2\left\{1 + \frac{16h^2}{\pi^2\omega^4}\left[1 + \frac{\pi\omega}{2a}\left(\frac{\pi}{2\mu} + \operatorname{tg}\frac{\pi\omega}{2}\right)\right]\right\};$$
$$\psi_{2n+1}^2 = \frac{16h^2}{\pi^2\omega^4}\left[\frac{2n+1}{\omega^2 - (2n+1)^2}\right]^2. \qquad (3.23)$$

Displacement of the resonance frequency.

As is known, inserting a damper leads to a certain displacement of the frequency, at which the amplitude of the fundamental harmonic has its maximum value. On expanding the amplitude of the fundamental harmonic (3.23) in series with respect to $\Delta\omega$, we get:

$$\psi_1^2 = |1 - 16h^2\pi^{-2} + \Delta\omega\,(1 + 8h^2\mu^{-1})|\,(2\Delta\omega)^{-2}. \qquad (3.24)$$

Whence we find the value $\Delta\omega^*$, at which ψ_1^2 has its maximum value ($\Delta\omega \neq 0$):

$$\Delta\omega^* = 2\,(16h^2\pi^{-2} - 1)\,(1 + 8h^2\mu^{-1})^{-1}. \qquad (3.25)$$

Fig. 9b shows the boundary of the regime in question for motion of type (3.21) and the curve of (3.25) for small values of $\Delta\omega$ and any μ. It is clear from the figure that when $h > \pi/4$ the maximum value of the amplitude lies in the region I in question. If $\Delta\omega \to 0$, then motion without slipping goes over into motion with slipping and there is no unbounded increase in amplitude in the region in question. If $\Delta\omega \to 0$ when $h < \pi/4$, then the amplitude increases without limit, as follows from (3.24).

Thus, we have found that for effective damping it is necessary to have a moment of friction $h > \pi/4$*. This corresponds to the known rule: that it is preferable to overtension the springs of the damper than not to tension them enough [13]. Note that the maximum value of the amplitude of the vibrations lies in the region of motion without stops when $h > \pi/4$, since the curve (3.21) passes above curve (3.25). This agrees with experimental results [13].

* Consequently, when $\omega = 1$ the simplest regime without slipping does not give damping.

Choice of optimum parameters.

On putting the frequency displacement (3.25) in (3.24), we get the amplitude of the fundamental harmonic for a displaced resonance frequency:

$$(\psi_1^2)^* = (0{,}25 + 2h^2\mu^{-1})^2 (16h^2\pi^{-2} - 1)^{-1}. \qquad (3.26)$$

From (3.26) we find the optimum value of the friction h, at wh $(\psi_1^2)^*$ has the minimum value:

$$h^2_{\text{опт}} = (\pi^2/8)(1 + \mu/\pi^2). \qquad (3.27)$$

On substituting (3.27) in (3.25) we get a resonance frequency displaced by the amount $\Delta\omega^* = 2\mu/\pi^2$. Since ordinarily $\mu \ll 1$, then approximately we have $h^2_{opt} \approx \pi^2/8$. Going over to dimensional parameters, we have: $F_{1\ opt} = 1.11\ F$, which agrees well with the "degree of tightness" normally recommended. When $\mu \ll 1$ the displaced resonance frequency $\omega^* \cong 1 + 2\mu/\pi^2$.

It is clear from (3.26) that the mass of the damper μ must be taken as large as possible. In practice its magnitude is limited by design considerations.

Energy dissipated by the damper.

In the regime in question, motion without stops, there is a continuous dissipation of energy in the damper in the form of heat. To find the energy dissipated per period (the so-called energy-capacity of the damper) it is necessary to integrate the product of the frictional force and the relative velocity of the damper:

$$E = 2h \int_{\tau^*}^{\tau^*+\pi} y(\tau)\, d\tau.$$

After the corresponding transformations we get:

$$E^2 = 16h^2\omega^2\alpha^2 \left|1 + h^2\alpha^{-2}\left|\pi\omega/2\mu + \operatorname{tg}(\pi\omega/2)\right|^2\right|. \qquad (3.28)$$

For small $\Delta\omega$ (3.28) can be written in the simpler form:

$$E^2 = (16h^2/\Delta\omega^2)\,|1 - 16h^2\pi^{-2}\Delta\omega\,(1 + 8h^2\mu^{-1}) - \pi^2 h^2 \mu^{-2}\,\Delta\omega^2|. \quad (3.29)$$

Ordinarily the optimum damper parameters are taken from the condition that its energy capacity is a maximum. In the general case this is incorrect, since the extreme values of ω and h for the amplitude of (3.23) and the energy of (3.28) do not coincide. However, it can easily be found from (3.29) that for small displacements of the resonance frequency maximum energy capacity also occurs at $h^2 \simeq \pi^2/8$ and resonance frequency $\omega = 1 + 2\mu/\pi^2$. This also explains why an essentially inaccurate condition for selecting optimum parameters has given satisfactory agreement with experiment in a number of practical cases.

Simplest regime with slipping.

The problem of investigating the simplest periodic motion with slipping reduces to a consideration of the point transformation T_+ST_-S and the defining of regions in the space of the parameters corresponding to a stable stationary point of this transformation. The point M' is linked with M^0 (Fig. 7b) by expression (3.11) and we can get the link between the coordinates of M' and M'' by solving the equation of slipping (3.10):

$$\begin{aligned}
&\omega^2(y''_1 + y''_2) = \omega\nu\,|A\cos\nu(\tau'' - \tau') - B\sin\nu(\tau'' - \tau')| + \\
&\qquad + \alpha(\omega^2 - \nu^2)(\nu^2 - 1)^{-1}\cos\tau'';\\
&-j\omega(y''_1 - y''_2) = \omega\,|A\sin\nu(\tau'' - \tau') + B\cos\nu(\tau'' - \tau')| + \\
&\qquad + \alpha(\omega^2 - \nu^2)(\nu^2 - 1)^{-1}\sin\tau'';
\end{aligned} \quad (3.30)$$

$$\omega^2 y''_3 = -\omega\nu\,|A\cos\nu(\tau'' - \tau') - B\sin\nu(\tau'' - \tau')| - \nu^2(\nu^2 - 1)^{-1}\cos\tau'';$$

$$(\nu^2 - 1)^{-1}\sin\tau'' + \omega|A\sin\nu(\tau'' - \tau') + B\cos\nu(\tau'' - \tau')| \quad h\omega^2(\omega^2 - \nu^2)^{-1} \quad 0,$$

where $\nu^2 = \omega^2(1 + \mu)^{-1}$, A and B are constants of integration defined by the expressions:

$$\begin{aligned}
&\omega^2(y'_1 + y'_2) = A\nu\omega + \alpha(\omega^2 - \nu^2)(\nu^2 - 1)^{-1}\cos\tau';\\
&-j\omega(y'_1 - y'_2) = B\omega + \alpha(\omega^2 - \nu^2)(\nu^2 - 1)^{-1}\sin\tau',
\end{aligned} \quad (3.31)$$

and τ'' is the least root ($\tau'' > \tau'$) corresponding to the moment of the arrival of the representative point at the "edge" of the slip plate $x(\tau'') = -h$.

Assuming $y_i'' = -y_i^0$ and $\tau'' = \tau^0 + \pi$, we get the equations of the symmetrical stationary point of the transformation. By varying (3.11), (3.30) and (3.31) with respect to all the variables and the parameters A, B in the neighborhood of the stationary point and assuming $\delta y_i'' = -z\delta y_i^0$ and $\delta\tau'' = z\,\delta\tau^0$, we arrive at the characteristic equation:

$$\begin{vmatrix} (1-z)B\omega\nu^2 + z[a\omega^2\sin\tau^0\cos\nu\tau - & z\omega^2\cos\nu\tau + \omega^2 - \nu^2 + \\ -\nu(\nu^2-1)^{-1}\cos\tau\sin\nu\tau] + a\omega^2\nu^2\sin\tau + & +\nu^2\cos\omega(\pi-\tau); \\ +a\nu^2\omega^{-1}\cos\tau\sin\omega(\pi-\tau) - a(\omega^2-\nu^2)\sin\tau; & \\ (1-z)A\omega\nu^2 + z[a\omega^2\sin\tau\sin\nu\tau + & z^2\omega^2\sin\nu\tau \\ +\nu(\nu^2-1)^{-1}\cos\tau\cos\nu\tau] + & -\omega\nu\sin\omega(\pi-\tau) \\ +a\omega^2\cos\tau + a\nu\cos\tau\cos\omega(\pi+\tau); & \end{vmatrix} = 0. \quad (3.32)$$

Here τ is the slipping time and A, B, τ^0, τ' are found from the equation of the stationary point of the transformation. Expression (3.32) is very complex for studying the surfaces N_{+1}, N_{-1} and N in the general form. Accordingly, we shall first find other boundary surfaces and then investigate their intersection with N_{+1}, N_{-1} and $N\varphi$. The surface C_h, corresponding to the bifurcation of the regime in question due to the stationary point of the transformation M' falling at the "edge" of the plate, coincides with the C_h for the stationary point of the transformation T_+T_- discussed above (3.16).

The other surface C_h' corresponds with the bifurcation, at which the slip trajectory M'M'' touches the "edge" of the plate, but then as h increases there are no intersections with it in general. In the space of the parameters this surface separates the region of the regime in question from the region corresponding to continuous slipping motion. The equation of C_h' is found from the condition that the trajectory of the slipping motion touches the "edge" $x = -h$ in the point M'' and has the form:

$$h^2\omega^4(1-\nu^2)^4=(\omega^2-\nu^2)^2. \quad (3.33)$$ *

In order to find the intersection of C_h (3.16) with the surfaces N_{+1}, N_{-1} and N_φ, we assume the slip time $\tau = \tau'' - \tau' \to 0$ in the equations of the stationary point of the transformation and in (3.32). The limiting case corresponds to a value of the parameters, satisfying (3.16). In this case eq. (3.32) assumes the form:

$$z^2+z|1+\cos\omega\pi-\nu^2\omega^{-2}(1-\cos\omega\pi)|+\nu^2\omega^{-2}(1-\cos\omega\pi)+\cos\omega\pi=0. \quad (3.34)$$

Putting $z = 1, -1, e^{i\varphi}$ in (3.34), we find that N_{+1} intersects C_n when $\omega = 1,3,5,\ldots$; N_{-1} when $\omega = 0,2,\ldots$ and $\mu = \infty$; N_φ intersects C_h when $\mu = 0$. It also follows from (3.34) that for other values of the parameters, satisfying C_h, the stationary point of the transformation is stable. In fact, taking $\omega = 1/2, 3/2, 5/2,\ldots$ when $0 < \mu < \infty$, we get:

$$\chi(z)=z^2(1+\mu)+\mu(z+1)=0,$$

both roots of which lie within the unit circle. Accordingly, C_h bounds the region defined from within, only touching N_{+1}, N_{-1} and N_φ at the values of the parameters mentioned above.

In order to find the intersection of C_h' (3.33) with the surfaces N_{+1}, N_{-1} and N_φ we insert in the equations of the stationary point of the transformation and in the characteristic equation (3.32) the slip time $\tau'' - \tau' \to \pi$ or $\tau' - \tau^0 \to 0$. The limiting case corresponds to the value of the parameters satisfying (3.33) and eq. (3.32) then takes the form:

$$\chi(z)=z^2+2z\cos\nu\pi+1=0.$$

Hence it is clear that C_h' coincides with $N_{\pm}$. If we consider a non-limiting case, then for small values of $(\tau' - \tau^0)$ the equation $\chi(z) = 0$ assumes the form:

---

* Note that (3.23) can also be obtained from the condition that the mass m break away from the mass M in the case of the forced vibrations of a body with the mass M + m.

$$\chi(z)=z^2-2z\left|\cos\nu\pi-(\tau'-\tau)(\nu^2-1)^{-1}\omega^2\nu\sin\nu\pi\right|+1-0.5(\tau'-\tau^0)^2=0. \quad (3.35)$$

If ν is not equal to an integer, then, as follows from (3.35), it is always possible to take $(\tau' - \tau^0)$ so small that both roots lie within the unit circle. If ν is an integer, then $\chi(z) = (z \pm 1)^2 - 0.5(\tau' - \tau^0)^2$ and one of the roots lies outside the unit circle when $(\tau' - \tau^0)$ is as small as desired.

Thus, excluding the neighborhood of whole values of ω and ν, which require special consideration, we have proved that with increase in h the simplest regime without slipping goes over into the simplest regime with slipping (3.16) and then into a continuous slip regime (3.23), if it is not disturbed by additional switchings of the relay (i.e. if the regions in the space of the parameters with which we are concerned are not intersected by C_τ).

From the condition of the occurrence of extraneous roots τ' during motion of the representative point in G_{+h} in accordance with (3.13) and (3.11) we get the equations for C_τ for the T_+-transformation:

$$\sum\left(y_i^0-h\frac{c_i}{\lambda_i}\right)e^{\lambda_i(\tau^*-\tau^0)}+a\cos\tau^*-h\sum\frac{c_i}{\lambda_i}=0;$$
$$\sum(\lambda_i y_i^0-hc_i)\,e^{\lambda_i(\tau^*-\tau^0)}-a\sin\tau^*=0, \quad (3.36)$$

where the parameter τ^* varies within the limits $\tau^0 \leqslant \tau^* \leqslant \tau_0'$. The equations of C_τ for the S-transformation, defining values of the parameters, at which extraneous roots τ'' occur, are obtained from the last equation of (3.30):

$$\omega\nu\left[A\cos\nu(\tau^*-\tau')-B\sin\nu(\tau^*-\tau')\right]+(\nu^2-1)^{-1}\cos\tau^*=0, \quad (3.37)$$

where the parameter τ^* varies within the limits $\tau' \leqslant \tau^* \leqslant \tau^0 + \pi$. (3.36) and (3.37) have not been plotted. However, for concrete values of the parameters a check shows that τ' and τ'' actually are the

least roots of (3.13) and (3.30). Accordingly, the C_τ can only reduce the region of existence and stability established.

The surfaces C_τ define regions of more complex periodic regimes, as, evidently, is also the case when $\omega = 2.8$ (Fig. 8). Note that motion with two stops per half-period has been observed for a simpler model by Den Hartog [11].

Further consideration has been devoted to the special case of resonance frequency $\omega = 1$. Finding the stationary point of the transformation reduces to a solution of the following system of four equations with respect to A, B, τ, τ^0:

$$\begin{aligned}
&(1-\nu^2)\,[A\sin\nu\tau + B\cos\nu\tau] - \cos(\tau^0+\tau) - h = 0;\\
&(1-\nu^2)\,[-A(1+\cos\nu\tau)+B\sin\nu\tau] + \nu h(\pi-\tau) - \nu\sin(\tau^0+\tau) = 0;\\
&2B+2\,[A\cos\nu\tau - B\sin\nu\tau]\,\nu\sin\tau - 2\,[A\sin\nu\tau + B\cos\nu\tau]\cos\tau -\\
&\quad -(\pi-\tau)\sin\tau^0 - \sin\tau\sin(\tau^0+\tau) + 2h(1+\cos\tau) = 0;\\
&2h\sin\tau + 2A\nu - 2\,[A\cos\nu\tau - B\sin\nu\tau]\,\nu\cos\tau -\\
&-2[A\sin\nu\tau + B\cos\nu\tau]\sin\tau - (\pi-\tau)\cos\tau^0 + \cos\tau\sin(\tau^0+\tau) - \sin\tau^0 = 0.
\end{aligned} \tag{3.38}$$

Fig. 10 shows the curves calculated for the dependence between the quantity h and the slip time for different values of μ. As can be seen from the figure, slipping begins at $h = \pi/4$ and when $h = 1$ the motion in question goes over into a continuous slip regime. In this case the equation $\chi(z) = 0$ has the form:

$$\begin{aligned}
z^2 - z\,|&2\nu(\sin\nu\tau\sin\tau + \nu\cos\nu\tau(\cos\tau) +\\
&+(1-\nu^2)(\cos\nu\tau - 1)\cos\nu\tau| +\\
&+\nu^2 + (\nu^2-1)\cos\tau = 0.
\end{aligned} \tag{3.39}$$

The boundaries of stability here coincide with the boundary values of the parameters $\nu = 0, 1$ and $\tau = 0, \pi$ but when $0 < \nu < 1$, $0 < \tau < \pi$ both roots $|z_{1,2}| < 1$ and, consequently, the regime is always stable.

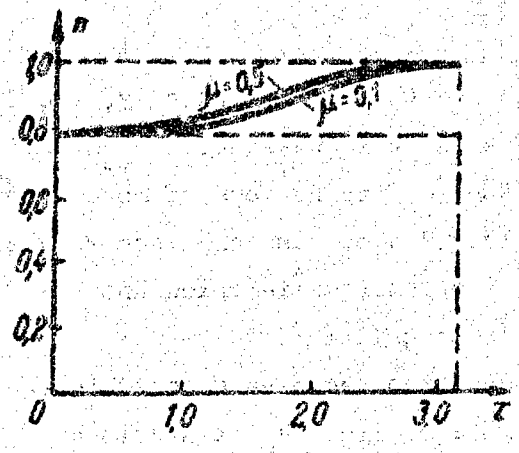

Fig. 10

Bibliography.

1. Paget, A.L.; Engineering, 3, 19 (1937).
2. Lieber, P; Jensen, D.P.: Trans. ASME, 67 (1945) 523.
3. Erlikh, L.B.; Slezinger, I.A.: Vestnik mashinostroyeniya (Herald of machine-building), 7 (1954) 5.
4. Kobrinskiy, A.E.: Vestnik mashinostroyeniya, 9 (1954) 42.
5. Sysoyev, V.I.: Issledovaniya po dinamike sooruzheniy (Investigations in the dynamics of structures), Publ. of Acad. of Construction and Architecture, M., 1957.
6. Royntenberg, Ya.N.: Inzh. sbornik,(Eng. collection), 3,1 (1946) 89.
7. Grubin, C: J.Appl.Mech., 23 (1956) 373.
8. Warburton, G.B.: J.Appl.Mech., 24 (1957) 322.
9. Kobrinskiy, A.E.: Trans. AS USSR, OTN, 5 (1957) 15.
10. Bespalova, L.V.: Trans. AS USSR, OTN, 5 (1957) 3.
11. Den Hartog: Trans. ASME, 53 (1931) 107.
12. Jendrassik, VDI, 37 (1933) 1,009.
13. Gopp, Yu.A.: Dempfery krutil'nykh kolebaniy valov bystrokhodnykh dvigateley (Dampers for torsional vibrations of the crankshafts of high-speed motors), GONTI, Khar'kov, 1938.
14. Lur'e, I.A.: Krutil'nye kolebaniya v dizel'nykh ustankov (Torsional vibrations in Diesel plant), Voemorizdat, M.-L., 1940.
15. Den Hartog: Theory of vibrations, GITTL, M.-L., 1942.
16. Dubrovskiy, K.K.: Trudy Gor'kovskovo instituta inzh. vodnovo transporta (Trans. Gor'kiy institute of water transport engineering), 5 (1939) 80.
17. Andronov, A.A.; Khaykin, S.E.: Teoriya kolebaniy (Theory of vibrations) ONTI, M., 1937.
18. Andronov, A.A.; Bautin, N.N.: Rep. AS USSR, 13 (1944) 95.
19. Zheleztsov, N.A.: PMM, 13 (1949) 3.
20. Neymark, Yu.I.: Avtomatika i telemekhanika, 13 (1953) 556.
21. Neymark, Yu.I.: Sci. papers GGU, phys. ser., 30 (1956) 159.

22. Neymark, Yu.I.: Radiofizika, 1, 1 (1958) 41.
23. Neymark, Yu.I.: Radiofizika, 1, 5-6 (1958) 146.

Physico-technical Research Institute of
Gor'kiy University

Submitted 2 Apr. 1959

ON THE THEORY OF VIBRO-SHOCK RAMMING

Pages 626-637 by L.V. Bespalova

This article deals with some of the principal cases of vibro-shock extracting and driving of piles, sheet-piling, pipe, etc.

This article is devoted to a study of the dynamics of driving and extracting piles . . A study of the motion of a system consisting of vibro-hammer, pile and soil presents considerable difficulties (see [1-3]). In view of this it is convenient to treat the problem of the motion of the vibro-hammer and the pile separately. A number of articles (see [4] and the references cited therein) have been devoted to an investigation of the dynamics of a vibro-hammer with a rigid stop. The second part - the investigation of the motion of a pile under the action of a series of shock impulses delivered from outside - is the subject of this article.

The model of the pile-soil system is assumed to take the same form as the ideal model employed in [5], i.e. as far as the forces of interaction are concerned, we assume that between the lateral surface of the pile and the soil there acts only a force of dry friction Q, the magnitude of which does not depend on the rate of slipping of the pile with respect to the soil; when there is no slipping, the soil is displaced together with the pile and its displacement is proportional to the applied force; under the pressure of the tip of the pile we first get an elastic deformation of the soil, the resistance being proportional to the amount of this deform-

ation; when a certain value R is reached, penetration begins.

In this article we shall discuss what is in practice the most interesting case, namely periodic motion of the pile with a period equal to the period of the external force, for vibro-shock extraction (R=0) and driving (Q=0) . In both cases the investigation is conducted by the method of point transformations [6]. Regions of existence and stability of single-impact, periodic motion are established in the plane of the system parameters; for this type of motion we investigated the change in the rate of extraction as a function of the magnitude and frequency of the shock impulses. In this connection it was observed that the rate of extraction increases with increase in the magnitude of the shock impulses and varies periodically with variation in the impact frequency, the maximum rate being attained at a frequency somewhat less then the natural frequency of the vibrations of the pile on an elastic basis. In the case of pile-driving we plotted curves of equal driving depth per period in the region of single-imapct, periodic motion. The results obtained help to define the optimum operating regime for vibro-shock ramming and extraction and may be used for designing and adjusting vibro-hammers.

1. Vibro-shock extraction (R = 0)

Equations of motion. Reduction of problem to a point transformation.

When R = 0 the model of the system may be given the form shown in Fig. 1. The adjacent soil is equivalent to plates on springs with a total rigidity K_{bok}. Between the plates and the pile we have dry friction, equal in magnitude to Q .

The pile is extracted under the action of a series of blows, occurring at equal intervals of time T. During the blow the position of the pile does not change and the velocity always varies by the same amount, independently of the velocity of the pile before the blow.

Let x and y be the displacements of the pile and the soil respectively, the positive direction of which is shown by the arrow (Fig.1). We shall consider the case in which the weight of the pile P = 0. With the assumptions stated the equations of motion of the pile and the soil will be

$$M\ddot{x} = F_{бок} - F\delta(t - nT), \qquad (1)$$

where M is the mass of the pile and $F_{бок} = -K_{бок}y$ when $|K_{бок}y| \leqslant Q$;

$$\dot{y} = \begin{cases} \dot{x} \text{ при } |K_{бок}y| < Q \text{ или при } Q \operatorname{sgn} \dot{\xi} = -K_{бок}\dot{y} \\ 0 \text{ при } Q \operatorname{sgn} \dot{\xi} = K_{бок}\dot{y} \end{cases}$$

Going over to the dimensionless variables $\xi = (K_{бок}/Q)x$, $\eta = (K_{бок}/Q)y$, $\tau = \omega_0 t$ $(\omega_0^2 = K_{бок}/M)$, we get:

$$\ddot{\xi} + \eta = -V\delta(\tau - n\Theta); \qquad (2)$$

$$\dot{\eta} = \begin{cases} \dot{\xi} \text{ при } |\eta| < 1 \text{ или при } \operatorname{sgn}\dot{\xi} = -\eta, \\ 0 \text{ при } \operatorname{sgn}\dot{\xi} = \eta \end{cases} \qquad (2a)$$

where $\Theta = 2\pi\omega_0/\omega_в$, $V = F\omega_0/Q$.

Thus, the system is characterized by the two parameters V and Θ.

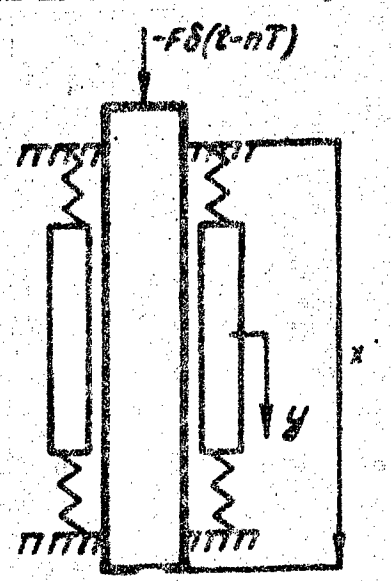

Fig. 1

We shall investigate the motion of the pile in the plane of η, $\dot{\xi}$. The upper part of the half-plane corresponds to movement of the pile downwards, the lower part to movement upwards. When $|\eta| < 1$, the mapping point moves in accordance with the equations (2)-(2a) along circles with their center in point O. At the moment of time $\tau = \tau_0$ let the pile be at the point A_0 (Fig. 2). The solution of eq. (2), satisfying the conditions $\xi = -1$ and $\dot{\xi} = 0$ when $\tau = \tau_0$, will be

$$\xi = -V\sin\left(\tau - \frac{n+1}{2}\Theta\right)\sin(n\Theta/2)/\sin(\Theta/2) - \cos(\tau - \tau_0).$$

where $n = E(\tau/\Theta)$. Consequently, before impact the mapping point moves along a circle of radius $r = 1$. When $\tau = \Theta$ the impact occurs; the mapping point goes over instantaneously, without changing its coordinates, to some circle of radius $r = r_1$ and moves along it until the next impact $\tau = 2\Theta$ and so on, while $|\eta| < 1$. The moment $\tau = \tau_1$, when the mapping point arrives at A_1 (Fig. 2), corresponding to the beginning of slipping between the pile and the soil, is determined from the condition $\xi = -1$:

$$1 = V\sin\left(\tau_1 - \frac{N+1}{2}\Theta\right)\sin(N\Theta/2)\sin(\Theta/2) + \cos(\tau_1 - \tau_0),$$

where $N = E(\tau_1/\Theta)$ and τ_1 is the least of the roots of this equation, greater than τ_0. At this moment the value of $\dot{\xi} = \dot{\xi}_1$ will be equal to:

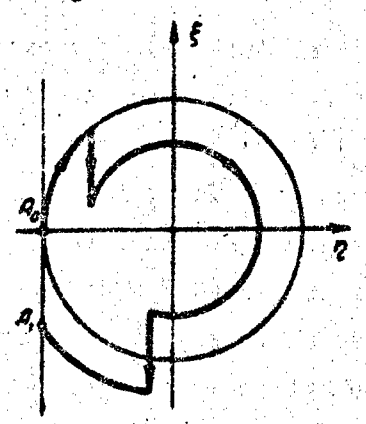

Fig. 2

$$\dot{\xi}_1 = -V\cos\left(\tau_1 - \frac{N+1}{2}\theta\right)\sin(N\theta/2)/\sin(\theta/2) + \sin(\tau_1 - \tau_0).$$

According to (2)-(2a) the further movement of the pile obeys the law

$$\xi = (\tau - \tau_1)^2/2 + \dot{\xi}_1(\tau - \tau_1) - 1 - mV(\tau - \tau_1),$$

where $m = E(\tau/\theta) - N$. The moment at which slipping ceases $\tau = \tau_2$ is found from the condition $\dot{\xi} = 0$:

$$\tau_2 = \tau_1 - \dot{\xi}_1 + MV, \tag{3}$$

where $M = E(\tau_2/\theta) - N$.

The amount the pile is driven in the interval from τ_0 to τ_2 is equal to:

$$\Delta\xi = -1 - \xi_2 = -(\tau_2 - \tau_1)^2/2 - \dot{\xi}_1(\tau_2 - \tau_1) + MV(\tau_2 - \tau_1).$$

During the slipping of the pile the coordinate η does not change, i.e. $\eta = -1$.

Thus, τ_0 and τ_2 are two successive moments of time, at which the mapping point arrives at the point A_0; the connection between τ_0 and τ_2 is then determined from the expressions:

$$1 = V\sin\left(\tau_1 - \frac{N+1}{2}\theta\right)\sin(N\theta/2)/\sin(\theta/2) + \cos(\tau_1 - \tau_0);$$

$$\dot{\xi}_1 = -V\cos\left(\tau_1 - \frac{N+1}{2}\theta\right)\sin(N\theta/2)/\sin(\theta/2) + \sin(\tau_1 - \tau_0); \tag{4}$$

$$\dot{\xi}_1 = MV - \tau_2 + \tau_1.$$

In virtue of the periodicity of the external force the study of the motion of the pile reduces to a study of the point transformation of $\tau_2 = f(\tau_0)$ (4) over the range from 0 to θ. We shall call this the S-transformation. The points of intersection of the curve of $f(\tau_0)$ with the straight lines $(N + M)\theta$ correspond to periodic motion with the period $(N + M)\theta$.

In this article we shall restrict ourselves to a consideration of the practically important, simplest periodic motion with a period equal to the period of the external force (single-impact, periodic motion).

Single-impact periodic motion

a) Region of existence and stability of the motion.

For N = 1 and M = 0, taking into account the condition of periodicity, the S-transformation may be written thus:

$$\begin{aligned} 1 &= V\sin(\tau_1-\theta)+\cos(\tau_1-\tau_0);\\ \dot{\xi}_1 &= -V\cos(\tau_1-\theta)+\sin(\tau_1-\tau_0);\\ \dot{\xi}_1 &= -\tau_2+\tau_1;\ \tau_2-\tau_0=\theta. \end{aligned} \qquad (5)$$

We shall find the boundary of the region of existence of this motion in the plane of the parameters V, θ. Single-impact periodic motion may be disturbed as a result of variation in the numbers M and N. The condition for a change in M will be $\tau_2 = 2\theta$; as a result of the periodicity of the motion, however, $\tau_2 = \tau_0 + \theta$, so that $\tau_0 = \theta$, i.e. the impact occurs at the straight line y = - 1. This means that $\tau_2 - \tau_1 = -V$ and, consequently, the boundary will be the straight line $V = \theta$, see Fig. 3. When $V > \theta$, clearly, the movement of the pile will be accelerated, in this case accelerated extraction. The quantity can change its value, if when $\xi = -1$ 1) $\tau_1 = 2\theta$ or 2) $\dot{\xi}_1 = 0$. Clearly the first possibility is not realizable, since $\tau_1 - \theta$ is less than $\theta - \tau_0$ and hence less than θ. In the second case, on substituting $\dot{\xi}_1 = 0$ in (5), we get:

$$\begin{aligned} 1 &= V\sin\tau_0+\cos\theta;\\ 0 &= -V\cos\tau_0+\sin\theta. \end{aligned}$$

Whence we find that the boundary will be formed by the curve $|\sin(\theta/2)| = V/2$ (see Fig. 3).

The periodic motion is stable, if at the stationary point of the S-transformation $|d\tau_2/d\tau_0| < 1$. From (5) $d\tau_2/d\tau_0 = \cos(\tau_1 - \tau_0)$. Consequently, the periodic motion is stable everywhere, with the exception of the line $\theta = V + 2\pi k$ when k is even and $\theta = \pm\sqrt{V^2 - 4} + \pi k$ when k is odd.

b) Investigation of the rate of extraction.

Taking into account (3) the amount of sinking (or withdrawal) of the pile during the period θ will be equal to $\Delta\dot{\xi} = \dot{\xi}_1^2/2$; consequently, the mean rate of extraction $v = \dot{\xi}_1^2/2\theta$. In order to determine $\dot{\xi}_1$ we shall write system (5) in the variables τ_0 and $\dot{\xi}_1$:

$$1 = V\sin(\tau_0 + \dot{\xi}_1) + \cos(\theta + \dot{\xi}_1);$$
$$\dot{\xi}_1 = -V\cos(\tau_0 + \dot{\xi}_1) + \sin(\theta + \dot{\xi}_1).$$

Eliminating τ_0 from these equations we get:

$$\dot{\xi}_1^2 - 2\dot{\xi}_1\sin(\theta + \dot{\xi}_1) - 2\cos(\theta + \dot{\xi}_1) - V^2 + 2 = 0 \qquad (6)$$

or (what amounts to the same thing)

$$v\theta + \sqrt{2v\theta}\,\sin(\theta + \sqrt{2v\theta}) - \cos(\theta + \sqrt{2v\theta}) - V^2/2 + 1 = 0. \qquad (7)$$

In Fig. 3 a series of lines of constant rate of sinking (v = 0.5; 1; 2) have been drawn in the plane of the parameters θ, V. Fig. 4 shows a graph of the dependence of the rate of sinking on for a constant value of V = 2. It is interesting to note that this curve has a series of maxima, the value of which decreases with increasing θ. The first of these maxima occurs at a frequency somewhat less than the natural frequency of the vibrations of the pile considered as a rigid body on an elastic foundation, the difference between these frequencies increasing with increase in V (see Fig. 3). Accordingly, to get the maximum rate of extraction (as with vibroextraction [4]) it is necessary to select an impact frequency close to the resonance frequency but somewhat less than the latter.

Allowing for the weight of the pile and the statical force during extraction.

We have just discussed the case in which the weight of the pile P was assumed equal to zero. This is correct, if the weight of the pile

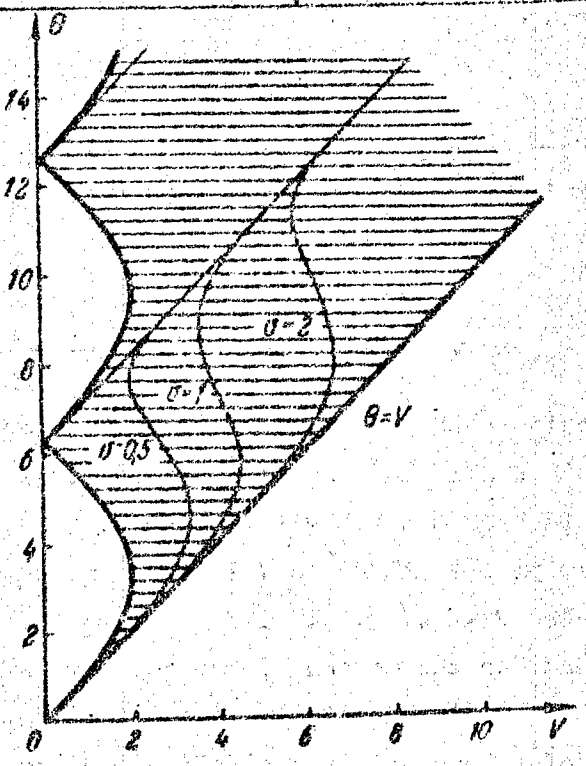

Fig. 3

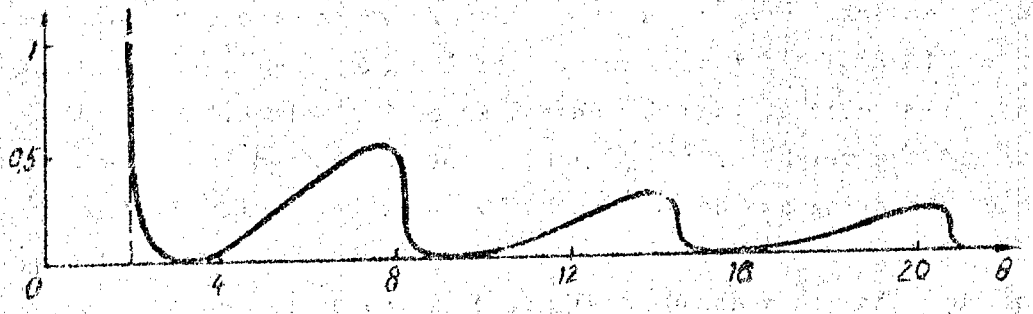

Fig. 4

is considered balanced by some constant external force.

In cases where there is no balancing force, but the weight of the pile is much less than Q, its effect can be taken into account by the method of small perturbations. Let a constant force, which may be its own weight or a statical force, act on the pile in addition to the impulse force. Then, on taking into account the constant applied force F, the equations of motion of the pile and the soil have the following form:

$$\ddot{\xi}+\eta=-\bar{V}\delta(\tau-n\Theta); \qquad (8)$$

$$\dot{\eta}=\begin{cases}\dot{\xi} \text{ при } -1<\eta<\rho; \text{ при } \eta=-1 \ \dot{\xi}>0; \text{ при } \eta=\rho \ \dot{\xi}<0\\ 0 \text{ при } \eta=-1 \text{ и } \dot{\xi}<0; \text{ при } \eta=\rho \ \dot{\xi}>0\end{cases} \qquad (8a)$$

In equations (8)-(8a)

$$\bar{V}=V\frac{Q}{Q+F}; \quad \rho=1-2\frac{F}{Q+F}.$$

If the force F acts in the same direction as the impulse force, i.e. $F = -L$ $(L > 0)$, then all that has been argued above remains valid after replacing the parameter V with $\bar{V} = VQ/(Q - L)$. If F is equal to the weight of the pile P, then $\bar{V} = V(1 - \mu^2)$ and $\rho = 1 - 2\mu^2$, where $\mu^2 = P/Q + P$. When $P \ll Q$, $\mu^2 \ll 1$.

Let us consider the motion of the mapping point in the plane η, ξ (Fig. 5) for single-impact periodic motion. After leaving point A_0 the mapping point moves along a circle of radius $r = 1$, until the impact occurs ($\tau = \theta$) or the point arrives at the straight line $\eta = \rho$ $(\tau = \tau_1)$. If impact occurs earlier ($\theta < \tau_1$), i.e. in the upper semi-circle, then the character of the motion, taking into account the weight of the pile, does not change and its effect on the rate of sinking can be calculated by replacing V with $\bar{V}$. When $\theta > \tau$ the mapping point arrives at the straight line $\eta = \rho$ (point $\bar{A}_1$), corresponding to a downward slipping of the pile.

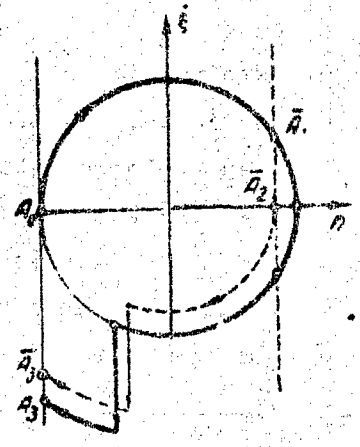

Fig. 5

It proves that the total time for the movement along the upper semi-circle and along the straight line $\eta = \rho$ (slipping) is equal as a first approximation to π, i.e. $\tau_2 - \tau_0 = \pi$. The subsequent movement of the mapping point starts from the point $\bar{A}_2$ and obeys the equations:

$$\xi = -\bar{V}\sin(\tau-\theta)+\rho\cos(\tau-\tau_2);$$
$$\dot{\xi} = -\bar{V}\cos(\tau-\theta)-\rho\sin(\tau-\tau_2).$$

The moment τ_3, at which the mapping point arrives at the straight line $\xi = -1$, is found from the equation

$$1 = \bar{V}\sin(\tau_3-\theta)-\rho\cos(\tau_3-\tau_2); \qquad (9)$$

At this moment $\dot{\xi}$ will be equal to:

$$\dot{\xi}_3 = -\bar{V}\cos(\tau_3-\theta)-\rho\sin(\tau_3-\tau_2). \qquad (10)$$

Taking into account the upward slipping time $\tau_4 - \tau_3 = -\dot{\xi}_3$, $\tau_4 = \theta + \tau_0$ (condition of periodicity) and $\tau_2 - \tau_0 = \pi$, it is possible to rewrite system (9)-(10) in the form:

$$1 = \bar{V}\sin(\tau_0+\bar{\xi}_3)+\rho\cos(\theta+\bar{\dot{\xi}}_3); \qquad (11)$$
$$\bar{\dot{\xi}}_3 = -\bar{V}\cos(\tau_0+\bar{\xi}_3)+\rho\sin(\theta+\bar{\dot{\xi}}_3).$$

Hence, assuming that $\bar{\xi}_3$ differs little from $\dot{\xi}_3$ - the velocity neglecting the weight, i.e. $\bar{\xi}_3 = \xi_3 + \alpha$, we find:

$$\alpha = \bar{\dot{\xi}}_3 - \dot{\xi}_3 = +\mu^2\frac{\dot{\xi}_3}{1-\cos(\theta+\dot{\xi}_3)}. \qquad (12)$$

Since α is assumed to be a small quantity, the method of small perturbations cannot be used, if $\theta + \dot{\xi}_3 = 2\pi n$ ($n = 0,1,2,\ldots$). In fact, when $\theta = -\dot{\xi}_3 + 2\pi n$ impact occurs close to the points A_0 and A_2 and, as is evident from (12), the increment in the rate of slipping due to the effect of the weight will not be small.

We shall find the effect of the weight of the pile on the rate of sinking in the region, where it can be taken into account by means

of the method of small perturbations. The upward displacement of the pile h will be equal to the difference between the upward and downward slip: $h = \Delta\xi_{up} - \Delta\xi_{down}$ and the rate of extraction $\bar{v} = h/\theta^*$. After a series of transformations (11) yields the following expression for the rate of extraction, taking into account the weight of the pile

$$\sqrt{\bar{v}} = \sqrt{v}\left[1 - \frac{P}{Q+P}\,\frac{1}{1-\cos\left(\theta - \sqrt{2\pi\theta}\right)}\right] - \sqrt{\frac{P}{2\theta(Q-P)}}. \qquad (13)$$

The rate of extraction neglecting the weight of the pile v is determined from equation (7).

2. Sinking a pile in the absence of lateral resistance.

Equation of motion; reduction of the problem to a point transformation.

With the assumptions made with respect to the forces of frontal resistance the system may be represented in the form of the model illustrated in Fig. 6. The soil under the toe of the pile is represented by a plug of the soil with a spring stiffness $K_{пр}$. Between the plug and the soil there is a force of dry friction R. As far as the external force is concerned, the assumptions are the same as those made previously.

The equations of motion of the system have the form:

a) Equation of motion of the pile

$$M\ddot{x} = P + F_{пр} + F\delta(t - n\Gamma), \qquad (14)$$

where M and P are the mass and the weight of the pile.

$$F_{пр} = \begin{cases} -R + K_{пр}(z - x) & \text{if } 0 < z - x < R/K_{пр} \\ 0 & \text{if } z - x > R/K_{пр} \end{cases};$$

---

* Note that in certain cases the displacement of the pile, taking into account the force of gravity, will be in a direction opposite to that of the impulse forces.

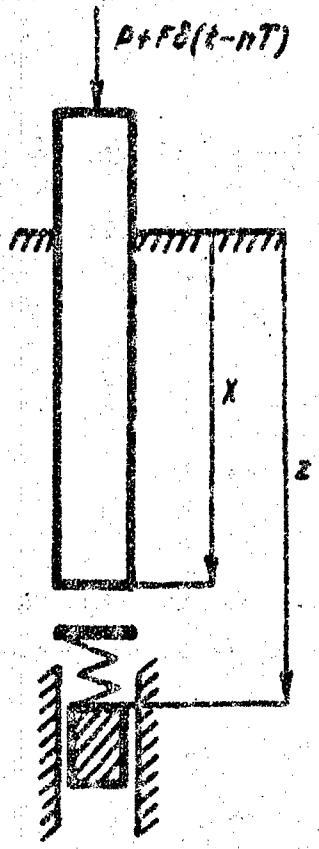

Fig. 6

b) Equation of motion of the soil:

$$\dot{z} = \begin{cases} \dot{x} & \text{при} \quad z - x = 0 \\ 0 & \text{при} \quad z - x > 0 \end{cases} \tag{15}$$

We shall introduce the dimensionless variables:

$$\xi = \frac{K_{пр}}{P-R}(z-x)+1; \quad \zeta = \frac{K_{пр}}{P-R} z;$$

$$\tau = \omega_0 t \left(\omega_0^2 = \frac{K_{пр}}{M} \right)$$

and write the equations of motion (14)-(15) for different stages:

1) Period of elastic compression of the soil, i.e. when

$0 < z - x < R/K_{пр}$,

$$\ddot{\xi} + \xi = V\delta(\tau - n\Theta);$$
$$\ddot{\zeta} = 0, \qquad (16)$$

where $$V = \frac{F\omega_0}{R-P}; \quad \Theta = 2\pi\frac{\omega_0}{\omega_n};$$

2) while the pile is jumping above the plug, i.e. when $z - x > R/K_{np}$,

$$\ddot{\xi} = \rho + V\delta(\tau - n\Theta);$$
$$\ddot{\zeta} = 0, \qquad (17)$$

where $$\rho = \frac{P}{R-P};$$

3) period of punching through the plug:

$$\ddot{\zeta} = 1 + V\delta(\tau - n\Theta), \qquad (18)$$

at the beginning of this stage $\dot{\xi}$ instantaneously vanishes and remains equal to zero throughout the whole of the period of punching.

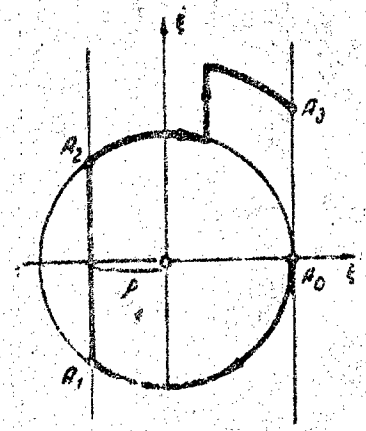

Fig. 7

The system (16)-(18) is characterized by three parameters, V, Θ and ρ. Let us consider the movement of the pile in the plane ξ, $\dot{\xi}$. As the starting moment we shall choose the position of the pile after the completion of the punching stage (the point A_0, see Fig. 7), i.e. at the moment $\tau = \tau_0$, $\xi = 1$ and $\dot{\xi} = 0$. After leaving A_0 the mapping point moves in accordance with the law:

$$\xi = V \sin\left(\tau - \frac{n_1+1}{2}\theta\right) \sin(n_1\theta/2) / \sin(\theta/2) + \cos(\tau - \tau_0),$$

where $n_1 = E(\tau/\theta)$, i.e. up to the moment of impact $\tau = \theta$ the mapping point moves along a circle of radius r = 1; after impact it passes instantaneously, without changing its coordinates, to a circle of radius $r = r_1$ and moves along it until the next impact $\tau = 2\theta$ and so on, until the mapping point arrives either at the straight line $\xi = -\rho$ (the pile begins to rebound) or at the straight line $\xi = 1$ (the pile begins to punch through).

We shall assume that the point first arrives at the straight line $\xi = -\rho$. Then the moment of its arrival τ_1 will be determine from the equation:

$$-\rho = V \sin\left(\tau_1 - \frac{N_1+1}{2}\theta\right) \sin(N_1\theta/2)/\sin(\theta/2) + \cos(\tau_1 - \tau_0), \quad (19)$$

where τ_1 is the least root, $N_1 = E(\tau_1/\theta)$. Note that in the moment $\tau = \tau_1$

$$\dot{\xi}_1 = V \cos\left(\tau_1 - \frac{N_1+1}{2}\theta\right) \sin(N_1\theta/2)/\sin(\theta/2) - \sin(\tau_1 - \tau_0). \quad (20)$$

Furthermore, the pile rebounds above the soil, during which the coordinate ξ varies in accordance with (17):

$$\xi = \rho(\tau - \tau_1)^2/2 + \dot{\xi}_1(\tau - \tau_1) - \rho + Vk\tau - V(k+1)k\theta/2,$$

where $k = E(\tau/\theta) - N_1$.

The moment τ_2 at which the pile falls back on the plug is found from the condition $\xi = -\rho$:

$$\rho(\tau_2 - \tau_1)^2 + 2\dot{\xi}_1(\tau_2 - \tau_1) + 2VK\tau_2 - V(K+1)K\theta = 0, \quad (21)$$

where $K = E(\tau_2/\theta) - N_1$ and

$$\dot{\xi}_2 = \rho(\tau_2 - \tau_1) + \dot{\xi}_1. \quad (22)$$

The further motion is again described by eq. (16), a solution of which for the starting conditions, taken at the moment τ_2, will be:

$$\xi = V\sin\left(\tau - \frac{n_2+1}{2}\theta\right)\sin(n_2\theta/2)/\sin(\theta/2) - \rho\cos(\tau-\tau_2) + \dot{\xi}_2\sin(\tau-\tau_2),$$

where $n_2 = E(\tau/\theta) - (N_1 + K)$.

The moment τ_3, at which the mapping point arrives at the point A_3 (Fig. 7), is found from the condition $\xi = 1$:

$$1 = V\sin\left(\tau_3 - \frac{N_2+1}{2}\theta\right)\sin(N_2\theta/2)/\sin(\theta/2) - \rho\cos(\tau_3-\tau_2) + \dot{\xi}_2\sin(\tau_3-\tau_2), \quad (23)$$

where τ_3 is the least of all the roots exceeding τ_2, $N_2 = E(\tau_3/\theta) - (N_1 + K)$. At that moment

$$\dot{\xi}_3 = V\cos\left(\tau_3 - \frac{N_2+1}{2}\theta\right)\sin(N_2\theta/2)/\sin(\theta/2) + \rho\sin(\tau_3-\tau_2) + \dot{\xi}_2\cos(\tau_3-\tau_2). \quad (24)$$

Finally, the pile punches through the plug in accordance with the law:

$$\zeta = -(\tau-\tau_3)^2/2 + \dot{\xi}_3(\tau-\tau_3) + 1 + Vm\tau - Vm(m+1)\theta/2,$$

where $m = E(\tau/\theta) - (N_1 + N_2 + K)$. The punching time is determined from the condition $\zeta = 0$, i.e.

$$\tau_4 - \tau_3 = \dot{\xi}_3 + VM, \quad (25)$$

where $M = E(\tau_4/\theta) - (N_1 + N_2 + K)$.

Thus, the mapping point comes back to the point A_0 and, after remaining there a certain time equal to $\tau_4 - \tau_3$, leaves it at the moment $\tau = \tau_4$. Accordingly, τ_0 and τ_4 are two successive moments, at which the mapping point leaves A_0. The point transformation of τ_0 into τ_4 (we shall call it the T-transformation) is described by the system of equations consisting of (19)-(25). Thus, the study of the movement of the pile reduces to an investigation of the T-transformati over the interval of variation of τ_0 from 0 to θ. As in the case R = 0, in what follows we shall confine ourselves to a discussion of

the simplest motion with a period equal to the period of the impacts.

Single-impact periodic motion with punching.

a) Region of existence.

Let us consider possible cases of single-impact periodic motion, differing from each other only in the moment of delivery of the impact: 1) impact occurs during decompression of the plug, 2) impact occurs during rebound, 3) impact occurs during compression of the plug, 4) impact occurs during punching.

Without attempting as yet to find the lines, delimiting these cases, we shall find the boundary for the surface of the parameters V, θ, dividing single-impact periodic motion with punching from other types of motion. First of all, starting from the condition $\dot{\xi}_3 = 0$, we shall determine the boundary of the region of single-impact periodic motion with punching and without punching for all the variants mentioned. In the first case this boundary coincides with the analogous boundary found previously for the case R = 0:

$$|\sin(\theta/2)| = V/2.$$

In the second case to find the boundary in the T-transformation it is necessary to put N_1, N_2, M, $\dot{\xi}_3$ equal to zero (K = 1). Taking into account the condition of periodicity $\tau_3 - \tau_0 = \theta$, we get:

$$\theta = 2\pi - 2\arccos\rho - V\rho + 2\sqrt{1-\rho^2}/\rho.$$

In the third case $\dot{\xi}_3 = 0$ only when V = 0. The fourth case does not yield the boundary required, since there can only be motion with punching in the presence of impact on the circle or during rebound; if in addition there is also impact during the punching period, then the motion cannot be single-impact.

Now we shall find in the region of single-impact periodic motion with punching (corresponding to the hatched part of the surface in Fig. 8) the boundaries delimiting the cases 1,2 and 3.

The condition for determining the boundary between cases 1 and 2 is the coincidence of impact with the point A_1 (Fig. 7): $\theta - \tau_0 = \pi - \arccos\rho$. Writing out the point transformation for the first case and taking into account the condition introduced above, after a series of transformations we get the equations defining this boundary, namely:

$$\theta = \beta + \pi - \arccos\rho + \sqrt{V(V-2\sqrt{1-\rho^2})};$$

$$\sin\beta = \frac{V-\sqrt{1-\rho^2}+\rho\sqrt{V(V-2\sqrt{1-\rho^2})}}{1+V^2-2V\sqrt{1-\rho^2}};$$

$$\cos\beta = \frac{(V-\sqrt{1-\rho^2})\sqrt{V(V-2\sqrt{1-\rho^2})}-\rho}{1+V^2-2V\sqrt{1-\rho^2}}.$$

Analogously the boundary between cases 2 and 3 is found from the point transformation, written for case 2, and the condition of the coincidence of impact with the point A_2: $\theta - \tau_0 = \pi - \arccos\rho + 2\sqrt{1-\rho^2}/\rho$. As a result we get:

$$\sin(\tau_3-\theta) = \frac{V+\sqrt{1-\rho^2}+\rho\sqrt{V(V+2\sqrt{1-\rho^2})}}{1+V^2+2V\sqrt{1-\rho^2}};$$

$$\cos(\tau_3-\theta) = \frac{(V+\sqrt{1-\rho^2})\sqrt{V(V+2\sqrt{1-\rho^2})}-\rho}{1+V^2+2V\sqrt{1-\rho^2}};$$

$$\tau_3-\theta = \theta - \arccos(-\rho) \quad \frac{2\sqrt{1-\rho^2}}{\rho} - \sqrt{V(V+2\sqrt{1-\rho^2})}.$$

The boundary between cases 3 and 1 is found from the T-transformation written for case 3 and the condition of impact in the point A_0: $\theta - \tau_0 = 2\arccos(-\rho) + 2\sqrt{1-\rho^2}/\rho$. From these we find:

$$\theta = 1 + 2\arccos(-\rho) + 2\sqrt{1-\rho^2}/\rho.$$

For $\rho = 1/2$ we get the boundaries shown in Fig. 8 (corresponding to lines I, II, III).

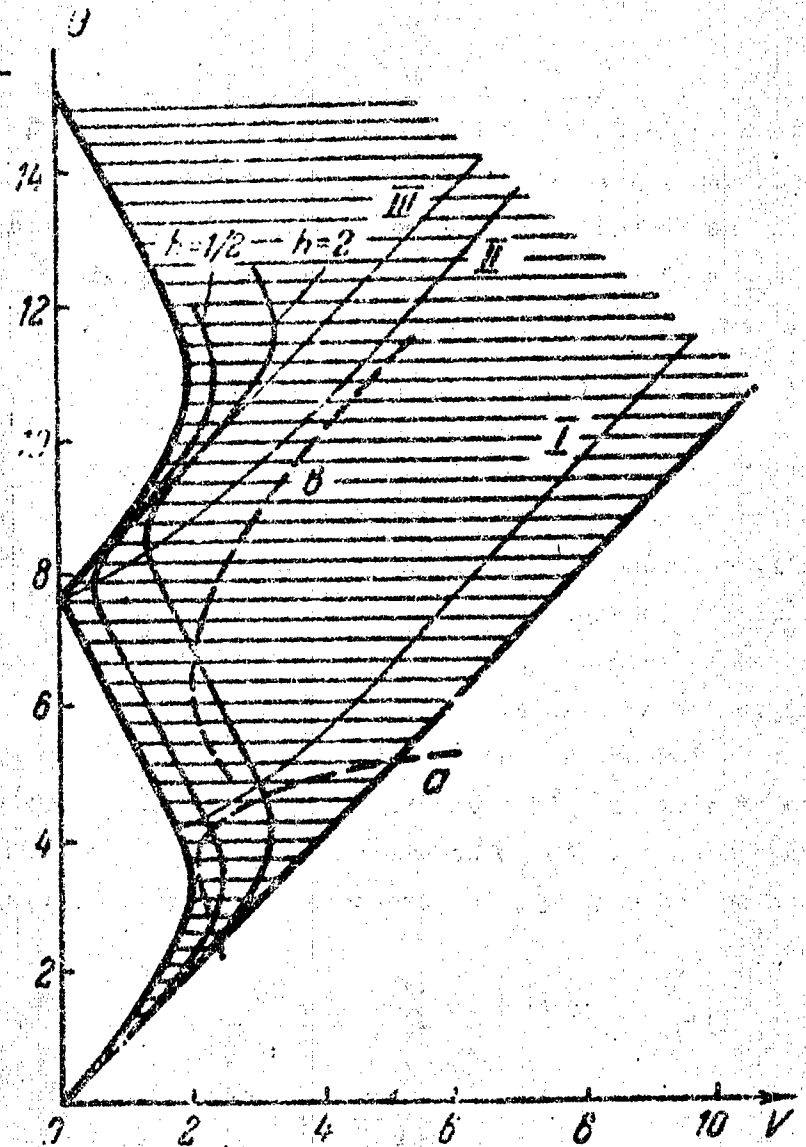

Fig. 8

b) Stability of the motion.

We shall investigate the stability of periodic motion with punching separately for all three cases.

In the first case, as in the case R = 0, the motion is stable everywhere, with the exception of the line $\theta = V + \pi k$ when k is even and $\theta = \pi k \pm \sqrt{V^2 - 4}$ when k is odd.

In the second case

$$\frac{d\tau_1}{d\tau_0} = \frac{p(\tau_2 - \tau_1) - \sqrt{1-p^2} - Vp\cos(\tau_3 - \tau_2)}{p(\tau_2 - \tau_1) - \sqrt{1-p^2} + V}.$$

For stability it is necessary and sufficient that $-1 < d\tau_4/d\tau_0 < 1$. The right-hand inequality is always fulfilled and the left-hand inequality gives the boundary (indicated in Fig. 8 by the dotted curve a), which for $\rho = 1/2$ lies wholly outside this region.

In the third case

$$\frac{d\tau_4}{d\tau_0} = 1 - V\sin(\tau_3 - \Theta).$$

From the condition of stability we find two boundaries: one of them coincides with the boundary of existence for the present case, the other lies wholly outside the corresponding region and is indicated by the dotted curve b in Fig. 8.

A check for individual points shows that the motion is stable in the whole region of existence.

c) Investigation of the rate of sinking.

The rate of sinking v is equal to $\dot{\xi}_3^2/2$. In the first case $\dot{\xi}_3$ is determined from eq. (6), where it is necessary to replace $\dot{\xi}_1$ with $\dot{\xi}_3$. In the second case $\dot{\xi}_3$ is determined from the following system of equations

$$\dot{\xi}_3^2 = \frac{\dot{\xi}_2^4 - \dot{\xi}_2^2 + 2\rho^2\dot{\xi}_2^2 - \rho^2 + \rho^4}{\dot{\xi}_2^2 + \rho^2};$$

$$\sin\left[\Theta - \dot{\xi}_3 - \arccos(-\rho) - \frac{\dot{\xi}_2 + \sqrt{1-\rho^2} - V}{\rho}\right] = \frac{\dot{\xi}_2 + \rho\dot{\xi}_3}{\dot{\xi}_2^2 + \rho^2};$$

$$\cos\left[\Theta - \dot{\xi}_3 - \arccos(-\rho) - \frac{\dot{\xi}_2 + \sqrt{1-\rho^2} - V}{\rho}\right] = \frac{\dot{\xi}_2\dot{\xi}_3 - \rho}{\dot{\xi}_2^2 + \rho^2}.$$

In the third case $\dot{\xi}_3$ is found by solving the equation

$$1 + \frac{\dot{\xi}_3^2}{2} - (\dot{\xi}_3\rho + \sqrt{1-\rho^2})\sin\left[\Theta - \dot{\xi}_3 - \frac{2\sqrt{1-\rho^2}}{\rho} - \arccos(-\rho)\right] +$$

$$+ (\rho - \dot{\xi}_3\sqrt{1-\rho^2})\cos\left[\Theta - \dot{\xi}_3 - \frac{2\sqrt{1-\rho^2}}{\rho} - \arccos(-\rho)\right] = \frac{V^2}{2}.$$

The lines in Fig. 8 represent equal rates of sinking per period θ ($h = 1/2$ and $h = 2$) for $\rho = 1/2$. The rate of sinking is found by dividing h by θ.

Bibliography

1. Tsaplin, S.A.: Vibroudarnye mekhanismy (Vibro-shock mechanisms) Avtotransizdat, M., 1953.
2. Osmakov, S.A.: Teoriya vibratsionnovo i udarnovibratsionnovo pogruzheniya svai (Theory of vibratory and impact-vibratory pile-driving), Dissertation, L., 1954.
3. Pchelin, I.K.: Issledovaniye dinamiki vibromolota dlya pogruzheniya svai (Investigation of the dynamics of a vibro-hammer for pile-driving), Dissertation, M., 1955.
4. Bespalova, L.B.: K teorii vibroudarnovo mekhanizma (On the theory of vibro-shock mechanisms), Trans. AS USSR, OTN, 5 (1957) 3.
5. Neymark, Yu.I.: Teoriya vibratsionnovo pogruzheniya i vibrovydergivaniya (Theory of vibro-driving and vibro-extraction), Inzh. sbornik, 16 (1953) 13.
6. Andronov, A.A.; Vitt, A.A.; Khaykin, S.E.: Teoriya kolebaniy (Theory of vibrations), Fizmatgiz, M., 1959.

Scientific Research Physico-technical Institute of
Gor'kiy University

Submitted 10 Apr. 1959

DETERMINING THE QUALITATIVE STRUCTURE OF A "COARSE" DYNAMIC SYSTEM BY MEANS OF APPROXIMATE PLOTTING OF SINGULAR TRAJECTORIES *

Pages 638-653

by L.N. Belyustina

It is proved that, in principle, it is possible to determine in a finite number of steps (operations) the qualitative structure of the partition of a phase-plane into trajectories for a "coarse" dynamic system, starting from an approximate plotting of singular trajectories. The concrete method of plotting singular trajectories proposed makes it possible to evaluate quantitative characteristics of the gravitational regions of limit cycles and equilibrium states.

In many practically important physical problems, when it is required to find the possible operating regimes of some system or other or to determine the system parameters corresponding to the most favorable operating regimes, the question reduces to the qualitative investigation of a system of differential equations on a phase-plane or a phase-surface (a cylindrical surface, for example), which can be developed into a plane. One of the first questions to arise is that concerned with the qualitative structure of the partition of the plane into trajectories of the system in question, namely the question

* Lecture at a scientific conference at Gor'kiy University, devoted to the celebration of the 40th anniversary of the Great October Socialist Revolution (20.12.1957).

of the existence of singular trajectories (equilibrium states, half-separatrixes and limit cycles) and their interrelationships. Moreover, qualitative investigations very often involve a consideration of the quantitative characteristics of singular trajectories (the dimensions of limit cycles, the dimensions of gravitational regions of equilibrium states and limit cycles, bounded by half-separatrixes, and so on.).

This article deals with the question of the qualitative structure of the partition of a plane into trajectories, starting from approximately plotted singular trajectories; a numerical method of qualitative integration may then successfully be applied to establish the quantitative characteristics of singular trajectories especially when electronic computers are used.

1. Let us consider the dynamic system, defined by the two first-order equations:

$$dx/dt = P(x, y), \quad dy/dt = Q(x, y), \tag{1}$$

and the modified system

$$dx/dt = P(x, y) + p(x, y), \quad dy/dt = Q(x, y) + q(x, y), \tag{2}$$

where P(x,y), Q(x,y), p(x,y), q(x,y) are functions of the class C', determined for the region G of the plane x,y. The region mentioned is bounded by a simple closed curve g, forming a cycle without contact*.

As is known,** the qualitative structure of the partition of a phase-plane into trajectories is determined by the singular (orbitally unstable) trajectories: equilibrium states, separatrixes, closed trajectories (limit cycles). The qualitative structure of the partition of the plane into trajectories of system (1) is uniquely defined if we are given a description, in which all the singular trajectories of

---

* Without making substantial changes in the subsequent argument, this boundary might be replaced with a more general type of boundary, namely, the boundary discussed in [1] consisting of a finite number of alternate trajectory arcs and arcs without contact.

** See [2].

the system are enumerated and their interrelationships established. Such a description is called a "complete scheme"* [1] of partition into trajectories as defined by system (1).

Article [3] (see also [4]) describes how "coarse", as distinct from "non-coarse" dynamic systems of type (1) are defined.

We shall assume that system (1) is coarse. As is known [3,4], all the equilibrium states and limit cycles of the coarse system are simple and half-separatrixes do not go from saddle point to saddle point, whence it follows that the number of singular trajectories in system (1) is finite.

In what follows an important part is played by the notion of the canonical neighborhood of equilibrium states and limit cycles, described below.

The region σ, containing a given equilibrium state of the focal or nodal point type (or a given limit cycle), is called a "canonical neighborhood" of this equilibrium state (or limit cycle), if the following conditions are fulfilled: a) besides the given equilibrium state (or the corresponding given limit cycle) no singular trajectory whatsoever lies within this region, b) if a singular trajectory enters this region in the course of an increase (decrease) in t, then in the course of further increase (decrease) in t it may not leave it again.

The canonical neighborhood of an equilibrium state of the saddle point type is called a circular neighborhood of this saddle point, satisfying conditions a) and b) above.

---

* In a region with a boundary consisting of a finite number of alternate trajectory arcs and arcs without contact a complete scheme of partition into trajectories of system (1) is established [1], i. all the singular trajectories and half-trajectories, boundary arcs without contact and trajectory boundary arcs of this partition are enumerated and we have the following data: 1) the nature of the boundary of the region G, 2) so-called "complete schemes" of all the equilibrium states, 3) "complete schemes" of all the ω, α, 0 limit continuums, 4) the interrelationships of all the so-called "free" ~~ω, α, 0 limit continuums.~~

We shall give geometrical illustrations of this.

It is clear that a region, containing only one limit cycle C_o, not containing any equilibrium states and bounded by two cycles without contact, is a canonical neighborhood of the cycle C_o. The saddle half-separatrixes S_1, S_2, S_3, which converge on this cycle, are shown in Fig. 1a. Fig. 1b shows a canonical neighborhood of the equilibrium state A of the focal or nodal point type and the saddle half-separatrixes S_1, S_2, S_3, which converge on this equilibrium state. The canonical neighborhood of a saddle point (Fig. 1c) cannot be traversed by the singular trajectories entering and leaving it, including the arcs of half-separatrixes of the saddle, which enter or leave it. The neighborhoods σ_1 and σ_2, shown in Fig. 1c, are canonical neighborhoods of the saddle point B but the neighborhood σ_3 is not canonical.

A wholly singular trajectory may lie at the boundary of a canonical neighborhood. Thus, if in addition to C_o there are two other cycles C_1 and C_2, adjacent to it, one lying within cycle C_o and the other outside it (Fig. 1d), then the doubly connected region, bounded by the cycles C_1 and C_2, will be the maximum canonical neighborhood of the cycle C_o. The simply connected region, bounded by the cycle C_1 (Fig. 1d), adjacent to the equilibrium state A of the focal or nodal point type, is the greatest canonical neighborhood of this equilibrium state.

According to [1], a description of the interrelationships of the singular trajectories, i.e. a "complete scheme" of partition into trajectories, as determined by the "coarse" system (1), in the region G with a boundary consisting of a cycle without contact is given, if all the equilibrium states, limit cycles and saddle half-separatrixes (their number is finite) are enumerated and we know: 1) the "scheme" of the boundary of region G (i.e. the order in which it is traversed*

* We shall speak of the boundary g of region G being traversed by trajectories of system (1), having in mind that since g is a cycle without contact and system (1) is coarse, there exists a certain neighborhood of g, outside the region G and other than zero, in which trajectories of system (1) can be continuously prolonged.

by saddle half-separatrixes), 2) "complete schemes" of all the equilibrium states (i.e. for each equilibrium state the order in which its canonical neighborhood is traversed by the half-separatrixes of various saddle points; see, for example, Fig. 1b), 3) "complete schemes" of all the "unfree" cycles (i.e. for each limit cycle, on which there converges at least one half-separatrix, the order in which the half-separatrixes traverse its canonical neighborhood; see, for example, Fig. 1a), 4) the mutual interrelationships of all the "free" cycles (i.e. the interrelationships of all the limit cycles, on which no saddle half-separatrix converges).

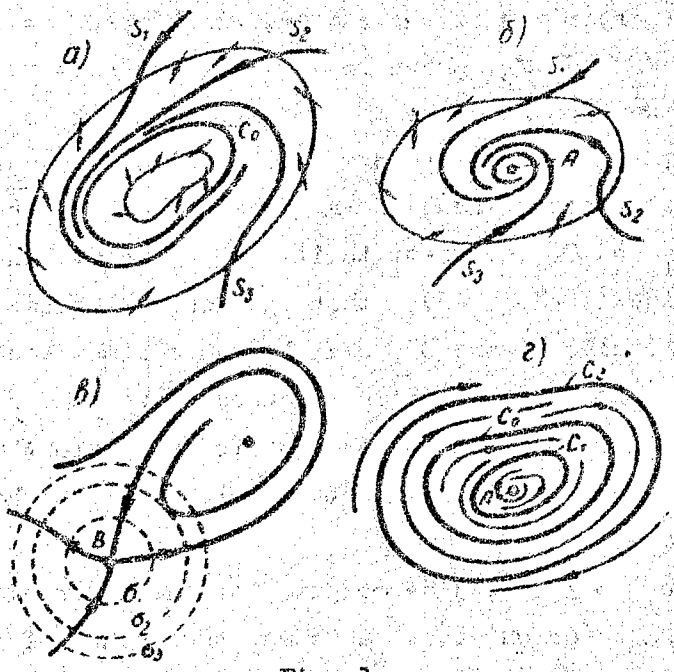

Fig. 1

We shall denote the greatest canonical neighborhoods of each of the equilibrium states and limit cycles of a coarse system (1) by C_λ ($\lambda = 1,2,\ldots,\Lambda$), where Λ is the total number of equilibrium states and limit cycles of the system; we shall denote the lower boundary of the least radii of neighborhoods C_λ by γ^*. For the coarse system (1) γ^* is clearly greater than zero.

The quantity γ^* characterizes the "coarseness" of the interrelationships of the singular trajectories of a given coarse system (1). It has been assumed that the boundary of the region G is a cycle without contact; consequently, there exists within G a neighborhood of the curve g of radius $\gamma^{**} > 0$, not containing singular trajectories of system (1) which might lie entirely within it or which might enter and leave it.

We shall call the quantity

$$\gamma_0 = \inf \{\gamma^*, \gamma^{**}\} \qquad (3)$$

the geometrical measure of coarseness of the qualitative structure of the partition into trajectories of the given coarse system (1) in the region G.

In connection with the derivation of the geometrical measure of coarseness γ_0 we note the following. We shall assume that system (1) (system D) is such that there exists a sequence $D_1, D_2, \ldots, D_i, \ldots$ of systems of the form of (1), for which the geometrical measure of coarseness γ_{oi} decreases with increase in i . If γ_{oi} approaches zero, this will mean that for the corresponding system D_i one of the following is close to zero: 1) either the distance between two or more equilibrium states or the distance between a state of equilibrium and a limit cycle (so that the states of equilibrium or the state of equilibrium and the limit cycle are close to merging into a complex equilibrium state) or 2) the distance between two or more limit cycles (so that these limit cycles are close to merging into a complex limit cycle, i.e. a cycle with a multiplicity factor equal to or greater than 2) or 3) the distance between an equilibrium state of the saddle point type and a singular trajectory, entering and leaving its neighborhood (so that two or more half-separatrixes are close to merging into one separatrix, going from saddle to saddle).

Thus, when γ_0 tends to zero coarse system (1) tends to a non-coarse system (1) of a degree equal to or greater than 1 [5].

(We note in passing that in his footnote to the translation of [6], (see [6], p. 103), M.I. Minkevich gives a, basically, incorrect explanation of the idea of the degree of non-coarseness, introduced in [5]. According to [5] non-coarse systems of a degree equal to or greater than 1 are defined as relatively coarse and at any rate cannot be defined starting from the "order of smallness of the additions", as stated in this footnote.) For any non-coarse system we consider that $\gamma_0 = 0$.

In this article we do not deal with the question of determining the magnitude of the geometrical measure of coarseness from the right-hand members of system (1). Note also that the idea of a geometrical measure of the coarseness of a qualitative structure may be introduced analogously into systems with a number of degrees of freedom greater than one. The coarseness of system (1) may also be characterized by a certain quantity δ_0, the so-called "analytical measure of coarseness of system (1), but we shall not dwell on this here*.

2. We shall call the continuous curve $\Delta(t)$, defined by the equations $x = \bar{x}(t)$, $y = \bar{y}(t)$, the γ-approximation of the curve $L(t)$, defined by the equations $x = x(t)$, $y = y(t)$ in the plane x,y for $0 \leqslant t \leqslant T$, if for any $t \leqslant T$ we have the inequality

$$\rho(\Delta, L) \equiv \sqrt{2}\,|\bar{z} - z| < \gamma, \qquad (4)$$

where $|\bar{z} - z|$ is the greater of $|\bar{x} - x|$ and $|\bar{y} - y|$.

We shall introduce one of the possible ways of plotting a γ-approximation of the arc of a trajectory of length equal to or greater than L, based on plotting the ε-solutions of system (1) for

* We shall mention that δ_0 is an analytical measure of the coarseness of system (1), if any system (2), to which there apply the inequalities

$$p \quad \delta_0 \quad q \quad \delta_0 \quad |p'_x| < \delta_0 \quad |p'_y| \quad \delta_0 \quad |q'_x| \quad \delta_0 \quad |q'_y| < \delta_0$$

is coarse and there does not exist a value $\delta^* > \delta_0$, for which this would hold true.

a limited length, not diverging more than for γ^*.

Taking the length of the arc as the parameter t, we shall evaluate the quantity $|\bar{z} - z|$ for two ε-solutions of system (1)** of length equal to or less than L, defined by the equations $x = x(t,x_0)$, $y = y(t,x_0)$, $\bar{x} = \bar{x}(t,x_0)$, $\bar{y} = \bar{y}(t,x_0)$ and satisfying the initial conditions $x_0 = x(0,x_0)$, $y_0 = y(0,y_0)$, $\bar{x}_0 = \bar{x}(0,x_0)$, $\bar{y}_0 = \bar{y}(0,y_0)$. Making use of a known inequality (see [7], chapter 1), we get:

$$|z - z| \leqslant (2\varepsilon L + |\bar{z}_0 - z_0|)\, e^{KL}, \qquad (5)$$

where K is the greater of the values of the first partial derivatives of the right-hand members of system (1) and $|\bar{z}_0 - z_0|$ is the greater of $|\bar{x}_0 - x_0|$, $|\bar{y}_0 - y_0|$.

Taking

$$\varepsilon < \gamma / \sqrt{2}\,(2L + 1)\, e^{KL}, \qquad (6)$$

we have: $|\bar{z} - z| < \gamma/\sqrt{2}$, when

$$|\bar{z}_0 - z_0| < \varepsilon. \qquad (7)$$

In order to plot the ε-solution of system (1) we may proceed in the following way (see [8], section 1). In the part $\bar{\Gamma}$ of region G, without equilibrium states, we shall consider, instead of system (1), the system

$$dx/dt = P(x, y)/\sqrt{P^2 + Q^2}; \quad dy/dt = Q(x, y)/\sqrt{P^2 + Q^2}, \qquad (8)$$

obtained from system (1) by substituting the variables $d\tau/dt = \sqrt{P^2 + Q^2} > 0$. The integral curves of systems (1) and (8) coincide. Geometrically the right-hand members of system (8) are

---

* An ε-solution of system (1) is a solution of system (1) with an error ω ($|\omega| < \varepsilon$), i.e. a solution of system (2), which has conditions applied only to p and q, namely $|p| < \varepsilon$, $|q| < \varepsilon$ and no conditions applied to their derivatives.

** A solution of system (1) is an ε-solution of this system when $\varepsilon = 0$.

defined, when $x = x_1$, $y = y_1$, by the sine and cosine of the tangent to the integral curve of systems (1) and (8) in the point $A_1(x_1, y_1)$ (direction cosines of the field given in $\bar{\Gamma}$ by systems (1) and (8)). According to /8/, to plot ε-solutions of system (8) in $\bar{\Gamma}$ it is sufficient to have a square grid with side d satisfying the inequali:

$$3\sqrt{2}\,d < \eta_\varepsilon(\bar{\Gamma}). \qquad (9)$$

and plot the ε-solutions as broken Euler lines. The quantity $\eta_\varepsilon(\bar{\Gamma})$ has the value defined from below:

$$\eta_\varepsilon(\bar{\Gamma}) \geqslant \varepsilon m^3/4\sqrt{2}\,LM^2,$$

where $m^2 = \inf\{1, P^2 + Q^2\}$ in $\bar{\Gamma}$, $L = \sup\{P'_x, P'_y, Q'_x, Q_y, 1\}$ and $M = \sup\{1, |P|, |Q|\}$ in G. At the starting point Euler's lines then have a direction coinciding with the direction of the field; they change direction only on crossing the boundaries of squares, their direction after each intersection coinciding with the direction of the field at the point of intersection*.

3. We shall consider a concrete coarse system of type (1) with a certain fixed geometrical measure of coarseness γ_0 greater than zero. We shall denote this system by "system $(1)_{\gamma_0}$".

Note particularly that open $\gamma_0/4$-neighborhoods of $\gamma_0/4$-approximations of equilibrium states and limit cycles of system $(1)_{\gamma_0}$ do not intersect. In fact, if this were otherwise, the distance between some equilibrium states or limit cycles or between an equilibrium state and a limit cycle would be less than γ_0, which is impossible from the definition of γ_0.

By virtue of what has been said, the plotting of $\gamma_0/4$-approximations of the equilibrium states and limit cycles is enough to

---

* Since the ε-solutions are plotted individually in the present article, the square grid may be replaced with a chain of squares (one with angles connected at points on the Euler line). This modification facilitates programming and reduces the number of necessary operations in using electronic digital computers.

establish the part of the scheme of system (1) γ_0, connected only with the existence of equilibrium states and limit cycles and with the interrelationships of equilibrium states and limit cycles.

The defining of "complete schemes" of equilibrium states and "unfree" cycles requires, together with the plotting of such approximations of parts of saddle half-separatrixes as might be established for each of these equilibrium states and limit cycles, a knowledge of the order in which the saddle half-separatrixes traverse the boundaries of their canonical neighborhoods.

We shall plot separately the approximations of the equilibrium states, half-separatrixes and limit cycles, which would be sufficient to define a complete scheme of partition into trajectories for the coarse system (1) γ_0. Except where specially stipulated, we shall not concern ourselves with the accuracy of the computations, assuming that it is sufficient for our purposes.

a) Equilibrium states.

The coordinates of the equilibrium states of the system (1) γ_0 are defined by the equations $P(x,y) = 0$, $Q(x,y) = 0$. The plotting in the region G of the curves $P = 0$ and $Q = 0$ with respect to points, the distance between which insures* the isolation of all the common points of these curves at a distance $\varepsilon \geq \gamma_0$, gives certain approximations to all the equilibrium states of the system (1) γ_0. These approximations are enough to compute and indicate the interrelationships between the equilibrium states of the system (1) γ_0. The coordinates of the equilibrium states computed can always be refined in accuracy (in particular, with respect to γ_0 and sufficiently to determine** the character and stability of an equilibrium state with respect to the

---

* The intervals with respect to x,y, sufficient for plotting the necessary number of points on curves $P = 0$, $Q = 0$, are determined by the quantity γ_0.

** The requirements with respect to accuracy in determining the coordinates of equilibrium states are higher for lower values of δ_0, the analytical measure of "coarseness" of the system (1) γ_0.

roots of the corresponding characteristic equations and the inclinations of the saddle separatrixes from the formulas of [4,11].

Let the system (1) γ_0 in question have n_1 equilibrium states A_i ($i = 1, \ldots, n_1$) of the focal or nodal point types and n_2 equilibrium states B_j ($j = 1, 2, \ldots, n_2$) of the saddle point type.

We shall distinguish the $\gamma_0/2$-neighborhoods of each of the equilibrium states, denoting them by $d\,\gamma_{0/2}(A_i)$ and $d\,\gamma_{0/2}(B_j)$ respectively.

b) Saddle half-separatrixes.

Every half-separatrix of a saddle point B_j is plotted starting from the equilibrium state, which it leaves with increase or decrease in t.

We shall introduce the construction of a certain γ-approximati of a finite part of a half-separatrix S of length L. Choosing ε s satisfying inequality (6), we shall carry out this construction in parts (see Fig. 2).

1) Construction in a certain neighborhood σ_1 of the saddle point B_j of an $\varepsilon/2$-approximation of part of the half-separatrix S traversing the neighborhood σ_1. Here the $\varepsilon/2$-approximation is found by the method of successive approximations. By N we shall denote the point of intersection of the $\varepsilon/2$-approximation of the half-separatrix and the boundary of the neighborhood σ_1.

2) Construction in the region $G - \sigma_1$ of an ε-solution of the system, passing through the point N and forming a γ-approximation of the arc of the half-separatrix S of length $\geqslant$ L.

Construction 1. By a linear substitution of the variables $\xi = c_1 x + y$, $\eta = c_2 x + y$ the equation, corresponding to the system (1) γ_0, in the neighborhood of the saddle point B_j is brought to the form:

$$\frac{d\eta}{d\xi} = \frac{-\lambda\eta + \lambda_1^{-1}(c_2 P_2 + Q_2)}{\xi + \lambda_1^{-1}(c_1 P_2 + Q_2)},$$

where $\lambda = -\lambda_2/\lambda_1$, λ_1, λ_2 are roots of the characteristic equation for the saddle point B_j. The directions $\xi = 0$ and $\eta = 0$ in the new coordinates correspond to the directions of the separatrixes in the saddle point $y_1 = c_1 x$ and $y_2 = c_2 x$. In the neighborhood of the saddle point we shall seek a solution in the form:

$$\eta = f_1(\xi); \quad \xi = f_2(\eta).$$

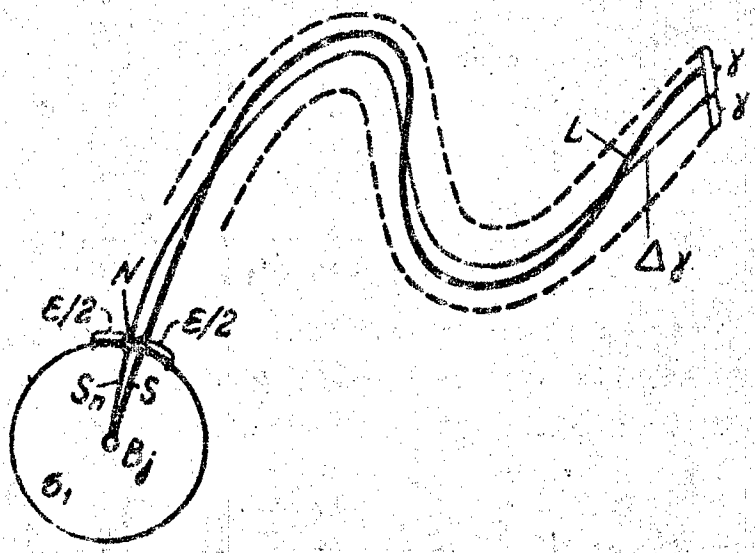

Fig. 2

By making the substitution $\eta = u\xi$, we get an equation of the form [9]:

$$\xi \frac{du}{d\xi} = -(\lambda + 1)u + \xi F_1(\xi) + u F_2(\xi, u). \qquad (10)$$

We shall seek a solution $u = u(\xi)$ for equation (10) by the method of successive approximations; then the n-th approximation

$$u_n = \xi^{-(\lambda+1)} \int_0^{\xi} |F_1(t) + u_{n-1} t^{-1} F_2(t, u_{n-1})| \, t^{\lambda+1} \, dt.$$

A solution exists for a ξ_0 and a u_0 satisfying the inequalities

$$\frac{M_2}{\lambda + 2} < 1; \quad \frac{M_1}{\lambda + 2} \left[\frac{1}{1 - M_2(\lambda + 2)^{-1}} \right] \xi_0 < u_0. \qquad (11)$$

where M_1 and M_2 are respectively the upper limits of the functions $\xi F_1(\xi) + uF_2(\xi,u)$ and $\partial[uF_2(\xi,u)]/\partial u$ for $|\xi| \leqslant \xi_0$ and $|\eta| \leqslant \eta_0$.

Inequalities (11) determine the maximum size of the neighborhood σ_1 of the saddle point B_j, belonging to the neighborhood $d_{\eta_0/2}(B_j)$ in which the method of successive approximations may be used.

The approximation of u_n, for which

$$|u_n(\xi) - u_{n-1}(\xi)| = \sum_{i=1}^{k} A_i \xi^{p_i}$$

(k is determined from the condition that $A_{k+1}\xi^{p_{k+1}}$ is less than the accuracy of calculation), is sufficient [10] and the values of p_i satisfy the inequalities

$$\frac{M_2}{\lambda + p_i + 1} < 1; \quad M_2 \sum_{i=1}^{k} \frac{A_i \xi^{p_i+1}}{p_i + \lambda + 1} \cdot \frac{1}{M_2} < \frac{\varepsilon}{2\sqrt{2}}(|c_2| + 1). \quad (12)$$

Conditions (12) are chosen so that in the coordinates x,y at the boundary of the neighborhood σ_1 the distance ρ between the half-separatrix S and its n-th approximation S_n is less than $\varepsilon/2$; then*

$$|u - u_n| < M_2 \sum_{i=1}^{k} \frac{A_i \xi^{p_i+1}}{p_i + \lambda + 1} \cdot \frac{1}{M_2} < \frac{\eta - \eta_n}{|\xi|} \leqslant$$

$$\frac{1}{|\xi|}\{|c_2||x - x_n| + |y - y_n|\} \cdot \frac{\varepsilon}{2\sqrt{2|\xi|}}(|c_2| + 1).$$

Thus, as a result of construction 1 we get at the boundary of the neighborhood σ_1 of the saddle point B_j a point N on the approximation S_n of the half-separatrix S of this saddle point; the point on the half-separatrix S, corresponding to this point N, is a distance equal to or less than $\varepsilon/2$ away from it (see Fig. 2).

---

* The value of ε is also chosen small enough for the $\varepsilon/2$-neighborhoods of the approximations of two half-separatrixes of the saddle point not to have common points at the boundary of σ_1.

Construction 2. If we now plot the ε-solution of system (1) passing through the point N and having a length $\geq L$, then, in accordance with the inequalities (6) and (7), the corresponding part of the half-separatrix S of length L will be found in the γ-neighborhood of this ε-solution (see Fig. 2). On completing the construction of the ε-solution passing through the point N, we obtain in a finite number of steps (operations) an approximation to a part of the half-separatrix S of length L. The ε-solution may be plotted in the manner indicated in section 2 above.

We shall consider the question of how to determine the quantities γ and L, sufficient for plotting the necessary approximations of all the saddle half-separatrixes of the system (1) γ_0. We shall call the arc $\overset{\smile}{M_1M_2}$ of the approximation Δ_γ the loop of a spiral (or simply a loop), if in moving along it the angle of inclination of the tangent to this arc varies from α to $\alpha + 2\pi$. We shall call the length of straight line $\overline{M_1M_2}$ joining the beginning and end of the spiral loop $\overset{\smile}{M_1M_2}$ the closure of the loop (and a loop together with its closure a closed loop). We shall call the line segment connecting the ends of the arc $\overset{\smile}{M_1M_2}$ the closure of the arc $\overset{\smile}{M_1M_2}$.

The quantity γ_0 permits us to find the γ_1-approximation Δ_{γ_1} ($\gamma_1 \leq \gamma_0/4$) of the part of the half-separatrix S of length L, the γ_1-neighborhood of which does not have common points with the γ_1-neighborhoods of the γ_1-approximations of all the other half-separatrixes and which 1) crosses the boundary of the region G or 2) crosses the boundary of the $\gamma_0/2$-neighborhood $[d_{\gamma_0/2}(A_i)]$ of an equilibrium state A_i of the focal or nodal point type or 3) describes outside the $\gamma_0/2$-neighborhood of the saddle point B_j $[d_{\gamma_0/2}(B_j)]$ a spiral loop, the closure of which does not contain (apart from the ends of the loop) points on the arc Δ_{γ_1}.

In the first case the half-separatrix S leaves the region G with increase or decrease in t. If this were not so, then the radius γ^{**} of the neighborhood of g would be less than $\gamma_0/4$, which

is impossible by virtue of (3).

In the second case, with increase (decrease) in t , the half-separatrix S enters an equilibrium state A_i of the focal or nodal point type, the boundary of the $\gamma_0/2$-neighborhood of which is intersected by the arc $\Delta\gamma_1$. If the contrary were assumed, the singular ha- trajectory-half-separatrix S would enter and leave the $(3/4)\gamma_0$-neighborhood* of the equilibrium state, which is incompatible with (3).

In the third case** the limiting behavior of the half-separatrix is investigated subsequently, after the third cases for the half-separatrixes for all the saddle points have been defined.

For a certain $\gamma \leqslant \gamma_0/4$ let it be established which of the three cases is realized for all the half-separatrixes of all the saddle points. This makes it possible to enumerate all the half-separatrixes of the saddle points; at the same time a finite number $m = m_1 + m_2$ of regions J_1^{k1} and J_2^{k2} ($k_1 = 1, 2, \ldots, m_1$; $k_2 = 1, 2, \ldots, m_2$) is establish in the region G. The region J_1^{k1}, simply connected, includes one equilibrium state A_{k1} of the focal or nodal point type and is bounded either by the loop of a $\Delta\gamma$-approximation of a half-separatrix and its closure (Fig. 3a) or by the boundary g of the region G (Fig. 3b). If the loop of the $\Delta\gamma_1$-approximation of the half-separatrix S and its closure bound a simply connected region, not containing equilibrium states, then increasing the length L ($L_2 > L_1$) of the arc being approximated and (where necessary) decreasing γ ($\gamma_2 < \gamma_1$) gives an approximation of a part of the half-separatrix S of length L_2, relating

---

* In fact, let the approximation $\Delta\gamma_1$ of the half-separatrix S intersect the boundary of $d_{\gamma_0/2}(A_i)$ in the point M_1. The point on the half-separatrix S, corresponding to M_1, lies at a distance $\leqslant \gamma_0/4$ from M_1 and, consequently, lies at a distance $\leqslant (3/4)\gamma_0$ from the equilibrium state.

** The third variant is realized, in particular, for the approximation of the half-separatrix, having as its limit a limit cycle.

to one of the cases mentioned above, while the loop $\Delta\gamma_2$ with its closure bounds a region, including at least one equilibrium state of the focal or nodal point type. The region J_2^{k2}, doubly connected, does not contain equilibrium states and is bounded from within by the loop of the $\Delta\gamma$-approximation of part of a certain half-separatrix S and its closure and from without (on the outside) either by the loop of the approximation of part of another half-separatrix and its closure (Fig. 3c) or by the boundary g (Fig. 3d)*.

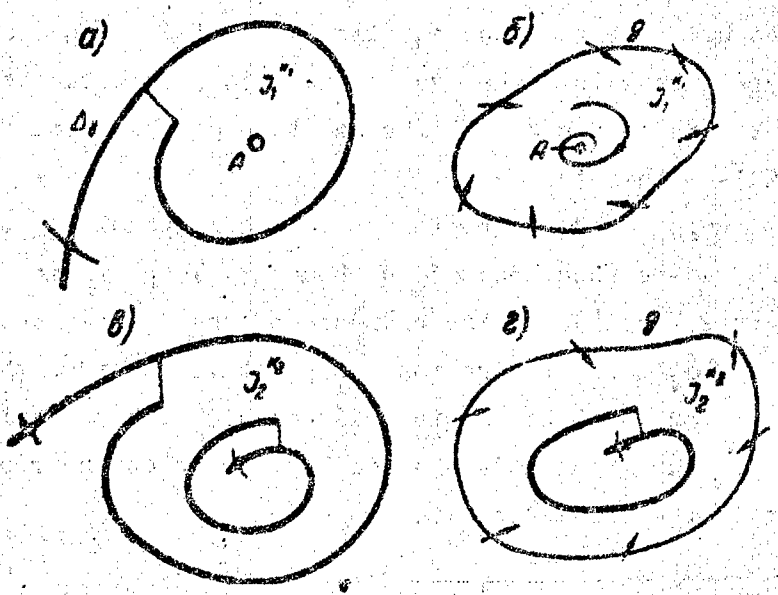

Fig. 3

We shall clarify the relationship between the regions J_1 and J_2 thus delimited and the limit cycles of the system (1) γ_0.

If the half-separatrix of a saddle point approaches a limit cycle, then there always exists a certain arc L forming a loop, the closure of which does not intersect this arc L. The validity of this assertion follows from the existence in a sufficiently small neighborhood of the limit cycle of an arc without contact, intersecting this

* In what follows the indices k1 and k2 will be omitted for the sake of simplicity.

limit cycle.

Every limit cycle either 1) lies within a simply connected region, bounded by the closed loop of a half-separatrix or the boundary g and containing only one equilibrium state of the focal or nodal point type or 2) lies in a ring, bounded by the two closed loops of two different half-separatrixes (or by the closed loop of a half-separatrix from within and by the boundary g from without) and not containing a single equilibrium state.

The first part of this assertion is easily proved on the assumption that not more than one equilibrium state of the focal or nodal point type lies within the cycle; the second part on the assumption that more than one equilibrium state of the focal or nodal point type exists within the cycle.

We shall supplement the region J_1 (J_2 correspondingly), mentioned above, with the γ-neighborhood of the boundary loop δ_γ and denote it by $\tilde{J}_1$ (or $\tilde{J}_2$) (see Fig. 4) and the boundary of the γ-neighborhood of the loop δ_γ by $\tilde{\delta}_\gamma$. For the region $\tilde{J}_1$ we shall consider the length l_1, connecting A (an equilibrium state within J_1) with the point on the boundary loop $\tilde{\delta}_\gamma$ or the boundary g (in dependence on the boundary of $\tilde{J}_1$) closest to the point A on l_1.

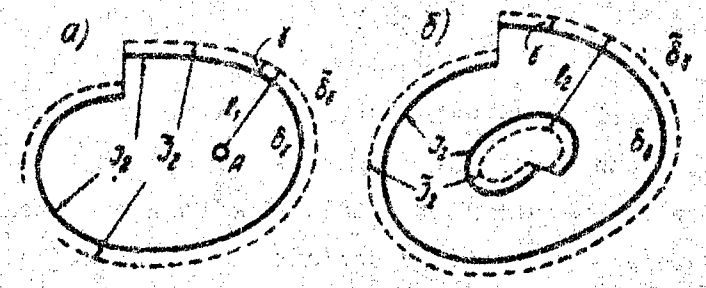

Fig. 4

For the region $\tilde{J}_2$ we shall consider a length l_2, connecting either two points belonging to different loops, entering into the boundary of $\tilde{J}_2$ (from the points on the second loop a point closest to the

point on the first loop is chosen on l_2) or two points, one belonging to the boundary g, the other the closest to it on l_2 and belonging to the inside loop of $\tilde{J}_2$. As follows from what has been argued above, every limit cycle of the system certainly cuts one of the lengths l_1 or l_2 of the regions $\tilde{J}_1^{k1}$ or $\tilde{J}_2^{k2}$. Below (see c) Limit cycles) we give one of the methods of distinguishing the rings, W_ν ($\nu = 1,2,\ldots, N$), of thickness $\gamma_0/4$, intersecting the lengths l_1 and l_2, such that the limit cycles of the system (1)$_{\gamma_0}$ exist only inside these rings in each of which there is no more than one cycle. For a coarse system the number of these rings is finite. Once we have established all the rings W_ν ($\nu = 1,2,\ldots, N$) and have clarified the stability of the cycles they contain, it will be possible to proceed to determine the limiting behavior of the half-separatrixes in the third case.

We shall plot the Δ_γ-approximation of the part $L = L_2 \quad L_1$ of the half-separatrix S for $\gamma = \gamma_2 < \gamma_1$. We then have the following possibilities for Δ_γ: either one of the first two cases enumerated above is fulfilled for the arc Δ_γ (then the half-separatrix S respectively intersects the boundary g or has as its limit an equilibrium state of the focal or nodal point type) or the arc Δ_γ intersects the boundary of the $\gamma_0/2$-neighborhood of one of the rings W_ν (then, in accordance with (3), the half-separatrix S has as its limit a cycle lying in the ring W_ν).

The limiting behavior is clarified successively for the half-separatrixes of all the saddles. Since in this connection we approximate integral arcs in a part G* of the region G, lying outside certain finite β-neighborhoods ($\beta \geqslant \gamma_0/2$) of the limit cycles and equilibrium states, the lengths of all the approximated arcs are limited by a certain finite quantity L*. Consequently, we always find in the final step (the greater, the less γ_0) a finite value of $\gamma_p > 0$ such that the γ_p-neighborhoods of the γ_p-approximations of the parts of the half-separatrixes concerned do not have common points in G*.

The order, in which the Δ_{γ_p}-approximations of parts of the half-

separatrixes intersect the boundary g, determines the complete scheme of the boundary of the region G. The order, in which $\Delta\gamma_p$-approximations of parts of the half-separatrixes intersect the canonical neighborhood of an equilibrium state of the focal or nodal point type, containing its $\gamma_0/2$-neighborhood, determines the complete scheme of the equilibrium state of the focal or nodal point type.

The complete scheme of an equilibrium state of the saddle point type is determined by the order, in which the approximations of the half-separatrixes of this saddle point intersect the boundary of its canonical neighborhood (see b) Construction of approximations of half-separatrixes).

We shall consider the canonical neighborhood of a limit cycle lying in a ring W_ν. For this purpose we shall choose the region forming a canonical neighborhood of this cycle and containing a ring W_ν and its $\gamma_0/2$-neighborhood.

The order, in which the approximations of the half-separatrixes intersect the boundary of this canonical neighborhood, determines the complete scheme of the limit cycle, lying in the ring W_ν. Rings W_ν, the $\gamma_0/2$-neighborhoods of which are not penetrated (with increase or decrease in t) by any half-separatrix, include free cycles of the system $(1)_{\gamma_0}$. A knowledge of the interrelationships of these rings makes it possible to enumerate all the free cycles of the system $(1)_{\gamma_0}$ and indicate their interrelationships.

Thus, the complete scheme of the partition of the region G into trajectories of the coarse system $(1)_{\gamma_0}$ in question will be wholly determined in a finite number of steps, if (as assumed above) we can point out a method of distinguishing in a finite number of steps rings W_ν of thickness $\leqslant \gamma_0/4$, intersecting the lengths l_1, l_2, such that the limit cycles of the system $(1)_{\gamma_0}$ can be found within them and only within them.

c) Limit cycles.

By plotting approximations of equilibrium states and $\Delta\gamma$-

approximations of parts of the half-separatrixes of saddle points of the system $(1)_{\gamma_0}$ we established regions $\tilde{J}_1$ and $\tilde{J}_2$ such that, if the system $(1)_{\gamma_0}$ has limit cycles, then all of them intersect one of the lengths l_1 or l_2 lying within $\tilde{J}_1$ or $\tilde{J}_2$. The line segments l_1 and l_2, not being, in general, line segments without contact, will be investigated for intersection with limit cycles with the aid of approximations of the integral arcs intersecting these lengths. Since the limit cycles of system $(1)_{\gamma_0}$ do not have points at distances of less than γ_0 from an equilibrium state (see (3)), for intersection with rings of thickness $\leq \gamma_0/4$, including limit cycles, it is sufficient to investigate the part of the length l_1 lying outside the $\gamma_0/2$-neighborhood of equilibrium state A. The investigation of the lengths l_1 and l_2 is the same in each case.

Construction of rings of thickness $\leq \gamma_0/4$, intersecting the lengths l_1, l_2 and containing limit cycles of the system $(1)_{\gamma_0}$.

Let the region $J_1(J_2)$ be represented with the aid of $\Delta\gamma_1$-approximations of parts of the half-separatrixes. We shall investigate one of the lengths $l_1(l_2)$: in the case, in which $l_1(l_2)$ (E_1E in Fig. 5) has a length greater than* $4\gamma_1$. We shall divide the length $l_1(l_2)$ into parts l_γ of length $\gamma \leq \gamma_1$ and we shall plot $\Delta\gamma$-approximations of the arcs of the trajectories ($\gamma \leq \gamma_1$), passing through the points $E_1, E_2, \ldots, E_r, \ldots, E_k = E$ dividing the length $l_1(l_2)$ into lengths l_γ. We shall agree to denote the $\Delta\gamma$-approximation of the part $t > t_0$ ($t < t_0$) of the arc of the trajectory, passing through the point E_r when $t = t_0$, by Δ^+_γ (Δ^-_γ). Then we may assume one of the following

* In the case in which the length of l_1 satisfies the inequality $l_1 \leq 2\gamma_1$, the limiting behavior of the half-separatrixes does not require further investigation, since in this case the separatrixes, approximations of parts of which are boundaries of the regions J_1 and J_2, enter (since $\gamma_1 \leq \gamma_0/4$) either the γ_0-neighborhood of an equilibrium state or the $\gamma_0/2$-neighborhood of a limit cycle.

possibilities for the arc* Δ_γ^+ (Δ_γ^-). The arc Δ_γ^+ (Δ_γ^-) either 1), without intersecting the length l_1, intersects the boundary of the $\gamma_0/2$-neighborhood of equilibrium state A or 2), without intersecting the length $l_1(l_2)$, leaves the region $\tilde{J}_1(\tilde{J}_2)$ or 3) has a common point with the length $l_1(l_2)$ in a certain point $D_i^+(D_i^-)$.

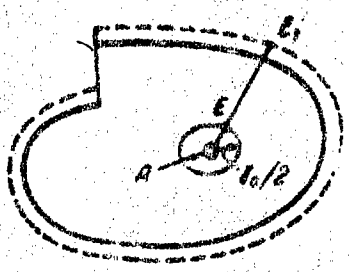

Fig. 5

It is clear that a length l_γ, for neither end of which case 3) is fulfilled, cannot have points in common with a limit cycle of the system $(1)_{\gamma_0}$. A length l_γ, for which at least one end satisfies case 3), may or may not have points in common with limit cycles of the system $(1)_{\gamma_0}$** in dependence on the disposition of the arcs $\smile E_r D_r^+$, $\smile E_r D_r^-$ and the closures $\overline{E_r D_r^+}$, $\overline{E_r D_r^-}$ of these arcs.

We shall say that for an arc $\smile E_r D_r$ with a closure $\overline{E_r D_r}$ we shall have case 3a on the length $l_1(l_2)$, if the arc $\smile E_r D_r$ is such that the closed curve $\smile E_r D_r, \overline{D_r E_r}$ bounds a simply connected region, including an equilibrium state A (Fig. 6a) or an inside boundary of the region

---

* The value of $\gamma \leq \gamma_1$ is taken sufficiently small for the arc Δ_γ not to intersect itself.

** Depending on whether $l_1(l_2)$ is a line segment with or without contact, limit cycles of the system $(1)_{\gamma_0}$ may intersect the length $l_1(l_2)$ one or more times. However, in either case, every limit cycle intersecting the length l_1, will enclose an equilibrium state A and every limit cycle, intersecting the length l_2, will enclose an inside boundary of $\tilde{J}_2$.

$\tilde{J}_2$ (Fig. 7a), and case 3b, if the arc $\overset{\smile}{E_r D_r}$ is such that the closed curve $\overset{\smile}{E_r D_r}, \overline{D_r E_r}$ bounds a simply connected region, not including an equilibrium state A (Fig. 6b) or an inside boundary of the region $\tilde{J}_2$ (Fig. 7b). We shall plot the following Δ_γ-approximations of the arcs of trajectories passing through the point E_r.

Fig. 6

If case 3a applies to the arc $\overset{\smile}{E_r D_r}$, then we complete the plotting by determining the length R_1 of the closure $\overline{E_r D_r}$ (construction P_1).

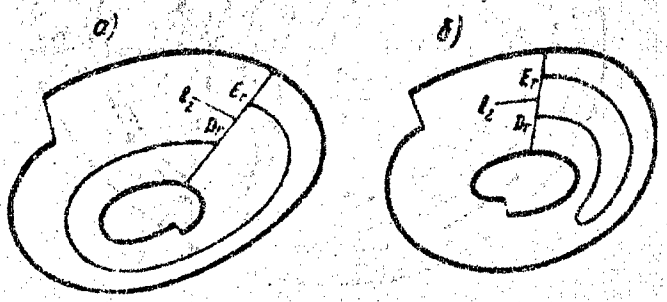

Fig. 7

If case 3b applies to the arc $\overset{\smile}{E_r D_r}$, then we continue the arc Δ_γ, passing through the point D_r, up to the following common point $Dr^{(1)}$ of the arc Δ_γ and the length $l_1(l_2)$. If case 3b applies to the arc $\overset{\smile}{D_r D_r^{(1)}}$ also, then we continue the construction to the common

point $D_r^{(m-1)}$ of the arc $\Delta\gamma$ and the length l_1; the point $D_r^{(m-1)}$ is such that either one of cases 1) and 2) is fulfilled for the $\Delta\gamma$-approximation of the arc of the trajectory, passing through the point $D_r^{(m-1)}$, or case 3a (construction P_2; see Fig. 7) applies to the arc $\cup D_r^{(m-1)} D_r^{(m)}$.

If construction P_2 is required for one of the arcs $\cup E_r D_r^+$, $\cup E_r D_r^-$ (for $\cup E_r D_r^+$, for example), then it is completed by determining the length R_2 of the line $E_r D_r^{(m_1)+}$; if construction P_2 is required for both the arcs $\cup E_r D_r^+$, $\cup E_r D_r^-$ (Fig. 8), then it is completed by determining the length R_3 of one of the lines $R_3' = D_r^{(m_1-1)+} D_r^{(m_2)-}$; $R_3'' = D_r^{(m_2-1)-} D_r^{(m_1)+}$.

The lengths R_μ ($\mu = 1,2,3$), obtained for $\gamma \leqslant \gamma_1$ from constructions P_1 and P_2, may or may not satisfy the inequalities:

$$R_\mu \leqslant 2; \qquad (\mu = 1, 2, 3). \tag{13}$$

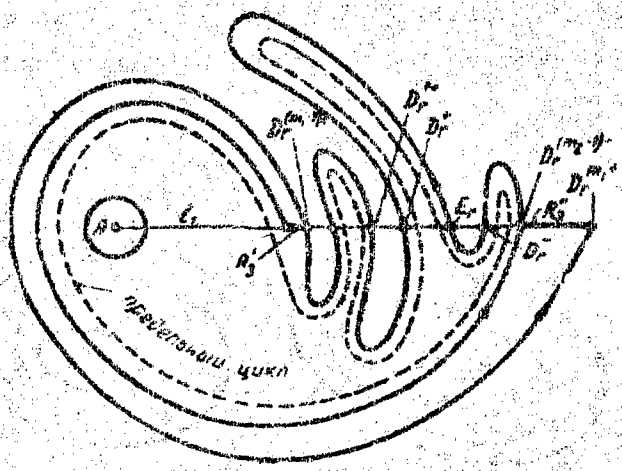

Fig. 8

The first step in investigating $l_1(l_2)$ is the following. $l_1(l_2)$ is divided into segments of length $\gamma \leqslant \gamma_1$. The segments l_γ, for at least one of the ends of which one of the inequalities (13) is fulfilled, are picked out for further investigation with respect to

intersection with limit cycles.

The second step consists in dividing the segments l_{γ}, picked out for further investigation, into segments $l_{\gamma/2}$ of length $< \gamma/2$. As before we single out segments $l_{\gamma/2}$ for further investigation with respect to intersection with limit cycles in a third step and so on.

In the k-th step the segments $l_{\gamma/(2k-1)}$, singled out for further investigation, form a series of non-intersecting segments U_μ ($\mu = 1,2,\ldots,M$) on $l_1(l_2)$ beginning from the outer boundary of $\tilde{J}_1(\tilde{J}_2)$. We shall single out from these segments U_ν ($\nu = 1,2,\ldots,N$) with ends $M'_\nu(M''_\nu)$ having the following properties.

Property 1. The arc of the γ_k-approximation of the arc of the trajectory, having its origin in the point $M'_\nu(M''_\nu)$ (with decrease or increase in t) intersects $l_1(l_2)$ in a point $\tilde{M}'_\nu(\tilde{M}''_\nu)$ such that the segment $\overline{M'_\nu \tilde{M}'_\nu}(\overline{M''_\nu \tilde{M}''_\nu})$ does not have points in common with the segment U_ν, besides $M'_\nu(M''_\nu)$, and forms a closure of the arc $\smile M'_\nu \tilde{M}'_\nu(\smile M''_\nu \tilde{M}''_\nu)$ and a line segment without contact*.

Property 2. The strip included between the arcs $\smile M'_\nu \tilde{M}'_\nu$ and $\smile M''_\nu \tilde{M}''_\nu$ does not intersect other segments U_ν**.

We shall distinguish the distance $\rho(M_\nu) = M_\nu \tilde{M}_\nu$ not only with respect to magnitude but also with respect to sign. We shall give $\rho(M_\nu)$ a positive (negative) sign, if movement along the arc $\smile M_\nu \tilde{M}_\nu$ occurs with increase in t (decrease in t). In the case shown in Fig. 9, the distances $\rho(M'_s)$ and $\rho(M''_s)$ have a positive sign. The ring W^*_ν, bounded by the two closed curves $\smile M'_\nu \tilde{M}'_\nu \overline{\tilde{M}'_\nu M'_\nu}$, $\smile M''_\nu \tilde{M}''_\nu \overline{\tilde{M}''_\nu M''_\nu}$ and supplemented by its γ_k-neighborhood (Fig. 9), will be designated

---

* For a certain finite k (possibly sufficiently large) there exists for every limit cycle of the system (1) γ_0, by virtue of the arrangement of the cycles (see above), at least one segment U_μ with the first property.

** Segments U_μ, which include successive points of intersection of $l_1(l_2)$ with the same limit cycle, do not have the second property.

W_ν.

The plotting of the approximations of the cycles is completed in the k-th step, in which 1) all the segments U_μ have a length $\leq \gamma_0/4$, 2) every segment U_μ either is one of the segments U_ν or is intersected by a certain ring W_ν, 3) the thickness of every ring W_ν does not exceed $\gamma_0/4$, 4) the distances $\rho(M_\nu)$ have the same signs. Such a finite k always exists*, since the cycles of a coarse system (1) lie at a finite distance $\geq \gamma_0$ from each other. The stability of the cycle lying in a ring W_ν, is determined by the sign of the distances $\rho(M_\nu)$. The cycle is stable if the sign is negative and unstable if the sign is positive.

Thus, the construction given for approximations of singular trajectories is sufficient to determine the complete scheme of the partition into trajectories of a coarse system $(1)_{\gamma_0}$. Consequently, the following theorem holds true.

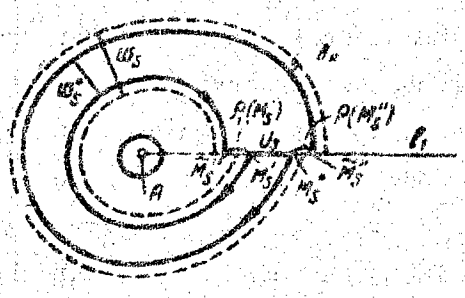

Fig. 9

Theorem 1. The qualitative structure of the partition of a plane region G into trajectories, i.e. the scheme of any coarse system, may be established in a finite number of steps (operations) by plotting approximately but with a sufficient degree of accuracy all the singular

* The number of these steps is always finite but depends on the density of the convolutions of a single trajectory outside a certain neighborhood of the limit cycle, i.e. it depends on the magnitude of the analytical measure of coarseness of the system $(1)_{\gamma_0}$ (see previous footnote).

trajectories (equilibrium states, limit cycles and half-separatrixes). The necessary accuracy of the approximations of singular trajectories depends on the magnitude of the geometrical measure of coarseness γ_0.

It clearly follows from this same method of plotting singular trajectories that the method outlined above can be used to establish the qualitative structure of a system (1) with a geometrical measure of coarseness greater than γ_0.

Note that in investigating a concrete system of type (1) we ordinarily do not know whether the system in question is a coarse or a non-coarse system [5] of degree $n \geqslant 1$. In cases in which certain considerations indicate that system (1) is coarse, then, as follows from what has been said, its qualitative structure can be established, if its geometrical measure of coarseness is defined from below (i.e. if it is established that the coarse system (1) has a geometrical measure of coarseness $\gamma_0 \geqslant \alpha > 0$). The quantity α may be evaluated by means of the Bendickson-Juliac criterion [11,12], with the aid of which it is possible to establish in individual cases the dimensions of the regions not containing limit cycles. The quantity α may also be evaluated by means of the dimensions a) of the simply connected region D_A, containing an equilibrium state $A(x_0,y_0)$ of the focal or nodal point type, for loops of the trajectories $x = x(t)$, $y = y(t)$ in which the quantity

$$h = \tau^{-1} \int_0^\tau \{P'_x \mid x(t), y(t)\mid + Q'_y \mid x(t), y(t)\mid\} dt \neq 0$$

and keeps the sign of the quantity $\sigma_0 = P'_x(x_0,y_0) + Q'_y(x_0,y_0)$ (when α is determined by the minimum distance between the equilibrium state A and the nearest cycle surrounding this equilibrium state), b) of the doubly connected region, containing a cycle C_0 with a characteristic index $h = h_0 \neq 0$, in which for loops of the trajectories $x = x(t)$, $y = y(t)$ the quantity $h \neq 0$ and keeps the sign of h_0 (when α is determined by the minimum distance between the cycle C_0 and the cycle nearest to C_0). However, as is customary in practice, the qualitative structure of a coarse system may be plotted with accuracy up to a certain

value α of the geometrical measure of coarseness, which may be made sufficiently small. This construction reduces to our plotting all the equilibrium states and limit cycles of system (1) lying at distances greater than α from each other and omitting equilibrium states and limit cycles lying at smaller distances apart. If, finally, a half-separatrix passes at a distance less than α from an equilibrium state of the saddle point type, then it remains uncertain whether the system in question is coarse (with a measure $\gamma_0 < \alpha$) or non-coarse; if it is coarse, then we do not know precisely how the separatrixes are disposed. Thus, it follows from what has been said above that it is not possible to prove the coarseness of any coarse system by numerical methods, starting only from an approximate construction of the singular trajectories. In order to establish the qualitative structure of the partition into trajectories of a system (1) by numerical methods (starting from an approximate construction for the singular trajectories) it is necessary to define from below the geometrical measure of coarseness γ_0.

Theorem 2. In principle the qualitative structure of the partition into trajectories of a non-coarse system (1) of degree $n \geqslant 1$ cannot be determined by the approximate plotting of its singular trajectories.

As a matter of fact, we have not made use of any additions to the right-hand members, however small, in plotting the approximations of singular trajectories; in view of their arbitrariness it is impossible to guarantee the preservation of the non-coarseness of the system. We note, without dwelling on this point in detail, that the qualitative structure of a non-coarse system may be approximated by the qualitative structures of coarse systems with a geometrical measure of coarseness as small as desired. Numerical methods, starting from such an approximation, make it possible to determine system parameters close to the bifurcation values of the system parameters. A method of approximating non-coarse systems is applied in reference [13]. There

approximating cases 3a and case 3b if the arc $\smile E_r D_r$ is such that the structurally coarse system with a sufficiently small geometrical measure of the arc $\smile E_r D_r$ bounds a simply connected region not including an equilibrium state is used to determine values of the system parameters close to the bifurcation values of the parameters, at which the arcs of separatrix of the system in question pass from saddle point to saddle point.

In conclusion I wish to express my sincere gratitude to E.A. Andronova-Leontovich for his constant interest and valuable advice.

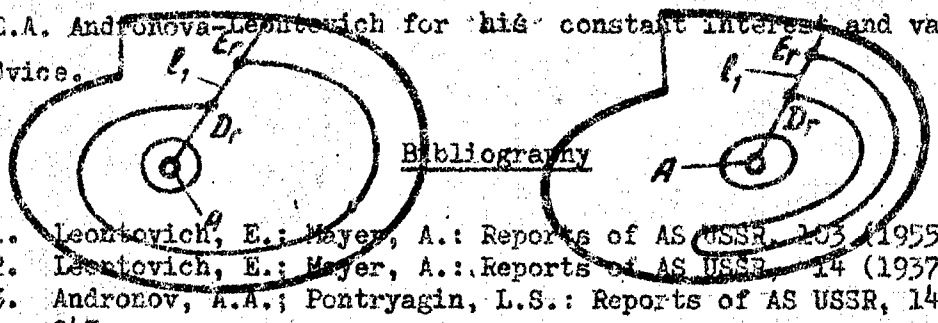

Fig. 6

Bibliography

1. Leontovich, E.; Mayer, A.: Reports of AS USSR, 103 (1955) 557.
2. Leontovich, E.; Mayer, A.: Reports of AS USSR, 14 (1937) 251.
3. Andronov, A.A.; Pontryagin, L.S.: Reports of AS USSR, 14 (1937) 247.
4. Andronov, A.A.; Khaykin, S.E.: Teoriya kolebaniy (Theory of vibrations), part 1, CNTI, M.-L., 1937.
5. Andronov, A.A.; Leontovich, E.A.: Reports of AS USSR, 21 (1938) 427.
6. Barris, G.F.: Uspekhi matemat. nauk, 10 (1955) 201.
7. Nemytskiy, V.V.; Stepanov, V.V.: Kachestvennaya teoriya differentsial'nykh uravneniy (Qualitative theory of differential equations), GITTL, M.-L., 1949.
8. Nemytskiy, V.V.: Matem. sb. 16 (1945) 307.
9. Leontovich, E.: Dissertation, Gor'kiy, 1946.
10. Myshkis, A.D.; Egle, K.Yu.: Matem. sb. 35 (1955) 491.
11. Andronov, A.A.; Vitt, A.A.; Khaykin, S.E.: Teoriya kolebaniy (Theory of vibrations), M.-L., 1959.
12. Belyustina, L.N.: Radiofizika, 1, 2 (1958) 118.
13. Belyustina, L.N.: Radiofizika, 2 (1959) 277.

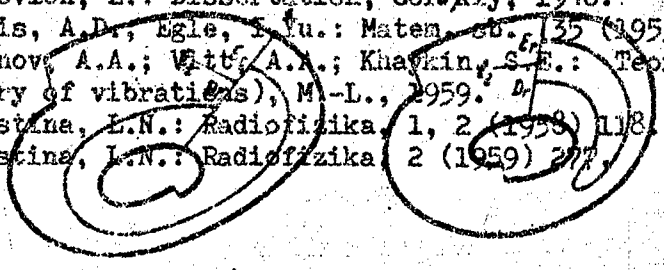

Fig. 7

Physical and Technical Scientific Research Institute of Gor'kiy University

Submitted: 10 Apr. 1959

If case 3b applies to the arc $\smile E_r D_r$, then we continue the arc Δ_γ, passing through the point D_r, up to the following common point $D_r^{(1)}$ of the arc Δ_γ and the length $l_1(l_2)$. If case 3b applies to the arc $\smile D_r D_r^{(1)}$ also, then we continue the construction to the common

SHORT COMMUNICATIONS AND LETTERS TO THE EDITOR.

ON LONGITUDINAL WAVES IN NON-ISOTHERMAL PLASMAS

by B.N. Gershman.

It is known that low-frequency as well as high-frequency longitudinal waves may be propagated in a homogeneous, isotropic plasma. In analyzing their properties it is necessary to take into account the thermal motion of the ions. It appears that, neglecting collisions, such perturbations can be propagated only in a non-isothermal plasma given that

$$T_e \gg T_i. \qquad (1)$$

where T_e and T_i are the temperatures of the electrons and the ions. The theory of the propagation of such waves has been developed in a number of papers, particularly in [1,2]. In this note we wish to draw attention to a series of peculiarities in the behavior of these waves, analogous to a known degree to certain peculiarities in the propagation of high-frequency waves in a magneto-active plasma. Furthermore, we shall introduce formulas for the damping ratio more complete than those given in [1,2].

In investigating low-frequency longitudinal waves we start from the kinetic equations for electrons and ions and the equations of electrodynamics. If at an initial moment of time t = 0 we have in an unbounded plasma a perturbation of the wave type $\sim e^{ikz}$ (k is the

wave number), then the asymptotic behavior of the component of the electric field E_z, defined by the law e^{pt}, where $p = -i\omega - \gamma$ (ω is the frequency, γ the damping ratio of the wave), may be established by Landau's method [3]. The quantities p and k are then linked by the dispersion equation

$$1 + \frac{\omega_e^2}{p\sqrt{2\pi}} \left(\frac{m}{\varkappa T_e}\right)^{3/2} \int_C \frac{V_{ze}^2 \exp\left(-mV_{ze}^2/2\varkappa T_e\right)}{p + ikV_{ze}}\, dV_{ze} + \tag{2}$$

$$+ \frac{\omega_i^2}{p\sqrt{2\pi}} \left(\frac{M}{\varkappa T_i}\right)^{3/2} \int_C \frac{V_{zi}^2 \exp\left(-MV_{zi}^2/2\varkappa T_i\right)}{p + ikV_{zi}}\, dV_{zi} = 0,$$

where m and M are the masses of an electron and an ion, $\varkappa$ is Boltzmann's constant, $\omega_e = \sqrt{4\pi e^2 N/m}$ and $\omega_i = \sqrt{4\pi e^2 N/M}$ are the natural frequencies of the electronic and ionic oscillations of the plasma (N is the density of electrons with a charge e). The equilibrium functions of electron and ion distribution are assumed to be Maxwellian. The limits of integration in (2) are chosen in the usual way (cf. Landau's method [3]).

Given that $\omega/k \equiv V_\phi \gg \sqrt{\varkappa T_e/m}$ it follows from (2) that the motion of the ions need not be taken into account. We then arrive at the known equation for high-frequency plasma waves.

Let us now assume that the phase velocity lies within the limit

$$\sqrt{\varkappa T_i/M} \ll \omega/k \ll \sqrt{\varkappa T_e/m}. \tag{3}$$

If the first of conditions (3) were broken, the damping would be considerable ($\gamma \sim \omega$), whereas when conditions (1) and (3) are simultaneously fulfilled the waves will always be weakly attenuated ($\gamma \ll \omega$). In this case, making use of the known expansions for the integrals in (2), we get:

$$1+\frac{\omega_e^2 m}{k^2 \varkappa T_e}\left(1-\frac{p}{k}\sqrt{\frac{m\pi}{2\varkappa T_e}}\right)+\frac{\omega_i^2 M}{k^2 \varkappa T_i}\left[\frac{k^2}{p^2}\frac{\varkappa T_i}{M}-\frac{3\varkappa^2 T_i^2 k^4}{M^2 p^4}-\frac{p}{k}\sqrt{\frac{M\pi}{2\varkappa T_i}}\exp\left(\frac{Mp^2}{2\varkappa T_i}\right)\right]=0. \tag{4}$$

As a first approximation, neglecting damping ($\gamma \ll \omega$), we assume $p = -i\omega$; then omitting the last terms in the brackets in (4), we arrive at the equation

$$3\beta_i^2 v_i n^4 + (v_i - 1) n^2 - v_i T_i/\beta_i^2 T_e = 0, \tag{5}$$

where $n = ck/\omega$ is the refractive index, $v_i = \omega_i^2/\omega^2$, $\beta_i^2 = \varkappa T_i/Mc^2$. Under our conditions $\beta_i^2 \ll 1$.

Equation (5) defines the propagation of two types of wave. However, we are only interested in the roots of the equation, for which $n^2 > 0$ (when $n^2 < 0$ propagation is generally impossible). To make things more graphic it is better to put the solution of eq. (5) in the form of a function of the parameter v_i for fixed values of β_i^2 and T_i/T_e (see Fig. 1). In this case our interest is focused on the curve lying in the upper half plane. The parameter v_i varies with the frequency or electron density. When $v_i < 1$, if the difference $1 - v_i$ is sufficiently great (namely, given that $(1 - v_i) \gg v_i \sqrt[3]{T_i/T_e}$), we have the relationship:

$$n^2 = \frac{1 - v_i}{3\beta_i^2 v_i}. \tag{6}$$

At the same time the difference $1 - v_i$ ought not to be very great, since then $n^2 \sim 1/\beta_i^2$; in this case one of the initial conditions (3) is unfulfilled and we get considerable damping. We may say that eq. (6) describes ionic plasma oscillations.

In the H.F. case we have analogous electron oscillations*.

* These oscillations are represented schematically in Fig. 1 by the dash-dot line. The behavior of the waves when $v_i \longrightarrow 0$ is not described by equation (5).

(In the H.F. case $n^2 = \frac{1 - v_e}{3\beta_e^2 v_e}$ [4]). However, it is more accurate to speak not of oscillations but of waves. We shall call the waves defined by formula (6) ionic plasma waves. The branch of the dispersion curve corresponding to these waves is represented by the broken line in Fig. 1.

The solution of eq. (5) will be substantially different when

$$v_i \gg 1 \quad (\omega_i \gg \omega). \tag{7}$$

Then we can neglect the first term in (6) so that

$$n^2 = \frac{T_i}{T_e \beta_i^2} \quad \left(V_\phi = \sqrt{\frac{\varkappa T_e}{M}}\right). \tag{8}$$

Expression (8) corresponds to the case in which sound waves are propagated in a non-isothermal medium; therefore we shall treat the wave described by (8) as a sound wave. The part of the dispersion curve corresponding to this wave is indicated by the double line in Fig. 1. The important thing is that the two types of wave mentioned, as follows from Fig. 1 , do not form isolated branches; the ionic plasma waves are, as it were, a prolongation of the sound waves. We then have an intermediate region between the waves mentioned.

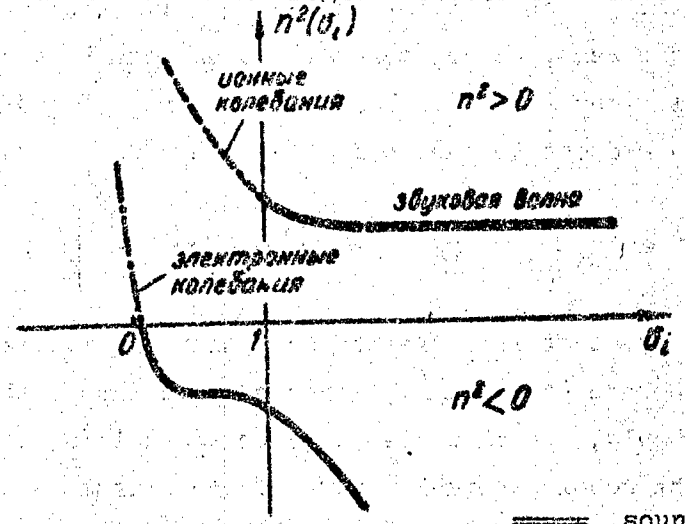

Fig. 1

═══ sound wave;
(– – – ionic oscillations; –·–·– electronic oscillations)

Thus, for example, according to (5) exactly when $v_i = 1$

$$n^2 = \frac{1}{\beta_i^2} \sqrt{\frac{T_i}{3T_e}}$$

The above-mentioned characteristic behavior of normal waves is found in accordance with the phenomenological theory of wave propagation taking into account space dispersion [5]. If it is a question of a plasma, then it is possible to point to an analogy with the propagation of high-frequency waves in a magneto-active plasma [4,6], where curves of the type shown in Fig. 1 are also obtained. Here the two waves - the extraordinary (or the ordinary) and the plasma wave - form part of the same dispersion curve.

We now get formulas for attenuation of the waves in question. Inserting in (4) $p = -i\omega - \gamma$, when $\gamma \ll \omega$ we obtain as the second approximation:

$$\frac{\gamma}{\omega} = \sqrt{\pi}\left[\left(\frac{m\omega^2}{2\varkappa T_e k^2}\right)^{3/2}\frac{M}{m} + \left(\frac{M\omega^2}{2\varkappa T_i k^2}\right)^{3/2}\exp\left(-\frac{M\omega^2}{2\varkappa T_i}\right)\right| \qquad (9)$$

$$= \sqrt{\pi}\left[\left(\frac{T_i}{2\beta_i^2 n^2 T_e}\right)^{3/2}\sqrt{\frac{m}{M}} + \frac{1}{2^{1/2}\beta_i^3 n^3}\exp\left(-\frac{1}{2\beta_i^2 n^2}\right)\right|.$$

Expression (9) differs from that introduced in [1,2] by virtue of the exponential component, which, generally speaking, is also substantial, especially for an ionic plasma wave. For an acoustical wave (8) expression (9) reduces to the form:

$$\frac{\gamma}{\omega} = \sqrt{\frac{\pi}{8}}\left[\sqrt{\frac{m}{M}} + \left(\frac{T_e}{T_i}\right)^{3/2}\exp\left(-\frac{T_e}{2T_i}\right)\right|. \qquad (10)$$

It follows from (10) that in correspondence with the initial assumptions we in fact do have $\gamma \ll \omega$. Although it is exponentially small, the second term should, in principle, also be taken into account, especially when the non-isothermal nature of the plasma is not strongly expressed. Note, by the way, that $T_e \sim T_i$ upsets the assumption that

$\gamma \ll \omega$.

For an ionic plasma wave (6):

$$\frac{\gamma}{\omega} = \sqrt{\frac{\pi}{8}} \left[\sqrt{\frac{m}{M}} \left(\frac{3v_i}{1 - v_i} \sqrt{\frac{T_i}{T_e}} \right)^3 + \frac{1}{\beta_i^3 n^3} \exp\left(-\frac{1}{2\beta_i^2 n^2} \right) \right]. \quad (11)$$

By virtue of the condition introduced just before formula (6) the first term is always much smaller than unity; the value of the second term increases with increase in the difference $1 - v_i$. Weakly attenuated waves can only occur, when the frequency ω is sufficiently close to the natural frequency ω_i.

Bibliography

1. Gordeyev, G.V.: ZhETF, 27 (1954) 19.
2. Bernstein, J.B.: Phys. Rev., 109 (1958) 10.
3. Landau, L.D.: ZhETF 16 (1946) 574.
4. Gershman, B.N.; Ginzburg, V.L.; Denisov, N.G.: UFN, 61 (1957) 561.
5. Ginzburg, V.L.: ZhETF, 34 (1958) 1593.
6. Gershman, B.N.: ZfETF, 31 (1956) 707.

Radiophysics Scientific ResearchInstitute of Gor'kiy University

Submitted 17 May 1959.

ON THE THEORY OF ARTIFICIAL ANISOTROPIC DIELECTRICS

Pages 656-658 by F.G. Bass.

A number of recent articles have been devoted to the question of the passage of particles and the propagation of electromagnetic waves in media, the dielectric constants and permeabilities of which are periodic functions of one coordinate [1-4]. In these articles it has been shown that if the period of variation of the dielectric constant and the permeability is much less than the electromagnetic wavelength, the electromagnetic field in the medium, averaged with respect to the space period of the structure, coincides with the field of a certain homogeneous, anisotropic medium. The authors of [1 - 4] solved a one-dimensional problem with a clearly given form of the dependence of the dielectric constant and the permeability on the coordinates.

In this note we shall derive equations defining the electromagnetic field, averaged with respect to period, assuming that the deviations of the dielectric constant and the permeability from their mean values $\overline{\epsilon}$ and $\overline{\mu}$ are small (the horizontal line denotes averaging with respect to the space period) and also that ϵ and μ are real functions. For the rest ϵ and μ are arbitrary scalar or tensor real periodic functions of the coordinates with a period much less than the wavelength in a medium with $\overline{\epsilon}$ and $\overline{\mu}$.

We shall put the electric and magnetic fields E and H in the form:

$$E = E_0 + \eta; \quad H = H_0 + \eta; \qquad (1)$$

$$E \quad E_0; \quad H \quad H_0.$$

In order to obtain equations defining E_0, H_0 and from Maxwell's equations for E and H, we shall use the method mentioned in / 5 / .

We shall average Maxwell's equations for E and H and subtract the averaged equations from the unaveraged ones. We then get this system of equations for E_0, H_0, ξ, η :

$$\operatorname{rot} E_0 = \frac{i\omega}{c}(\bar{\mu} H_0 \quad \overline{\beta\eta}); \quad \operatorname{rot} H_0 = -\frac{i\omega}{c}(\bar{\varepsilon} E_0 + \overline{\alpha\xi}); \tag{2}$$

$$\operatorname{rot}\xi = \frac{\omega}{c}(\mu\eta + \beta H_0); \quad \operatorname{rot}\eta = \frac{i\omega}{c}(\bar{\varepsilon}\xi + \alpha E_0). \tag{3}$$

where

$$\beta = \mu - \bar{\mu}; \quad \alpha = \varepsilon - \bar{\varepsilon}.$$

In system (2)-(3) we have neglected terms of the order of $\alpha\xi/\bar{\varepsilon}$ and $\beta\eta/\bar{\mu}$. We shall put alpha and beta in the form of a Fourier series:

$$\alpha = \sum_n \alpha_n e^{inr}; \quad \beta = \sum_n \beta_n e^{inr} \left(\alpha_n^* = \alpha_{-n}, \ \beta_n^* = \beta_{-n}\right). \tag{4}$$

From (3) and (4) we get for ξ and η :

$$\xi = -\sum_n \frac{\alpha_n n}{\bar{\varepsilon} n^2}(nE_0) e^{inr}; \quad \eta = -\sum_n \frac{\beta_n n}{\bar{\mu} n^2}(nH_0) e^{inr}. \tag{5}$$

Note that for a solution correct to terms $\sim \frac{\omega}{c}\sqrt{\bar{\varepsilon}\bar{\mu}}\,L$ it is possible to consider that E_0 and H_0 do not depend on the coordinates (L - a quantity of the order of the space periods α and β).

Substituting (5) in (2) and averaging for E_0 and H_0, we find the following equations:

$$(\operatorname{rot} E_0)_i = \frac{i\omega}{c}\mu'_{ik} H_{0k}; \quad (\operatorname{rot} H_0)_i = -\frac{i\omega}{c}\varepsilon'_{ik} E_{0k}. \tag{6}$$

where

$$\mu'_{ik} = \bar{\mu}\delta_{ik} - \frac{1}{\bar{\mu}}\sum_n \beta_n 2\frac{n_i n_k}{n^2}; \quad \varepsilon'_{ik} = \bar{\varepsilon}\delta_{ik} - \frac{1}{\bar{\varepsilon}}\sum_n |\alpha_n|^2 \frac{n_i n_k}{n^2}. \tag{7}$$

The results obtained are easily generalized to include the case in which the mean specific inductive capacitance and the mean permeability are tensors.

The tensor expressions have the following form:

$$\varepsilon'_{ik} = \bar{\varepsilon}_{ik} - \sum_n \frac{a^{(n)}_{lm}\, a^{(-n)}_{kl}\, n_l n_m}{\bar{\varepsilon}_{pq} n_p n_q}; \quad \mu'_{ik} = \bar{\mu}_{ik} - \sum_n \frac{\beta^{(n)}_{lm}\, \beta^{(-n)}_{kl}\, n_m n_l}{\bar{\mu}_{pq} n_p n_q} \quad (8)$$

The notation is self-evident. In the calculations we have neglected terms of the order of $(\omega/c)\sqrt{\bar{\varepsilon}\bar{\mu}}\,L$ and $(\omega^2/c^2)\bar{\varepsilon}\bar{\mu}L^2$. Terms of the order of $(\omega/c)\sqrt{\bar{\varepsilon}\bar{\mu}}\,L$ specify the optical activity of the artificial dielectric. However, if alpha and beta have central symmetry, then terms of the first order with respect to $(\omega/c)\sqrt{\bar{\varepsilon}\bar{\mu}}\,L$ are equal to zero. Retaining terms of the second order with respect to $(\omega/c)\sqrt{\bar{\varepsilon}\bar{\mu}}\,L$ leads to a quadratic space dispersion, which in a number of cases may be substantial [6]. The investigation of the optical activity and quadratic dispersion will be the subject of a special report.

In conclusion the author wishes to thank P.V. Blokh and E.A. Kaner for useful discussion.

Bibliography

1. Faynberg, Ya.B.; Khizhnyak, N.A.: ZhTF, 25 (1955) 712.
2. Faynberg, Ya.B.; Khizhnyak, N.A.: ZhETF, 32 (1957) 883.
3. Rytov, S.M.: ZhETF, 29 (1955) 605.
4. Blokh, P.V.: Dissertation, Kharkov, 1955.
5. Lifshits, I.M.; Kaganov, M.I.; Tsukernik, M.V.: Transactions of the KhGU, 2 (1950) 41.
6. Ginzburg, V.L.: ZhETF, 34 (1958) 1993.

Institute of Radiophysics and Electronics AS USSR

Submitted: 15 May 1959

A RING SORTING SYSTEM FOR A MOLECULAR GENERATOR

Pages 658-659

by A.F. Krupnov.

Tests have been made on a sorting system for molecular generators and amplifiers, consisting of a series of rings, surrounding the molecular beam. Neighboring rings bear charges of different sign. The minimum of the electric field E is then obtained at the axis of the system and the maximum at the periphery, making it possible to sort molecules according to level (Fig. 1). The optimum ratio of ring radius ρ_0 to the distance between rings x_0 ought to be of the order of unity:

$$\xi_{opt} = (\rho_0/x_0)_{opt} \quad 1,$$

since when $\xi \ll 1$ the field is almost uniform in cross section and when $\xi \gg 1$ the whole field is concentrated at the periphery of the system (i.e. the central part works badly).

As distinct from the field of a quadripole condenser the field of the system is on average parallel to the field in the resonator. The length, over which the molecules interact with the field, is less than the real length of the system, since there are sections inside the rings where the field is close to zero.

Tests on ring sorting systems have been made for a molecular generator with the following characteristics: source - one aperture 1 mm in diameter, length 10 mm (without diaphragm), resonator for

E_{010}, length 100 mm ($Q \simeq 7{,}000$), working pressure in the molecular generator $(2 - 3)\ 10^{-5}$ mm Hg. Tests were made on ring sorting systems with a length equal to the length of the quadripole condenser (100 mm) and a diameter equal to the diameter of the inside part of the condenser (6 mm), made of nickel wire 1 mm in diameter, with different values of $\xi = 0.7,\ 1.15,\ 1.55$. With all the specimens we got generation beginning with roughly the same sorting voltages as in the quadripole system; the amplitudes of the oscillations with the ring and quadripole systems are of the same order. The test specimen with $\xi = 1.15$ gave the greatest amplitude of oscillation of all the specimens tested.

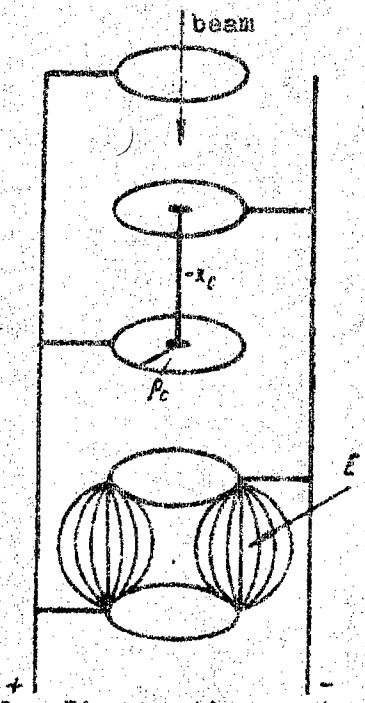

Fig. 1: Ring sorting system

As a variant the ring sorting system may be a double spiral.

In our opinion the basic advantage of the proposed system consists in its giving more freedom to vary the shape of the cross section of the beam and its area than does the quadripole condenser. Evidence for this is afforded by, for example, a) the possible design

of a molecular generator in the sub-millimater range with a disk resonator, as proposed by Prokhorov [1] (Fig. 2), b) the method of increasing the power of a molecular generator by using an annular beam of molecules and a resonator for the higher mode of oscillations E_{020} (Fig. 3).

From the design point of view the virtue of the system consists in its compactness, simplicity of manufacture and the ease with which it can be adjusted. Note also that in the system proposed it is possible to change from ring to ring the potentials, the ring dimensions and the direction of the axis of the system.

Fig. 2: Sorting system with disk resonator. The beam sources are disposed around the periphery of the sorting system.

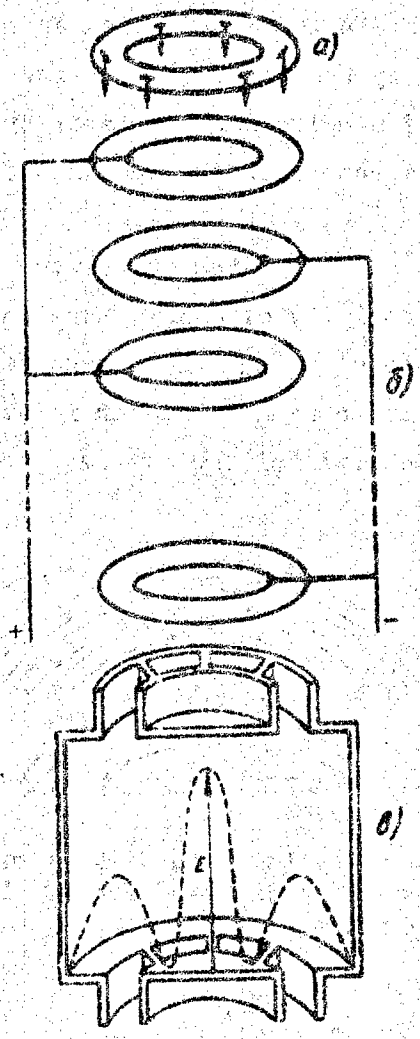

Fig. 3: Generator with resonator for higher mode of oscillations:

a) annular beam source;
b) sorting system consisting of a series of coaxial rings, giving an annular beam of active molecules;
c) E_{020} resonator with annular terminal waveguides with diaphragms.

Bibliography

1. Prokhorov, A.M.: ZhETF, 34 (1958) 1658.

Radiophysics Scientific Research Institute of Gor'kiy University

Submitted: 17 May 1959.

APPLICATION OF THE PARAMAGNETIC RESONANCE METHOD FOR DETERMINING THE CONCENTRATION OF OXYGEN DISSOLVED IN WATER

Pages 660-661

by S.E. Tokar' & L.N. Litvinenko.

In studying paramagnetic resonance absorption in coal (anthracite) it has been noted that when the coal is finely pulverized (conversion of lump coal to dust) the amount of absorption falls sharply and recovers again, if the pulverized coal is placed in an evacuated vessel. The sharp reduction in paramagnetic absorption in pulverized coal is ordinarily attributed to the effect of paramagnetic atoms of atmospheric oxygen. This phenomenon has been used as the basis for the design of a gas analyzer for determining the oxygeb content of any gaseous mixture [1].

We made experiments showing that the "quenching" of paramagnetic resonance absorption when coal is pulverized is due not only to atmospheric oxygen but also to oxygen dissolved in water. Preliminary measurements confirmed that the reduction in paramagnetic resonance absorption is linked with the effect of atoms of oxygen adsorbed on the surface of the coal. In fact, if the reduction in absorption is linked with the effect of adsorbed oxygen atoms, then there must be a relationship of inverse proportionality between the total surface of the coal particles S and the intensity of absorption Q (for constant weight of the sample). From Fig. 1 it is clear that there actually is such a dppendence; we obtained it experimentally using Zavoyskiy's

method at a frequency of 3.10^6 cps.

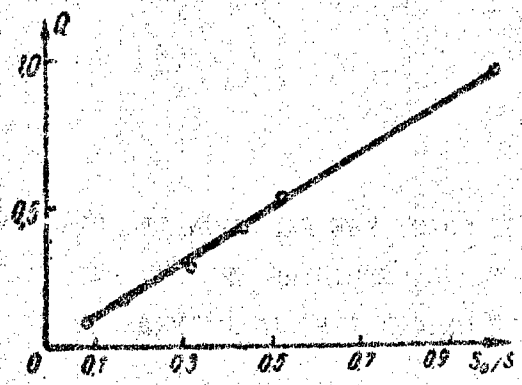

Fig. 1: Relative paramagnetic resonance absorption Q as a function of S_o/S (S_o is the surface of the sample before pulverization and S the total grain surface of the pulverized sample).

On subsequent degasification of the surface of the coal particles by boiling in distilled water the absorption returned to a level equal to that observed originally with the lump coal.

We also made the following experiment: for several hours we passed oxygen through the mixture (distilled water - pulverized coal), degasified by boiling, until the saturation point was reached (at room temperature and atmospheric pressure) and observed the change in paramagnetic resonance absorption. As the concentration of oxygen in the water increased, the amount of absorption by the pulverized coal decreased.

In order to establish the nature of the dependence of the intensity of absorption in pulverized coal (in distilled water) on the concentration of oxygen dissolved in the water we made the following measurements. The mixture (distilled water and pulverized coal), which had first been degasified by boiling, was saturated with O_2. Then we recorded the temperature dependence of the intensity of absorption for the pulverized coal in the mixture. The measurements were made at atmospheric pressure. The dependence obtained is shown in Fig. 2a. Plotted along the ordinate axis is the relative amount of absorption

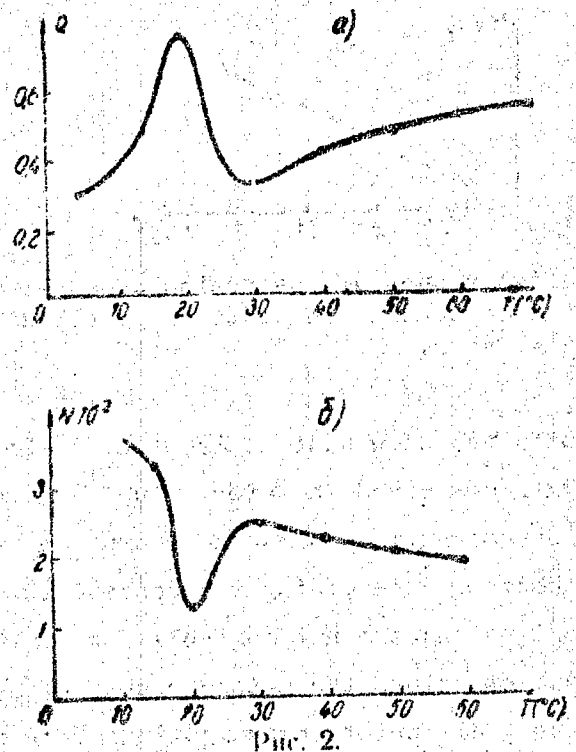

Рис. 2.

Фиг. 2.

Q and along the abscissa the temperature of the mixture T. Fig. 2b shows the dependence of the concentration N of oxygen dissolved in the water on the temperature T at atmospheric pressure, the curve being taken from a handbook [2,7]. A comparison of these curves shows that there is a proportionality between the quantity 1/Q and the concentration of oxygen dissolved in the water N (see Fig. 3).

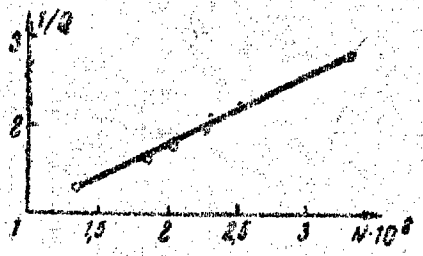

Fig. 3: Relative amount of absorption Q as a function of the concentration of the oxygen N dissolved in the water.

The results obtained show that it is possible to measure the concentration of oxygen dissolved in water by using Zavoyskiy's method of observing paramagnetic resonance absorption with a special Whereas existing methods of determining the concentration of dissolved oxygen are very laborious and are not suitable for continuously observing varying concentration, the method proposed may find very wide application in very different investigations (for example, in studying problems of oxygen exchange connected with the activity of living organisms and in certain technical processes, etc.).

Bibliography

1. Kichigin, D.A.: Paramagnitnyy gazoanalizator (Paramagnetic gas analyzer), Report to the Jubilee Session of the AS USSR in honor of the 100th anniversary of the birth of A.S. Popov, M., 1959.
2. Key, D.; Lebi, T.: Spravochnik fizika-eksperimentatora (Physics experimenter's handbook), IL., M., 1949.

Kharkov State University Submitted: 12 May 1959

ON CERTAIN POSSIBILITIES OF USING THREE-LEVEL SYSTEMS FOR RECEIVING WEAK VHF SIGNALS

Pages 661-663

by Ya.I. Khanin.

Three-level masers have the disadvantage that for them to operate it is absolutely necessary to have a sufficiently powerful source of oscillations with a frequency exceeding that being amplified. This limits the possibilities of applying these amplifiers to the range of higher frequencies. It is therefore of interest to discuss other possibilities, free from this disadvantage, of using three-level molecular systems for receiving purposes.

We shall therefore consider a paramagnetic, in the spin level system of which, when a constant magnetic field is applied, there are three suitable levels E_1, E_2 and E_3, linked by allowed transitions with the frequencies $\nu_{12} < \nu_{23} < \nu_{13}$*. The susceptibility χ_{ik} at any of these frequencies appears to depend on the presence within the volume of the specimen of oscillations of the magnetic field at other resonance frequencies [1,2] (the action of the maser is based on this circumstance). Placing this paramagnetic in a resonator, simultaneously tuned to the frequencies ν_{13} and ν_{12}, and measuring χ_{12} (the real (χ'_{12}) or imaginary (χ''_{12}) component), it is possible

* In what follows all the quantities relating to these frequencies will be written with the same indices.

to estimate the magnitude of P_{13}, the power being supplied to the resonator, i.e. to fix higher-frequency radiation from measurements at a given frequency. Here, as distinct from the maser, the auxiliary role is played by a lower frequency*.

We shall find the connection between χ''_{12} and P_{13}. [2] gives the following expression for χ''_{12}:

$$\chi''_{12} = 2\mu_{12}^2 S_1/\hbar. \qquad (1)$$

Whence clearly,

$$\Delta\chi''_{12} = 2\mu_{12}^2 \Delta S_1/\hbar. \qquad (2)$$

where $\Delta S_1 = S_1(0) - S_1(P_{13})$ is the difference in the values of S_1 for $P_{13} = 0$ and for the final P_{13}. In expressions (1)-(2) S_1 is the solution of a system of algebraic equations [2]. Omitting intermediate steps, we shall give the final result, true for the case in which the power P_{12} is small compared with the saturation power:

$$\Delta S_1 = (n_1 - n_3)\, T_1 T_2^2 \mu_{13}^2 H_{13}^2/4\hbar^2. \qquad (3)$$

Here n_1^0 and n_3^0 are the Boltzmann populations of the levels E_1 and E_3, T_1 and T_2 are relaxation times, μ_{13} and μ_{12} are dipole moment matrix elements and H_{13} is the amplitude of the magnetic field within the volume of the specimen V_0. Using the formula for the Q-factor of a resonator, we can express H_{13} in terms of P_{13}:

$$H_{13}^2 = 4Q_{13}P_{13}\left(1 - \Gamma_{13}^2\right)\varepsilon_{13}/\nu_{13} V_0. \qquad (4)$$

---

* There are other ways of using three-level systems for receiving purposes. For example, [6,7] contains a discussion of the case in which ν_{13} lies in the optical part of the spectrum and ν_{12} in the radio range. Similar spectra are observable in the vapors of certain metals in a magnetic field. By irradiating vapors with resonance light it is possible to estimate the amount of oscillation with a frequency ν_{12} from the light re-radiated.

In formula (4) we have: Q_{13}, the Q-factor of the resonator, V_p, its volume, ξ, a coefficient close to unity determined by the geometry of the resonator, Γ^2_{13}, the reflection coefficient of the resonator with respect to the power. Since $\xi_{13} \simeq 1$ and $\Gamma^2_{13} \ll 1$, the corresponding terms can be neglected, so that

$$\Delta \chi''_{12} = 2\mu^2_{13}\mu^2_{12}\left(n^0_1 - n_3\right) T_1 T_2^2 Q_{13} P_{13}/h^3 \nu_{13} V_p \qquad (5)$$

and consequently

$$(P_{13})_{\min} = \frac{h^3 \nu_{13} T_1^{-1} T_2^{-2}}{2\mu^2_{13}\mu^2_{12}\left(n^0_1 - n^0_3\right) Q_{13}} \cdot \frac{V_p}{V_0} \left(V_0 \Delta \chi''_{12}\right)_{\min} \qquad (6)$$

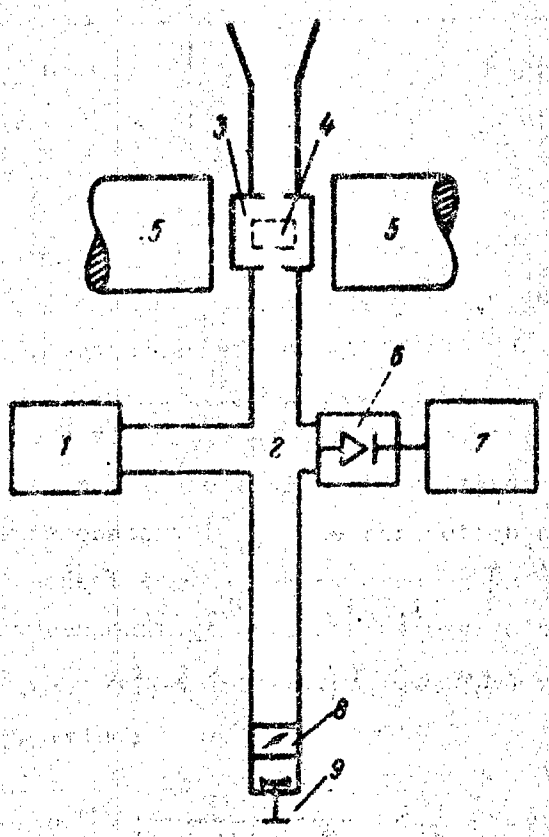

Fig. 1: Block diagram of radiospectroscope:
1 - source of oscillations with a frequency ν_{12}; 2 - waveguide bridge; 3 - resonator; 4 - paramagnetic; 5 - magnet; 6 - detector; 7 - receiver; 8 - attenuator; 9 - plunger.

$\Delta\chi''_{12}$ can be measured by means of a slightly modified radiospectroscope, the block diagram of which is shown in Fig. 1. According to the literature [3,4] the sensitivity of the spectroscope may be as much as $(V_0\chi'')_{min} = 10^{-13}$. For numerical calculations we shall assign the following values to the parameters entering into (6): $\mu_{12} = \mu_{13} = 10^{-20}$; $Q_{13} = 10^3$; $\nu_{13} = 10^{11}$ cps; $V_p/V_0 = 10$. Table 1 shows the computed values of the minimum observable P_{13} at the temperature of liquid helium and at room temperature.

Table 1.

T (°K)	T_1 (sec)	T_2 (sec)	$n_1^0 - n_3^0$ (c.u^{-3})	P_{13} (erg)
293	10^{-8}	10^{-7}	10^{16}	10^{-6}
4	10^{-2}	10^{-7}	10^{18}	10^{-14}

It was remarked above that formula (6) was obtained on the assumption that the auxiliary power P_{12} was small compared with the saturation power. The criterion is the validity of the inequality [5]

$$\frac{1}{4}\gamma^2 T_1 T_2 H_{12}^2 \ll 1,$$

i.e.

$$P_{12} \ll \frac{\nu_{12} V_p}{\gamma^2 T_1 T_2 Q_{12}\left(1-\Gamma_{12}^2\right)\xi_{12}} \equiv P_{kp}, \qquad (7)$$

where γ is the gyromagnetic ratio for an electron. Values of the critical power (P_{kp}), computed from this formula, are given in Table 2 as a function of the relaxation time for $\nu_{12} = 10^{10}$ cps, $Q_{23} = 10^3$.

Table 2.

T_1T_2 (sec^2)	10^{-14}	10^{-12}	10^{-10}	10^{-8}
P_{kp} (erg)	1	10^{-2}	10^{-4}	10^{-6}

When T_1, T_2 are large, another operating regime is possible, namely one involving, given $P_{12} \gg P_{kp}$, complete saturation of the levels E_1 and E_2. In this case, when $P_{13} > 0$, the distribution becomes $n_2 > n_1$ and it is possible to observe amplification of the oscillation ν_{12}. However, the paramagnetics presently available do not have sufficiently large relaxation times and the second regime can only be brought about with powers P_{12} substantially greater than those required by the first method. This reduces the sensitivity and, accordingly, the practical value of employing a saturation regime.

The values given above in fact determine the total power P_{13} in the receiving band, which will be of the order of 1.5 mc for the given $Q = 10^3$ and $T_2 = 10^{-7}$ seconds.

Thus, the existence of a link between P_{13} and χ''_{12} makes it possible to use a paramagnetic spectroscope, working at a frequency of ν_{12}, to receive oscillations at a higher frequency ν_{13}. On cooling the active material to the temperature of liquid helium very high sensitivity is obtained.

Bibliography

1. Clogston, A.M.: J.Phys.Chem.Solids, 4 (1958) 271.
2. Malakhov, A.N.; Fayn, V.M.: Radiofizika, 1, 5-6 (1958) 66.
3. Ingram, D.J.E.: Radiospectroscopy at microwave frequencies, London, 1955.
4. Feher, G.: Bell System Techn. J., 36 (1957) 449.
5. Bloembergen, N.; Wang, S.: Phys. Rev., 93 (1954) 72.
6. Kastler, A.: J.Opt.Soc.Amer., 47 (1957) 460.
7. Arditi, M.: IRE National Convention Record, 1 (1958) 3.

Radiophysics Scientific Research Institute of
Gor'kiy University

Submitted: 12 Apr. 59

ON THE STABILITY OF THIRD-ORDER NONLINEAR SYSTEMS

Pages 664-665 by I.N. Pechorina.

If the dynamics of a control system can be described by equations of the form

$$dx/dt = f_1(x) + a_{12}y + a_{13}z;$$
$$dy/dt = f_2(x) + a_{22}y + a_{23}z;$$
$$dz/dt = f_3(x) + a_{32}y + a_{33}z,$$

then, according to [1], the stability of the system can be checked with the aid of the inequality

$$4k_2c(x)[a(x) - k_1] \quad \{c(x)(1 + k_2)/k_1 + k_2[a(x) - k_1]k_1 - k_2b(x)\}^2 \quad 0. \qquad (1)$$

Here a(x), b(x) and c(x) are the coefficients of an equation set up on the basis of the matrix

$$-\begin{vmatrix} \frac{f_1(x)}{x} - \lambda & a_{12} & a_{13} \\ \frac{f_2(x)}{x} & a_{22} - \lambda & a_{23} \\ \frac{f_3(x)}{x} & a_{32} & a_{33} - \lambda \end{vmatrix} = \lambda^3 + a(x)\lambda^2 + b(x)\lambda + c(x).$$

k_1 and k_2 are positive constant numbers.

The stability can be checked by means of inequality (1) for any perturbations of the control system. However, it is inconvenient to use the inequality in practice. In order to investigate the stability

of a system it is necessary to select two numbers k_1 and k_2, which, being inserted in expression (1), insure the inequality. In this article expression (1) is transformed in such a way that it becomes perfectly possible to use this inequality in calculations.

We shall consider that $a(x) > 0$, $b(x) > 0$ and $c(x) > 0$. This condition is usually satisfied in practice. Then expression (1) can be put in the following form:

$$4c(x)\,A(x)\,k_2 - \{c(x) + k_2\,[A(x) - (k_1 b(x) - c(x))]\}^2 \quad 0.$$

Here $A(x) = k_1^2\,[a(x) - k_1]$.

The inequality written out above may exist if $A(x) > 0$ and $k_1 b(x) - c(x) > 0$. Accordingly, the first condition for the stability of a third-order nonlinear control system of a given class may be formulated as the inequality:

$$a(x) > k_1 > c(x)/b(x). \qquad (2)$$

i.e. $[a(x)]_{min} > [c(x)/b(x)]_{max}$. This expression is analogous to Hurwitz's stability criterion.

The determination of the magnitude of the constant k_1, which bounds the functions $a(x)$ and $c(x)/b(x)$, is not sufficient for investigating a control system. To check the stability it is necessary to inquire into the value of the constant k_2.

We shall consider the polynomial

$$F(k_2) = 4c(x)\,A(x)\,k_2 - \{c(x) - k_2\,[A(x) - (k_1 b(x) - c(x))]\}^2$$

and find the values of k_2, at which the function $F(k_2) = 0$. In order that $F(k_2) = 0$, k_2 must be equal to

$$k_2' = c(x)\left[\sqrt{k_1^2\,[a(x) - k_1]} - \sqrt{k_1 b(x) - c(x)}\right]^{-2}$$

or

$$k_2'' = c(x)\left[\sqrt{k_1^2\,[a(x) - k_1]} + \sqrt{k_1 b(x) - c(x)}\right]^{-2}.$$

The inequality $F(k_2) > 0$ is possible only on condition that

$$c(x)\left[\sqrt{k_1^2\,[a(x) - k_1]} - \sqrt{k_1 b(x) - c(x)}\right]^{-2} \quad k_2 \quad c(x)\left[\sqrt{k_1^2\,[a(x) - k_1]} + \sqrt{k_1 b(x) - c(x)}\right]^{-2}. \qquad (3)$$

If we put

$$\varphi_1(x) = k_1^2 [a(x) - k_1]/c(x);$$
$$\varphi_2(x) = |k_1 b(x) - c(x)|/c(x). \qquad (4)$$

then we can write:

$$\varphi_1(x)\ \varphi_2(x) - 2\sqrt{\varphi_1(x)\varphi_2(x)}\ k_2^{-1}\ \varphi_1(x)\ \varphi_2(x) - 2\sqrt{\varphi_1(x)\varphi_2(x)}. \qquad (5)$$

Inequality (5) shows that in a stable control system the range of variation of the functions $\varphi_1(x)$ and $\varphi_2(x)$ is bounded. Inequalities (2) and (5) are not difficult to use and are recommended for practical calculations.

Bibliography

1. Krasovskiy, N.N.: Prikladnaya matematika i mekhanika (Applied mathematics and mechanics), 17 (1953) 339.

Ural Polytechnic Institute

Submitted: 22 Jan. 1959.

JPRS: 2962

OSO: 3332-N

THIRD ALL-UNION CONFERENCE ON RADIO ELECTRONICS

[This is a translation of an unsigned article in Izvestiya Vysshikh Uchebnykh Zavedeniy - Radiofizika, Vol. II, No 4, 1959, pages 666-673.]

The third All-Union Conference on Radio Electronics of the Ministry of Higher Education USSR, devoted to the memory of A. S. Popov was held from 22 through 27 January 1959 at Kiev. About 500 delegates of institutions of higher learning and various scientific industrial establishments of the Academy of Sciences USSR, and Academy of Sciences Ukrainian SSR, took part in the Conference.

The following sections worked at the Conference: Ultrahigh Frequency Electrophysics, Ultrahigh Frequency Electronics, General Electronics, Quantum Radio Engineering and Radio Spectroscopy, Radio Wave Propagation and Radio Astronomy, Semiconductors and their Application in Radio Equipment, and General Radio Engineering.

The following survey reports were read at the plenary sessions: V. K. Tkach "Certain Results of the Application of Radio Electronics to the Study of Biological Media," V. I. Siforov "Problem of Channels of Communication with Random Changes of Parameters," I. A. Kukurite, G. I. Rukman, O. Ya. Savchenko, M. K. Safronova, G. M. Khaplanov "Prospects of the Use of Certain Optico-Radiophysical Phenomena for the Creation of New Ultrahigh-Frequency Devices."

In the decision taken by the Conference, there are a number of recommendations relating to the trend of scientific research work at higher education institutions and scientific research institutes, as well as certain suggestions of an organizational character. It was proposed that the next, Fourth Conference of the Ministry of Higher Education on Radio Engineering and Electronics, be held in November 1960 at Khar'kov.

The Work of Conference Sections

Radio Wave Propagation and Radio Astronomy Section

The evening session of 24 January opened with a report by V. V. Zheleznyakov, entitled "On Magnetic Retarding Radiation and Unsteadiness of the System of Charged Particles in Plasma." The report gives the results of the evaluation of the magnetic retarding radiation of the unbalanced electronic system obtained on the basis of the quantum theory on radiation and absorption of electromagnetic

waves. The criteria of amplification and unsteadiness of electromagnetic waves at the frequencies of magnetic retarding radiation within the system of magnetoactive plasma and the flow of charged particles were formulated.

The paper read by B. N. Gershman entitled "On the Theory of the Propagation of Low Frequency Waves in Magnetoactive Plasma" was devoted to the problems of the propagation of electromagnetic waves with frequencies $\omega < \omega_0, \omega_H$ where ω_0 is the plasma freugency and ω_H is the gyro frequency of the electrons. In this case the index of waves refraction is far greater than one, i.e., the wave is slow. The attenuation of these waves due to the thermal movement of particles (Landau mechanism) was estimated. The results obtained were utilized in the theory of "whistling atmospherics."

B. S. Shapiro in his report on "Investigation of the Distribution of Ionization with Altitude by the Method of Vertical Radiosondage of the Ionosphere" gave an account of the method devised by him of determining geometrical parameters of ionospheric strate (altitude, half-thickness, etc.) according to the tabulated ionospheric data. As a result, it appeared to be possible to study variations of geometrical parameters of the ionosphere on the basis of vast material provided by observations of the ionosphere, in conformance with the program of the International Geophysical Year.

V. D. Gusev, S. R. Mirkoman, L. A. Drachev, Yu. V. Berezin and M. P. Kiyanovskiy read a paper on "Results of the Investigation of Parameters of Large-Scale Heterogeneities of the Ionosphere by the Phase Method." The experiments were conducted from January 1957 through May 1958. The method used was that of three space-diversity antennas with base 30 to 40 km, through which the variations of the phase path of reflection of ionospheric signals were measured. It was established that large-scale heterogeneities have an elongated form with a ratio of semiaxes 1.5 to 2.0. The dimensions of heterogeneities along the major axis are of the order of several hundred kilometers and the velocity of their drift is 130 to 170 m sec^{-1}.

The second communication by the same authors, "On the Correlative Treatment of Fluctuations in the Presence of a Slowly Changing Nonstationary Component" was, in fact, a continuation of the preceding report. In this, the possibilities of exclusion of a slow daily course of the phase path in correlative treatment of the data on fluctuations of the reflection of signals by the ionosphere were discussed, and the influence of this factor on the precision of the measurements was evaluated.

The communication of Ye. A. Benediktov and N. A. Mityakov on "Evaluation of the Influence of the Earth is Magnetic Field in the Study of Ionospheric Heterogeneities," set forth the results of calculation of the intensity of the signal dispersed by ionospheric heterogeneities in the approximation of quasi-longitudinal propagation of the wave in relation to the magnetic field. Comparison of the results of evaluation with published data on the vertical sondage of the ionosphere gives, for the relative deflection of the concentration of the particles in the heterogeneities, the value of $\Delta N/N \sim 4 \cdot 10^{-4}$.

At the morning session of 26 January, M. M. Kobrin read a communication on "Radio Echo from the moon on 3 and 10 cm Waves." He spoke on the results of the investigation of radio signals reflected by the moon, which were sent by a transmitter of continuous action and received by means of a radio-astronomical receiver of high sensitivity. It was found that the reflection from the moon of $\lambda = 3$ cm and $\lambda = 10$ cm has a mirror character and is mainly determined by the central part of the moon disc.

The communication entitled "On Nonthermal Cosmic Radio Emission" was contributed by G. G. Getmantsev. In this, an attempt was made to explain the radio emission of the plane component of cosmic radio emission on the basis of the ideas on the magneto-retarding origin of radio emission.

V. A. Razin read the communication on "Observation of the Ring-Shaped Solar Eclipse of 19 April 1958 on Waves of 1.63 cm, 3.2 cm and 10 cm" on behalf on the group - Du Len-Yao, A. N. Malakhov, V. M. Plechkov, V. A. Razin, V. L. Rakhlin, K. M. Strezhneva, K. S. Stankevich, Tan Shou-Pe, V. S. Troitskiy, V. V. Khrulev and N. M. Tseytlin. The eclipse was observed on the island of Hainan in China. From curves of the change of intensity of radio emission during the eclipse, it was possible to determine the distribution of radio brightness on the solar disc on the day of the eclipse, to evaluate the effective temperature of the active radio emitting regions and to measure the integral flow of radio emission.

In the communication of V. L. Ginzburg and V. Ya. Eydman, "On Certain Peculiarities of the Emission of Electromagnetic Waves by Particles Moving with Faster-than-Light Speed in a Medium," the peculiarities of the emission of electromagnetic waves by "faster-than-light" particles were discussed. The classical calculation of the force of radiation friction during movement of the charged particle in a magnetic field showed that with "faster-than-light" speeds the force of the emission reaction altering the rotation radius of the particle decreases as compared with the case of movement "up-to-the-speed-of-light" and, in an anisotropic medium, it can even change the sign, that is, correspond not to the "friction" but to the drive of the oscillations.

A. A. Semenov and G. A. Karpeyev spoke on "The Connection of the Frequency of Fluctuations of the Field Amplitude with the Speed of the Drift of Heterogeneities." They quoted the results of the evaluation and experiment in the determination of the frequency of fluctuations of the reflected radar signals in the centimeter band. The connection between the frequency of fluctuations and the speed of movement of the heterogeneities was established.

The morning session of 26 January ended with a lecture by G. Ye. Brengauz, "On the Possibilities of Detection of Monochromatic Lines of Absorption in the Spectrum of Radio Emission of the Sun." The speaker quoted the results of evaluations of the intensity of radio lines of hydrogen and singly-ionized helium in the spectrum of

solar radio emission.

At the evening session of 26 January, four papers were read.

The communication of I. D. Gits, B. A. Ioshpy and E. I. Mogilevskiy on "Electronics of Solar NIZMIR Magnetographs" contained a description of the circuits of a radio electronic meter separating the signal with the frequency magnetographs.

In the next communication entitled "Electro-Optic Light Modulators of the NIZMIR Magnetograph," I. A. Zhulin gave a description of an electronic light modulator based on the use of the Kerr ce...

In the communication "On the Statistical Properties of the Intensity of the Field of Atmospheric Radio Noise," Ya. I. Likhter and G. I. Gurina quoted experimental data on the distribution of the probability of the envelope of the field of radio noise.

V. Ye. Kashprovskiy, in the communication on "A New Method of Measuring the Conductivity of Soils according to the Attenuation of Waves and Results of Measurements," proposed to utilize for the determination of the conductivity of soils at the frequencies of the broadcasting bands, the measurement of the depth of penetration of the field into soil, using for this wells, boreholes, etc. The experimental checkup of the method showed its effectiveness.

Section of Ultrahigh Frequency Electrodynamics

At the sessions of the Section of Ultrahigh Frequency Electrodynamics, 30 papers and communications were read, which were devoted to the theoretical and experimental investigation of retarding systems, waveguide structures and transmission lines, coordination of ultrahigh frequency structures, study of cavity resonators, as well as problems of the measurement of ultrahigh frequencies.

The reports of Yu. G. Al'tshuler (theoretical analysis of counter-pin systems), B. M. Bulgakov (exact and approximate estimates of spirals with magneto-dielectrics), I. G. Gladyshev (investigation of diaphragm-type waveguides with additional coupling elements in the form of π-shaped slots, inductive loops and capacitive pins), V. N. Ivanov (study of properties of stacked pin connecting strips) were devoted to treatment of the theory and experimental studies of retarding systems. Likewise devoted were two reports of N. M. Chirkin, one of them to a study of the dispersion properties of coaxial systems in which both conductors are loaded with discs, the other to an investigation of a coaxial system with a spiral chute on the inside conductor. The report of A. S. Bondarev and G. F. Semenov set forth an investigation of the dispersion properties of spirals with dielectric mounts achieved by means of a sonde with high-ohmic supply. V. D. Ivanov and V. S. Mikhalevskiy reported on the findings of an investigation of a retarding system of the spiral type in the presence of plasma. Systems representing a combination of spiral and ribbed structure (spiral in ribbed waveguide and ribbed rod in spiral) were studied by V. A. Slyusarskiy. Under certain

conditions such systems are analogous to a combination of spiral and anisotropic dielectric.

Z. I. Taranenko investigated a wave-like bent waveguide of rectangular cross section with openings for passing the electron beam. He established that when the transit channel is made in the form of alternating openings of two different dimensions, the dispersion of such a retarding system becomes positive in the longwave range of the pass band.

A. G. Sveshnikov made an interesting report on evaluating a bent waveguide of variable cross section. In this paper general equations of the electromagnetic field were given, approximate solution methods in case of slowly varying waveguide characteristics were examined and methods of calculating by means of highspeed computers were discussed. V. S. Il'in extended to four-pole symmetrical systems the Levin-Shvinger variation method for calculating sudden nonuniformities in rectangular waveguides. In another paper V. S. Il'in reported on a method of computing waveguide nonuniformities by means of an equivalent resonator. The calculation was made with use of the variation method and illustrated in concrete examples (dielectric rods of different forms, bearing washers in coaxial cables, and others.).

In V. M. Sedykh's paper the constant attenuation of H-waveguides was determined and it was demonstrated that in such waveguides the attenuation is less than it should be from the Cohn theory. The dependence of the constant attenuation of a cross-shapped waveguide on the oscillation frequency and dimensions of the waveguide cross section were determined in the paper of V. M. Sedykh and A. F. Zorkin.

V. V. Tyazhelov set forth an approximation method of computing the effect of nonuniformities on single-wire lines, that is similar to the problem-solving method with diffusion of a plane wave on a sphere.

V. P. Sazanov and Ye. V. Skazochkin devoted their paper to problems of balancing a coaxial-spiral crossing by means of a multi-sectional transformer formed from segments of spiral with distribution of their wave resistances according to Chebyshev. Experimental investigations demonstrated that such crossings designed according to a deveoped method, can secure balancing in the range of three and more octaves with KSVN [probably coaxial-spiral wave norm] less than 1.5. Ya. M. Turover studied the balancing of a coaxial line with a rectangular waveguide by means of a conic antenna with a small angle of apertura. G. I. Shmel'kova determined on the basis of the variation method, the parameters of the equivalent circuit of a slot power lead from a toroidal resonator.

Spatial overtones in cavity resonators, and also a new type of resonance depending on the driver position and partially on the ratio of sides in a rectangular resonator and called "wandering," were studied in the work of B. P. Petrov. Distortions of the electromagnetic field configuration in a cavity resonator with non-

ideal walls was evaluated in the paper of A. S. Bondarev.

A. I. Fursayev examined the dispersion of a resonator system with double ties.

The paper of Ye. D. Mayboroda gave the theoretical grounds of a method for determining the full resistance of a point-contact diode (semiconductor) at super-high frequency in small signals conditions according to the rectified current's dependence on the position of a short-circuiting plunger situated beyond the diode. The measurement of the full input resistance of a detector according to the rectified current's dependence on the position of s short-circuiting plunger situated beyond the detector was the subject of the report of R. N. Bondarenko, Ye. D. Mayboroda and V. I. Strikh. This method can be employed in the case when measurement by means of a measuring line becomes difficult or impossible. For raising the sensitivity of ponderomotor measurers of power, V. D. Kukysh proposed that the circuit of a structure with travelling wave be used. Examined in the paper of K. P. Yatsuk was the possibility of measuring the dielectric permeability of solid and liquid dielectrics when they are placed inside a spiral retarding system.

Super-High Frequency Electronics Section

The reports and communications of the super-high frequency electronics section were devoted to the problem of studying the new methods of generation and amplification, and also problems of making theory more precise, raising the efficiency and improving the paramaters of tubes operating on known principles.

The papers were in considerable number devoted to phasochronic generators based on effective multiple energy exchange between the electron flow and the electromagnetic field with velocity parity of the flux of charged particles and the wave phase. The work of K. Ya. Lidzhvoye performed an experimental investigation of a phasochronic generator with cross interactions in which the electrons travel in crossed electrical and magnetic fields along a non-retarding system over roughly trochoidal trajectories. The experimental study of another phasochronic generator was done in the work of Z. I. Taranenko. A Phasochronic generator with combined interaction employing a retarding system was examined in the paper of I. V. Akalovskiy. In a generator of this type the electrons interact both with the cross and the longitudinal components of the high frequency field, which makes it possible, with less magnetic fields, to get shorter wave lengths than in generators without a retarding system.

The interaction of a trochoidal beam with the electromagnetic wave in waveguides was examined in the report of A. V. Gaponov. It was demonstrated that amplification of high frequency oscillations in such systems is possible only in case the velocity of the electron drift exceeds the wave's phase velocity, i.e. only in the case when the interaction of the electromagnetic wave is accomplished with one

of the "slow" harmonics of the beam current. The interaction of a trochoidal beam of electrons with a non-retarded wave under the conditions of the takeoff of unfavorably phased electrons was studied in the paper of V. M. Bokov. The basic properties of this type trochoidal amplifier were described and an evaluation was made of the maximal efficiency at high levels of power. An experimental investigation of a trochotron amplifier in the three-centimeter range was made by I. I. Antakov and R. P. Vasil'yev. It was established that amplification occurred in those conditions when the electrons having taken energy from the high-frequency field settled on one of the tube electrodes. In the authors' opinion, the trochotron amplifier can be used in the capacity of an adjustable amplifier of average power.

In the investigation of focusing beams of charged particles with high-frequency fields, D. M. Bravo-Zhivotovskiy, B. G. Yeremin, Ye. V. Zagradskiy, M. A. Miller and S. B. Mochenev obtained interesting experimental findings.

The excitation of waveguides and retarding systems with modulated linear flows of charged particles travelling with variable velocity was examined in the work of V. A. Ginzburg, V. A. Solntsev and A. S. Tager. It was demonstrated that for the flow of a finite line the intensity of radiation depends on the ratio between the average velocity of particles and the group velocity of the waves in the waveguide, and for an infinitely long flow the ratio between these velocities is immaterial. The interaction of electromagnetic waves with electron fluxes of variable velocity was studied also by V. A. Sosunov, who derived an expression for the generated power, frequency and efficiency of the electronics.

The paper of V. M. Lopukhin, B. D. Charkin and N. G. Zeveke cited the findings of an experimental investigation of the parametric amplification in LOV [possibly a wave deflection tube] with two dual-approach spirals in series. The first cascade operated as a generator of feed and the second was used as a signal amplifier. The findings of an experimental investigation of parametric amplification in a travelling-wave tube with two spirals in series were reported also by D. A. Akulina, S. A. Akhmanov, A. S. Gorshkov and I. T. Trofimenko. In this case the feed signal from the outside generator was introduced in the travelling-wave tube's first spiral, and the amplified signal in the second.

At section sessions the paper of V. G. Karamzin about development of a continuous action amplifier klystron with output power of 10 kwts was read and also the report of Ya. Ya. Akmentynykh, S. A. Zusmanovskiy and Z. I. Khaplanova about a new approach to calculation of bunchings in powerful straight-transit klystrons. For the case of small amplitudes, simple expressions have been derived for the induced current giving good concurrence with results of the theory of Kahn and Ramo [Rameau?]. In the case of large amplitudes the continuous electron flux is represented as comprising charged

discs and rings, the travel of which is also investigated. The problem of bunching at large amplitudes is solved on a computer.

Presented in the paper of S. D. Gvozdover and G. G. Solodar were the findings of elaboration of the travelling-wave tube theory for medium currents; it was shown that in case of medium currents the factor of amplification is found to be less, while the factor of depression is more than the weak current theory gives. The papers of A. M. Kats, and also of A. M. Kats and M. B. Tsaytlin were devoted to elaboration and making the travelling-wave tube theory more precise.

Yu. L. Klimontovich reported on the results of an analysis of non-linear oscillations that arise in the plasma during the passage of a beam of electrons through it. The author's original treatment of the mechanism of exciting these oscillations aroused a discussion.

The paper of D. M. Petrov was devoted to problems of engineering nomographic calculation of a reflex klystron. The stabilization of a reflex klystron's frequency by means of an outside cavity resonator was studied in the work of Yu. N. Kuznetsov. V. A. Malyshev reported on the findings of an experimental verification of the theory of super-high frequency generators with complex oscillating systems.

Examined in the paper of I. R. Gekker was the possibility of raising the efficiency of transit klystrons, traveling wave tubes and other super-high frequency divices by means of multi-cascade retarding of electrons in a sectionalized collector. G. N. Rapoport devoted his report to the problem of raising the efficiency of LOV by means of a sudden or gradual reduction of couplings of the initial section of a retarding system with an electron beam. Great interest was aroused by the report of V. S. Yergakov and A. A. Shaposhnikov about a two-span klystron with cross control in which cross modulation of the electron beam by the super-high frequency field is accomplished in the first resonator and the amplified signal is taken from the second resonator. It was demonstrated that in a klystron of such type amplification of the order of 25 db with a noise factor of 3 to 5 db is achievable.

At the section's concluding session a discussion was held devoted to an evaluation of the possibilities of the preset field method in analysis of the interaction of an electron beam with electromagnetic waves. S. D. Gvozdover, V. M. Lopukhin, V. N. Shevchik, A. S. Tager, M. B. Goland and S. I. Averkov participated in the discussion.

Quantum Radio Engineering and Radio-Spectroscopy Section

At the section's morning session on 25 January data on the installation, operating principle and technical possibilities of atomic-radiation standards of frequency were given in the survey report of I. A. Kalyabina, V. P. Laguzov, G. I. Rukman and Ya. A. Yukhvidin, entitled "Modern Atomic-radiation Means of Stabilizing Super-High Frequency."

In the report of V. M. Fayn, entitled "Theory of Coherent

Spontaneous Radiation," certain questions were examined about the theory of coherent spontaneous radiation in the radio range. It was demonstrated that interaction through the general field of radiation leads to a shift of the system's natural frequencies. The paper of G. L. Suchkin devoted to the theory of a parametric mixer in ferrites was read at the same session.

At the evening session of 23 January the paper of Ya. N. Shamfarov, entitled "A Highly-Sensitive Paramagnetic Spectrometer at Frequency of 9,000 Mc," described a paramagnetic radio-spectrometer with stabilization of the spiral klystron frequency by a measuring resonator and an automatic frequency control heterodyne. With the receiving channel band 25 kc, the experimentally verified sensitivity amounted to 5.10^{-9} moles of diphenyltrinitrophenylhydrosil. The paper of I. A. Deryugin and M. A. Sigal was devoted to an investigation of the dispersion properties of isotropic artificial dielectrics in the 500 to 25,000 Mc range. Cited in the report were the results of measurements of magnetic and dielectrical permeability of copper-paraffin mixtures depending on the concentrations of the conducting particles. The findings of the measurements are in good accord with theory. The dispersion of dielectric permeability was detected at frequencies in which the skin-layer becomes less than the particle dimensions.

The report of V. S. Ptkin and Z. M. Gershenzon, entitled "Parametric Regeneration in the Super-High Frequency Range in a Semiconductor Diode," was devoted to a description of a parametric amplifier of the centimeter range built by the authors in a germanium diode and the results of its testing.

The paper of Yu. S. Konstantinov describes an autodyne spectroscope with quartz stabilization in the fundamental frequency for measurement of chemical shifts of the nuclear magnetic resonance. The device's resolving power is $\Delta f/f \leq 10^{-6}$.

At the section's last session 24 January the nuclear and electronic paramagnetic resonance during ultrasonic excitation of a cyrstallic grid were examined theoretically in the report of L. L. Myasnikov and Ye. N. Plotnikova, entitled "On the Quantum Magnetic-Acoustic Effect."

The theory of the propagation of electromagnetic shock waves in ferrites was set forth in the report of A. V. Gaponov and G. I. Freydman. In the report were formulated the conditions of the formation of breaks in electromagnetic waves, and the structure of a shock wave front was also examined in the simplest example (in the case of wave propagation in the direction of the primary magnetization). The possibility of applying this phenomena in super-high frequency technology was noted in the report.

The papers of V. P. Tychinskiy and Yu. T. Derkach gave the elements of the theory of a parametric super-high frequency amplifier and generator in ferrite, and also cited certain findings of experimental investigations of such systems.

I. A. Deryugin's paper, entitled "The Doubling of Frequency in Ferrites," was devoted to the non-linear effect in mixed ferrites. The author investigated experimentally the dependence of the level of the second harmonic of signal value on the fundamental frequency of 9,400 Mc of the external magnetic field and the technique of preparing specimens.

V. M. Vamberskiy made a report, entitled "Variation of Tensor of Magnetic Permeability of Ferrites at High Level of Power."

General Radio Engineering Section

The reports read at the general radio engineering section were devoted to problems of radio measurements, raising the realiability of radio-electronic divices, accomplishing the best amplitude-phase modulation, the problems of getting laminar and three-dimensional X-ray pictures and so forth.

The report of V. A. Koval'chuk on division of frequencies in two-circuit autogenerators aroused great interest among those present. The audience heard with keen attention the paper of V. P. Lyannіy about the investigation of errors of an integrator for achieving optimal amplitude-phase modulation and the correction of errors. In the report were set forth the chief considerations in choice of the parameters of the integrator's line of retardation, the integrator's errors on account of the discreteness of summation and the terminal limits of integration were examined, also the means of correcting errors.

V. P. Kovalev told about determining the modulus and phase of the intensity of an electrical field at super-high frequency by means of simultaneous measurement of transient components of the field. The block diagram of a unit based on the proposed method was shown in the report, characteristics of circuit elements were examined and the findings of experimental measurements discussed.

Interest was aroused also by A. A. Tyutin's report on the elements of a television computer for deriving laminar and also three-dimensional X-ray pictures. The conditions of the roentgeno-technical examination of subjects were so selected that the corresponding integral equation had a single solution. The information about the subject recorded on photographic film during its roentgenoscopy was transformed in the picutre by the television computer which performed by instrumental means the appropriate integral transformation. One of the possible circuits of a television computer was described in the report and data given on its main elements.

The findings of work in the investigation of performance characteristics of the screens of electron-beam tubes (visual range characteristics) were set forth in M. M. Gratsianskiy's report. An equation was derived that makes it possible to calculate the visual range characteristics of a signal on the screen of an indicator operating with a brilliance modulator.

The reports of A. G. Kislyakov on the sensitivity of measurers of weak signals with continuous spectrum and I. A. Fastovskiy on a device for analysis of radio noise were devoted to problems of radio measurements. V. A. Malyshev's paper was devoted to a theoretical investigation of autogenerators with a single non-linear element. Questions of relaxation oscillators were expounded in the paper of G. L. Sobolev.

Ye. A. Domanov reported about an investigation of an attenuato based on the effect of changing the concentration of current carriers in a thin semiconductor, situated in a magnetic field, during the flow of an electric current through it.

In the communication of A. A. Bassonov about evaluation of the reliability of radio-electronic devices, the averages were given between the estimated and the experimental values of the reliability magnitude of certain standard unit elements, which can be used in rough appraisal of the reliability of these devices. The method of reserve elements was shown to be approximately five times more effective than the method of duplicating.

General Electronics Section

At three sessions of the general electronics section, 14 reports were read, devoted to the investigation of intensive electron beams, the modelling of fields and electron trajectories; also read were several communications of interest for the design and operation of electric vacuum devices.

P. V. Golubkov and I. G. Kozlov reported about the results of an experimental investigation of the distribution of the velocities o electrons in a ribbon plane-parallel beam of the Pearse gun by the method of the Hughes-Rozhanskiy cylindrical capacitor. The effect of various factors (filament voltage, degree of vacuum, etc.) on distribution of velocities was investigated.

The paper of B. M. Tseytlin examined theoretically the question about the limit current in an electron beam of finite length and varied configuration of cross section with conducting walls around the beam present.

The question of practical interest on the neutralization, by ions, of the space charge of an electron beam in a relatively high vacuum, was treated in V. P. Tarasov's report. Tarasov made an experimental investigation of the action of an ion trap on the passage of current. It was found that the use of ion traps leads to improvement of current passage in parallel beams and reduces the destruction of the cathode by ion bombardment.

I. K. Ovchinikov and I. S. Zinchenko spoke about the method of measuring parameters of an electron beam by radial distribution of current densities, the potential and axial velocities of electrons by means of an intersecting beam of a vibrating sonde. The report gives theoretical grounds of the method and experimental findings.

Described in the paper of Yu. I. Anisimov and A. I. Vystavkin is a unit for modelling the trajectories of relativist electrons in the shifting field of a magnetic undulator by means of low-volt electron beams. A method is cited for measuring and plotting projections of trajectories according to the position of spots on a sliding screen.

G. M. Gershteyn's paper substantiated a new experimental method of determining the intensity of an electrical field along the line of travel of a small charged body, by means of measuring the induced current. The method is based on the Rameau-Shokley [?] theory. The possibility was examined of applying the method for investigating the fields of certain periodic structures; results of experiments are given. Also read was Polyakov's report: "Investigation of Certain Functional Properties of Arbitrary Electrical Systems with Equivalent Electrodes by means of Models with Rubber Membranes."

S. M. Levitskiy and I. P. Shamshurin reported about the method of measuring the concentration of electrons in gas-discharge plasma by means of a high-frequency sonde which is a single-wire or two-wire line, the pole of which penetrates the plasma. The method gives results that are lower (1.5 to 2 times less as compared to the method of Langmuir's probe); this discrepancy can be qualitatively explained.

The report of K. I. Kononenko and G. A. Sobol set forth the results of an experimental study of the detector properties of gas discharge plasma of varied origin and chemical composition as they depend on a number factors (pressure, frequency, conditions and so forth.)

The report of V. D. Sobolev and M. N. Urlapova was devoted to the problem of measuring the thermo-electron emission of oxide cathodes in ionic devices. It appeared that horizontal sections corresponding to the cathode emission current are detected in the volt-ampere pulse characteristics of thyratrons at lowered current densities. This permits more precise evaluation of the cathode emission properties, whereas only very rough estimates can be made from characteristics measured at high current densities. The proposed method of measuring thermo-electron emission of an ionic device's oxide cathode is convenient for checking the manufacture of cathodes and investigating their changes in the process of divice operation.

G. L. Golub, P. A. Tarasov and L. I. Gubanov described three types of oscillographic tubes they had developed for recording super-high frequency oscillations in the frequency range to 1,000, 5,000 and 10,000 Mc.

The reports of N. V. Rabodzeya, entitled "Thermo-mechanical Processes that Determine the Static and Dynamic Form-Resistance of Electric Vacuum Device Designs," and S. A. Tiktin, entitled "Electric and Thermal Ratios in Modelling Electric Devices," read in the section were of interest for designing and engineering estimates of various electric vacuum devices.

Also read at the section was A. A. Genio's report, entitled

"Chief Characteristics of Tyratrons with Gold Cathodes and the Prospects of their Application."

Section of Semiconductors and Their Use in Radio Devices

In this section the reports were devoted to analysis of the physical processes in semiconductor devices; the properties of semiconductor materials were examined as well as the analysis of the work of circuits employing semiconductor devices and materials.

An investigation of the electrical and recombination properties of germanium with an admixture of beryllium in a wide temperature interval was reported in the peper of V. Ya. Lashkarev, R. N. Bondarenko, V. N. Dobrovol'skiy, V. G. Litovchenko, G. P. Zubrin and V. I. Strikh. It was demonstrated that beryllium is twice ionized at room temperature by the acceptor impurity capable of strongly alloying the germanium without reducing substantially the life time of the outside carriers.

The paper of V. N. Vertoprakhov was devoted to the problem of the anisotropy of a number of the properties of germanium monocrystals. The author showed that monocrystals manifest a number of anisotropic properties - anisotropy of hardness determined by the method of mutual abrasion, anisotropy of corrosion, anisotropy of the electric discharge routes on the germanium monocrystal surface, anisotropy of variation of resistance in the magnetic field and anisotropy of the cross photomagnetic effect. It is essential to take these phenomena into account when manufacturing devices as well as when using the finished devices.

The findings of experimental investigations of contacts of germanium with a series of metals and alloys were set forth in the report of A. P. Myatkin.

Experimental dependence of noises on temperature in the low-frequency part of the spectrum was examined for monocrystallic specimens of germanium in the paper of V. V. Potemkin and G. A. Chukina.

On the basis of ideas about bipolar and monopolar recombination, V. A. Malyshev examined the problem about the inertness of semiconductor devices which convert pulses of light or electron irradiation into secondary pulses of current or light emission (Luminescence). The principles derived make it possible, by the kind of frequency characteristic, to determine the recombination character and, by a certain kind of recombination, to select a photoconductor for getting the needed frequency characteristic.

N. S. Spiridonov examined the frequency characteristics of drift semiconductor triodes and analyzed their equivalent circuit. The derived results have importance for calculating the circuits of these triodes.

The phenomenon of "closing" in semiconductor triodes and its several applications were discussed in Ye. K. Vasil'yev's report.

The effect of a germanium plate, having variously processed

surfaces, on the propagation of waves in a waveguide was examined in the paper of N. V. Aleksandrov, L. B. Gorskaya, Ye. M. Gershenzon and V. S. Etkin. The findings of an investigation of amplitude and phase modulation of a passed and reflected wave when electrical and magnetic fields are applied to the plate indicate the possibility of utilizing the given phenomenon in parametric circuits.

In the paper of G. P. Petin a theoretical and experimental examination was made of the determination of threshold voltages of the Schmitt trigger in junction transistors. The dependence of threshold voltages on temperature was determined experimentally and means of temperature stabilization indicated. The conditions for deriving hysteresis loops closest to rectangular were also determined.

Ye. F. Doronkin made a report on the theme: "Design of Temperature Compensation Circuits of Semiconductor Relaxation Oscillators."

V. V. Voskresenskiy made an analysis of phantastron type semiconductor oscillators of linearly variable voltage.

The excitation mechanism of a generator in a point-contact semiconductor triode was examined in the report of Yakunkin. The analysis method, proposed by Yakunkin, however aroused serious objections from a number of conference participants.

Also read at the section were the reports of I. N. Magulin, entitled "Investigation of Certain Semiconductor Amplifier Circuits," of P. V. Bespalov, entitled "Investigation of Certain Methods of Frequency Stabilization in Semiconductor Generators," S. I. Malashenko, entitled "Means of Raising the Stability of Direct Current Amplification in Semiconductor Triodes," and G. I. Oliferenko, "Semiconductor Triodes in a Line Scanning Generator."

END